https://theses.gla.ac.uk/

Theses Digitisation:

https://www.gla.ac.uk/myglasgow/research/enlighten/theses/digitisation/

This is a digitised version of the original print thesis.

Copyright and moral rights for this work are retained by the author

A copy can be downloaded for personal non-commercial research or study, without prior permission or charge

This work cannot be reproduced or quoted extensively from without first obtaining permission in writing from the author

The content must not be changed in any way or sold commercially in any format or medium without the formal permission of the author

When referring to this work, full bibliographic details including the author, title, awarding institution and date of the thesis must be given

Enlighten: Theses
https://theses.gla.ac.uk/
research-enlighten@glasgow.ac.uk

REDISPERSION REACTIONS OF PLATINUM / ALUMINA REFORMING CATALYSTS.

by

LAURA JANETTE BUTTERLY

A Thesis for the Degree of Ph.D submitted to the Science Faculty of the University of Glasgow.

May 1988

© L.J. Butterly, 1988

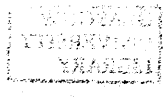

ProQuest Number: 10997943

All rights reserved

INFORMATION TO ALL USERS
The quality of this reproduction is dependent upon the quality of the copy submitted.

In the unlikely event that the author did not send a complete manuscript
and there are missing pages, these will be noted. Also, if material had to be removed,
a note will indicate the deletion.

ProQuest 10997943

Published by ProQuest LLC (2018). Copyright of the Dissertation is held by the Author.

All rights reserved.
This work is protected against unauthorized copying under Title 17, United States Code
Microform Edition © ProQuest LLC.

ProQuest LLC.
789 East Eisenhower Parkway
P.O. Box 1346
Ann Arbor, MI 48106 – 1346

DEDICATION

I dedicate this thesis to my parents - William and Margaret Butterly - to thank them for their support and encouragement throughout my education.

ACKNOWLEDGEMENTS

I am grateful to my academic supervisors Dr. John Fryer and Dr. Tom Baird for their advice and comments on this work. I am also grateful to fellow research students in the electron microscopy group for useful discussions, and to Davi Thom for his technical assistance.

I thank the SERC and ICI Petrochemicals and Plastics Division for the provision of a CASE award. I am particularly indebted to my industrial supervisor Dr. Mike Day, for his keen interest in this work. Thanks also to Ali, Rob and Alan for their assistance with experimental work, and to Dr. S. Norval for X-ray diffraction analysis.

I use this section to show my appreciation to Mrs Anne Martin for her patience in typing this thesis. Also to mum, dad, Michelle and Sharon for their encouragement over the past three years. I would especially like to thank my fiance, Raymond Murphy, for proof reading, diagram drawing - and putting up with me while writing this thesis.

CONTENTS

SUMMARY

Platinum metal supported on alumina is used industrially as a reforming catalyst, converting linear hydrocarbons to unsaturated cyclised and isomerised species. With prolonged use the platinum tends to agglomerate and carbon is deposited on the surface of the alumina, decreasing the catalytic activity. The catalyst can be reactivated by burning off the carbonaceous residues in oxygen and redispersing the platinum by an oxychlorination treatment.

Two models have been proposed to explain the redispersion of platinum. The crystallite splitting model suggests that large platinum particles split. The second model suggests that redispersion occurs via the spreading of a layer of platinum oxide on the alumina due to the decrease in surface tension as platinum is oxidised to platinum oxide.

Previous studies in this department suggest that no redispersion occurs following an oxychlorination treatment. X-ray diffraction data suggests that most of the platinum exists at the contrast limit of the electron microscope and below the resolution of X-ray diffraction analysis. The aim of the present study is to identify any sub-10Å platinum particles following oxychlorination treatment and to gain a better understanding of the optimum regeneration treatment and to propose a model for the redispersion of platinum following oxychlorination treatment.

X-ray diffraction line broadening, chemisorption, transmission electron microscopy have been used and catalytic measurements from a lab-scale micro-reformer have been used to study the regeneration and dispersion of the catalyst following oxychlorination treatments.

Small sub-10Å platinum particles have been identified by high resolution electron microscopy following oxychlorination treatment indicating that redispersion occurs. Following oxychlorination over 50% of the platinum particles detected by TEM were <15Å in diameter. Quantitative XRD has shown that 80% of the platinum exists in a highly dispersed state following oxychlorination treatment. Hollow Cone Illumination was used to resolve small platinum particles. A method was attempted using a Te compound to 'stain' the platinum but this was unsuccessful in since it combined with the support as well as the platinum and hence was non-selective.

Conditions of oxychlorination treatment were varied to find optimum conditions and to gain an understanding of the mechanism. CCl_4 concentration was found to increase the redispersion indicating that a platinum oxychloride complex may be responsible for redispersion.

Redispersion was found to increase with time of oxychlorination, although some large platinum particles still remain after the attempted regeneration treatments. With the higher metal loading (C3 0.8% by weight Pt) the size of the large particles,as determined by XRD, increases with the time of oxychlorination. The splitting model is therefore not a good representation of platinum redispersion as energetically large particles split more readily than smaller particles. A model is proposed where redispersion occurs via the spreading of a layer of a platinum oxide due to the decrease in surface tension as the platinum is oxidised to platinum oxide. Large particles may be protected by a layer of platinum oxide and require very long redispersion times to completely spread out. A sintering mechanism is proposed which competes with the redispersion mechanism and so large platinum particles co-existing with the highly dispersed material grow at the expense of

the smaller particles. CCl_4 must be injected into the gas stream during regeneration to give better metal dispersion.

Catalytic data compare well with physical measurements of particle size and dispersion. The catalytic activity decreases following the ageing treatment and increases following the regeneration treatments. The catalytic activity is less stable following oxychlorination for 18 hours. An optimum redispersion treatment is therefore oxychlorination for 9 hours.

1. Introduction

1.1 Previous Work and Aims of Present Study

1.2 Catalytic Naphtha Reforming

1.3 Ageing of Reforming Catalysts

1.4 Catalyst Regeneration

1.5 Catalyst Characterisation

1.1 Previous Work and Aims of Present Study

Platinum metal on a γ - alumina support is industrially used as a reforming catalyst, converting linear hydrocarbons to unsaturated, cyclised and isomerised hydrocarbons. With prolonged use the platinum tends to agglomerate and carbon is deposited on the surface of the alumina, hence decreasing the catalytic activity. The catalyst can be reactivated by burning off the carbonaceous residues in oxygen and redispersing the platinum with an oxychlorination treatment.

Two models have been proposed to explain the redispersion of platinum;
(1) The crystallite Splitting Model:- Where redispersion is due to the splitting of large Pt particles.
(2) Redispersion by spreading :- Where redispersion occurs via the spreading of a layer of a platinum oxide species on the alumina, due to the decrease in surface tension as platinum is oxidised to platinum oxide.

Previous work has been carried out in this department, in an attempt to explain the redispersion effect. Transmission electron microscopy (TEM) was used, as the actual particle size distribution can be found, as compared to average valves found by other techniques, such as gas adsorption. However, TEM studies on supported catalysts are inhibited by the high contrast from the porous support, making identification of small metal particles ($< 20\text{Å}$) difficult. For this reason initial studies were carried out on model catalysts, especially prepared for TEM examination. (White, 1982; Smith et al., 1983). These model catalysts consist of a thin film of γ - alumina, prepared by vacuum evaporation of alumina.

Platinum was deposited on the alumina by vacuum evaporation of platinum wire.

The model catalysts were treated in different temperatures, atmospheres and Pt loading, and then examined by electron microscopy. Sintering of highly dispersed metal particles occured in both a reducing and an oxidising atmosphere, resulting in an increase in particle size. Higher temperature and higher platinum loading also enhanced sintering.

Redispersion of the sintered model catalyst was attempted by oxychlorination at 480°C under a 2% by volume O_2/N_2 gas flow of $21h^{-1}$. Controlled amounts of chlorine were added via a carbon tetrachloride carrier. The platinum particle size was found to increase after this treatment, suggesting that no redispersion of the platinum crystallites occurred. No complementary data, such as H_2 chemisorption, could be obtained from the model catalysts. Catalytic activity could not be obtained due to the flat surface of the alumina film, as compared to the complex macroporous structure of γ - alumina, and also due to the very small amounts of model catalysts available.

For this reason it was decided to carry out similar experiments using industrial Pt/ γ- Al_2O_3 catalysts. The catalysts (0.4-2.0 w/o Pt) were prepared by the impregnation of γ - Al_2O_3 ($200\ m^2\ g^{-1}$) with chloroplatinic acid ($H_2\ Pt\ Cl_6$). TEM examination showed an increase in platinum particle size on sintering and a subsequent increase in metal particle size following an oxychlorination treatment, although H_2 Chemisorption results showed an increased H_2 uptake following oxychlorination. (White, 1982; White et al. 1983).

A second study was undertaken to study the redispersion of industrial catalysts (Spanner et al; 1983A, 1983B). The treated catalysts were characterised by; transmission electron microscopy (TEM); X-ray diffraction line broadening (XRD) and H_2 chemisorption. The catalytic activity was determined, after each treatment, by pulsing n-heptane in a carrier gas of 5% H_2 in N_2 over the samples in a lab - scale micro-reformer.

Results from TEM and XRD indicate that the large platinum particles formed during sintering were not apparently redispersed on oxychlorination treatment, although catalytic activity was regained and hydrogen chemisorption showed enhanced surface area. Quantitative XRD was used to measure the amount of Pt being detected by comparison to standards of known Pt content. It was found that over 50% of the platinum was at a size below the resolution of this technique. Monolayer Volumes were estimated from XRD results by assuming particle diameters for the undetected Pt, and comparing to the measured monolayer volumes from hydrogen chemisorption. The minimum deviation from the measured monolayer volume was found by assuming a Pt particle diameter of 9Å. These sub 10Å particles are below the resolution of a standard electron microscope.

The present aims are to use high resolution electron microscopy in further structural studies of the catalyst after different stages of oxychlorination treatment, in an attempt to explain the redispersion process. In particular it is hoped to resolve sub - 10Å platinum particles and to identify platinum compounds that may form during oxychlorination.

1.2 CATALYTIC NAPHTHA REFORMING

Catalytic reforming is one of the most important industrial applications of catalysis. Reforming is the process whereby the naphtha fraction of crude oil (consisting of C_6 - C_{10} straight chain hydrocarbons) is converted to branched, unsaturated and cyclised hydrocarbons, improving the fractions octane rating. Hydrocarbons are given research octane numbers (RON) in relation to the amount of energy which can be recovered from use as fuels; aromatics, branched and unsaturated compounds have higher ratings; Ciapetta et al (1958) have tabulated octane numbers for naphtha constituents and reformed products.

Initial research work on catalytic reforming studied molybdena and chromium oxide hydrogenation - dehydrogenation catalysts. Commercial reforming units in operation between 1940 and 1950 employed molybdena - alumina catalysts. In about 1950 a new reforming process was introduced with the discovery of bifunctional catalysts, such as platinum/alumina. These catalysts could operate for longer periods of time before replacement was required. This discovery, together with the increasing demand for high octane motor fuels, increased the capacity for catalytic reforming.

In a modern reforming unit the naphtha feed is composed of hydrocarbons (boiling point 370 - 470K). The reaction temperature is 700 - 800K, under a pressure of 10 - 35 atm. (Sinfelt, 1981). The catalyst consists of a metal part (e.g. Platinum) dispersed on an acidic support (e.g. $Si\ O_2$ - $Al_2\ O_3$ or chlorinated $Al_2\ O_3$). The support materials are generally high surface area porous materials. The catalyst is termed a bifunctional catalyst as both the metal and the support exhibit catalytic properties.

Heinemann et al.(1953) identified the dual functional nature of reforming catalysts and the mechanism was proposed by Mills et al. (1953). Dehydrogenation reactions are due to the metal part and isomerisation reactions are due to the acidic sites on the support. Commercial catalysts showing these properties have been patented as follows; platinum on silica - alumina (British patent 1958). Platinum on chlorinated alumina (US patent 1960, British patent 1969). Bimetallic catalyst systems have replaced the Pt/Al_2O_3 system as they have higher activity and are more resistant to deactivation. One of these catalysts is the platinum - rhenium - alumina catalyst first introduced by Chevron (US patent 1969) and more recently Alumina supported platinum-iridium bimetallic cluster catalysts (US patent 1976).

The main reactions in catalytic reforming are- (a) dehydrogenation of cyclohexanes to aromatics; (b) dehydroisomerisation of alkylcylopentanes to aromatics; (c) isomerisation of paraffins; (d) dehydrocyclisation of paraffins to aromatics; and (e) hydrocracking of hydrocarbons, as shown by figure 1.1.

As aromatics have a high octane rating the dehydrogenation of cyclohexanes is one of the most important reactions in catalytic reforming. Sinfelt and co workers (1962) investigated the role of the dehydrogenation activity in catalytic isomerisation and dehydrocyclisation of hydrocarbons. They found that the dehydrogenation activity of a platinum - alumina catalyst increases with increasing platinum content.

Figure 1.1

Hydrocarbon reactions in the presence of Reforming catalysts. (after Ciapetta and Wallace 1971).

1. Dehydrogenation of cyclohexanes to aromatics.

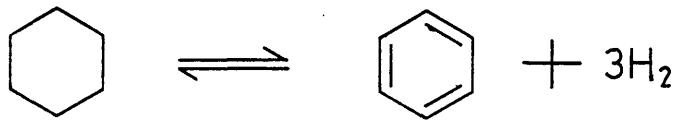

cyclohexane benzene

2. Dehydroisomerisation of alkylcyclopentanes to aromatics

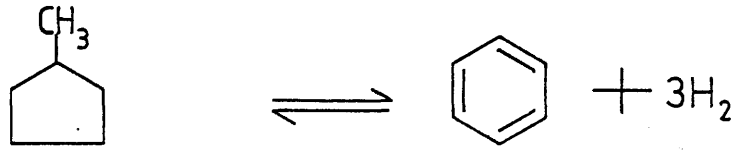

methylcyclopentane benzene

3. Isomerisation of paraffins

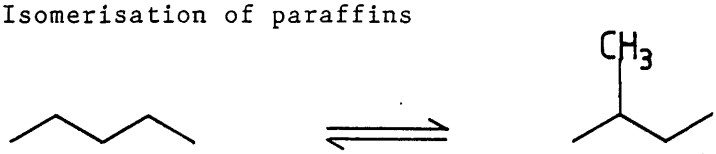

n-pentane 2-methylbutane

4. Dehydrocyclisation of paraffins to aromatics

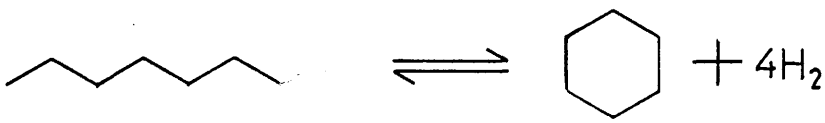

n-hexane Benzene

5. Hydrocracking of hydrocarbons

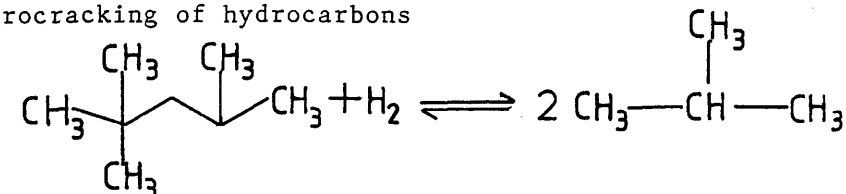

2,2,4-trimethylpentane Isobutane

Cusamano et al (1966) studied cyclohexane dehydrogenation over alumina and silica-aupported platinum and found the specific catalytic activity for cyclohexane dehydrogenation is unaffected by the support. Davis and Veneto (1969) studied dehydrocyclisation of paraffins over Pt - $A1_2\ 0_3$ catalysts. They found that using non-acidic supports 95% of aromatics produced were formed by direct six - membered ring formation. Using an acidic alumina support 50% of the aromatics produced were aromatic isomers, resulting from dual-functional catalytic reactions. Isomerisation reactions occur mainly on the acidic sites on the support. The nature of the acidic sites on alumina has been the subject of much discussion. The surface hydroxyl groups exhibit a Brønsted (protonic) type acidity. The presence of chloride ions enhances the Brønsted acidity of the alumina support by interaction with the hydroxyl groups (Gates et al., 1979). A Lewis type acidity is reported by Pines and Hagg (1960).

The acidic strengths of aluminas have been determined by measuring the ammonia adsorption of dehydrated aluminas (MacIver, Tobin and Barth; 1963).

Tanaka and Ogasawara (1970A) measured the surface acidity of HCl - treated aluminas by n-butylamine titration and infra-red measurements of adsorbed pyridine on the treated aluminas. They reported on increased alumina acidity with increased HCl adsorption. In a second paper by the same others, (Tanaka and Ogasawara, 1970B), the catalytic activity of n-butene isomerisation was reported as four times greater on the HCl treated alumina compared to that of pure alumina. Several reviews have reported the developments of catalytic naphtha reforming. (Ciapetta et al, 1958; Ciapetta and Wallace, 1971; Sinfelt, 1981).

1.3 Ageing of Reforming Catalysts

$Pt/\gamma - Al_2O_3$ reforming catalysts consist of small platinum particles (< 2nm), highly dispersed on a porous, high surface area alumina support. These catalysts deactivate with time as a result of; (1) the formation of carbonaceous deposits blocking catalytic sites; (2) poisoning of active sites by impurities present in the naphtha feed (e.g. S, As); and (3) the loss of metal surface area due to the agglomeration of platinum crystallites (sintering).

Catalyst poisoning can be limited to a tolerable level by the use of appropriate feed treatments. Catalyst regeneration is achieved by removing the carbonaceous residues by a carbon 'burn-off' treatment in oxygen at 600°C. This carbon 'burn-off' treatment causes further sintering of the platinum particles, resulting in an increase in the average platinum particle size. This loss of platinum surface area leads to a decrease in the catalytic activity and to changes in selectivity. Several reviews have discussed the deactivation of reforming catalysts (Butt (1984); Franck and Martino (1985)).

In this section I aim to briefly discuss the factors causing catalyst deactivation and to consider the sintering process in some detail. This will include a discussion of the proposed models for the sintering of supported metal particles.

1.3.1 Changes in Activity and Selectivity

A great deal of research has been undertaken to find the extent to which catalytic activity varies with metal particle size in supported catalysts. Many studies have reported the absence of any crystallite size effect (e.g. Basset et al. (1975)). Other studies have found the catalytic activity and selectivity to be particle size dependent, in reforming catalysts.

Basset and co-workers (1975), studied benzene hydrogenation over a Pt - Al_2O_3 catalyst. The specific activity was found to be independent of crystallite size, in the range studied (1.5 - 8.4nm). The particle sizes were measured by O_2 - H_2 titration and confirmed by electron microscopy.

A recent study by Guenin et al.(1984) studied the effect of particle size in n-hexane conversion, using a Pt/γ- Al_2O_3 catalyst. The authors reported that the selectivity for aromatisation does not depend on particle size, although the selectivities for isomerisation and hydrogenolysis were size dependent.

The influence of platinum particle size on the activity and selectivity of reforming reactions was studied by Arai et al (1980), using zeolite supported platinum catalysts. The metal dispersion was determined by hydrogen chemisorption and electron microscopy. The catalytic activity was measured by studying the change in product distribution, following n-heptane conversion. Their results show that platinum particles below 15Å, in diameter, were extremely active in reforming reactions. The catalytic activity was found to decrease with an increase in the platinum particle size.

Similar results were obtained by Spanner, Baird and Fryer (1983), who found that the catalytic activity of Pt/γ - Al_2O_3 catalysts decreases with an increase in platinum crystallite size. The catalytic activity was measured by pulsing n-heptane over the catalyst and measuring the major products of toluene, benzene and un-reformed heptane The selectivity for toluene and benzene was also found to change with an increase in platinum particle size.

Carbon deposition and particle size effects in the conversion of n-hexane, over a silica supported platinum catalyst, have been considered by Lankhorst et al. (1980). A series of catalysts with varying particle sizes was prepared and particle sizes determined by X-ray diffraction line broadening analysis. The activity and selectivity of the catalyst were determined, at each particle size, for untreated catalysts and for catalysts modified by carbon deposition. Their results, for the untreated series, show that an increase in platinum crystallite size causes a drop in catalytic activity. The selectivity of the catalyst is also changed. The activity is further decreased by carbon deposition and the changes in selectivity enhanced.

The build up of carbonaceous residues on reforming catalysts is one of the main causes of deactivation. Several workers have studied the effect of carbon build-up (coking) on catalysts, as reviewed by Franck and Martino, 1985.

1.3.2 Sintering of Supported Metal Particles

As discussed in the previous section, the sintering of supported metal particles causes changes in the activity and selectivity of reforming catalysts. In this section the factors affecting sintering will be outlined and the proposed models for sintering discussed.

Several factors can affect the sintering of supported metal particles.

White (1982) studied Pt/ γ-Al_2O_3 by electron microscopy and reports an increase in particle size with increasing temperature, treatment time and catalyst metal loading. He also reports changes in the degree of sintering due to changes in the chemical atmosphere. He finds that treatment in an oxygen environment lead to larger platinum particles than in a reducing environment. Similar results have been reported by other authors (e.g. Chu and Ruckenstein (1977, 1978); Yao et al (1979); Rothschild et al. (1986)).

The effect of chemical atmosphere on the sintering of platinum on alumina model catalysts is reported in an electron microscopy study by Chu and Ruckenstein (1978). H_2, N_2, O_2, wet N_2 and H_2 atmospheres were examined. Significant increases in particle growth is reported in wet H_2. Sintering is increased with higher treatment temperature. In an earlier paper by the same authors (Chu and Ruckenstein, 1977) an oxygen environment and the presence of water vapour was found to strongly affect the sintering of carbon supported platinum particles.

Yao et al. (1979) studied the effect of atmosphere, temperature and metal loading on the sintering of platinum supported on alumina. Temperature programmed reduction, transmission electron microscopy, and selective gas adsorption were used to study the catalyst after various treatments. The authors report that heating the catalyst at 500°C in H_2 causes an increase in particle size, and hence a decrease in surface area. Subsequent heating in an O_2 atmosphere at 500°C increases the surface area. However, O_2 treatment at temperatures > 600°C causes further sintering of the metal particles. More sintering is reported with higher metal loading.

These results are explained by assuming the formation of a platinum oxide phase, which will redisperse the metal in oxygen at 500°C. Above 600°C this complex decomposes to platinum which agglomerates, decreasing the metal surface area.

Two models have been suggested to explain the sintering of supported metal catalysts.

(i) The Crystallite Migration Model

The crystallite migration model was developed by Ruckenstein and Pulvermacher (1973). It suggests that sintering occurs by the migration of metal crystallites over the surface of the support, followed by a collision and subsequent coalescence of the metal particles.

(ii) The Atomic Migration Model

The atomic migration model for sintering is based on individual metal atoms (or molecules) leaving crystallites, migrating over the support and being captured by collision with larger metal crystallites (Flynn and Wanke, 1974A, 1974B).

Ruckenstein and Pulvermacher (1973) proposed the crystallite migration model to explain the growth of supported metal particles. Their model is based on a two stage process; (a) migration of the crystallites on the support and, (b) sintering of the migrating particles by collision and subsequent coalescence. In a later paper by the same authors (Pulvermacher and Ruckenstein, 1974), results from electron microscopy, X-ray line broadening, small angle X-ray scattering and static chemisorption were compared to theoretical models, in an attempt to find which of these two steps is rate determining.

The crystallite migration model was used to explain results obtained by Chu and Ruckenstein (1977, 1978) from two electron microscopy studies on model catalyst systems. In each study the size, shape and position of each platinum crystallite was monitered following treatment in various chemical atmospheres. The first study (Chu and Ruckenstein, 1977) examined platinum on a carbon substrate; migration of particles larger than 20nm was reported. In a study of platinum on alumina (Chu and Ruckenstein, 1978) migration of crystallites larger than 10nm was reported.

Although crystallite migration has been used to explain sintering, several factors remain unexplained by this model; e.g. the increased particle growth in an oxidising environment, as compared to a reducing environment. The migration times required for the observed rates of sintering are also questionable. Wynblatt and Gjostein (1975), in a theoretical discussion of supported metal crystallites, conclude that particle migration is too slow a process to explain sintering for particles greater than 5nm.

The atomic (or molecular) diffusion model can be used to explain differences in sintering with changes in chemical environment, the migrating species being platinum atoms in a reducing atmosphere and molecules of platinum oxide in an oxidising atmosphere (Flynn and Wanke, 1974). The rate of growth of particles would be smaller in a reducing atmosphere, as the sublimation energy for platinum is 135Kcal $mole^{-1}$, whereas the activation energy for the removal of a platinum atom as PtO_2 is only -42 Kcal $mole^{-1}$ (Slinkin, 1980).

The basis for the atomic migration model is the growth of larger particles at the expense of smaller ones (Ostwald Ripening). Small particles have a larger surface energy than larger particles and, therefore, the driving force of sintering would be an overall decrease in surface energy.

Flynn and Wanke (1974A) used the atomic migration model to explain results obtained on the sintering of alumina supported paltinum. McVicker et al. (1977) studied Ir/Al_2O_3 catalysts by electron microscopy and concluded that sintering occurs in an oxygen environment by a molecular migration mechanism.

Wynblatt and Ahn (1975) considered the two mathematical models for sintering and concluded that particle growth of supported metals is due to ripening.

Harris et al. (1983) studied the sintering of alumina supported platinum catalysts by transmission electron microscopy. Specimens were prepared by a novel technique based on the sol-gel process. The samples were sintered in air at 600°C. Sintering times were varied from 30 minutes to 24 hours in an attempt to explain which mechanism, atomic migration or particle migration and coalescence, represents the sintering

of supported platinum particles. A decrease in the sintering power-law exponent from 14 to 7 suggested that a change in sintering mechanism occurs after 2 hours of sintering. The authors propose that in the initial stages platinum particles grow by the migration and subsequent coalescence of small Pt particles. In the later stages, fast growing large platinum crystallites suggest that sintering occurs via an Ostwald ripening process. These results are supported by a later paper (Harris, 1986). In this study the catalyst was treated in O_2 in 700°C from 10 minutes to 8 hours. The particle size distribution and particle structure were noted after each treatment. Results show that initially the sintering mechanism is dominated by the migration and coalescence of small particles. Many twinned platinum particles are observed. In the later stages the presence of abnormally large particles (> 1500Å) suggest growth via an Ostwald ripening process with PtO_2 as the migrating molecular species, due to the oxygen atmosphere. It is suggested that the twin boundaries formed in the initial stages of particle sintering can provide nucleation sites for growth via molecular migration. Sintering at 700°C (Harris, 1986) causes an increase in the rate of particle growth compared to sintering at 600°C (Harris et al., 1983).

Several reviews have considered the possible mechanism of sintering (e.g. Wanke and Flynn (1975), Wynblatt and Gjostein (1975)).

1.4 Catalyst Regeneration

As explained in the previous section, reforming catalysts are deactivated by: coking, sintering of highly dispersed metal crystallites and the decrease in chlorine content on the acidic support. These catalysts are expensive to manufacture so their ability to undergo regeneration is an important factor in an industrial process.

An aged catalyst can be regenerated by the following treatment (as shown by figure 1.2). The carbonaceous residues are removed by a mild oxidation treatment (Phase I - III), until there is less than 100ppm CO_2 in the resulting gas stream. The carbon burn-off stage is followed by an oxychlorination stage to restore the chlorine level in the support to its original value (o.5 - 1 per cent by weight). An increase in metal surface area as measured by H_2 chemisorption, following oxychlorination treatment is responsible for a redispersion of the sintered metal crystallites.

Several processes have been patented for the regeneration of reforming catalysts. (e.g. Hayes (1973), Yates (1973), U.S. Patent (1976)). Hayes (1973) found that the octane rating of an aged catalyst could be returned to that of a fresh catalyst, following regeneration in an oxygen environment at 500 - 550°C in the presence of small amounts of HCl. Similarly Yates (1973) found a reduction in metal particle size and a restoration of catalytic activity for hydrocarbon conversion following an oxychlorination treatment on alumina supported Pt - Ir catalysts.

COMBUSTION			OXYCHLORINATION
PHASE I	PHASE II	PHASE III	
0.3% O_2 in N_2 to 425°C complete when CO_2 < 500 ppm in off gas	0.3% O_2 in N_2 to 440°C complete when CO_2 < 200 ppm in off gas	0.5/0.8/1/1.6/2% O_2 in N_2 to 500°C complete when CO_2 < 100 ppm in off gas	480°C 2% O_2 in N_2 260 ppm CCl_4

Figure 1.2 Regeneration/Oxychlorination Procedure.

Mills et al. (1961) considered catalyst regeneration in their study on the state of platinum in a Pt/ γ-Al_2O_3 reforming catalyst The catalytic properties were measured by the ability to chemisorb H_2, CO, O_2 or benzene. Platinum crystallite size was determined by X-ray measurements. The fresh catalyst consisted of small, highly dispersed platinum particles. Regeneration of a coked catalyst by a mild oxidation (0.5 percent volume O_2 in N_2 at 370°C) restored the catalyst to its original activity. An increase in the temperature of coke combustion led to a loss of catalytic activity, together with a substantial growth of platinum particles.

Bishara and co-workers (1983) studied the Ageing - regeneration cycle of an industrial Pt - Ir/Al_2O_3 catalyst. The authors reported that the sintering of metal crystallites during the carbon burn-off stage can be controlled by mild treatment. An increase in the combustion temperature from 370 - 450°C led to considerable sintering of the metal. The metal crystallites were subsequently redispersed by an oxychlorination treatment.

The metal dispersion was found to increase with an increasing chlorine content in the support.

The reactivation of sintered alumina supported platinum catalysts was examined by Spanner, Baird and Fryer (1983). The catalytic activity was measured by pulsing n-heptane over the catalyst at 400°C and particle sizes measured by hydrogen chemisorption, transmission electron microscopy and X-ray diffraction measurements. As the platinum particle size increased the catalytic activity decreased and the selectivity for the main products of toluene and benzene changed. The catalytic activity and selectivity were restored to that of a fresh catalyst following

an oxychlorination treatment. Chemisorption results showed an increase in hydrogen uptake, suggesting a redispersion of the platinum agglomerates, although no decrease in platinum particle size was detected by electron microscopy or x-ray measurements.

The redispersion of sintered metal crystallites has been studied by many workers. Studies on the effect of temperature on supported metal particles show that heating in oxygen above 600°C causes particle growth. Oxygen treatment at temperatures 400 - 550°C causes redispersion of the sintered metal (e.g. Johnson and Keith, 1963; Straguzzi et al. 1980; Adler and Kearney, 1960; Fiedorow and Wanke, 1976). The chemical atmosphere also has an effect on catalyst regeneration. Redispersion has been widely reported in oxygen containing environments. (e.g. Fiedorow and Wanke, 1976; Ruckenstein and Chu, 1979; Lee and Kim, 1984; Johnson and Keith, 1963), and by an oxychlorination treatment (e.g. Lieske et al, 1983; Straguzzi et al. 1980). Foger and Jaeger (1985) reported an increase in platinum dispersion following treatment at 320 - 700K in a stream of Cl_2 (0.2 - 100 % by volume) in N_2. Similar results were reported for the redispersion of supported Ir and Pt - Ir bimetallic catalysts. (Foger, Hay, Jaeger, 1985A, 1985B).

In 1960 McHendry and co-workers noted an increase in the dehydrocyclization rate of n-heptane at 490°C, using alumina - supported platinum catalysts. They proposed that the active component consists of a platinum - alumina complex. This is based on their findings that dehydrocyclization activity was dependent on the amount of complex present, defined as the amount of platinum soluble in HF or acetylacetone. ("Soluble" platinum). The complex exists in an oxidized state and is responsible for high platinum metal dispersion upon reduction.

Platinum - alumina complex formation in an oxidising environment was supported by Johnson and Keith (1963). Johnson and Keith studied the regeneration of a deactivated 0.6% Pt on alumina catalyst. They find that treating a sintered catalyst at 500° C in air converts some of the supported metal to the "soluble" form. The amount of "soluble" platinum increases with increasing exposure time and increasing oxygen partial pressure. The authors suggest that the soluble platinum represents a complex formed between the supported platinum, oxygen and the alumina support. The platinum particles are dispersed by the complex formation and subsequent reduction removes the oxygen, leaving platinum in a highly dispersed state on the support. The degree of dispersion increases with an increase in the amount of platinum "soluble" in the oxidized state.

The findings of Johnson and Keith remain unchallenged to this day. The formation of a complex responsible for redispersion has been suggested by many authors, although the structure is not yet known. Some mechanisms have been proposed to explain the redispersion phenomena.

The models for the regeneration of sintered supported metal crystallites fall into two main categories. One category attributes the increase in surface area to the actual splitting of the particles, (crystallite splitting model), while the other category suggests that redispersion occurs by the formation and spreading of a platinum complex on the support, (spreading model).

(i) The Crystallite Splitting Model

The crystallite splitting model was proposed by Ruckenstein and Malhotra following studies on the platinum - alumina system. The

platinum - alumina complex, suggested by Johnson and Keith (1963), forms at the support - metal interface. A strain energy is induced on the metal due to the lattice mismatch between the complex and the metal. This strain is relaxed by the fracture of the particle.

(ii) The Spreading Model

This model assumes that redispersion occurs via the spreading of a layer of metal oxide (or some metal complex, formed by the regeneration treatment) on the support in an oxidising atmosphere, dispersing through molecular migration. The thermodynamic basis for this model is the decrease in surface tension as metals are oxidised to their corresponding metal oxides. Consider a cap-shaped particle resting at thermodynamic equilibrium on a support surface as shown:

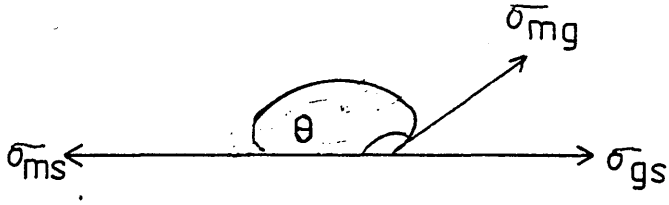

Its contact angle, θ, is determined by Young's equation.

$$\sigma_{gs} - \sigma_{ms} = \sigma_{mg}\cos\theta$$

Where, σ is the surface tension, the subscripts ms, mg and gs refer to the metal-substrate, metal-gas and gas-substrate interfaces; θ is the contact angle. When a metal is oxidised to its corresponding metal oxide, $\sigma_{gs} - \sigma_{ms} > \sigma_{mg}$, hence the contact angle $\theta \longrightarrow 0$ causing a surface layer of metal oxide to wet the support. In a reducing atmosphere the metal oxide is reduced to metal, which does not wet the support, hence redispersing the sintered metal.

The splitting of platinum crystallites supported on thin non-porous alumina films was studied by Ruckenstein and Malhatra (1976). Particle sizes and positions were studied at each stage by transmission electron microscopy. The specimens heated in air at 600°C showed sintering of the platinum crystallites. Reheating these samples in air at 500°C led, due to splitting, to a decrease in the average size of the crystallites.

Dadyburjor (1979) considered the results of Ruckenstein and Malhatra and proposed two theatrical explanations of splitting in an oxidising atmosphere. In each case he assumes the formation of platinum oxides, on the surface of the platinum particles. The lattice parameters of platinum oxide is much larger than the lattice spacings of the pure metal, this creates an internal stress on the particle. When the oxide thickness reaches a critical value (l_{crit}) the stress is relieved by the fracture of the particle. In Dadyburjor's first model only the oxide layer fractures and the particle does not split. The oxidation continues and a stressed oxide layer builds up inside the particle which in turn fractures and the process continues until the particle splits. In the second model the oxide again cracks to relieve the stress; in this case the crack propagates through and the particle splits.

Gollob and Dadyburjor (1981), studied the regeneration of a model platinum alumina catalyst as a function of time, using a TEM. The changes in dispersion were measured after short time intervals. Results show that initial regeneration rate is rapid and falls after 2 hours. These results were explained by the crystallite splitting model, particularly valid for short times and large particles. Smaller particles do not split as readily as they require a greater critical thickness before a crack can be initiated.

Dadyburjor (1980) applied a mathematical approach to consider the two models for redispersion. His calculations indicate that splitting of platinum particles, due to internal stresses caused by metal - metal oxide lattice mismatch, is more favourable for large particles and short regeneration times. The spreading model, requiring all of the platinum to be converted to PtO_2, is more favourable for smaller particles and longer regeneration times. Below a critical particle diameter, $\sim 10\text{Å}$, splitting of the platinum will not occur and so the platinum redisperses by a spreading mechanism.

By the "splitting" mechanism particle splitting occurs more easily as particle size increases (Dadyburjor, 1979), but redispersion of particles as small as 3nm has been reported (Fiedorow and Wanke, 1976) and large particles have been observed after regeneration (e.g. Yao et al., 1979; Spanner et al., 1983). The above observations suggest that crystallite splitting does not adequately explain the redispersion phenomena.

The redispersion of supported platinum in oxygen was studied by Fiedorow and Wanke (1976). Metal dispersions were measured by hydrogen chemisorption. Redispersion was reported at 500°C and 550°C and explained by a molecular migration mechanism, due to the formation of PtO_2. Above 600°C sintering of the platinum crystallites was observed, due to the decomposition of PtO_2 to platinum.

Ruckenstein and Chu (1979) considered the role of wetting to the redispersion of model alumina supported platinum catalysts. Changes in particle size, shape, and position were followed by examining the same

specimen, after each treatment, by transmission electron microscopy. The specimens were treated alternately in oxygen and hydrogen at 750°C. Several cycles of oxygen and hydrogen treatment were required before redispersion was observed. Thereafter redispersion occurs in an oxygen atmosphere and sintering in a reducing atmosphere. Redispersion occurs in oxygen due to the spreading of platinum oxide over the surface of the alumina. Spreading occurs either because the crystallites are completely oxidized and hence no wetting angle can exist between the crystallites and the support, or because a "two - dimensional fluid" of platinum oxide co-exists with the metal crystallites. The authors suggest that heating in hydrogen causes sintering as the platinum oxide is converted to platinum metal, which does not wet the alumina support. Baker (1980) considered the explanation of Ruckenstein and Chu, and used wetting to explain results from earlier work on the behaviour of platinum on a titanium oxide support (Baker et al., 1979A, 1979B) Deoraune et al., (1984), studied copper on magnesium oxide by controlled atmosphere electron microscopy. Dramatic changes in particle morphology were observed by treating the catalyst in oxygen at 200°C. The changes in morphology, and in particle size, were explained by wetting of the magnesium oxide support by copper oxide.

The support also has an effect on the redispersion of supported metals. Platinum supported on γ - Al_2O_3, SiO_2 and TiO_2 was studied by hydrogen chemisorption, X-ray diffraction, TEM and temperature programmed reduction (TPR) (Lee and Kim, 1984). An increase in dispersion following O_2 treatment below 600°C occurs only for $Pt|\gamma\text{-}Al_2O_3$. The presence of chlorine during oxidation was required to redisperse TiO_2 supported platinum. No redispersion was observed for $Pt|SiO_2$. The authors report that redispersion can only occur by the formation of platinum oxide which is stabilised by forming a complex with the support.

Redispersion occurs via the spreading of platinum oxide and the trapping of migrating species. The effect of chlorine may be explained by the formation of oxychloroplatinum complexes which are strongly bound to the support. These chlorinated compounds create acidic oxidising sites on the support. No redispersion was observed on the SiO_2 support since SiO_2 has no acidic sites, even in the presence of chlorine.

The effect of chlorine to redispersion in oxygen has been considered by many authors. Straguzzi, Aduriz and Gigola (1980) studied changes in platinum dispersion, in a chlorided $Pt|Al_2O_3$ catalyst, by hydrogen chemisorption. Heating the catalyst in H_2 at 600°C led to a decrease in metal dispersion and a loss of chlorine. Air treatment at 500°C led to a recovery of metal dispersion, although successive sintering-regeneration cycles showed a slow decrease in the final dispersion and a parallel loss in chlorine content. Air treatment at 500°C with 0.85% HCl in the gas stream returned the metal dispersion to its original value. Redispersion was explained by a spreading model. The role of chlorine is to enhance the oxidising properties of the alumina support.

Bournoville and Martino (1980) considered the sintering-redispersion of alumina supported platinum. The effect of temperatures and atmosphere was considered. In a hydrogen atmosphere sintering was prevented by the injection of CCl_4 into the gas stream. In air, sintering of the platinum is observed above 600°C, and redispersion between 400-500°C. The addition of CCl_4 inhibits the rate of sintering at higher temperatures (>600°C). and increases the redispersion rate at lower temperatures (400-500°C). This phenomenon may be explained by the shift in the equilibrium between sintering and redispersion, equilibrium being reached at lower

dispersions with platinum oxides than platinum oxychlorides.

Lieske et al., (1983) studied Pt| γ-Al_2O_3 catalysts, with and without chlorine, at different temperatures in oxygen and hydrogen. Chlorine was introduced to the gas stream via the addition of 0.85% HCl. Four surface complexes were identified by TPR; two oxides, α- and β - PtO_2; and two chloride containing complexes, $[Pt^{IV}(OH)_x Cl_y]s$ and $[Pt^{IV} O_x Cl_y]s$. Redispersion was only observed in oxygen in the presence of chlorine. The authors suggest that redispersion occurs by a molecular migration mechanism, via the formation of $[Pt^{IV} O_x Cl_y]s$.

Contrasting results were obtained by Smith et al., (1983) and White et al., (1983) from electron microscopy studies on model and real catalysts respectively. No platinum redispersion was observed in 3% O_2/N_2 in the temperature range studied (300-600°C). The addition of CCl_4 enhanced the sintering of the platinum.

Although there appears to be good evidence that redispersion can occur, Smith et al., (1983) and White et al., (1983) observe no redispersion of sintered platinum following oxychlorination treatment by a TEM examination, although H_2 chemisorption increased. Stulga et al., (1980) repeated the experiments of Ruckenstein and Malhotra (1976), and found no significant decrease in metal particle size. Dautzenberg and Wolters (1978) studied the effect of heat treatment in air and hydrogen on the dispersion of platinum in alumina - supported catalysts. Their results suggest that regeneration in oxygen does not actually redisperse the large crystallites, but recovers the fraction of platinum lost by severe heat treatment.

The mechanism of redispersion will be further discussed and compared to the results of this study in the discussion chapter.

1.5 Catalyst Characterisation

In a study of the redispersion of supported metal the changes in metal dispersion must be measured at each stage in the ageing - regeneration cycle. A method must be available to measure the changes in particle size, particle size distribution and the metal dispersion. The metal dispersion is the metal surface: volume ratio. An ideal catalyst would have a dispersion close to one, where every metal atom is on the surface, and therefore available for catalysis. Several techniques have been used in the study of supported metal crystallites. Two basic modes of measurements exist. The first being techniques sensitive to the number of metal atoms available for catalysis, or the metal surface area, such as selective gas chemisorption. The mean particle size can then be calculated by assuming a spherical geometry for the metal crystallites. The second type of measurement is methods sensitive to the particle size of the metal component, such as transmission electron microscopy and X-ray diffraction line broadening analysis.

Earlier studies on supported catalysts used X-ray diffraction line broadening to determine metal dispersion. This technique is limited to particles greater than ca. 3nm, so highly dispersed metal particles are undetected by X-ray diffraction line broadening analysis (XRD). Spenadel and Boudart (1960), used hydrogen chemisorption and X.R.D. to determined the dispersion of platinum on alumina supported catalysts. Good agreement was obtained between platinum particle sizes calculated from chemisorption and X-ray diffraction, for particles above the resolution limit of XRD. In addition chemisorption could be used to determine the surface area of the highly dispersed platinum crystallites. Similar results were reported by Adler and Keavney (1960).

Selective gas chemisorption is now the most extensively used method of measuring metal dispersion, although care must be taken in deriving the average metal particle size from chemisorption data alone. (Dautzenberg and Wolters, 1978).

Renouprez and co-workers (1974) studied supported platinum catalysts by small - angle X-ray scattering (SAXS); chemisorption; and transmission electron microscopy. They report that for finely dispersed catalysts, results from all three techniques are in good agreement. When the metal dispersion is poor, results from electron microscopy were less reproducible, whereas the results from SAXS and chemisorption were in good agreement.

Conflicting dispersion measurements were obtained by White (1982; 1983) on studies of industrial $Pt/\gamma - Al_2O_3$ reforming catalysts. The dispersion was measured at each stage in an ageing - regeneration cycle by hydrogen chemisorption and transmission electron microscopy (TEM). For an aged catalyst both techniques show a decrease in metal dispersion, hence an increase in platinum particle size, following a regeneration treatment TEM shows no change in particle size although chemisorption shows an increase in dispersion.

Similar results were obtained by Spanner et al. (1983) on a study of the same catalyst. The dispersion was measured by H_2 chemisorption, TEM, X-ray diffraction line broadening (XRD), and the catalytic activity was noted at each stage by pulsing n-heptane over the catalyst. Results from TEM and XRD indicate that the large platinum particles formed during sintering were not apparantly redispersed following a regeneration treatment, although catalytic activity was regained and hydrogen chemisorption showed enhanced surface area. Quantitive XRD was used to measure the amount of platinum being detected. It was found that over 50% of the platinum is below the resolution limit of the technique, i.e.

sub - 30Å particles. Comparing XRD results with results from chemisorption suggests that the undetectable platinum mainly exists in the form of sub - 10Å particles below the resolution limit of the modern TEM, as recently reported (Butterly et al., 1986).

Each characterisation technique has both advantages and disadvantages in the study of alumina supported platinum catalysts. The use of a combination of techniques is therefore required to ensure that results are reliable. In this section I wish to introduce the three characterisation methods used in this study; selective gas chemisorption; X-ray diffraction line broadening analysis and electron microscopy.

1.5.1 Gas Adsorption

Selective gas adsorption is the most common method for measuring the metal dispersion of supported catalysts. Adsorption occurs when molecules of a gas stick to the surface of the catalyst. The amount of gas adsorbed by the metal in the catalyst is measured and converted to a metal dispersion by assuming an adsorption stoichiometry (i.e. the ratio of the number of adsorbate atoms or molecules adsorbed per surface metal atom). For H_2 and CO on platinum the adsorption stoichiometry is taken as 1:1. Physical adsorption occurs where adsorption is via van der Waals forces. The valency forces can also cause surface combinations between the elements on the surface of a solid and the molecules (atoms) of a reactive gas. This is called chemical adsorption or chemisorption.

Physical adsorption is nonselective whereas chemisorption can be selective to combine with either the metal or the support in supported metal catalysts. It is also used with metal catalysts containing various promoters (e.g. Emmett and Brumauer (1937). The use of H_2 chemisorption to study reforming catalysts is outlined by Lemaitre et al., (1984). The adsorption of H_2 by the support is negligible. However, the assumption that H_2 spillover does not occur has lead to errors in H:Pt stoichiometries. The characterisation of platinum|silica catalysts is considered in a series of reports by Bond et al., (1985). Frennet and Wells (1985) considered the chemisorption of hydrogen on the platinum|silica catalyst. A H:Pt stoichiometry was reported as exceeding 1.1:1. This suggests that H_2 chemisorption on platinum catalysts may have problems with spillover effects. The adsorption stoichiometry of CO on platinum was reported as 1.1 (Wells, 1985). Results from CO adsorption were in good agreement with electrom microscopy. Conflicting results were obtained from Renouprez et al., (1974) who found

results from H_2 and CO adsorption to be in good agreement.

Care must therefore be taken to ensure that the gas adsorption is selective and that no adsorption is due to the support.

1.5.2 X-ray Diffraction Line Broadening Analysis (XRD)

X-ray diffraction line broadening has been widely used to characterise supported metal catalysts (e.g. Adler and Kearney (1960); Ganesan et al (1978); Sashital (1977)), giving information on the average particle size. The technique is limited to detecting crystalline particles greater than 3nm.

The relationship between the size of small crystallites and the width of diffraction lines was recognized by Scherrer in 1918. It was shown that the broadening, β, of the diffraction line corresponding to the Bragg angle, θ, using a wavelength λ was related to the thickness, t, of the crystal in a direction perpendicular to the diffracting planes as:

$$t = \frac{K\lambda}{\beta \cos\theta}$$

where K is a constant, depending on the definition of β.

Two main definitions of β are used: the full breadth at half maximum height, $\beta_{\frac{1}{2}}$; and the integral breadth, β_i, is the width of a rectangle having the same surface area as the observed line.

The main problem with this method (Scherrer formula) in calculating crystallite sizes, is that it assumes that all broadening is due to a decrease in particle size. Lattice distortions, the presence of microstrains and instrumental factors, also contribute to line broadening.

A fourier method of analysis is used which takes account of the above factors. Using a Fourier analysis all the information of the diffraction peak is used, i.e. both the size and shape, as compared to the Scherrer method where only the line width is taken into account. Correction for instrumental broadening and the effects of strain is also possible with a Fourier method. Warren and Averbach (1950) developed a method for seperating broadening, due to particle size and due to lattice strains. Information on lattice distortions and strains of supported metal catalysts has been reported (Sashital et al, 1977; Ganesan et al; 1978). The development of the fourier method is discussed in a recent review by Matyi and co-workers (1987).

The determination of metallic platinum, by X-ray diffraction line broadening analysis, in platinum - alumina catalysts has been discussed by Van Nordstrand, Lincoln and Carnevale (1964). The main difficulties in using XRD for crystallite size determination of platinum supported on alumina are outlined. The total platinum concentration in an industrial catalyst is low (0.3 - 1%), this can be partially compensated by the strong scattering power of the platinum atom. The second difficulty is that due to a structural similarity between platinum and alumina, the major diffraction peaks of alumina nearly coincide with those of platinum. The strongest platinum line is from the platinum (111) reflection. The line can not be used for line broadening analysis as it almost coincides with the γ - alumina (222) reflection, as shown by figure 1.3. For this reason the platinum (311) line is selected for line broadening analysis, as it has the least background interference from the γ - alumina profile. The platinum (311) line is only one third the intensity of the platinum (111) line.

Figure 1.3: XRD profile showing interference between γ-Al_2O_3 (222) and Pt (100) peak.

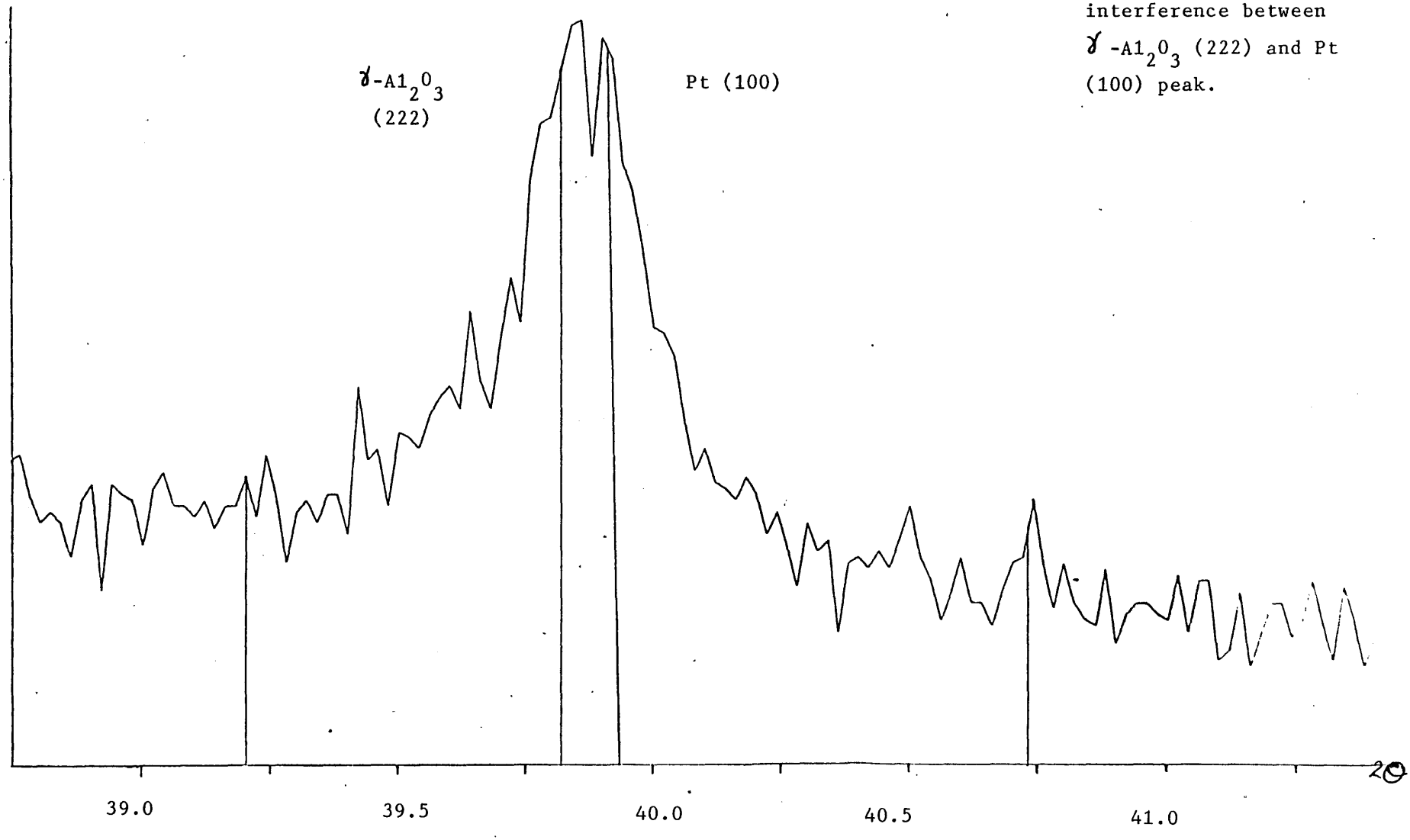

The use of X-ray diffraction line broadening analysis in the study of supported metal catalysts has been discussed by many authors (e.g. Lemaitre et al (1984); Matyi et al (1987)).

1.5.3 Transmission Electron Microscopy

The use of the electron microscope was first applied to study supported metal catalysts in the mid - 1940's (Turkevich, 1945; Anderson et al., 1947). The electron microscope has been developed since and the structure of catalytic particles identified (Sanders, 1986). Electron microscopy can be used to directly observe the metal catalyst particles on the support and can provide particle size, size distribution and metal dispersion data for comparison with chemisorption and X-ray measurements. The theory of electron microscopy is outlined in chapter 2.

The main advantage of TEM is that it is a direct technique. However, the major limitations are outlined by Flynn et al., (1974). Particle size distributions are based on three assumptions:

(i) the size of the metal particle is equal to the size of its image recorded (corrected for magnification).

(ii) Detection of a particle at a given size implies that all particles of that size and larger are being detected.

(iii) Image contrast of the metal particles is distinguishable from contrast arising from the support material.

Particle detectability and apparent size are found to be sensitive to defocus. Contrast is shown to vary with orientation of both particles and the support. More error is reported from particle size distribution as the fraction of particles with sizes below about 25Å increases.

Contrast effects from supported particles was discussed by Treacy and Howie (1980). For particles >30Å the main scattering is Bragg reflection, whereby electrons are scattered outside the objective aperture. For particles <30Å electrons scatter by a phase contrast mechanism. Detection of these particles is therefore very sensitive to the defocus of the objective lens.

The detection of small particles becomes more difficult with an increase in the crystallinity of the support. For this reason many methods have been adopted where the contrast from the support is decreased (eg. Hollow cone illumination), or the scattering of the particle is enhanced (eg. Z-contrast, where scattering is proportional to the atomic number).

Image intensity varies with defocus and so detection of small particles depends on their elevation, specimen thickness should be therefore kept to a minimum (Oikawa et al., 1970). Tilting specimens in bright field images causes contrast changes within individual particles allowing more information to be obtained (Flynn et al., 1974).

Dark field methods may offer some advantage over bright field method (Zenith et al., 1980). For example by selecting a small portion of a diffraction ring with the objective aperture some details of the inner structure of the particle may be obtained (Avery and Sanders, 1970). Freeman et al., (1977) used an annular condenser aperture to produce hollow cone illumination of alumina supported palladium particles. Varying the depth of the specimen in the objective lens field allows different Bragg reflections to be selected. A second method is used whereby an annular objective aperture is generated be electronic control of the deflection coils (Heinenmann and Poppa, 1970; Karkow and Howland,

1976). The advantages of hollow cone illumination are outlined by Saxton et al., (1978).

The use of scanning transmission electron microscopy for catalyst characterisation is considered by Treacy et al., (1978). By using a Z-contrast technique structural details in platinum particles as small as 2nm may be imaged.

Several reviews have outlined the use of electron microscopy to catalyst characterisation (e.g. Baird, 1982;Matyi, 1987; Howie, 1980; Poppa and Heinemann, 1980).

2. ELECTRON MICROSCOPY

2. ELECTRON MICROSCOPY

In 1924 de Broglie (de Broglie, 1924) discovered the wave nature associated with an electron, and found that the wavelength of an electron is shorter than the wavelength of light (λ light $\sim$ 3000Å ; λ electron $\sim$ 0.036Å , at 100KV). As the light microscope is limited by the wavelength of light, it was thought that improvements could be offered on light microscopy.

Knoll and Ruska built the first electron microscope in 1931 (Knoll and Ruska, 1932) and the first high resolution instrument in 1933. This was capable of resolving 0.05μm structural information, greatly exceeding the resolving power of the light microscope. Since its invention, the electron microscope has been developed to the stage where atomic scale resolution has been acheived on modern commercial high resolution microscopes (e.g. Hall and Hines, 1970; Murata et al., 1976; Iijima, 1977; Fryer, 1983; Smith et al., 1983). Electron optical theories and development of the electron microscope have been extensively reviewed (Zworykin et al., 1945; Hillier and Vance, 1945; Coslett, 1951, 1970, 1981; Hall, 1953; Hirsch et al, 1965; Spence, 1981) with the practical techniques used in modern microscopy described by Kay (1965).

2.1 TEM Instrumentation

The basic design and ray diagram of a high resolution transmission electron microscope are shown in figure 2.1. A coherent beam of electrons is accelerated through a potential of thousands of volts (120KV for the JEOL 1200EX) and is focussed on to the specimen by means of a condenser lens system. The electron source usually takes the form of an electrically heated tungsten hairpin filament. Improved coherence and an increase in source brightness can be obtained using special pointed tungsten

Figure 2.1

A Schematic features of a modern TEM (altered geometrically to fit ray diagram B).

B Ray paths for conventional imaging.

KEY TO FIGURE

HV	:	Stabilised high voltage supply
F	:	Electron - emitting filament
WC	:	Wehnelt cylinder
A	:	Anode
C1	:	First condenser lens
CA1	:	First condenser aperture (fixed)
C2	:	Second condenser lens
CA2	:	Second condenser aperture (variable)
S	:	Specimen stage
O	:	Objective lens
OA	:	Objective aperture (variable)
SA	:	Area selection aperture
I	:	Intermediate lens
P	:	Projector lens
FS	:	Fluorescent viewing screen
C	:	Camera
SS	:	Electronics and vacuum support systems

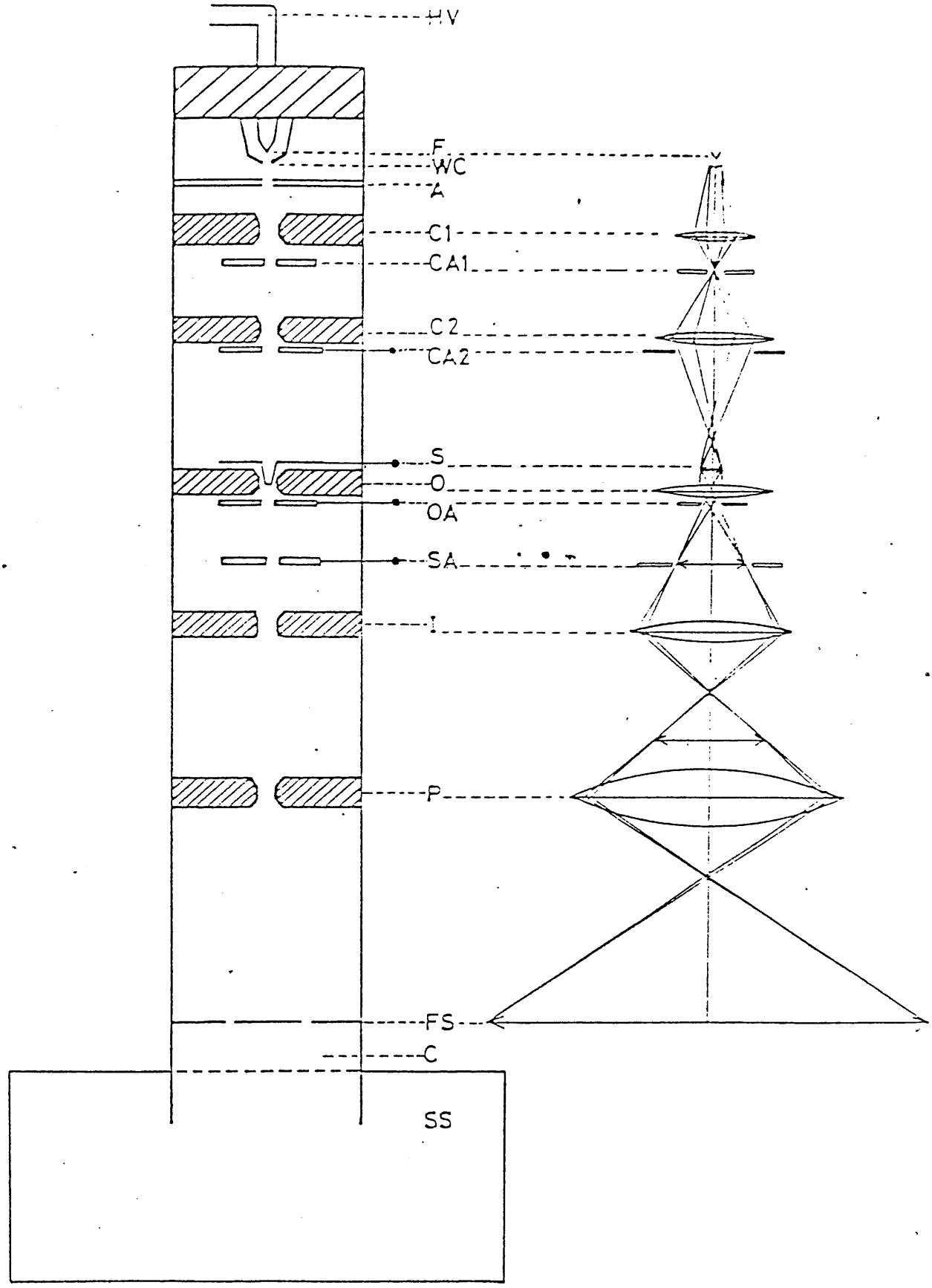

A

B

filaments (Wolf and Joy, 1971) or from lanthanum hexaboride single crystal Cathodes (Ahmed, 1971). Field emission cathodes (Crewe et al., 1968) can replace electrical heating with similar benefits.

A three lens system (objective, intermediate and projector) magnifies the electron image of the specimen, up to one million times, onto a fluorescent screen or an image intensifier screen (both used for viewing) or onto a photographic plate to record image detail.

The objective lens detects, transmits and magnifies the modified electron beam and therefore its performance is critical to overall microscope performance. Light microscopy employs a series of convergent and divergent lenses to compensate for individual lens defects. However the nature of electromagnetic lenses is always convergent and as such lens defects cannot be compensated for in the same manner. Electromagnetic condenser and objective lenses are fitted with astigmatism correction devices which control the current density of the lens and improve the electron optics which suffers from lens aberrations. High resolution TEM (transmission electron microscopy) requires an objective lens of extremely high quality. The intermediate and projector lenses, although less critical to overall microscope performance, transmit and further magnify the modified electrons from the objective lens.

The information recoverable from TEM is contained in the electrons scattered during passage through the specimen. The information desired is represented by perturbations in the electron waves. Electron optical defects can cause similar perturbations. However, if these are suppressed to a lower level than specimen perturbations then meaningful resolution may result, although interpretation can be complicated by lens aberration.

2.2 Image Formation and Contrast

The electron microscope is based on the interactions of fast electrons with the electrostatic potential of the specimen (coulomb interactions). The specimen is usually so thin that almost all the incident electrons pass through, and only those passing close to the atoms are deflected. (figure 2.2).

Image formation, in the transmission mode, can arise from recombination of scattered and transmitted electron waves, or by physical exclusion of scattered electrons. The two dominant mechanisms of electron scattering are:-

(i) ELASTIC SCATTERING - occurs when the electrons of the probe interact with the nuclei in the specimen and are deflected without loss of energy. The scattering angles are related, in crystalline specimens, to the geometry of the crystal lattice and to the electron wavelength by the Bragg Law.

(ii) INELASTIC SCATTERING - produced when the probe electrons interact with orbital electrons in the specimen and are deflected at reduced energy. Inelastic interactions with delocalised electrons in the specimen can give rise to collective oscillations of the whole system of conduction electrons. This effect is known as plasmon scattering (Pines, 1956; 1963).

Increasing atomic number, of the specimen nuclei, or increasing specimen thickness increases the elastic scattering of electrons. If scattering occurs at very large angles to the optical axis of the incident electron beam, or if an aperture is inserted such that electrons scattered greater than the aperture angle are cut out, then image contrast arises and is referred to as 'mass thickness' contrast or

amplitude contrast, or for a specimen with a defined periodic structure 'diffraction contrast'. In such cases, areas of the specimen from which elastically scattered electrons have been removed are dark in contrast. Diffraction contrast is sensitive to crystal orientation with respect to the incident beam.

Inelastic scattering results in small angle deflections to the electrons, altering their energies and hence their wavelengths. Recombination of these inelastic electrons with similarly altered unscattered electrons results in reinforced or diminished intensities in the image contrast, depending on the relative phases of the interacting waves. This is known as Inelastic Phase Contrast. Elastic phase contrast occurs, in the same way, by the interference between the transmitted beam and the elastically scattered electrons arise from periodic structure in the specimen (e.g., a crystalline specimen with at least one lattice plane orientated parallel to the beam direction) then a related periodicity in the image can be obtained. Such information can only be obtained for periodicities normal to the incident beam. Care must be taken in interpreting the observed lattice fringes at the position of the lattice planes in the specimen since the transfer of information from the object to the image plane, through the optical system, is subjected to phase modulations by lens aberrations and defect of focus as described by transfer theory (Cowley, 1975).

Scherzer (1949) considered the theoretical resolution limit of the TEM and derived a wave - mechanical formulation of image formation. Phase contrast effects in high resolution electron microscopy are generated as a result of the phase distortion function, $\mathrm{Sin}\chi$, due to any sort of wave abberation associated with the objective lens. For a perfect lens $\mathrm{Sin}\chi = 1$. The presence of wave abberations can be accounted for by an instrumental modulation factor χ is) where;

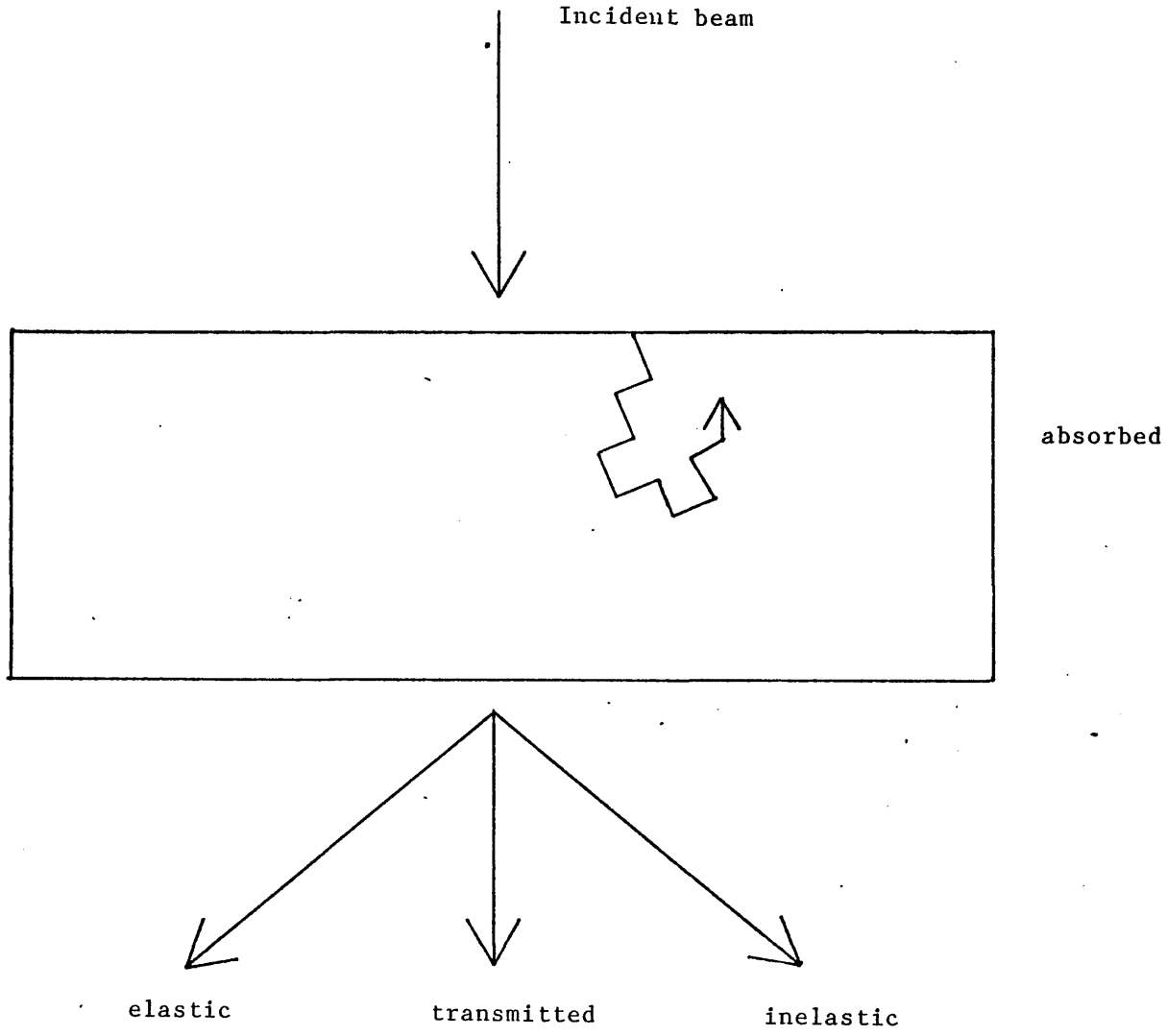

figure 2.2: Scattering of electrons on passing through a specimen.

amplitude contrast, or for a specimen with a defined periodic structure 'diffraction contrast'. In such cases, areas of the specimen from which elastically scattered electrons have been removed are dark in contrast. Diffraction contrast is sensitive to crystal orientation with respect to the incident beam.

Inelastic scattering results in small angle deflections to the electrons, altering their energies and hence their wavelengths. Recombination of these inelastic electrons with similarly altered unscattered electrons results in reinforced or diminished intensities in the image contrast, depending on the relative phases of the interacting waves. This is known as Inelastic Phase Contrast. Elastic Phase Contrast occurs, in the same way, by the interference between the transmitted beam and the elastically scattered beams that pass through the objective aperture. If the elastically scattered electrons arise from periodic structure in the specimen (e.g., a crystalline specimen with at least one lattice plane orientated parallel to the beam direction) then a related periodicity in the image can be obtained. Such information can only be obtained for periodicities normal to the incident beam. Care must be taken in interpreting the observed lattice fringes at the position of the lattice planes in the specimen since the transfer of information from the object to the image plane, through the optical system, is subjected to phase modulations by lens aberrations and defect of focus as described by transfer theory (Cowley, 1975).

Scherzer (1949) considered the theoretical resolution limit of the TEM and derived a wave - mechanical formulation of image formation. Phase contrast effects in high resolution electron microscopy are generated as a result of the phase distortion function, $\sin \chi$, due to any sort of wave aberration associated with the objective lens. For a perfect lens $\sin \chi = 1$. The presence of wave aberrations can be accounted for by an instrumental modulation factor $\chi(s)$ where:

$$\chi_{(s)} = \frac{2\pi}{\lambda}\left[\Delta f \frac{\alpha_{(s)}^2}{2} - C_s \frac{\alpha_{(s)}^4}{4}\right]$$

$\alpha(s)$ is the scattering angle for the diffracted beam.

C_s is the spherical, aberration constant of the objective lens.

Δf is the lens defocus value.

The function $\sin\chi(s)$ can be plotted against spatial frequency, giving the Phase Contrast Transfer Function (PCTF). This is a function of defocus, Δf, and spherical aberration, C_s. Figure 2.3 shows the PCTF of an optimized function for C_s = 0.7mm and a defocus, Δf = 600Å at 100KV (solid line). Spatial frequencies between A and B will appear in the reversed contrast to those in region BC. Frequencies corresponding to valves of $\sin\chi = 0$ will not be visible in the image. Structural imaging is limited by the Scherzer cut-off, at B. Therefore structural imaging would be expected for spacings > 2.86Å for a defocus of Δf = - 600A°. A change of defocus, for example Δf = - 200Å, gives a different function (dotted line).

In practice it is desirable to operate the microscope at a defocus value where the appropriate transfer function is identical and near unity over the maximum range of spatial frequencies, without contrast reversal. This 'optimum defocus' value Δf, first found by Scherzer (1949), is given by

$$\Delta f = 1.2\sqrt{C_s\lambda}$$

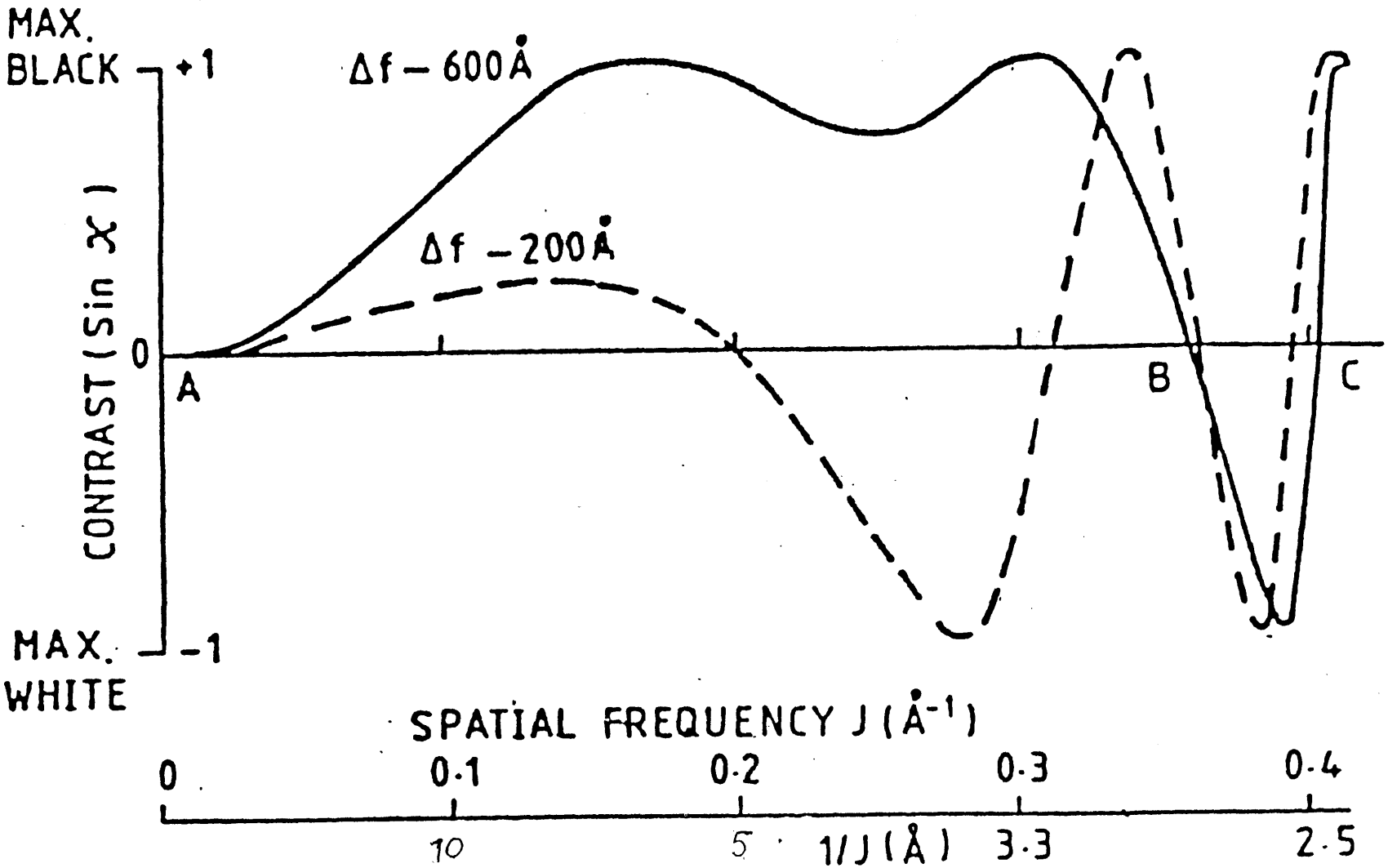

figure 2.3: Phase contract Transfer Functions for a range of defocus values, 4f = - 200Å and 600Å, with ~50 μm objective aperture cut-off.

For the JEOL 1200 EX, C_s = 2.3mm, and Δf = 100nm, at 120KV.

Full details of high resolution imaging methods are given by Spence (1981). Detailed mathematical treatment of dynamical theory of electron optics have been outlined by various authors (Cowley and Moodie, 1957; Lynch and O'Keefe 1972; Allpress et al., 1972; Goodman and Moodie, 1974; Cowley, 1975).

2.3 Limitations to High Resolution Information

2.3.1 Astigmatism

Information available from TEM is limited by the effect of astigmatism, most critical in the objective lens. Astigmatism arises from rotational variation in the focal length of the lens. This can be due to inaccuracies in manufacture, or induced by contamination within the microscope column causing distorting fields due to charging. The latter can be minimised by maintaining extreme cleanliness on all surfaces, especially apertures, which are exposed to the electron beam. Astigmatism is compensated by applying a compensating field, this is established when the grain of a carbon support film appears symmetrical, or a symmetrical Fresnel fringe is obtained around a hole in a 'holey' carbon film (Haine and Mulvey, 1954).

2.3.2 Specimen Stability

Electron beam irradiation will damage most specimen to same extent, and is prohibitive to the study of many organics of polymers in which it can lead to total loss of specimen structure (Holland et al., 1983).

To aid focus adjustment, with radiation sensitive specimens, image intensifiers have been used at low beam doses (English and Venables, 1971, 1972) and minimal exposure techniques have been developed (Williams and Fisher, 1970) so that the specimen is subjected to the electron beam for the duration of the photographic exposure only.

2.4 Electron Diffraction

Specimens with crystal planes parallel to the electron beam diffract electrons in accordance to Bragg's Law. The electron diffraction patterns are formed in the back focal plane of the objective lens (fig. 2.4). In the transmission mode the intermediate lens is focussed on the intermediate image, for electron diffraction the intermediate lens is focussed on the diffraction pattern and corresponding adjustment of the projector system magnifies this onto the final screen. A comparison of both imaging modes is shown by figure 2.5. The diffraction pattern from a small specimen area can be obtained by inserting a suitable aperture in the projector lens system. This is termed selected area electron diffraction (Andrews et al., 1968).

Figure 2.6 shows the construction of a diffraction pattern from a set of lattice planes, spacing d, at an angle θ to the incident electron beam. From this diagram:

$$\tan 2\theta = \frac{D}{2L} \quad \ldots\ldots\ldots 1$$

Where D = diameter of the diffraction pattern.

Using the Bragg Law for first order diffraction

$$\lambda = 2d \sin\theta \quad \ldots\ldots\ldots\ldots\ldots 2$$

Since θ is normally very small ($\theta < 3^{\circ}$)

$$\tan 2\theta \sim 2 \sin\theta \ldots\ldots\ldots 3$$

Using this approximation and combining equations 1 and 2.

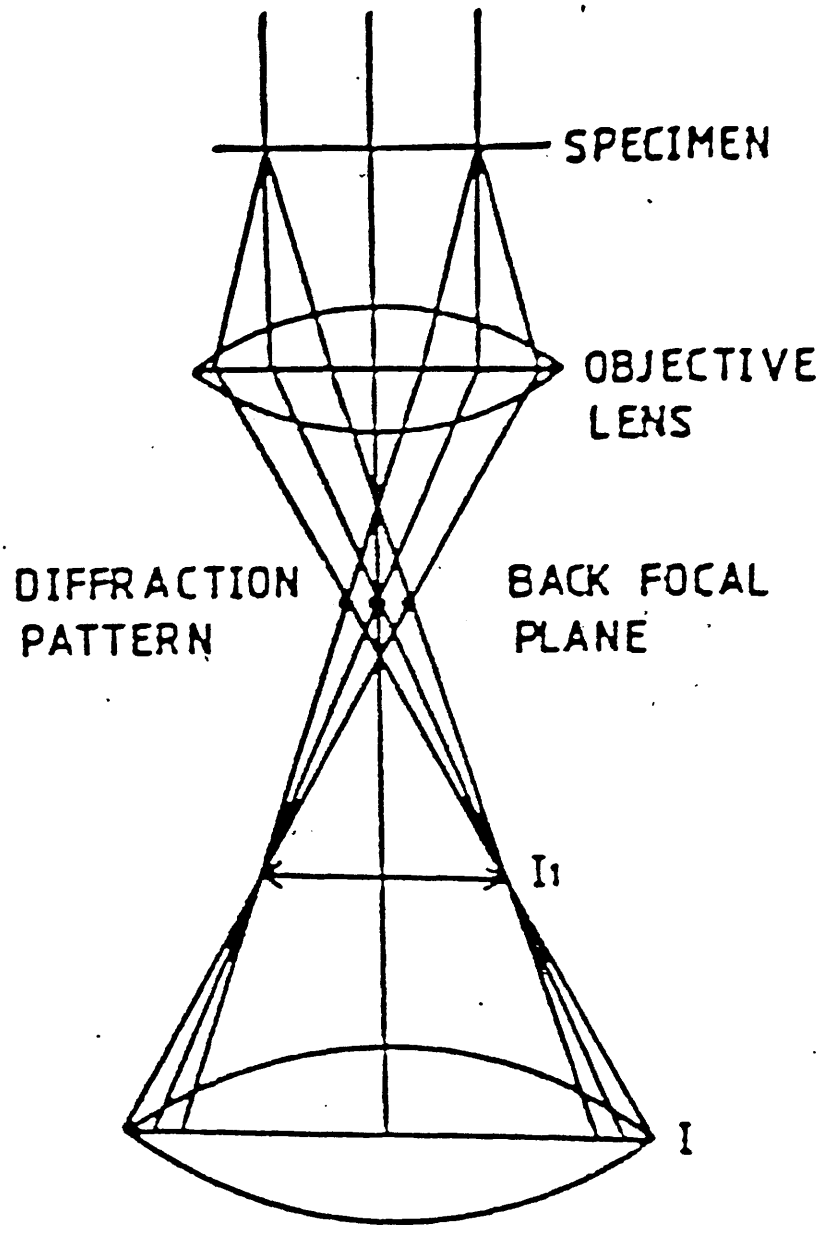

figure 2.4: Diffraction pattern and intermediate image (I_1) formation from a crystalline specimen. The intermediate lens (I) can be used to image either I_1 or the diffraction pattern.

Figure 2.5: Ray paths in the electron microscope for

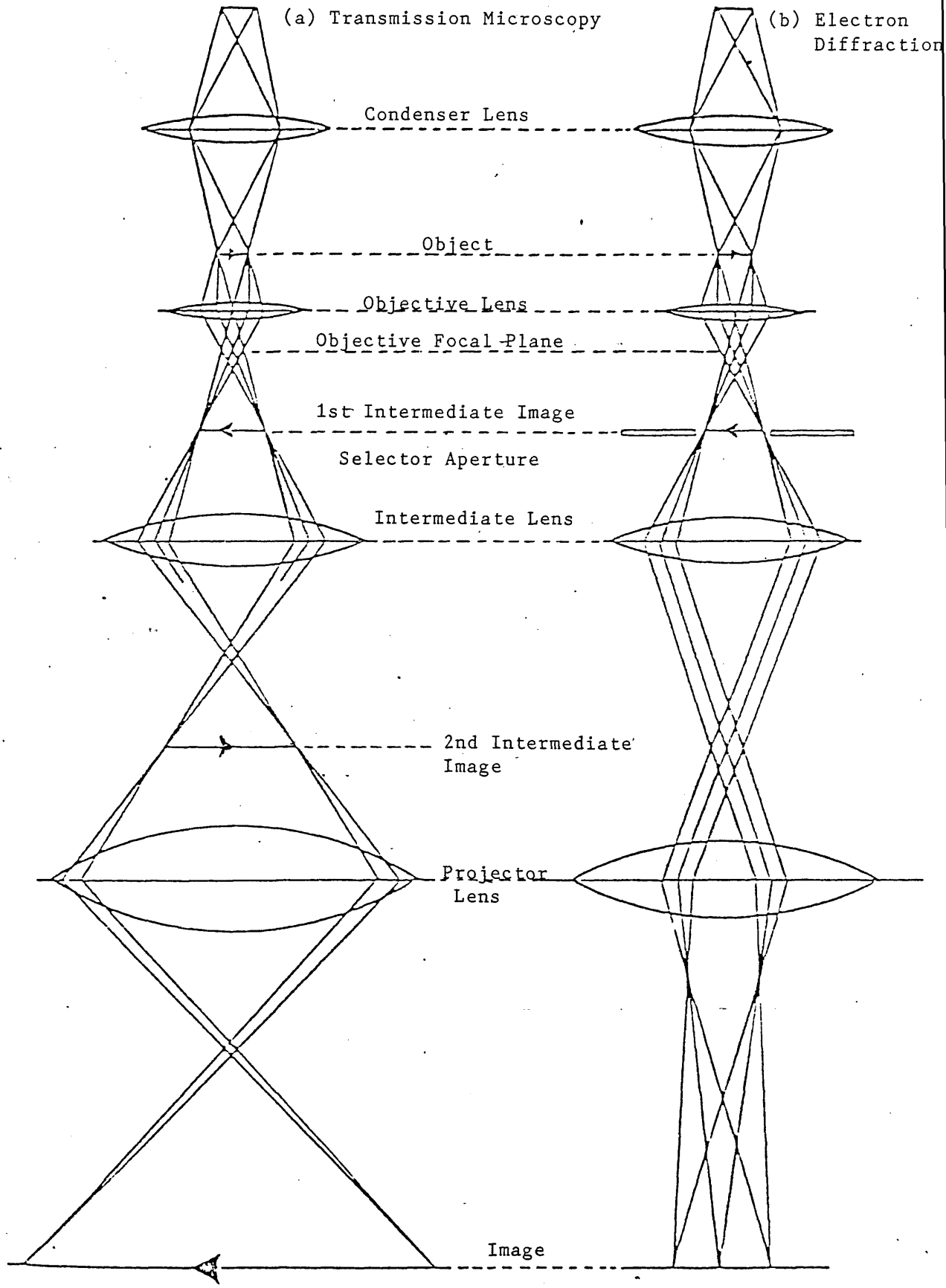

Figure 2.6: The electron microscope as simple diffraction camera.

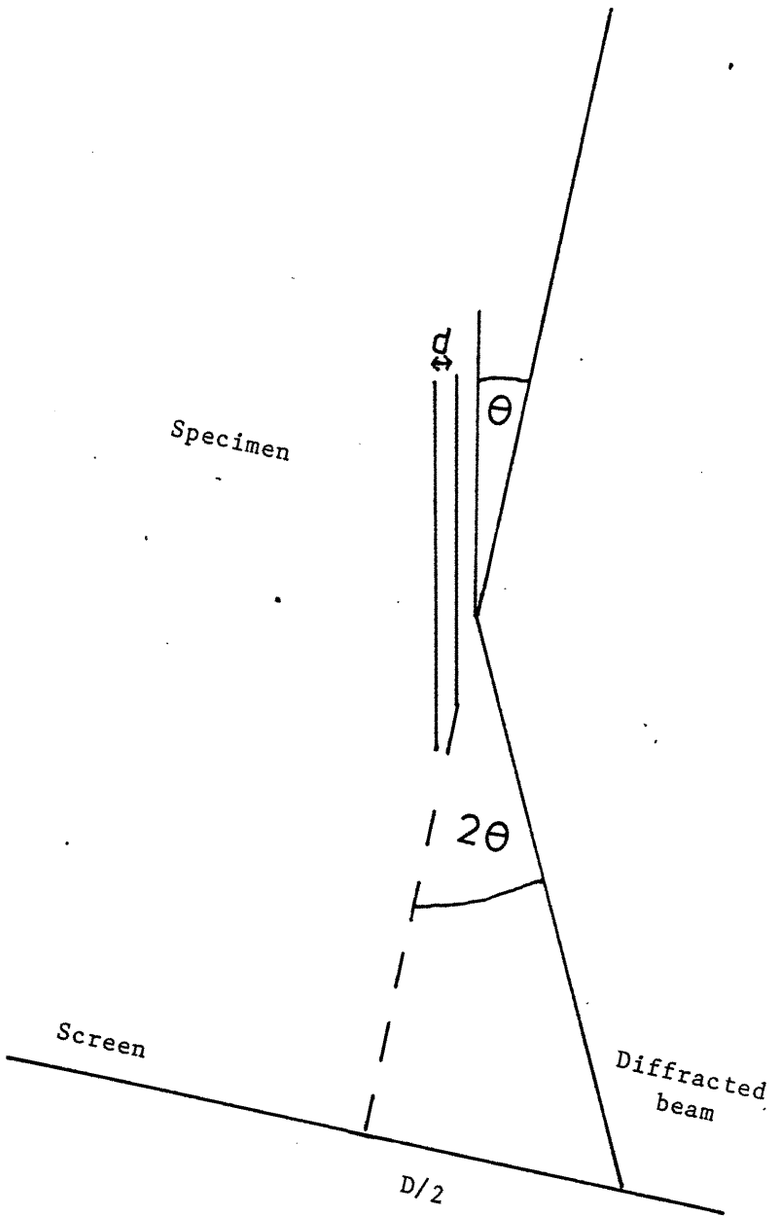

$$Dd = 2\lambda L = K \quad \ldots\ldots\ldots \quad 4$$

$2\lambda L$ is the camera constant, K, and is fixed by the operating conditions; λ is the electron wavelength and L the effective camera length, which is the equivalent distance between the diffraction plane and the final image, given by

$$L = f_o M_1 M_2 M_3 \quad \ldots\ldots\ldots \quad 5$$

where f_o is the focal length of the objective lens; M_1, M_2, M_3 are the magnification of the intermediate and projector lenses.

The camera constant can be determined using a standard of known d - spacings. Unknown diffraction patterns are identified by comparing spacings with tabulated X- ray data in the A.S.T.M. index (1965). Lattice spacings can be obtained with an accuracy of 1%, if care is taken in setting up the diffraction mode.

2.5 Optical Processing

Optical processing of micrographs can be used to measure lattice periodicities, the resolution limit of the microscope, and to detect astigmatism and specimen drift (Millward and Jefferson, 1978). An optical diffraction pattern (optical transform) is obtained from the micrograph on an optical bench, as shown in figure 2.7. The optical transform provides and intensity map of spatial frequencies pertaining to the optical density distribution on the micrograph, and therefore reflects the microscope transfer function at the time the micrograph was recorded. Spatial frequencies for which no information is contained in the micrograph ($\sin\chi(s) = 0$) appear dark in the optical transform and bright areas in the transform correspond to spatial frequencies for which contrast information was transferred to the

Figure 2.7: Schematic diagram of an Optical Diffractometer

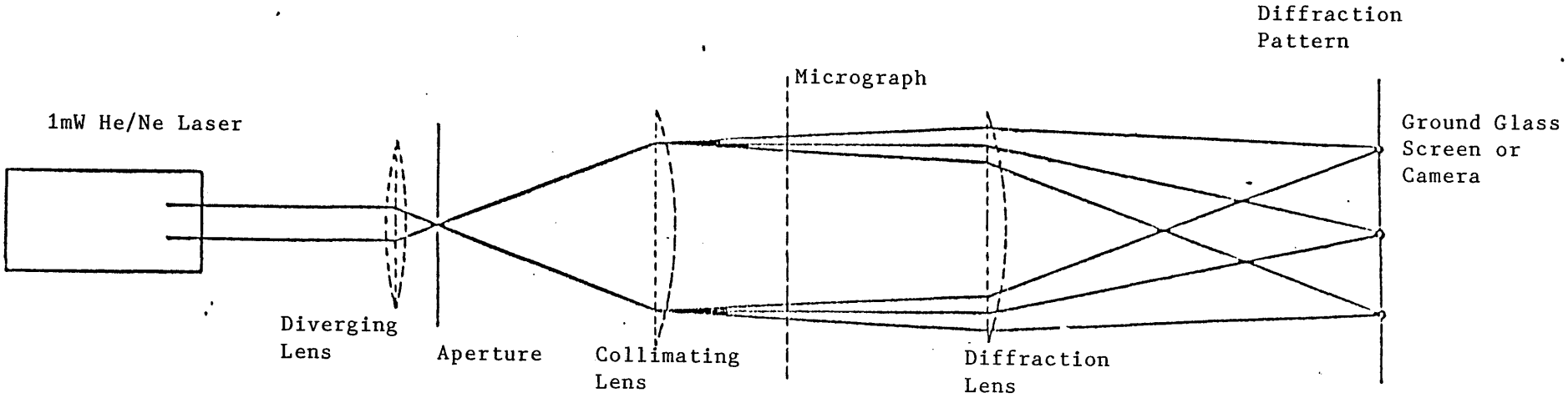

Figure 2.8: Schematic representation of Holow Cone Illumination

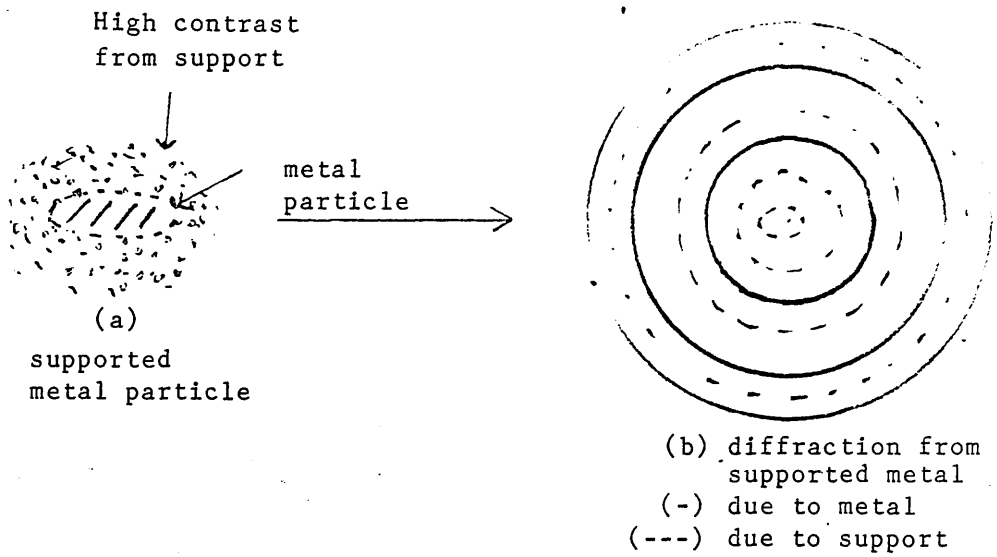

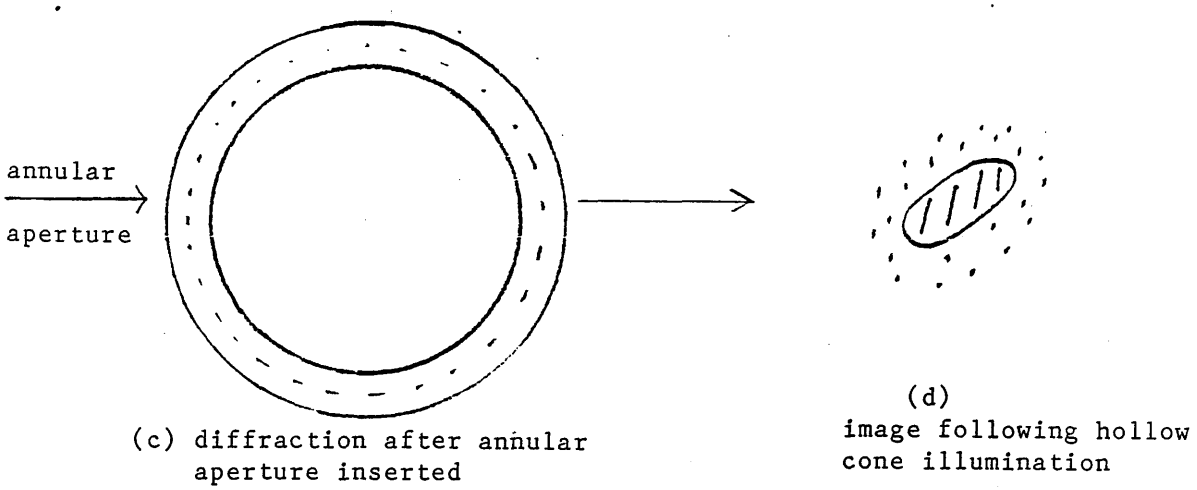

original micrograph ($0 \leq \sin\chi(s) \leq 1$, $0 \geq \sin\chi(s) \geq -1$).

Astigmatism leads to an eliptically shaped Fourier transform for the amorphous (carbon) support film as opposed to the circular pettern present for well corrected micrographs (Thon and Siegel, 1970). Specimen drift leads to loss of Fourier components in the direction of drift. Image filtering and reconstruction can also be carried out, although care must be taken to avoid artefacts (Fryer, 1979).

2.6 Hollow Cone Illumination

In supported metal catalysts the contrast from the support often inhibits the detection of small metal particles. The high contrast from the support can be reduced by using hollow cone illumination which is an annular dark field imaging technique. The principle of hollow cone illumination is that an annular aperture removes certain periodicities from the image. A basic schematic representation of hollow cone illumination is shown by figure 2.8. 2.8(a) shows a supported metal particle 2.8(b) is the diffraction pattern, if an annular aperture is inserted some periodicities from the support would be removed as shown (2.8(c). The image is then formed from 2.8(c) hence the high contrast from the support is removed and the metal particle can be more easily detected.

Freeman et al. (1977) used an annular condenser aperture to produce hollow cone illumination of alumina supported palladium particles. Varying the depth of the specimen in the objective lens field allows different Bragg reflections to be selected. In this way it is possible to pick up the major reflections of the supported crystallites. A second method is used, whereby an annular objective aperture is generated by electronic control of the deflection coils. (Heinemann and Poppa, 1970; Krakow and Howland, 1976). The advantages of hollow cone illumination

are outlined by Saxton et al. (1978).

3. Experimental

3.1 Catalyst Preparation

3.2 Ageing Regeneration Treatments

3.3 Electron Microscopy

3.4 Surface Area Measurements

3.5 Chemisorption

3.6 XRD

3.7 Micro-Reformer Runs

3.8 Neutron Activation Analysis

3.9 Te-staining

3.10 Stability of Pt (IV) O_2 in the Electron Beam

3. Experimental

3.1 Catalyst Preparation

50g of powdered Condea SB alumina was mixed with 10ml of 10% acetic acid and 5ml of deionised water in a mortar and pestle. 15g batches of the resultant paste were pelletised in a 3cm diameter press at 8000 psig; reground and sieved to obtain granules in the range 400 - 1000 μm in diameter. The granules were calcined at 650°C for 84 hours in air at 20l/Hour, ready for impregnation.

To achieve approximately 0.3wt % Pt on the support, 5g of H_2 Pt Cl_6 were dissolved in 25ml of deionised water. 2.2ml of solution were dissolved in 25ml deionised water with 0.5ml conc. HCl, filtered and made up to 50ml with deionised water. 2.2ml of solution were added to 47.5ml deionised water, plus 0.05ml conc. HCl and 25g of alumina granules were added and left to stand overnight. After decantation, the granules were dried at 110°C for 3 hours in air at 20 l/hour.

The calcined catalyst was reduced by the following treatment: cooled to 300°C, purged in N_2 at 2l/hour. Hydrogen at 2l/hour was then introduced at 300°C and the temperature increased to 460°C and held for 4 hours. The reduced sample was cooled to room temperature under flowing N_2.

Fresh catalyst samples were then subjected to various ageing and attempted regeneration treatments and then characterised by transmission electron microscopy, gas chemisorption and X-ray diffraction. Platinum and chlorine levels were determined by neutron activation analysis.

Three catalyst samples were prepared. Catalysts 1 and 2 have a platinum metal loading of 0.3 w|o Pt and catalyst 3 has a higher metal loading of 0.8 percent by weight platinum.

3.2 Ageing | Regeneration Treatments

One gram catalyst samples were packed into a stainless steel reactor tube (6mm diameter, 300mm long). The tube was fitted to a brass heating plate, placed between two insulated blocks, and heated under N_2 to the required temperature at a rate of 60°C rise per hour. Once the required temperature was achieved the gas flow was changed to 3% O_2 | N_2 at the required flow rate, and maintained for the chosen duration of the treatment. The samples were then cooled to room temperature under flowing N_2.

If required, the catalyst was reduced overnight at 460°C in flowing H_2 at 21|hour and then cooled to room temperature in N_2.

Table 3.1 lists the purities of the gases used in the ageing and regeneration treatments.

Table 3.1: Trade names and purities of the gases used in the ageing and regeneration cycles.

	Supplier	Purity
CCl_4	BDH	AnalaR
H_2	Air Products	High Purity
O_2	Air Products	High Purity
N_2	Laboratory Grade	(< 2ppm H_2O)

3.2.1 Ageing

Sintering of the fresh catalyst was achieved by the following treatment: 4 hours at 600°C in N_2, 3% O_2 in N_2 was introduced for 4 hours.

The sintered material was then reduced as described. The time of sintering was varied in a few experiments as indicated by table 3.2.

3.2.3 Oxychlorination Treatments

Redispersion of the sintered catalyst was attempted by various oxychlorination treatments at 480°C, using a carrier gas of 3% O_2 in N_2. A predetermined amount of CCl_4 was injected into the gas stream, as illustrated by figure 3.1.

As very small amounts of carbon tetrachloride (400 - 1400 ppm) are required, the CCl_4 has to be blended with N_2 and a portion of this blend injected into the gas stream. The blend is prepared as follows. A round bottomed flask, calibrated volume 5260ml, is first purged with N_2 and sealed. The calculated amount of CCl_4 (l) is vapourised, 100ml of the mixture is drawn into a 100ml syringe. The rate of injection is set so that all of the required CCl_4 is expelled in the period of the experiment.

The gas flow rate, rate of injection and the amount of CCl_4 required for injection are all dependent on the requirements of the experiment. For example to add 0.6 percent by weight (0.6 w/o) of chlorine to 1g of catalyst, the volume of CCl_4 required can be calculated as follows:-

Weight of chlorine required	= 0.006g Cl
Weight of CCl_4 required	= 0.0065g CCl_4
Density of CCl_4	= 1.595g /ml
Volume of CCl_4 (l) required for 100ml syringe	= 0.004ml
Volume of CCl_4 (l) required for 5260ml flask	= 0.21ml

Figure 3.1: Aparatus for oxychlorination treatments.

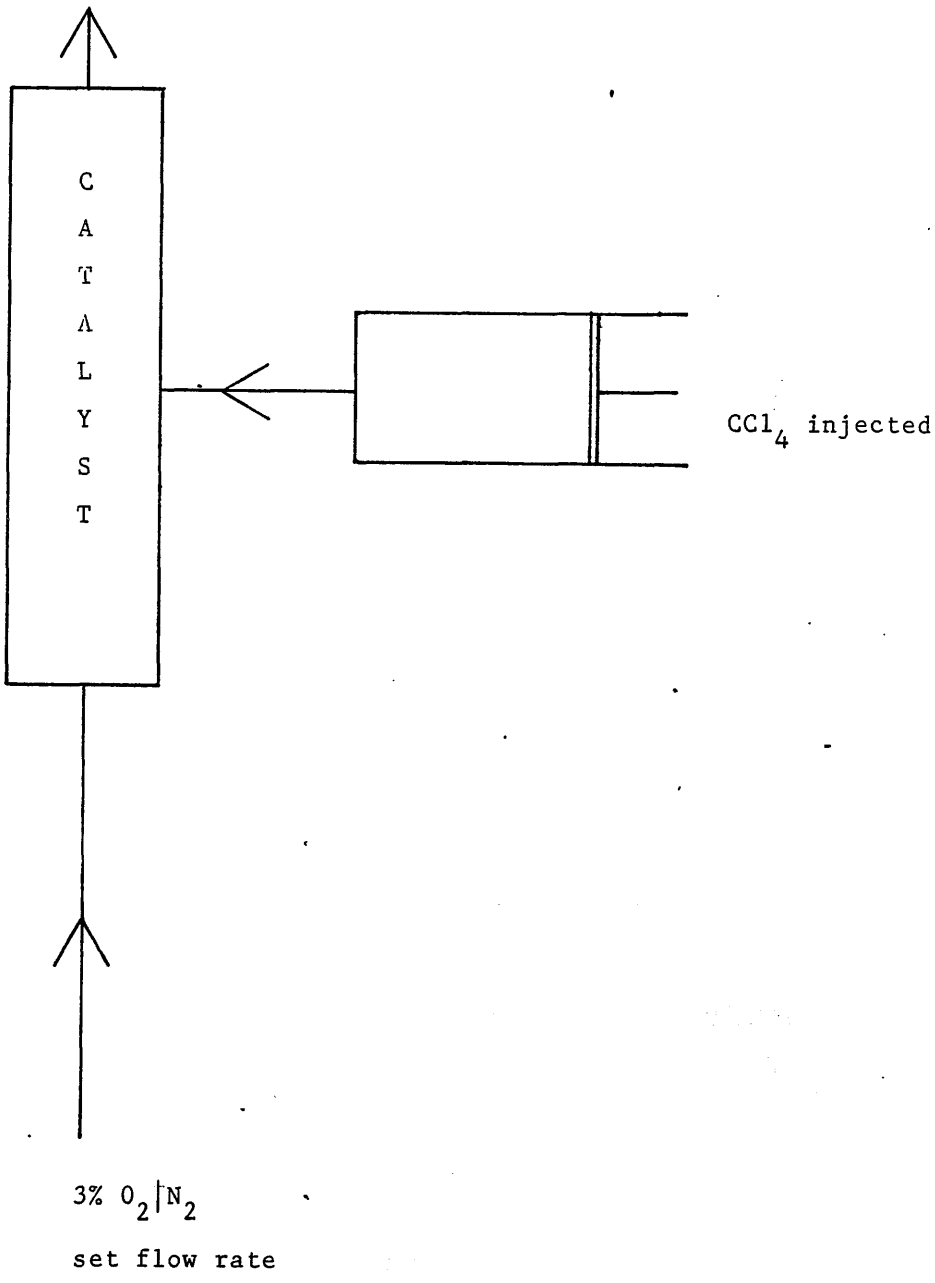

The flow rate for the reaction is calculated, depending on the desired Cl increase, CCl_4 concentration in the resultant gas stream, and the time for the reaction:-

Time of oxychlorination = 3 hours

Concentration of CCl_4 = 400 ppm

Volume of O_2 | N_2 required = 2425ml

Carrier gas flow rate = 0.81 l|h

The rate of injection of the CCl_4 | N_2 blend was 33.3ml|h for a 3 hour oxychlorination.

After oxychlorination the system was cooled under flowing N_2. The catalyst samples, where required, were reduced as described.

Table 3.2

Table of Ageing treatments on catalysts

	Time of Sinter	Catalyst
Sinter 1	4h	1
Sinter 2	4h	2
Sinter 3	2h	3
Sinter 4	4h	3

Table 3.3

Table of oxychlorination Treatments of Catalyst 1.

No.	Attempted W/o Cl increase	[CCL4] (ppm)	3% O_2/N_2 Gas flow rate (l/hour)	Time (hours)
1.1	0.6	400	0.81	3
1.2	-	-	0.85	3
1.3	1	400	1.40	3
1.4	2	400	2.80	3
1.5	0.6	800	0.39	3
1.6	0.6	1400	0.21	3
1.7	-	400	0.81	0.25
1.8	-	400	0.81	17

A. Catalyst 1 : 0.3w/o Pt Catalyst

All sintered catalysts have been treated as explained on page 54. (Sinter 1). All oxychlorination treatments have been carried out at 480°C and are tabulated in table 3.3.

(i) Standard Oxychlorination Treatment (Oxychlorination 1.1)

(1) Sintered Catalyst

Redispersion of a sintered catalyst was attempted by the following oxychlorination treatment. A gas flow of 3% O_2 in N_2 was passed over the catalyst with a flow rate of 0.81 h^{-1}. A 0.6 w/o Cl increase was attempted by injecting CCl_4 in N_2 into the gas stream to a concentration of 400 ppm CCl_4 in the gas flow. The time for oxychlorination was 3 hours, as tabulated in table 3.2.

(2) Fresh Catalyst

The standard oxychlorination treatment (oxychlorination 1.1) was repeated using a sample of fresh catalyst.

(3) Platinum Wire

Oxychlorination 1.1 was used to treat a piece of platinum wire (gauge 0.5mm).

(ii) Oxygen treatment of a sintered Catalyst

(Oxychlorination 1.2)

The O_2/N_2 gas flow was set up as with the standard oxychlorination. No CCl_4 was injected in this experiment. All other conditions of oxychlorination 1.1 were kept constant.

(iii) The Effect of A CCl_4 Increase to the Redispersion of a Sintered Catalyst.

The amount of CCl_4 injected into the gas stream was varied, maintaining a CCl_4 concentration of 400 ppm by controlling the gas flow of the 3% O_2/N_2. All other conditions of the standard oxychlorination (oxychlorination 1.1) were kept constant. A 1 w/o Cl increase was attempted by oxychlorination 1.3, and a 2 w/o Cl increase was attempted by oxychlorination 1.4. The conditions of the treatments are tabulated in table 3.3.

(iv) The Effect of the CCl_4 concentration to the Redispersion of a Sintered Catalyst.

Redispersion of sintered catalyst samples was attempted by oxychlorination 1.5 and 1.6. The treatments were carried out as described for oxychlorination 1.1, except that the concentration of CCl_4 in the gas stream was varied by the adjusting the carrier gas flow. In oxychlorination 1.5 the CCl_4 concentration was increased to 800 ppm, and with oxychlorination 1.6 a CCl_4 concentration of 1400 ppm was used, as indicated in table 3.3.

(v) The Effect of Time to the Redispersion of a Sintered Catalyst.

Oxychlorination 1.7

The reaction system was set up as described for oxychlorination 1.1, and stopped 15 minutes after commencement of the oxychlorination treatment. The sample was then cooled under flowing N_2 and then reduced as described.

Oxychlorination 1.8

The sintered catalyst was oxychlorinated for 17 hours. The carrier gas flow and the amount of CCl_4 injected per hour were as with oxychlorination 1. The CCl_4 injection was carried out in two 100ml syringes. For the first eight hours the first syringe was used to inject the CCl_4/N_2 blend into the gas stream, at an injection rate of 11.1 ml/h. The second syringe was used for the final 9 hours at the same injection rate.

After 17 hours the gas flow was changed to N_2 and the system cooled. After cooling the catalyst was reduced at 460°C overnight.

(vi) Oxychlorination of γ-Al_2O_3

Oxychlorination 1.6 was repeated using a 1g sample of γ- Alumina, in place of the catalyst sample.

B. Catalyst 2: 0.3 w/o Pt Catalyst

The fresh catalyst was aged by sinter 2 (Table 3.2). All oxychlorination treatments were carried out at 480°. The carrier gas flow rate and the amount of CCl_4 added per hour were kept constant throughout all of the experiments. All reductions were carried out in flowing H_2 at 460° overnight, then cooled to room temperature in flowing N_2.

(i) Oxychlorination 2.1

Regeneration of the sintered catalyst was attempted by the following oxychlorination treatment. (as with oxychlorination 1.3). A carrier gas of 3% O_2/N_2 was passed over 1g of sintered catalyst at a flow rate of 1.4l/h, for 3 hours. CCl_4 was injected into the carrier gas giving a concentration of 400 ppm CCl_4 in the resulting gas stream, via 100ml of a CCl_4/N_2 blend containing 1.69 vol % CCl_4. The blend was prepared by injecting 0.36ml of CCl_4 (l) into a N_2 filled 5260ml flask and withdrawing a 100ml portion, which was then injected into the carrier gas at a rate of 33.3ml/h. The catalyst was then cooled to room temperature under flowing N_2 and reduced.

(ii) Oxychlorination - Reduction Cycles.

(Oxychlorinations 2.2, 2.3)

"Pulse oxychlorination" treatments were carried out on the sintered catalyst, by short oxychlorination treatments, followed by reduction. The system was set up as for oxychlorination 2.1 and all conditions were maintained. The oxychlorination was stopped after 30 minutes, the gas flow changed to N_2 and the catalyst cooled to room temperature. The catalyst was then reduced in the usual manner. After reduction oxychlorination was continued for a further 30 minutes, cooled under N_2 and reduced. The oxychlorination - reduction cycles were continued, in this manner, the required number of times. Details of "pulse" oxychlorinations are given in table 3.4

C. Catalyst 3: 0.8 w/o Pt Catalyst

(i) Oxychlorination of a 2 hour Sintered Catalyst

Oxychlorination 3.1

The catalyst was sintered as described on page 54 (sinter 3, Table 3.2). Redispersion was attempted by a 3h oxychlorination treatment, conditions of the treatment were as described by oxychlorinations 1.3 and 2.1.

TABLE 3.4

Details of oxychlorination treatments on catalyst 2.

No.	$[CCl_4]$	Carrier gas flow Rate (l/h).	CCl_4 injection Rate (ml/h)	No. of Cycles *	Total Oxychlorination time (h)
2.1	400	1.4	33.3	-	3
2.2	400	1.4	33.3	6	3
2.3	400	1.4	33.3	10	5

* No. of cycles = No. of 30 minute oxychlorination treatments followed by reduction.

(ii) Oxychlorination of a 4 hour Sintered Catalyst

Oxychlorinations 3.2, 3.3 and 3.4

The catalyst was sintered as described on page 54 (sinter 4, Table 3.2).

The aim of the following experiments was to find how Pt redispersion varies with the time taken for an oxychlorination treatment. The carrier gas flow rate was maintained at 1.4 l/h. The amount of CCl_4 injected into the carrier gas per hour was maintained by increasing the concentration of CCl_4 in the CCl_4/N_2 blend and adjusting the injection rate for the required time. (Table 3.5). For the 18 hour treatment (oxychlorination 3.4) two 100ml syringes were used, one for the first 9h of treatment and the second for the next 9h. The concentration of CCl_4 in the resultant gas flow was 400 ppm CCl_4 for all three treatments. The temperature for oxychlorination was 480°C. Oxychlorination 3.2 was carried out in the same way as oxychlorination 3.1.

The treatments were carried out over three times, 3 hours (oxychlorination 3.2); 9 hours (oxychlorination 3.3) and 18 hours (oxychlorination 3.4). Details of all three treatments are tabulated in table 3.5.

TABLE 3.5

Conditions for regeneration treatments on catalyst 3.

No.	Time(h)	Vol % CCl_4 in blend	CCl_4/N_2 injection rate (ml/h)
3.1	3	1.69	33.3
3.2	3	1.69	33.3
3.3	9	5.07	11.1
3.4*	18	5.07	11.1

* 2 syringes used for injection.

3.3 Electron Microscopy

3.3.1 Transmission Electron Microscopy (TEM.

The catalyst samples were characterised at each stage by transmission electron microscopy (TEM). Samples (catalyst samples, alumina, platinum (IV) oxide), were prepared for analysis as follows: The catalyst was crushed to a fine powder, in an agate mortar and pestle. A small amount of this powder was then placed in a micro test tube and suspended in de-ionised water. A slurry of the 'catalyst' / water mixture was then withdrawn from the test tube using a finely drawn Pasteur pipette and a drop placed on a carbon-coated copper electron micrscope grid. The microscope grids were then allowed to dry at around 30°C, in a laboratory oven, before transfer to the microscope.

Samples were run on a JEOL 1200 EX electron micrscope, operated at an accelerating voltage of 120KeV. The microscope was fitted with a lanthanum hexaboride ($La B_6$) pointed filament to increase the coherence of the electron beam. The microscope was also fitted with an image intensifier system to aid in viewing specimens. The images were recorded on photographic plate film (Ilford EM film).

Some specimens were also run on the Cambridge University 600 KeV Microscope (Nixon et al., 1977; Cosslett, 1980; Smith et al., 1983) in order to gain some high resolution information.

Particle size distributions are presented as histograms, determined from diameter measurements of between 100 and 400 particles per catalyst.

When catalysts had small particles, particle diameters were measured from photographic enlargements of high resolution micrographs; larger particle diameters were mainly measured directly from negatives. The mean of the longest and shortest diameters was taken for irregularly shaped particles.

The normal statistical formulae were used to calculate the mean diameter, $\bar{d}$, and the variance on the mean, σ, for counts of n particles, each of diameter d:-

$$\bar{d} = \frac{\Sigma d}{n}$$

$$\sigma = \sqrt{\frac{\Sigma(\bar{d} - d)^2}{n}}$$

3.3.2 Hollow Cone Illumination

A thin film of γ-alumina was prepared by vacuum evaporation of Condea alumina. Model Pt/ γ- Al_2O_3 catalysts were then prepared by vacuum evaporation of platinum wire onto a thin film of γ-alumina. The model catalysts and a thin film of alumina were studied by axial and hollow cone illumination at the Fritz - Haber Institut der Max - Planck - Gesellschaft, Berlin, using the Deeko 100 electron microscope.

3.3.3 Scanning Electron Micrscopy (SEM)

Platinum wire, before and after an oxychlorination treatment, were studied by SEM. A Philips PSEM 500 B microscope was used, operated at an accelerating voltage of 30 KeV. The scanning micrscope was fitted with an Energy Dispersive X-ray Analysis system, which was used to determine the relative amounts of chlorine in the two wire samples.

Samples were prepared by mounting the platinum wire on aluminium stub spindles using silver dag paint.

3.3.4 Scanning Transmission Electron Microscopy (STEM)

The HB5 Scanning Transmission electron microscope with an energy dispersive X-ray analysis system was used, operated at 100kV. Samples for STEM were prepared as for TEM.

3.4 Surface Area Measurements

Surface area measurements on alumina samples were determined using the Micromeritics High Speed Surface Area Analyser, Model 2200.

3.5 Chemisorption

3.5.1 H_2 Chemisorption

Catalyst samples were first reduced in flowing hydrogen, transferred to the Micromeritics Digisorb 2500, reduced at 400°C in 200 torr static H_2 for 2.5 hours followed by evacuation at 400°C for 4 hours. An adsorption isotherm was measured at four pressures from 100-260 torr. The monolayer volume (V_m) was derived by extrapolation to zero pressure. The H: Pt ratio was taken as 1.1. A simple spherical particle geometry was assumed and, on this basis, mean particle diameters were calculated (d_{calc}), from the following algorithm:-

$$A = 3.4Vm$$

$$A^1 = \frac{3.4Vm.100}{W}$$

$$\overline{d}calc = \frac{6 \times 104}{\rho_{Pt} \cdot A^1}$$

Where V_m = Monolayer volume of chemisorbed hydrogen

W = Catalyst Pt loading (weight percent).

ρ_{Pt} = Density of platinum.

A = Surface Area per g of catalyst

A^1 = Surface Area per g of platinum.

3.5.2 CO Pulse Chemisorption

The micromeritics Digisorb 2500 was used for CO Chemisorption.

The following method was used:

1. Dry catalyst at 100°C in air, 2hr at 100°C.
2. Calcine for 2 hr at 500°C, in air.
3. Cool to 25°C, in air.
4. Purge in He, 4l/hr, 1 hr.
5. Reduce to 500°C, 2 hr at 500°C, (5°C/min) in 5% H_2 in Ar
6. Purge at 500°C in He, 4l/hr, 2 hr.
7. Cool to 25°C.
8. Pulse at 25°C in He carrier gas at 200ml/hr (20ul pulses).

The surface areas measured from CO adsorption are used to find mean platinum particle diameters. The CO: Pt ratio is taken as 1:1. A simple spherical particle geometry is assumed and the algorithm on page 70 used to calculate the mean platinum particle size.

3.6 X-ray Diffraction Line Broadening Analysis (XRD)

X-ray diffraction line broadening analysis was carried out on γ-alumina and selected catalyst samples. A Philips TW1730 X-ray diffractometer was used. Platinum sizes were calculated by measuring the line broadening of the Pt (311) diffraction line.

Quantitative X-ray diffraction, to determine the amount of platinum being detected by the diffractometer, was carried out by comparing the size of the Pt (311) peak to those of standard samples. Two standard samples of known platinum content were used. The standards were sintered so that all of the platinum was detectable by XRD. Standard 1 contained 0.73 percent by weight platinum, and standard 2,1.66 percent by weight platinum. The standards were prepared by mixing platinum black with Condea alumina.

Due to the small amounts of catalyst sample available for XRD, the samples were prepared on SiO_2 coated Al sample holders. The SiO_2 is orientated in such a way as to be transparent to the X-ray beam. The catalyst was ground in an agate mortar and pestal. To maximise the amount of sample, on the sample holder, the powder was then suspended in ethanol and dropped onto the sample holder.

3.7 Micro-Reformer Runs

Experiments were carried out in a lab-scale micro-reformer to test the catalytic activity in a reforming process.
A naphtha feed was used initially to compare the activity to standard results to ensure that the catalyst behaves as a reforming catalyst. n-Heptane was then used as the feed to compare fresh, sintered and oxychlorinated catalysts, as information is obtained on aromatic conversion. Four catalysts were tested, as listed below.

(a) Catalyst 3, fresh

(b) Catalyst 3 following 4h sinter (sinter 3.2)

(c) Catalyst 3, sinter 4h, oxychlorination 9h (oxychlorination 3.3).

(d) Catalyst 3, sinter 4h, oxychlorination 18h (oxychlorination 3.4).

The catalyst charge of 0.25g catalyst (400-800 um) was placed in the micro-reformer. The catalyst was heated to 400°C in H_2 at a rate of 1°/min, with a H_2 flow rate of 6ml/min.

The H_2 rate was the increased to 13ml/min and the naphtha feed introduced with a weight hourly space velocity (WHSV) of $2.5h^{-1}$, under a pressure of 300 psig. The H_2 : hydrocarbon ratio was 6:1. The temperature was then increased to 480°C. The naphtha yield was recorded at four hourly intervals to check the stability of the catalyst.

The temperature was increased to 500°C for 3 days and the stability recorded every four hours. The temperature was then reduced to 480°C for a further 3 days and the stability of the catalyst recorded.

The temperature was then increased to 500°C and the n-heptane passed over the catalyst in place of the naphtha feed. The yield was recorded at four hourly intervals for 210 - 280 hours.

3.8 Neutron Activation Analysis

Platinum and chlorine concentrations were determined by neutron activation analysis. Irradiation of the samples was carried out at the Scottish Universities Research and Reactor Centre. γ - decay spectra were obtained by monitoring the γ- decay with a Ge (Li) detector. Platinum and chlorine levels were calculated from the γ- spectra by comparison to a standard sample, of known platinum and chlorine contents, irradiated at the same time as the unknown catalyst sample.

3.9 Te - Staining

3.9.1

Samples of catalyst 1 fresh, Catalyst 1 sintered (Sinter 1, table 3.1) and alumina were prepared for electron microscopy as explained in section 3.3.1.

The above samples, together with a carbon-coated copper specimen grid, were treated with di ethyltellurium (Et_2 Te) as follows:-

A portion of Et_2 Te was diluted with ethanol in a small beaker, the microscope grids were placed in the solution, after 2 minutes the grids were removed, placed in a vacuum descicator and dried under vacuum for 10 minutes. The samples were then examined by transmission electron microscopy. Elemental analysis of the treated samples was carried out using energy dispersive X-ray analysis.

3.9.2

An untreated sample of catalyst 3 was prepared for electron microscopy as explained in section 3.3.1.

A portion of Et_2 Te was diluted in ethanol and allowed to vapourise over the sample for 5 minutes (as shown in figure 3.2). The grid was removed, placed in a vacuum desiccator and vacuum dried for 10 minutes. The sample was then examined by transmission electron microscopy. Elemental analysis was carried on a HB5 STEM fitted with energy dispersive X-ray analysis.

Figure 3.2: Diagram showing how Et_2Te was vapourised over the catalyst sample

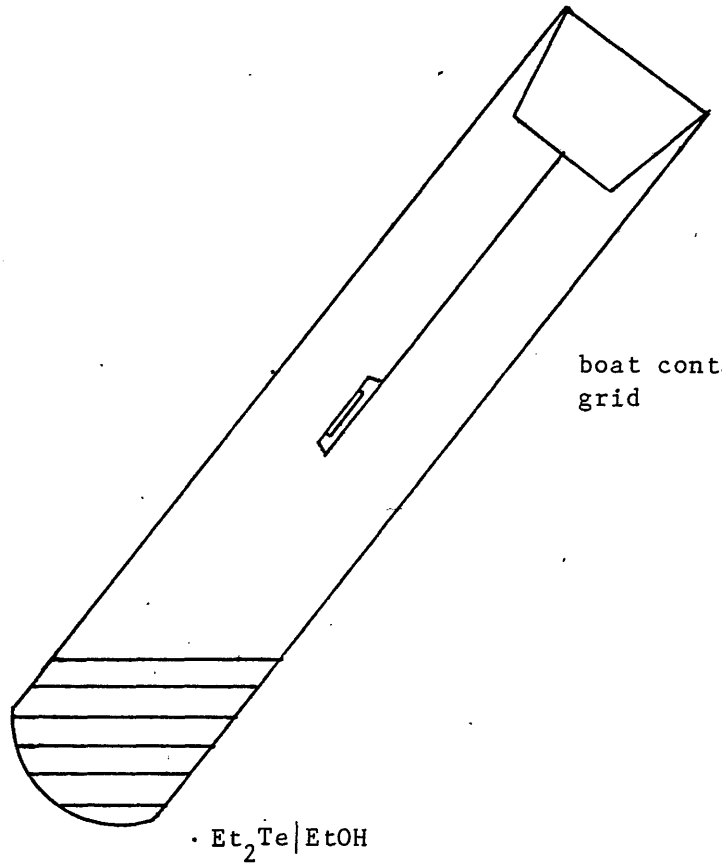

3.10 Stability of Pt (IV) oxide in the Electron Beam

A sample of Pt (IV) oxide (PtO_2) was prepared for study in the electron microscope, as explained on page 66. The stability of PtO_2 in the electron beam was studied by recording the diffraction pattern of the oxide, over a period of time.

4. Results: Identification of Small Platinum Particles

4.1 Hollow Cone Illumination

4.2 Tellurium Staining

4.3 High Resolution Electron Microscopy

4 Results: Identification of Small Pt Particles

4.1 Hollow Cone Illumination

A thin film of alumina was studied by axial and hollow cone illumination. The results show that the contrast is reduced using hollow cone conditions. Platinum particles evaporated on to the alumina films were then examined by axial and hollow cone illumination and the advantages and disadvantages of the hollow cone method noted.

Plates 1(a) and 1(b) show the same area using axial and hollow cone illumination respectively. Examination of the two micrographs shows that the background granularity is reduced by using hollow cone illumination. Particles A, B, E and F are difficult to detect in plate 1(a), removing the contrast by inserting an anular aperture (plate 1(b)), makes the resolution of these particles possible. The edges of all particles are more clearly defined using hollow cone illumination (plate 1(b)).

A second area is shown by axial (plate 2(a)) and hollow cone (plate 2(b)) illumination. 1.9Å Pt lattice periodicities have been resolved on particles A and B using axial illumination (plate 2(a)). This high resolution information is lost using hollow cone illumination, as shown by plate 2(b). Areas C, D and E are difficult to identify using axial illumination and are more defined using the hollow cone method.

No differences were observed in the relative positions of particles between the two methods. No change in particle size was observed by using an annular aperture. The hollow cone method was able to resolve 20Å particles (e.g. particle A, plate 1(b); particle E, plate 2(b)), which are difficult to resolve by axial illumination due to the contrast from the alumina support.

Plate 1

Platinum particles on an alumina support.

(a) Axial Illumination

X 4.7 M

(b) Hollow Cone Illumination.

X 4.7 M

B
E
A
D
C
F
B
E
A
D
C

Plate 2

Platinum particles on an alumina support.

(a) Axial Illumination

X 4.7·M

(b) Hollow Cone Illumination

X 4.7·M

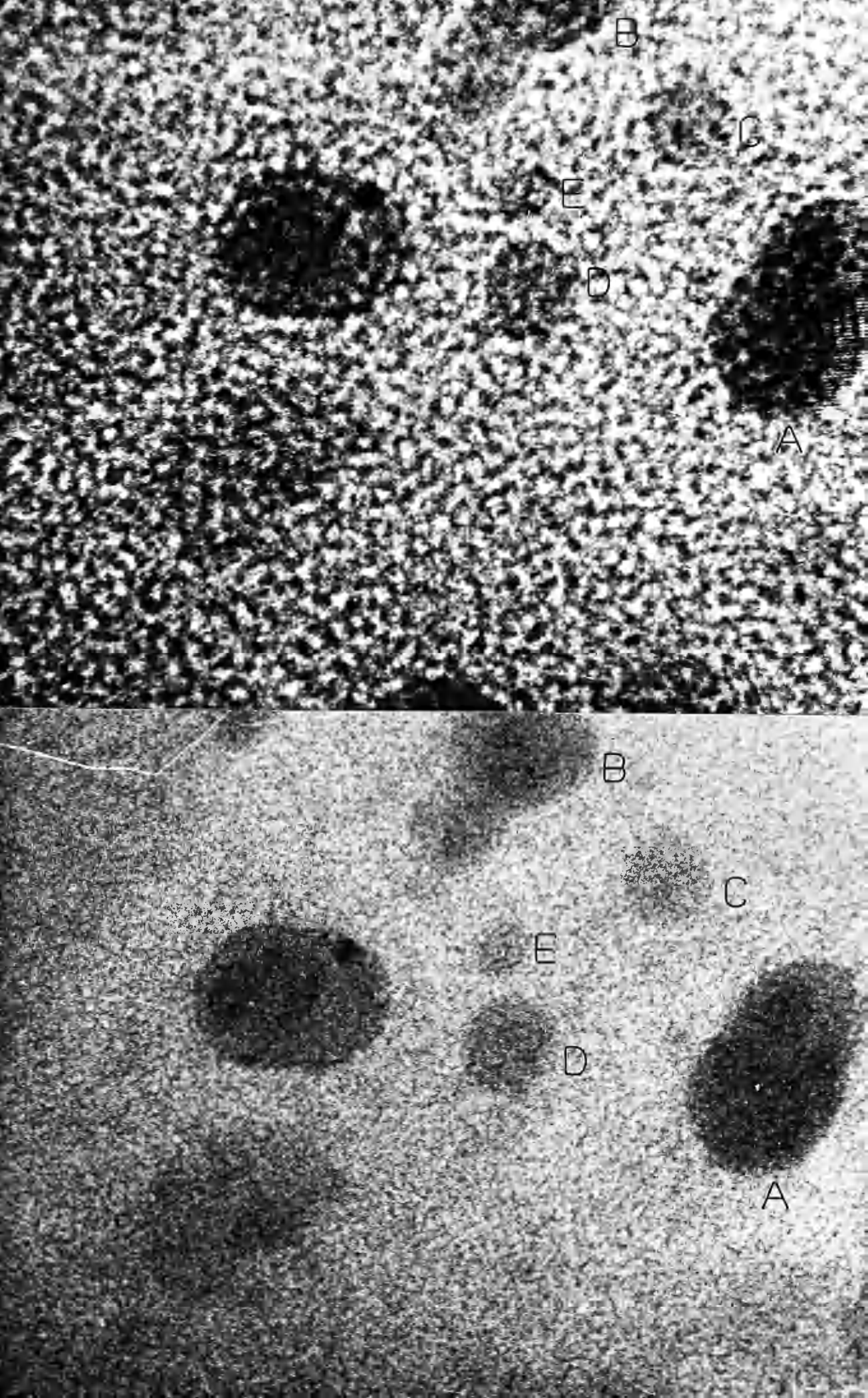
B
C
E
D
A
B
C
E
D
A

4.2 Tellurium Staining

Diethyl tellurium (Et_2 Te) diluted in ethanol (EtOH) was used for the attempted "stainings". In the first experiment the samples were placed into the solution as described by section 3.9.1. As a check that the tellurium compound did not combine with the alumina or the carbon film used coat electron microscope specimen grids, a γ- alumina specimen and a carbon-coated microscope specimen grid were treated in the same way as the catalyst samples. Transmission electron microscopy showed that an amorphous material was deposited onto the carbon support (plate 3). X-ray elemental analysis showed that Te could be detected on carbon film, γ- alumina and on the catalyst samples. No enhanced Te concentration was found where platinum was detected. It was apparent that the Te was too concentrated, in this experiment, to selectively combine with the platinum.

The experiment was repeated allowing the Te to vapourise over a catalyst sample (section 3.9.2). Again an amorphous material was deposited on the carbon film and no enhancement in the Te concentration found at platinum particles. Plate 4(a) shows an amorphous material, deposited after Te treatment. After a few minutes under the electron beam the material is damaged, as shown by plate 4(b). Following changes in the diffraction pattern (inserts a, b and c) it can be seen that the initially amorphous material becomes more crystalline with radiation damage.

Plate 3

Amorphous deposit on carbon-film following an attempted Te-stain.

X 182,000

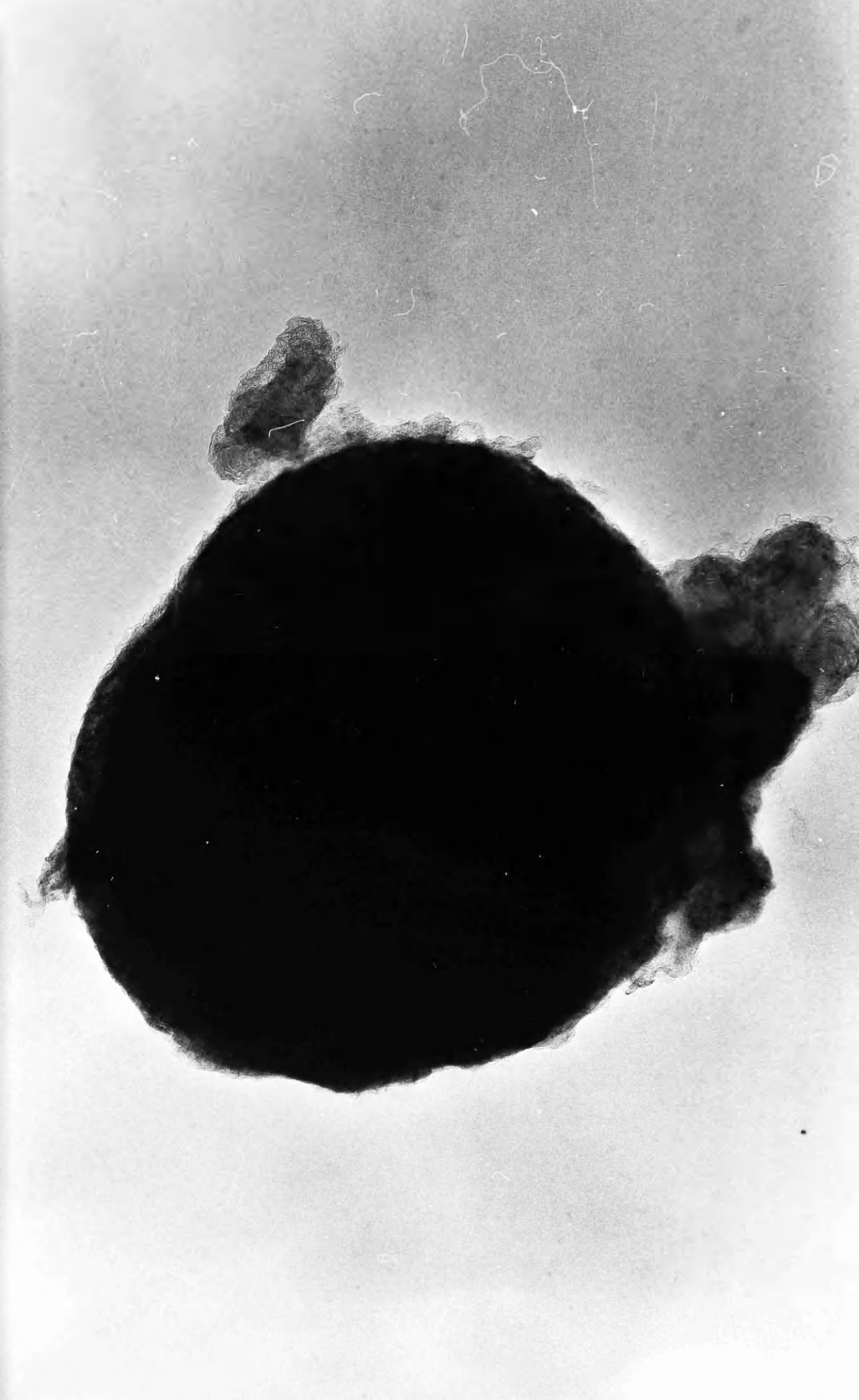

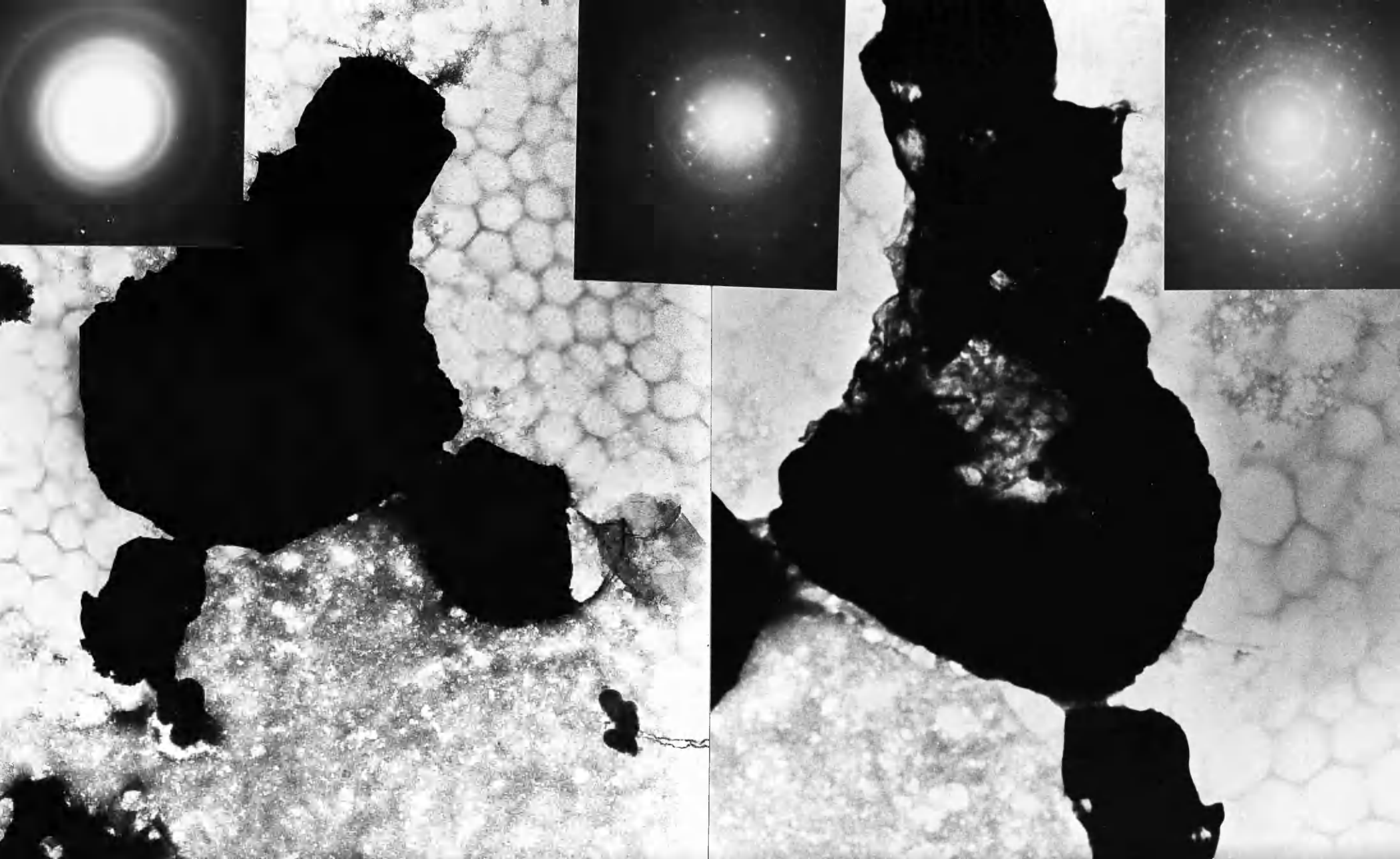

4.3 High Resolution Electron Microscopy

High resolution electron microscopy has been used in an attempt to resolve small platinum particles. Taking care in sample preparation, making the alumina as thin as possible, and with careful imaging conditions, sub - 10Å platinum particles can be resolved, as shown by plates 5 and 6, if the platinum is in the correct orientation.

The resolution of some sub - 10Å particles proves that platinum exists in this form, however this technique is not quantitative and only a fraction of the platinum in this form is resolved.

Plate 5(a)

Sub - 10Å platinum particles on the alumina support, C1 following oxychlorination 1.1.

X 2.43 M

Plate 5(b)

Sub - 10Å platinum particles. C3 following oxychlorination for 9 hours.

X 2.43M

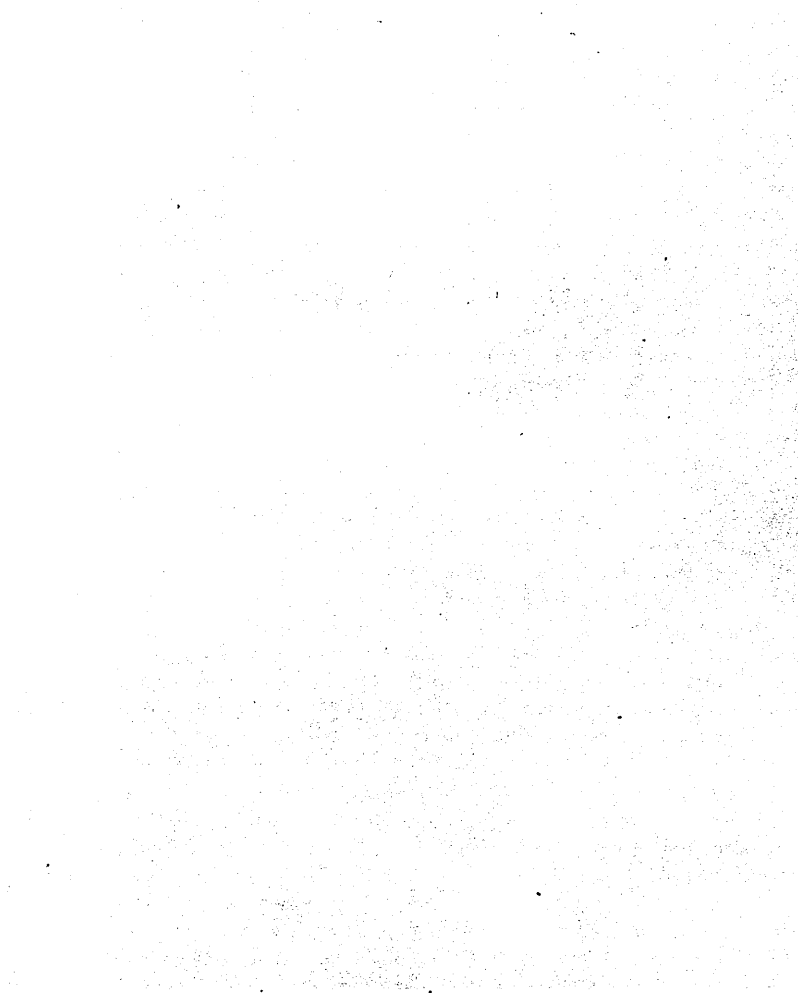

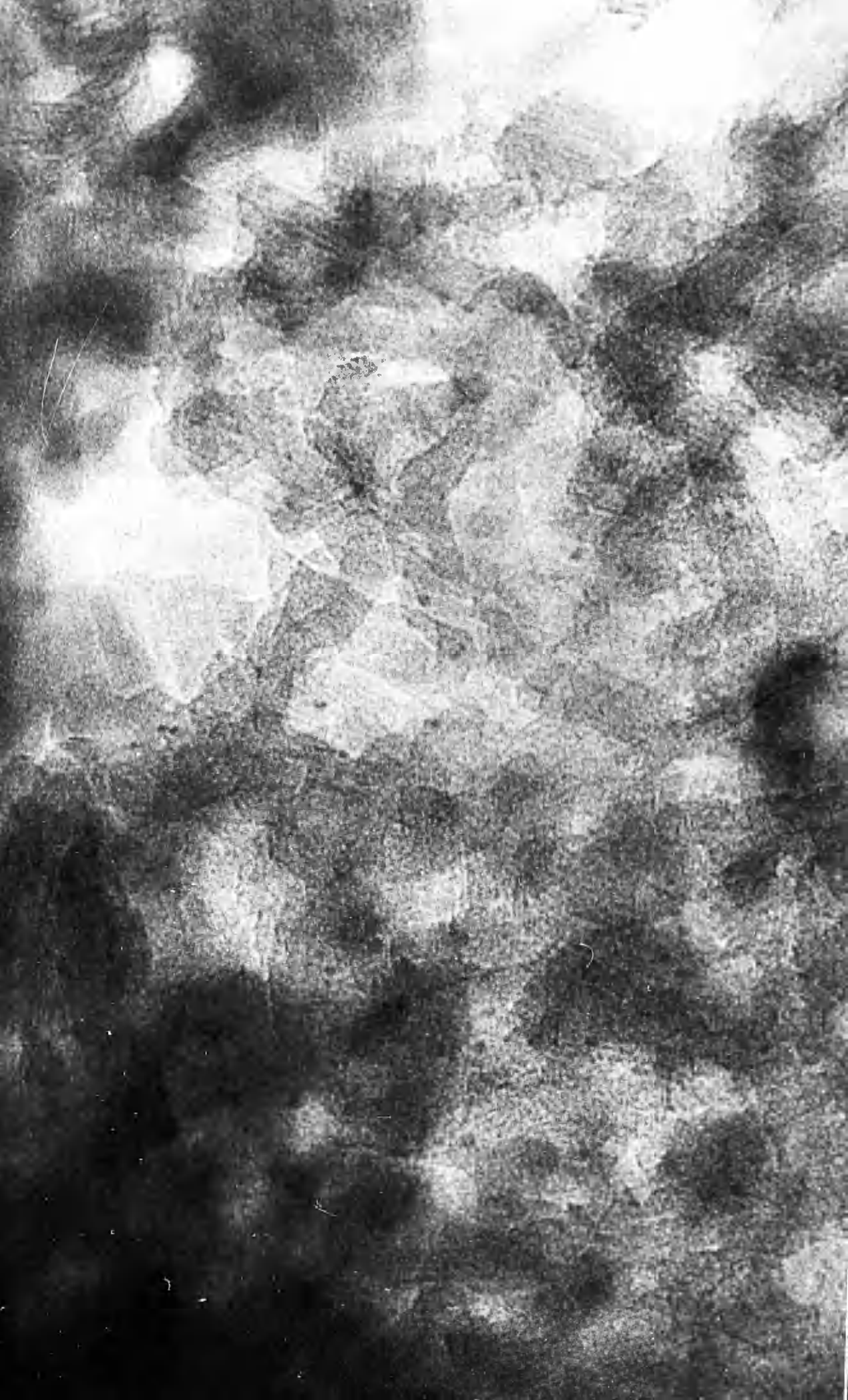

5. Results : Catalyst Regeneration

5. RESULTS : Catalyst Regeneration

5.1 Catalyst 1 (C.1)

5.1.1 Catalyst Characterisation

The alumina - supported platinum catalysts were examined at various stages in their preparation. After calcination of the Condea alumina, the alumina was examined by transmission electron microscopy (TEM) and X-ray diffraction analysis. Plate 6 shows the structure of the alumina, and the electron diffraction pattern is insetted. The diffraction pattern indicates that the alumina consists of a randomly orientated polycrystalline material. The diffraction spacings were measured and corresponded to those tabulated, by the A.S.T.M. index, for γ-Al_2O_3. Plate 6 shows the 2.39 Å lattices from the γ- Al_2O_3 (222) plane and the 1.9Å from the γ - Al_2O_3 (400) plane. The X-ray diffraction line profile from the alumina is shown by figure 5.1, and shows the periodicities due to γ - Al_2O_3. Table 5.1 lists the A.S.T.M. indexed values for γ- Al_2O_3 together with the experimentally obtained X-ray and electron diffraction values. Nitrogen adsorption measurements indicated a surface area of about. $200m^2/g$ for the γ- alumina.

The γ-alumina granules were then impregnated with hexachloroplatinic acid, as described by section 3.1. The impregnated catalysts were studied by TEM, both by the transmission and the diffraction mode. No hexachloroplatinate was detected by either technique.

The fresh catalyst was obtained following reduction of the impregnated alumina. Discrete, supported platinum particles were observed by TEM. The particles were difficult to resolve and only those in a suitable orientation were detected. This is due to the contrast effects and

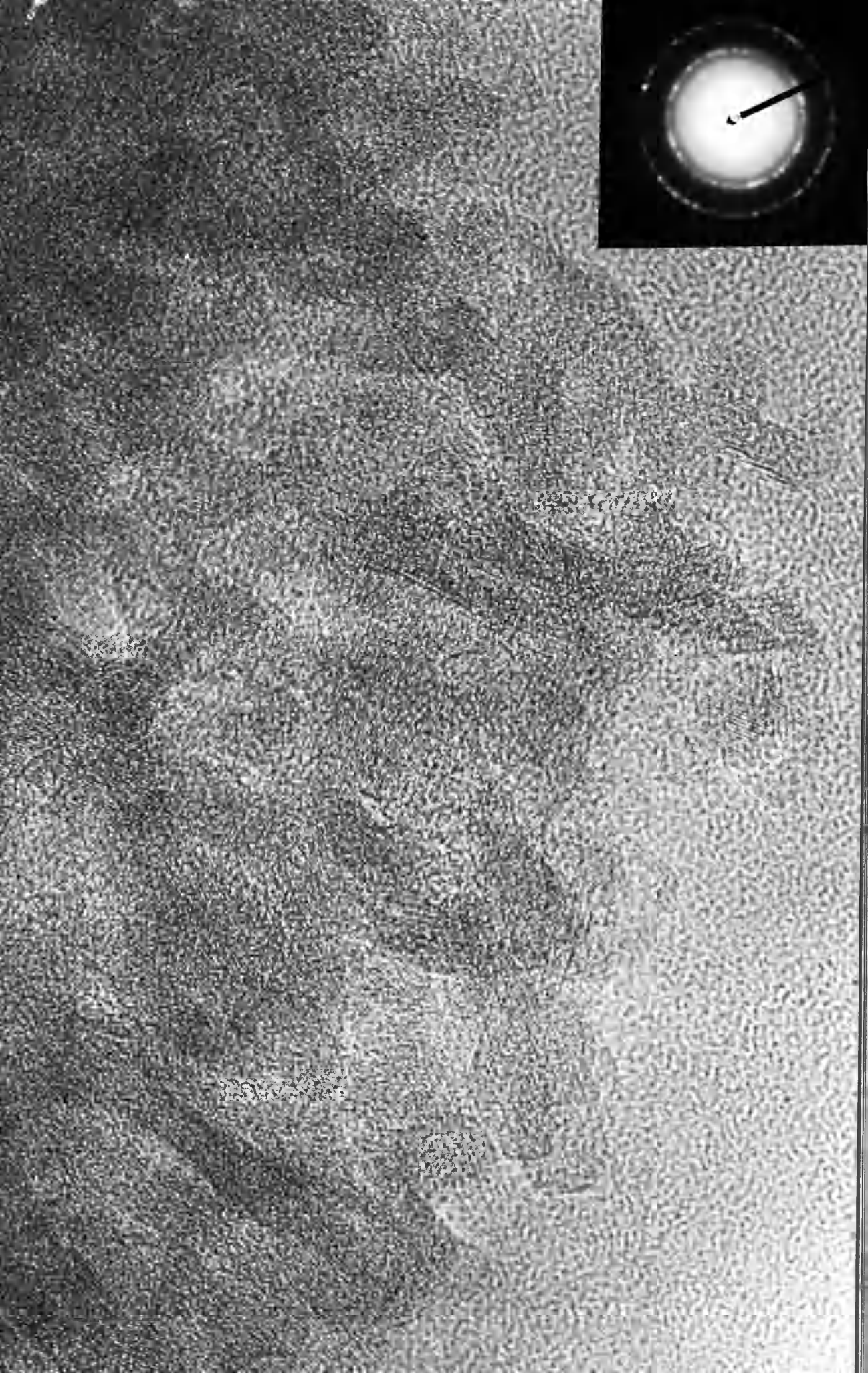

Figure 5.1

XRD profile

of γ-Al_2O_3

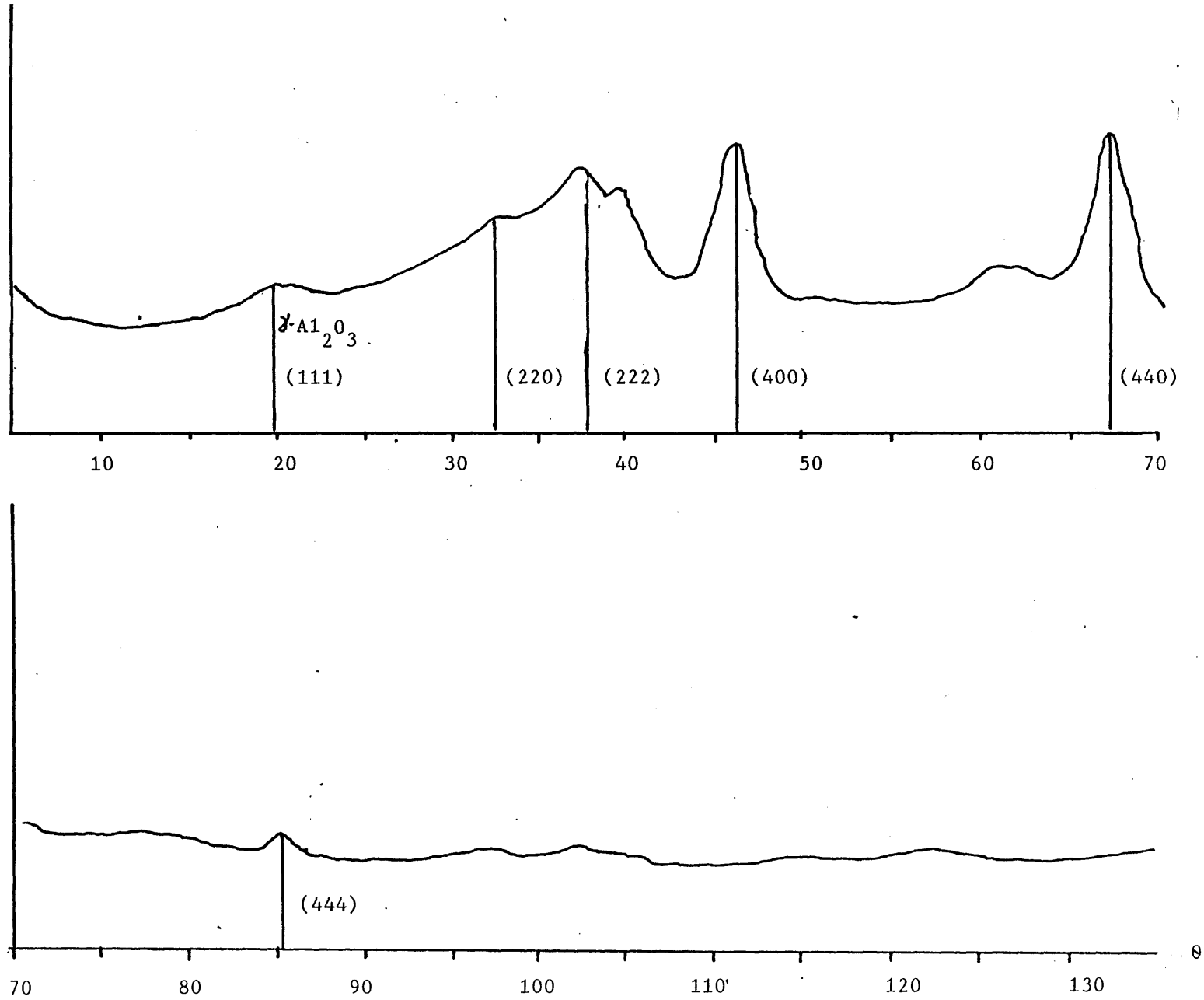

Table 5.1: Measured electron diffraction and X-ray periodicities, and A.S.T.M. indexed X-ray diffraction data for γ- Al_2O_3.

Measured		γ-Al_2O_3 A.S.T.M. Indexed		
electron-diffraction d (Å)	X-ray d (Å)	d(Å)	I/I_o	(hkl)
	4.60	4.56	40	111
2.78	2.82	2.80	20	220
2.32	2.39	2.39	50	222
1.94	2.07	1.977	100	400
1.39	1.38	1.395	100	440
1.13	1.13	1.140	20	444
1.07		1.027	10	731
		0.989	10	800
		0.805	20	844

limitations of resolution, described in section 1.5. Catalyst 1 had a mean platinum particle diameter, resolvable by TEM, of 16Å with a standard deviation = ± 5Å (Plate 7). The Pt particle size distribution is indicated in figure 5.2.

Chemisorption results, indicated on tables 5.2 and 5.3, suggests that the catalyst is highly dispersed. X-ray diffraction line profile analysis was attempted on the fresh catalyst. No platinum was detected by XRD, suggesting that the platinum exists at a size below the resolution of the technique.

Neutron activation analysis confirmed that catalyst 1 contained 0.31 % by weight platinum. The chloride levels of the fresh catalyst was 1.27 % by weight chlorine.

5.1.2 Ageing of Catalyst 1

Catalyst 1 was aged as described in the experimental section. An increase in particle size was observed by TEM, together with a decrease in the hydrogen uptake by H_2 chemisorption. The mean particle size, measured by TEM, increased to 55Å. This value is in agreement with the value calculated from H_2 chemisorption results of 54Å. Plates 8 and 9 show typical sintered platinum particles on the alumina support. The particle size distribution of the aged catalyst is shown in figure 5.3. TEM, H_2 chemisorption and CO chemisorption data are shown in tables 5.1 - 5.4. X-ray diffraction line broadening analysis was attempted for the aged catalyst. The X.R.D. trace, shown by figure 5.4, shows the Pt (311) line for the standard sample and for the aged catalyst. No Pt reflection is detectable, by XRD, from the sintered catalyst due to the low metal loading of catalyst 1.

Plate 7

Fresh catalyst 1, showing highly dispersed Pt crystallites.

X 1.84M

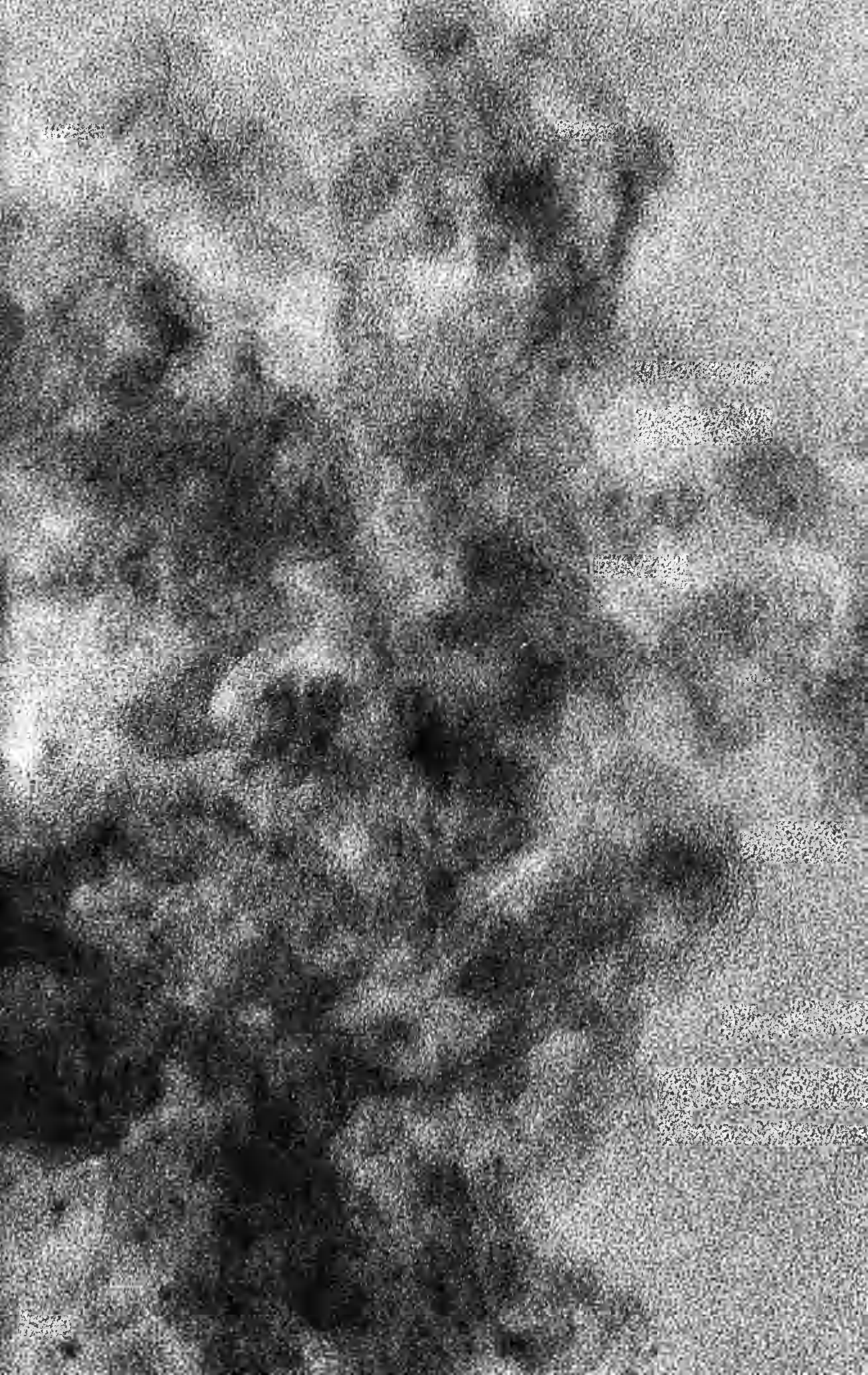

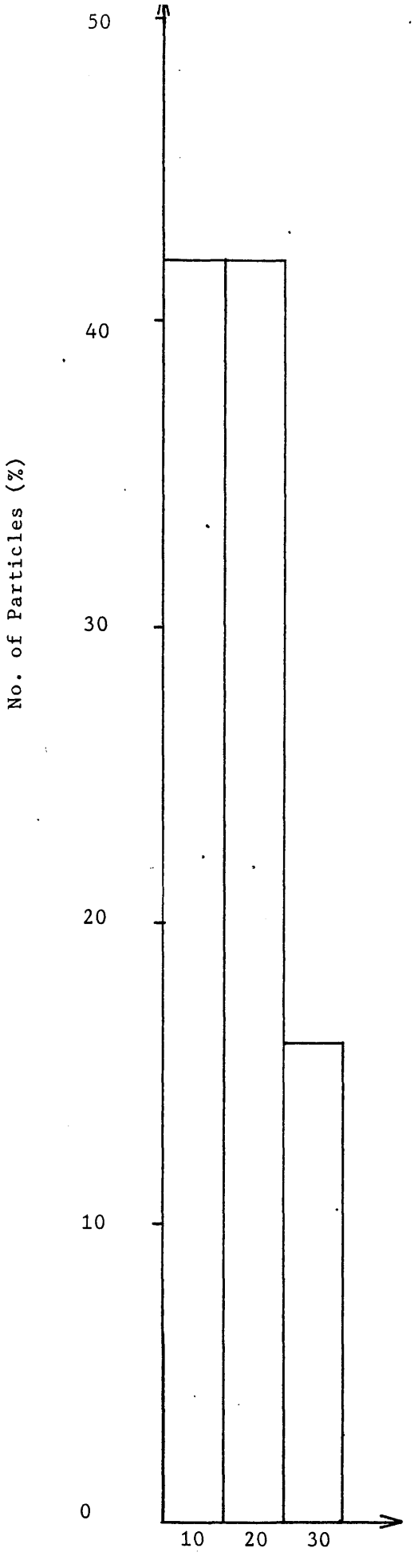

figure 5.2: Particle size distribution of fresh catalyst 1 (C1).

Table 5.2: H_2 chemisorption data for catalyst 1 following ageing and oxychlorination (oxy) treatments.

	H_2 Chemisorption	
	Vm (ml/g)	Pt d_{calc} (Å)
fresh	0.204	12.5
fresh, oxy	0.265	10.5
sintered	0.047	54.0
sinter, oxy 1.1	0.234	11.0
sinter, oxy 1.2	0.271	9.0
sinter, oxy 1.3	0.314	8.0
sinter, oxy 1.4	0.291	8.5

Table 5.3: CO Chemisorption data for catalyst 1 following ageing and oxychlorination (oxy) treatments.

	Surface Area (m^2/g)	Pt dcalc (Å)
fresh	0.74	11.7
sintered	0.32	27.1
sinter, oxy 1.1	0.66	13.1
sinter, oxy 1.7	0.50	17.3
sinter, oxy 1.8	0.64	13.5

Table 5.4: Electron microscopy data for catalyst 1 following ageing and oxychlorination (oxy) treatment.

	TEM		
	$\bar{d}$mean (Å)	σ (± Å)	n
fresh	16	5	40
fresh, oxy	13	15	102
sintered	60	38	229
sinter, oxy 1.1	28	31	200
sinter, oxy 1.2	38	22	110
sinter, oxy 1.3	26	21	147
sinter, oxy 1.4	43	39	81
sinter, oxy 1.5	<20	-	-
sinter, oxy 1.6	52	48	93
sinter, oxy 1.7	31	19	283
sinter, oxy 1.8	<20	-	-

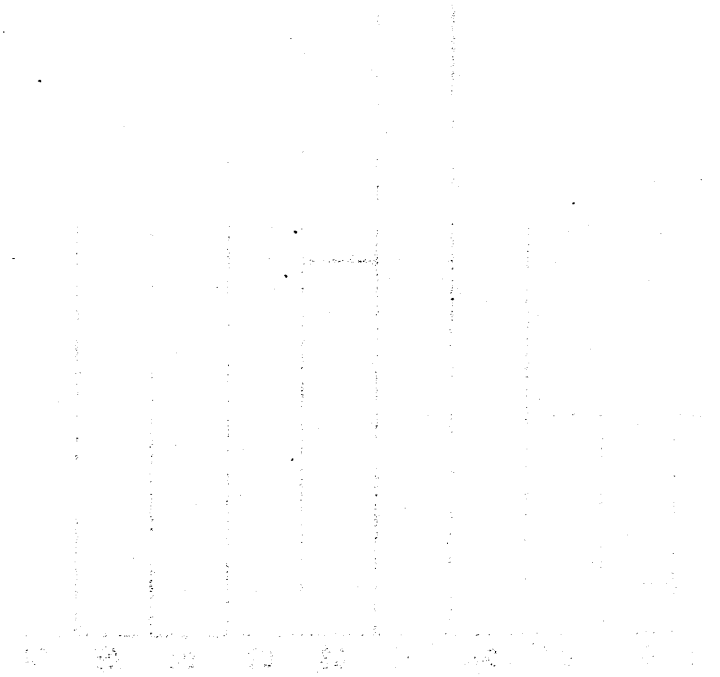

figure 5.3: Particle size distribution of catalyst 1 following sintering in 3% $O_2|N_2$ at 600°C for 4 hours

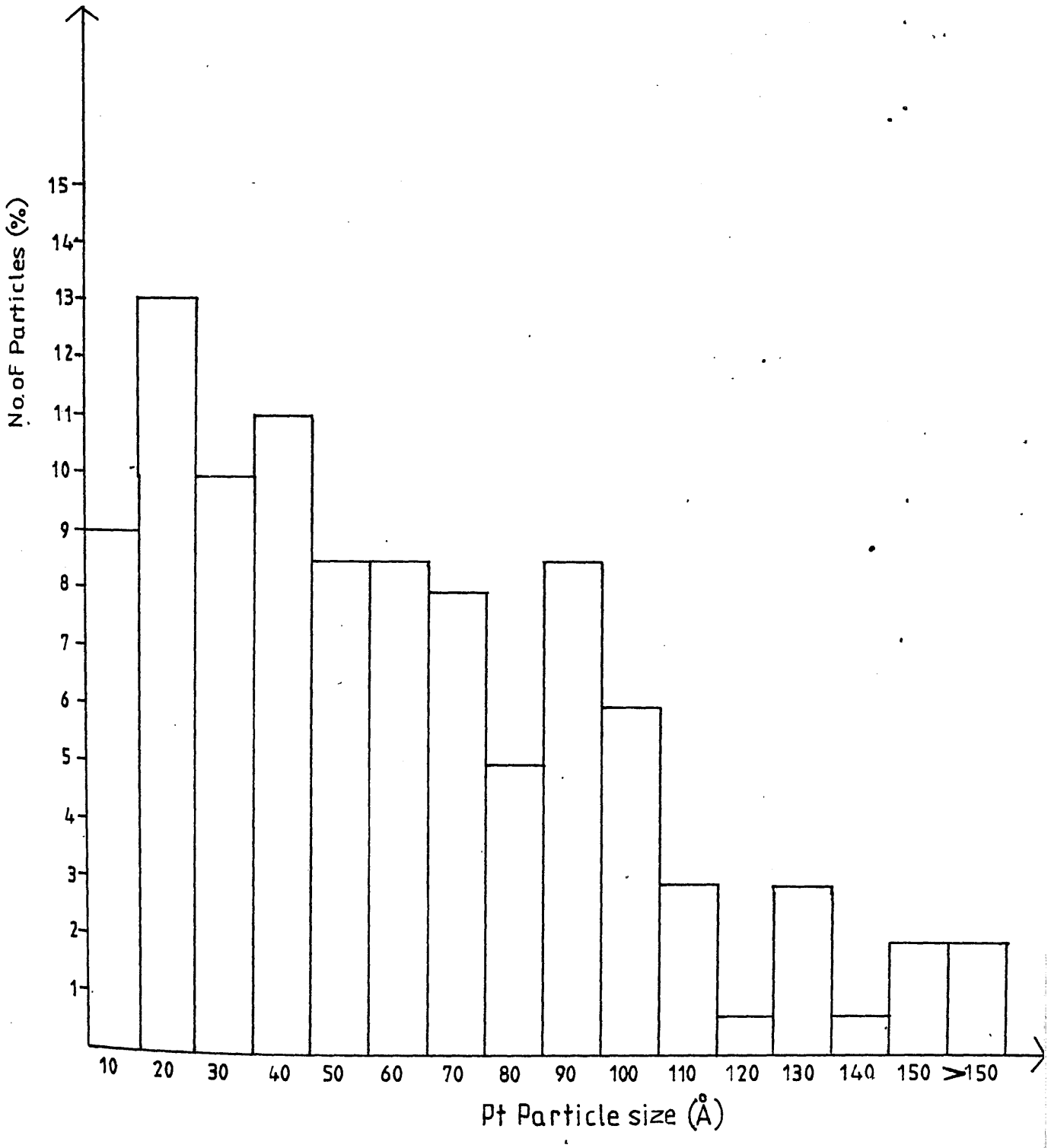

5.1.3 Oxychlorination treatments of Sintered C.1.

Redispersion of the sintered platinum crystallites was attempted by a series of oxychlorination treatments, as described in the experimental section. Results from H_2 chemisorption are indicated on table 5.2; CO chemisorption, Table 5.3; and TEM results, Table 5.4

X-ray diffraction line broadening analysis was attempted following each oxychlorination treatment. In each case no Pt was detected due to the low metal loading of the catalyst.

(i) Standard oxychlorination (1.1)

Figure 5.5 shows the platinum particle size distribution, for the catalyst, following the standard oxychlorination treatment. A decrease in particle size is shown by TEM, with a mean particle size measured at $28\text{Å} \pm 31\text{Å}$. Plate 10 shows sintered platinum particles remaining after this treatment. Plate 5a shows highly dispersed sub - 10Å platinum particles on the alumina support following the standard oxychlorination.

(ii) Oxygen Treatment (oxychlorination 1.2)

No CCl_4 was injected into the O_2/N_2 gas flow in oxychlorination 1.2. The platinum particle size distribution, measured from TEM examination, is indicated in figure 5.6.

Plate 8

Typical area of C1 following ageing for 4 hours.

X 2.26 M

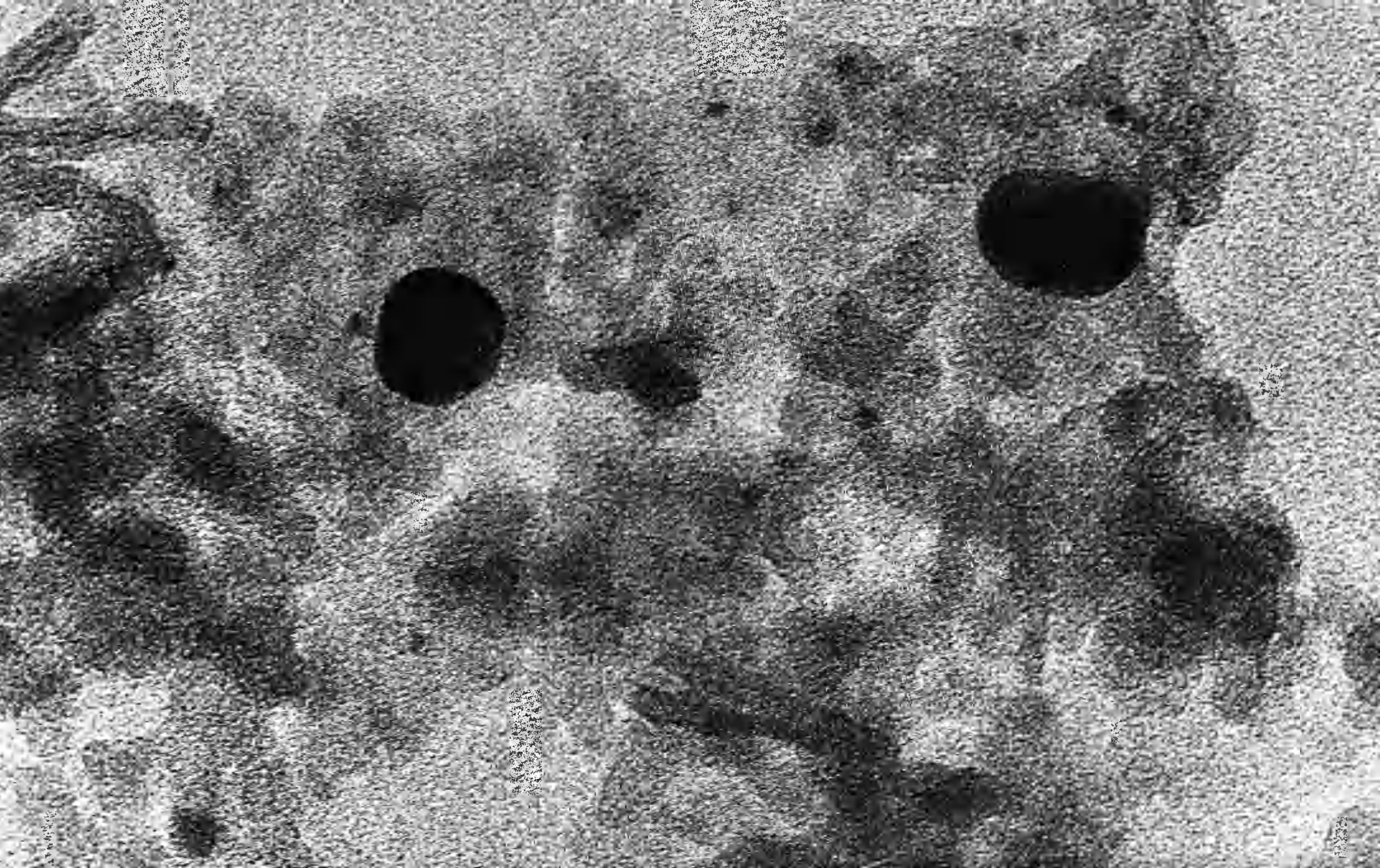

Plate 9

C1 following ageing for 4 hours, showing typical sintered Pt particles.

X 3.0 M

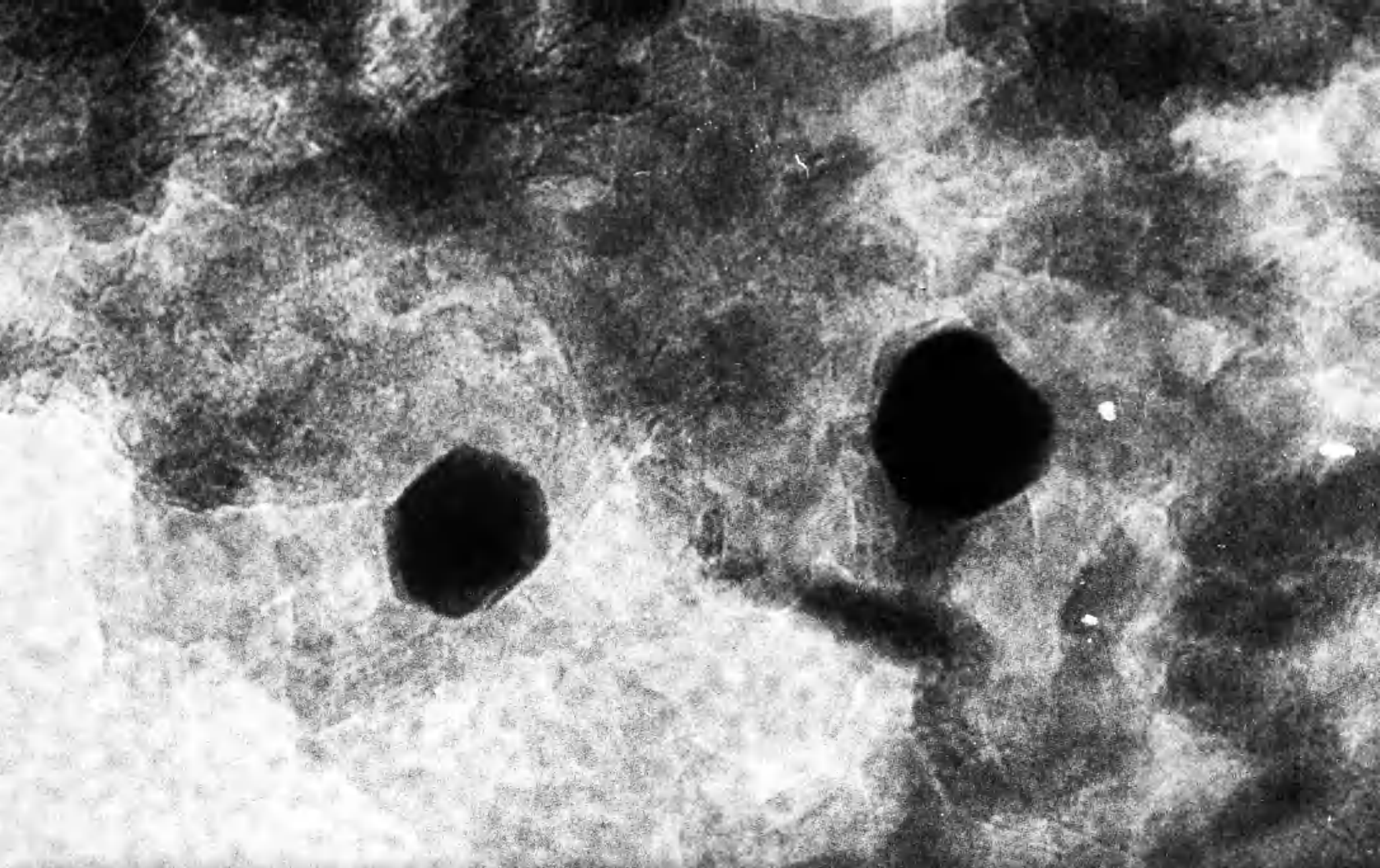

figure 5.4: XRD of standard sample and C1 sintered showing the Pt(311) reflection.

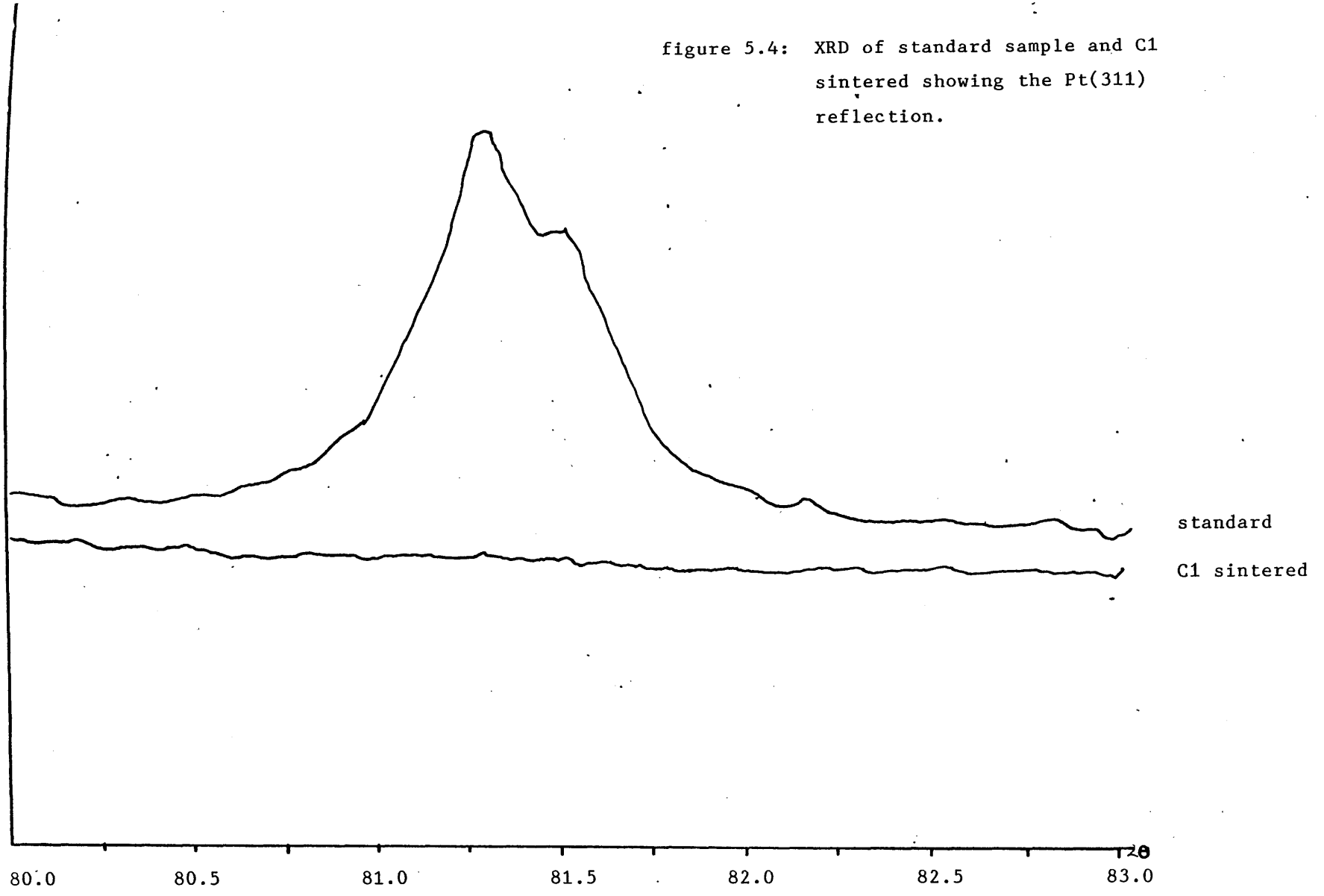

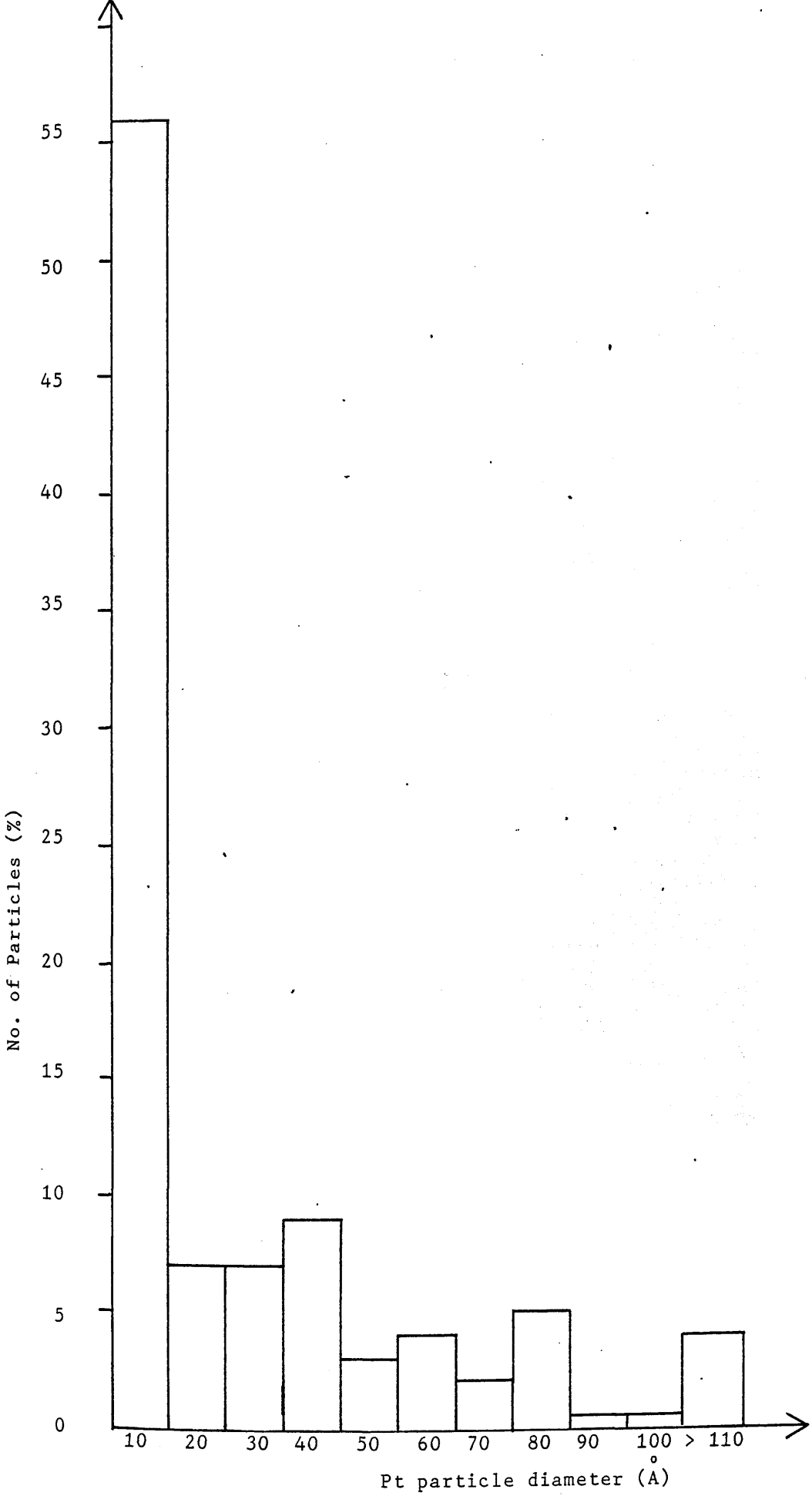

figure 5.5: Particle size distribution of C1 following sintering for 4 hours and oxychlorination 1.1.

Plate 10

Large Pt particles on C1 following oxychlorination 1.1

X 1.41M

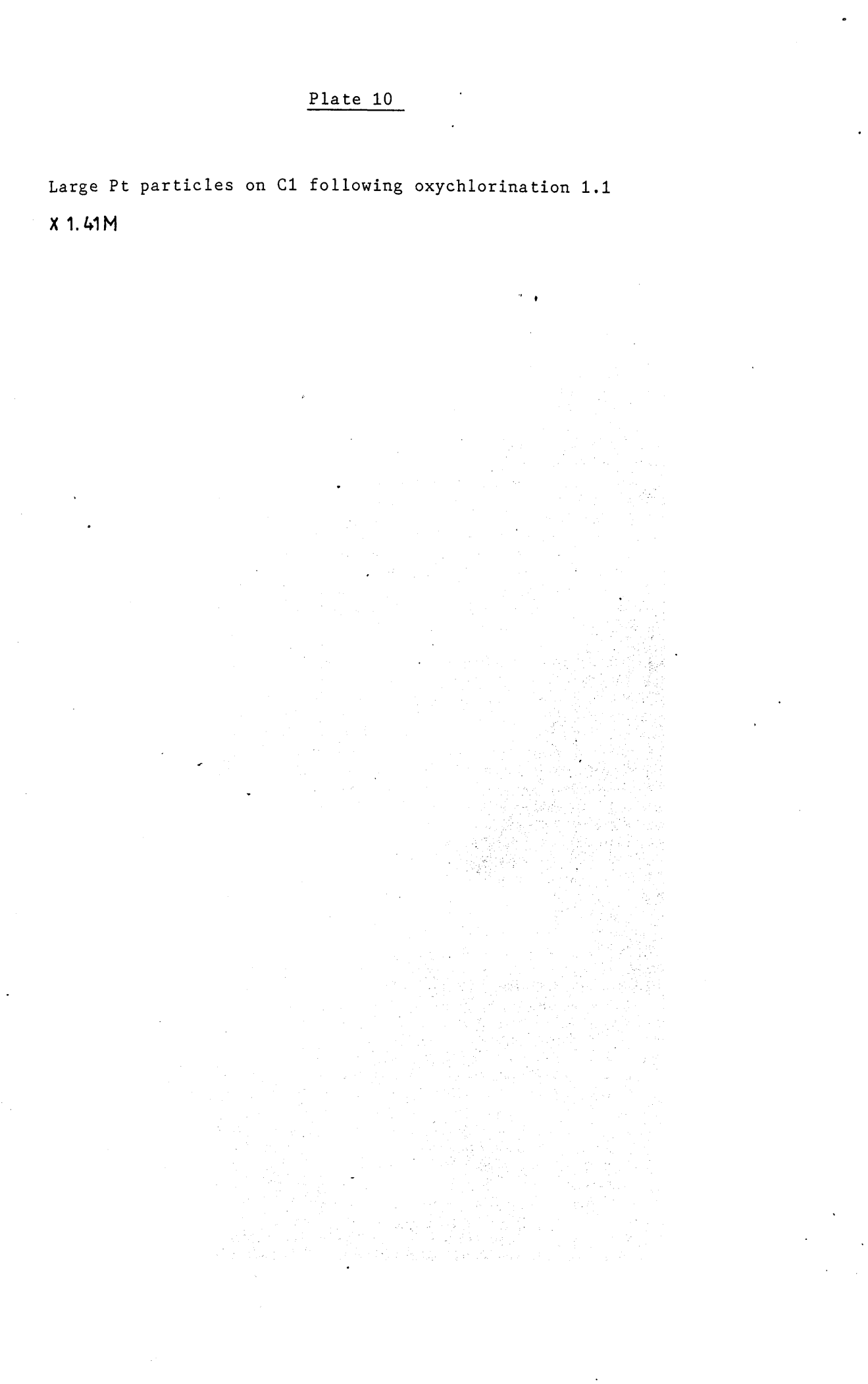

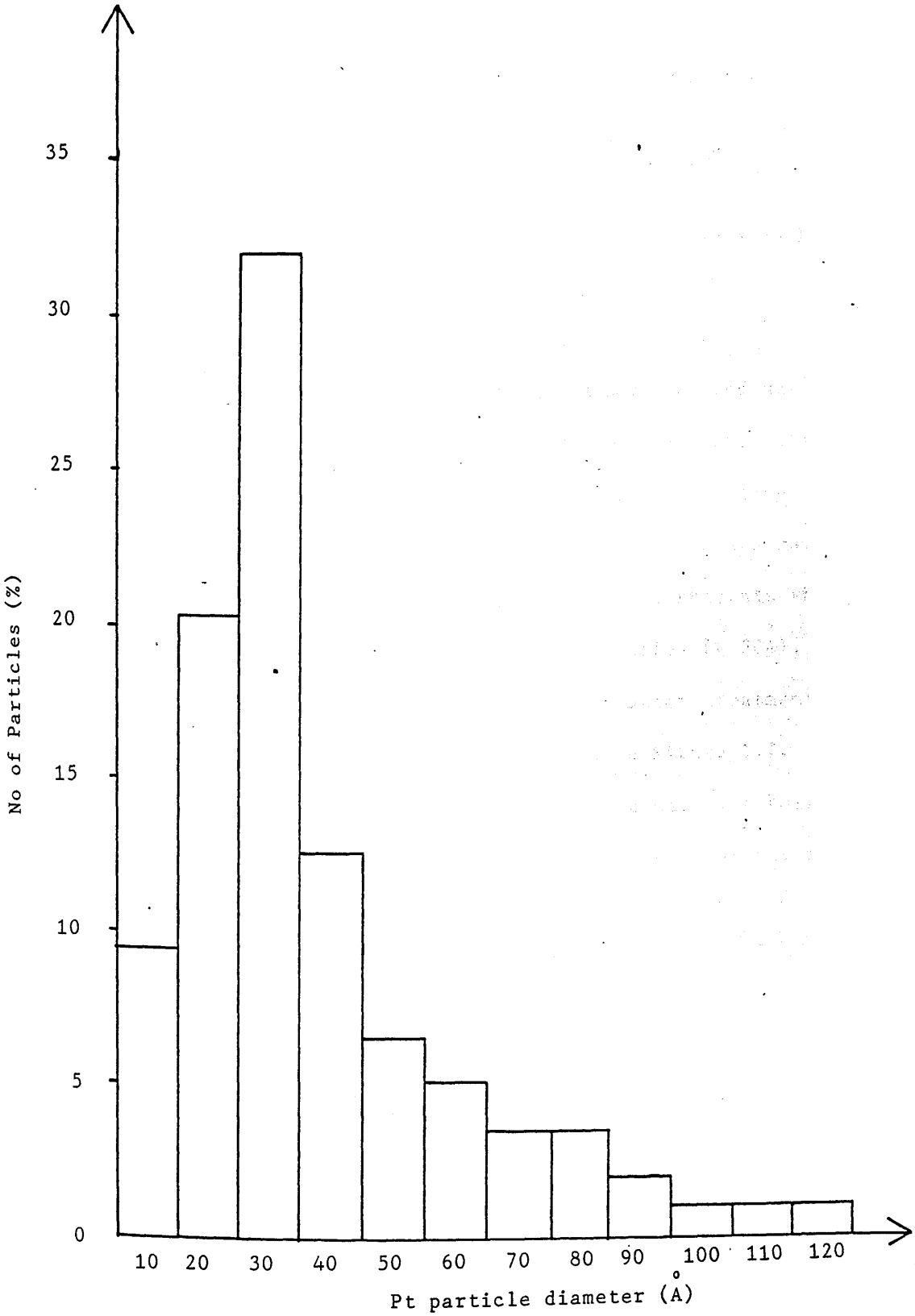

figure 5.6: Particle size distribution of C1 following (i) Ageing for 4 hours (ii) Oxychlorination 1.2

(iii) The Effect of CCl_4 Increase to the Redispersion of a Sintered Catalyst

Oxychlorinations 1.1, 1.3 and 1.4 show the effect of increasing the amount of CCl_4 passed over the catalyst to the redispersion of sintered platinum particles.

H_2 chemisorption results (Table 5.2) indicate that varying the amount of CCl_4 has no effect on the redispersion process.

TEM results indicate that all three treatments redisperse the platinum. Adding 2w/o chlorine over the sintered catalyst (oxychlorination 1.4), the platinum was very difficult to resolve, by TEM, indicating that the platinum is highly dispersed. The platinum detected was mainly in the form of large Pt crystallites (Plate 11). This suggests that most of the platinum exists in the form of small particles ($< 30\text{Å}$), with large sintered particles remaining after oxychlorination treatment. The particle size distribution for 1.4 is shown in Figure 5.7. Figure 5.8 shows the Pt particle size distribution of the catalyst following oxychlorination (1.3). TEM shows that redispersion of the sintered particles occurs following this treatment.

Plate 11

Large Platinum crystallites following oxychlorination 1.4

X1.47M

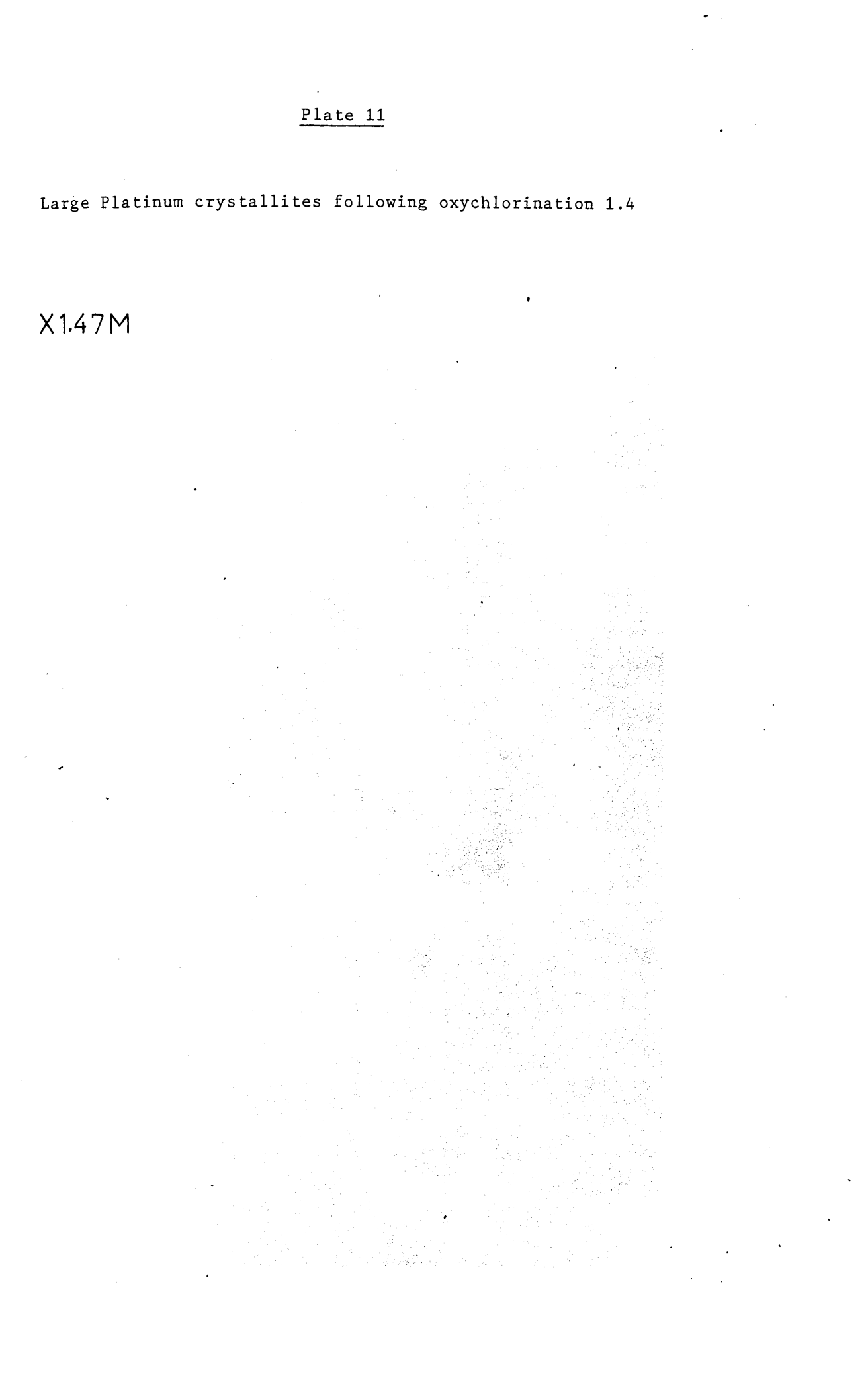

figure 5.7: C1 following sintering for 4 hours + oxychlorination 1.4

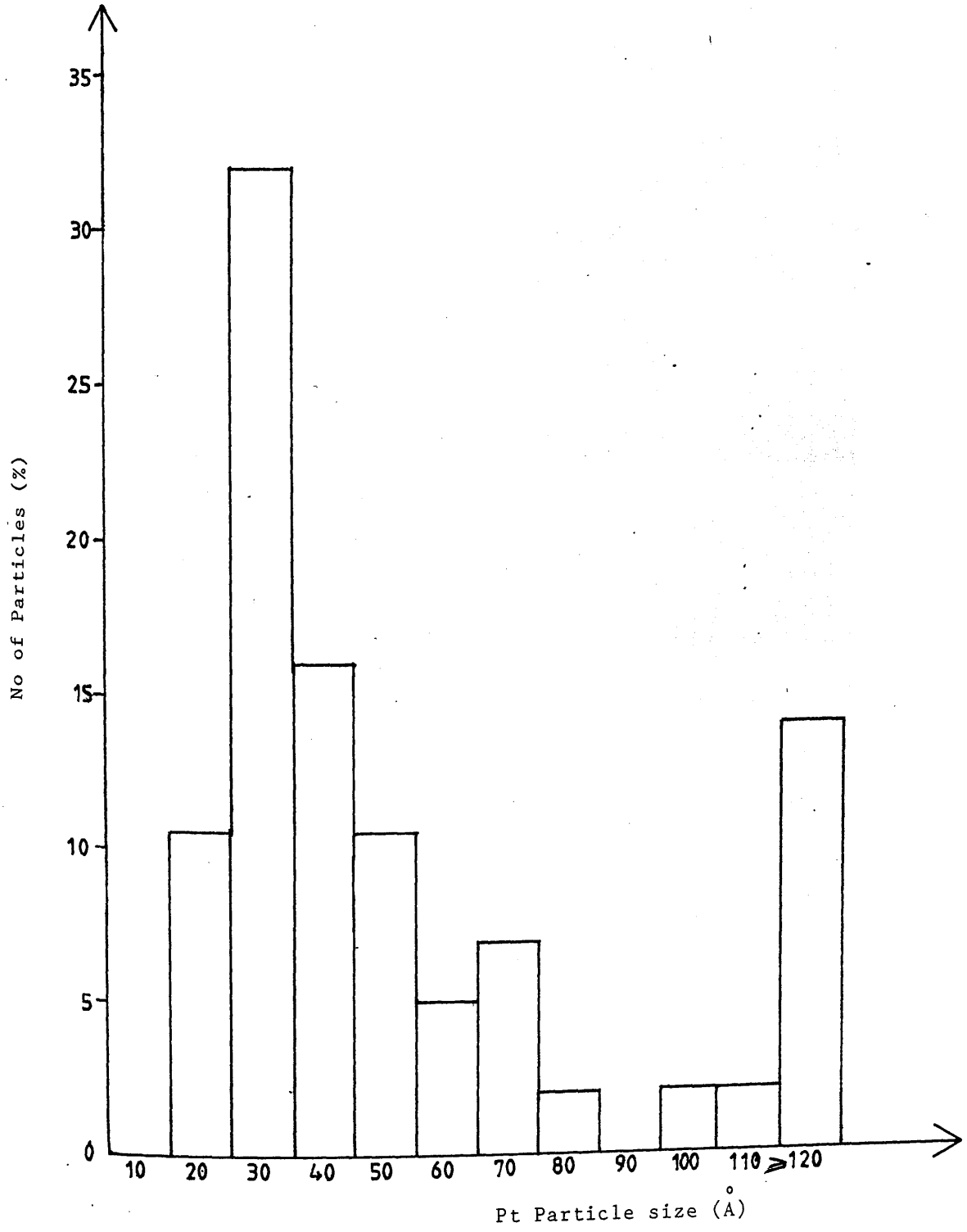

figure 5.8: Particle size distribution of C1 following
(i) Ageing for 4 hours (ii) Oxychlorination 1.3

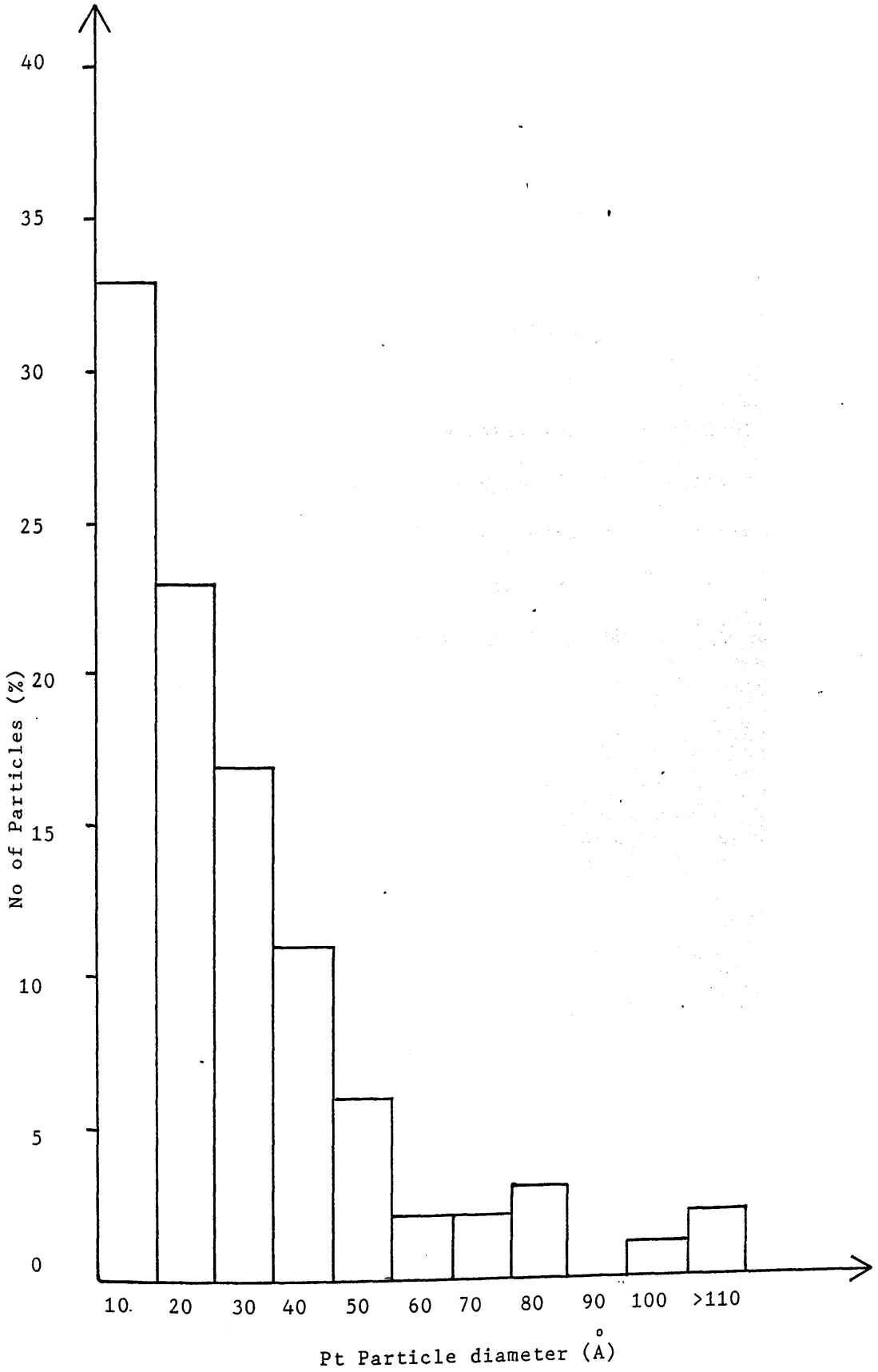

(iv) The Effect of Increasing [CCl_4]

The concentration of CCl_4 in the gas stream was increased to 800ppm (oxy 1.5) and 1400 ppm (oxy 1.6) as described in section 3.2.3.

TEM examination following oxy 1.5 indicated a successful resdispersion as no platinum was detected by electron microscopy.

Plate 12 shows large platinum particles of up to 240Å in diameter, following oxychlorination with a 1400ppm CCl_4 concentration. The surface of the alumina appears to have been affected by this treatment, and some twinned platinum particles have been observed (Plate 12). The platinum particle size distribution, as determined by TEM, for the catalyst following oxy 1.6 is shown in figure 5.9.

Plate 12

Typical area of C1 following oxychloriantion with a 1400 ppm CCl_4 concentration (oxychlorination 1.6).

X 1.35M

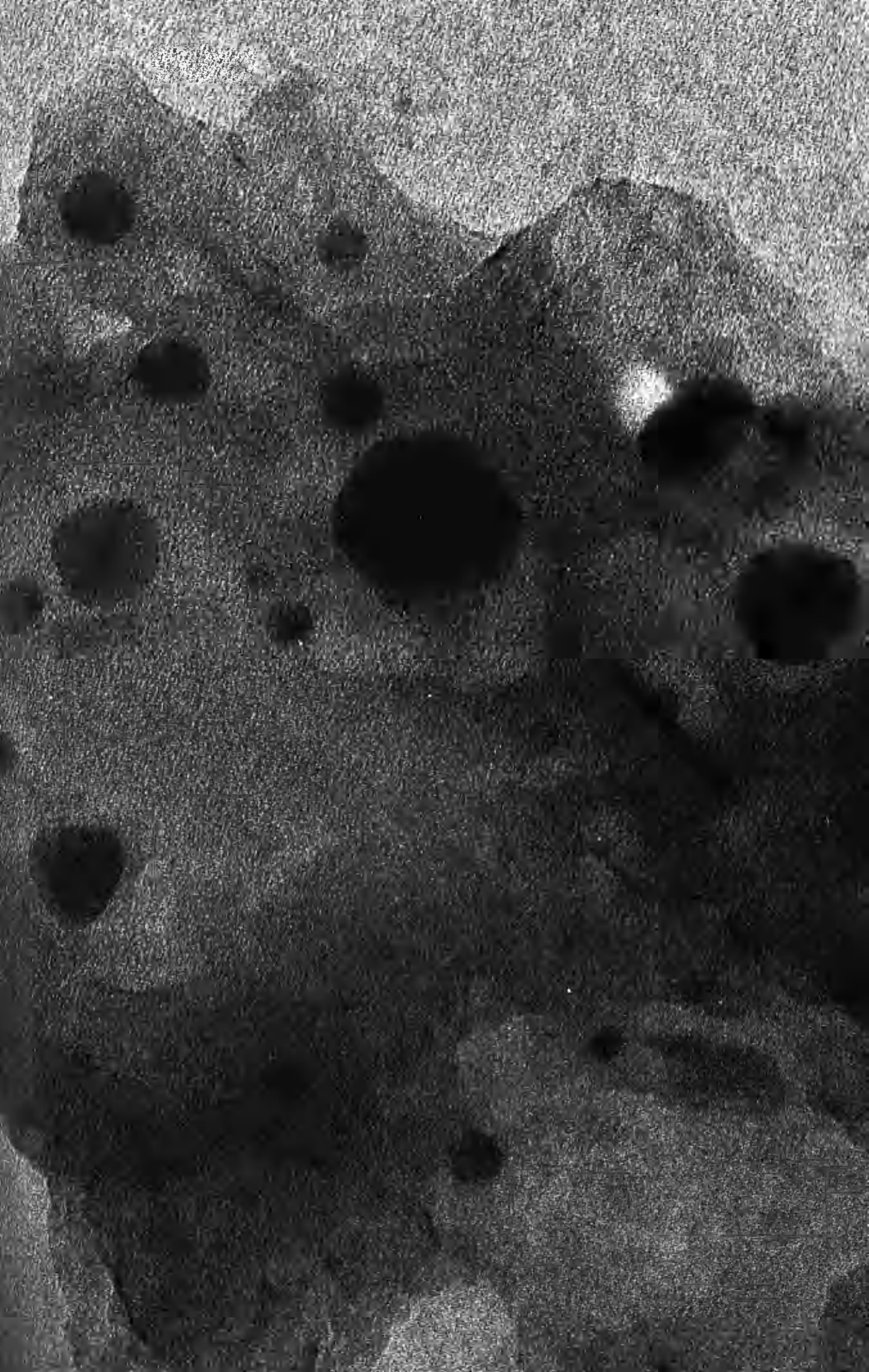

Figure 5.9: Particle size distribution of Cl following sintering for 4 hours and oxychlorination 1.6.

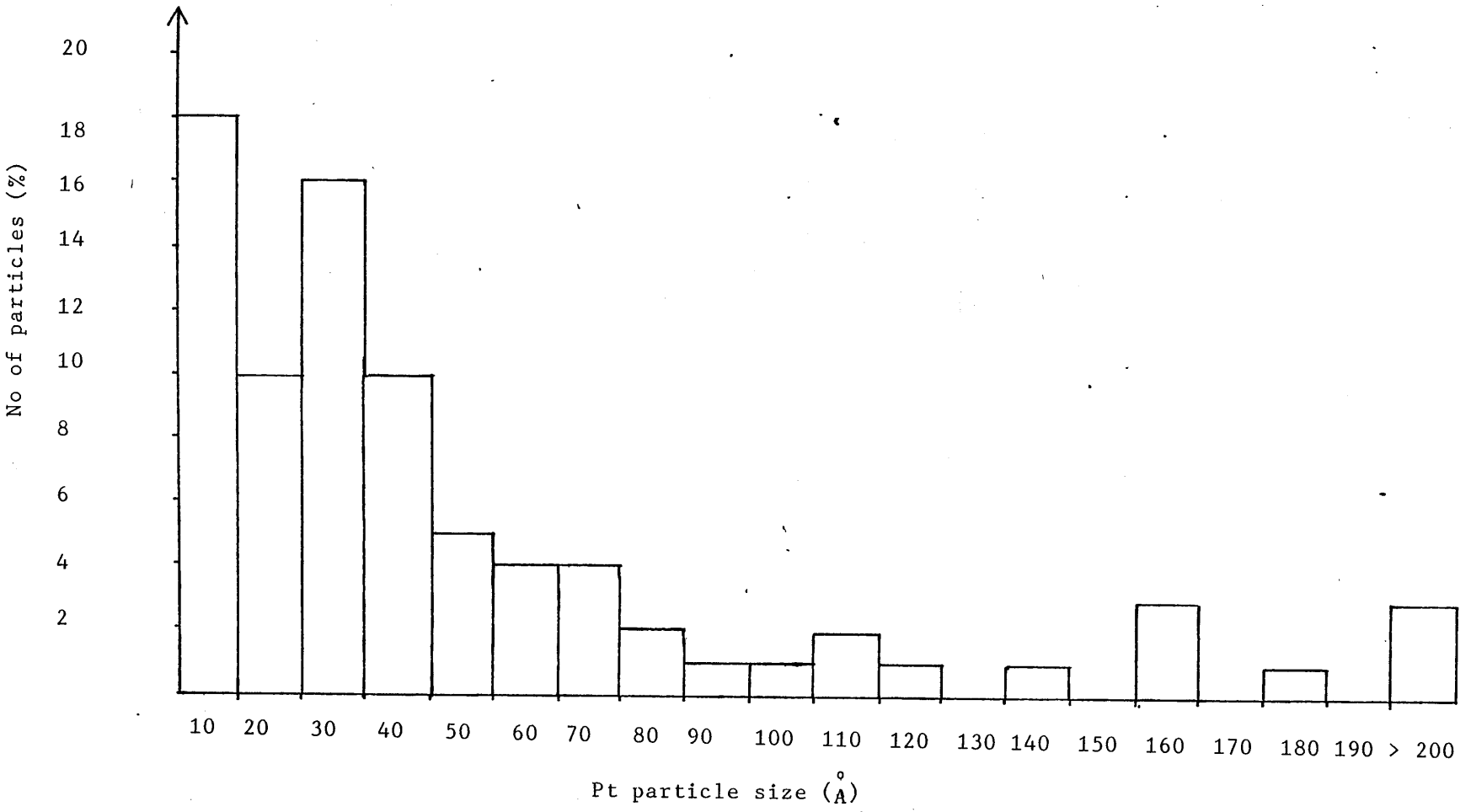

(v) The Effect of Time to the Redispersion of a Sintered Catalyst

Figure 5.10 shows the platinum particle size distribution, measured by TEM, following oxychlorination of an aged catalyst for 15 minutes (oxychlorination 1.7). Plate 13 shows a typical area of the catalyst following oxychlorination for 15 minutes. TEM suggests that some redispersion occurs (Table 5.4). CO chemisorption results (Table 5.3) indicate a recovery of platinum surface area.

After oxychlorination for 17 hours (oxychlorination 1.8), both TEM and CO chemisorption results suggest complete platinum redispersion.

5.1.4 Oxychlorination of a Fresh Catalyst

A fresh catalyst was treated by oxychlorination 1.1., as explained in the experimental chapter. No sintering of the platinum particles was observed by TEM (Table 5.4), and hydrogen chemisorption indicates a mean platinum particle size of 10.5Å (Table 5.2). Plate 14 shows highly dispersed platinum, following the oxychlorination treatment on the fresh catalyst. The particle size distribution is indicated by figure 5.11.

figure 5.10: Particle size distribution of C1 following (i) Ageing for 4 hours (ii) Oxychlorination for 15 minutes (oxy 1.7).

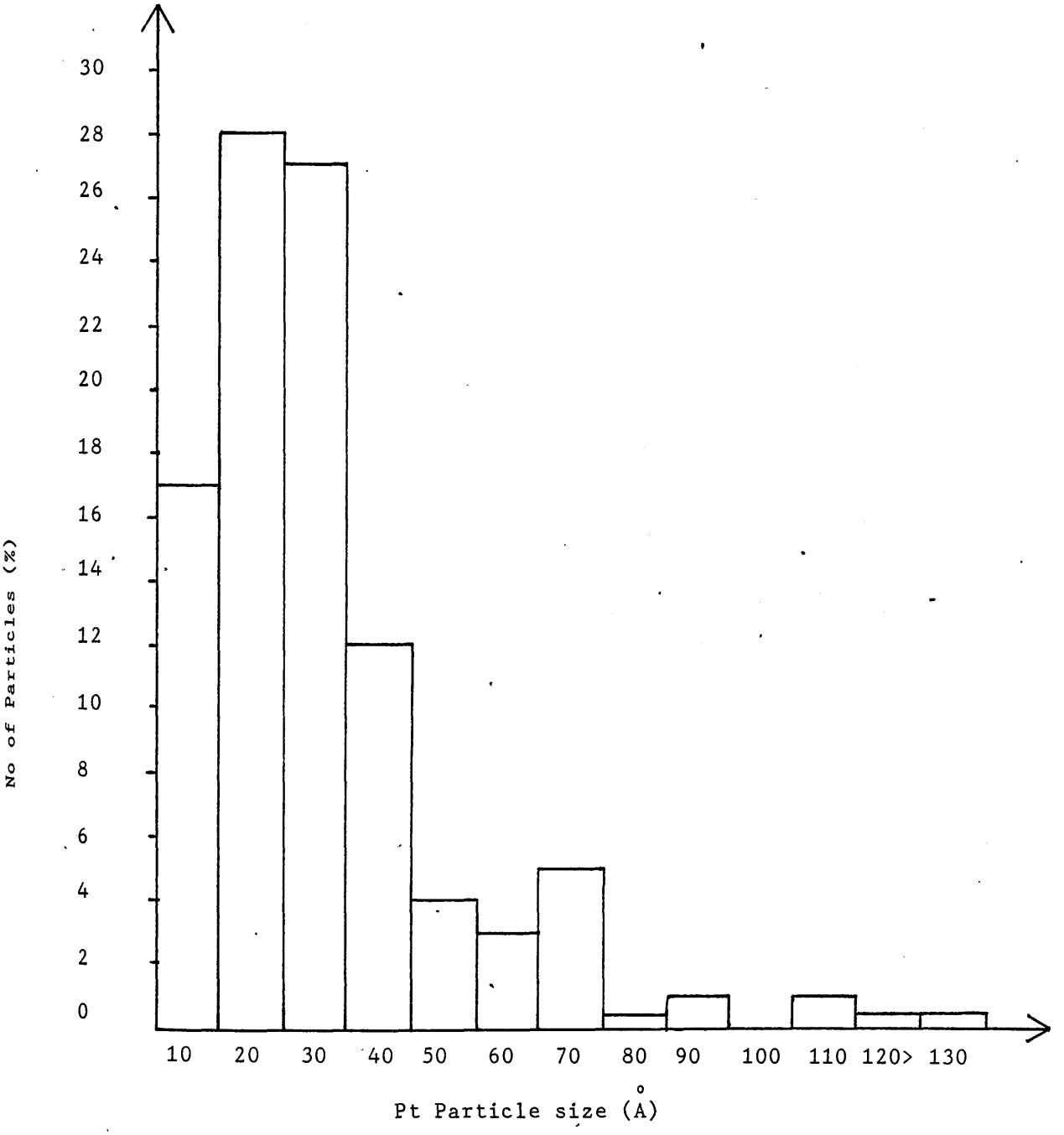

Plate 13

Typical area of C1 following oxychlorination treatment for 15 minutes.

X1.35M

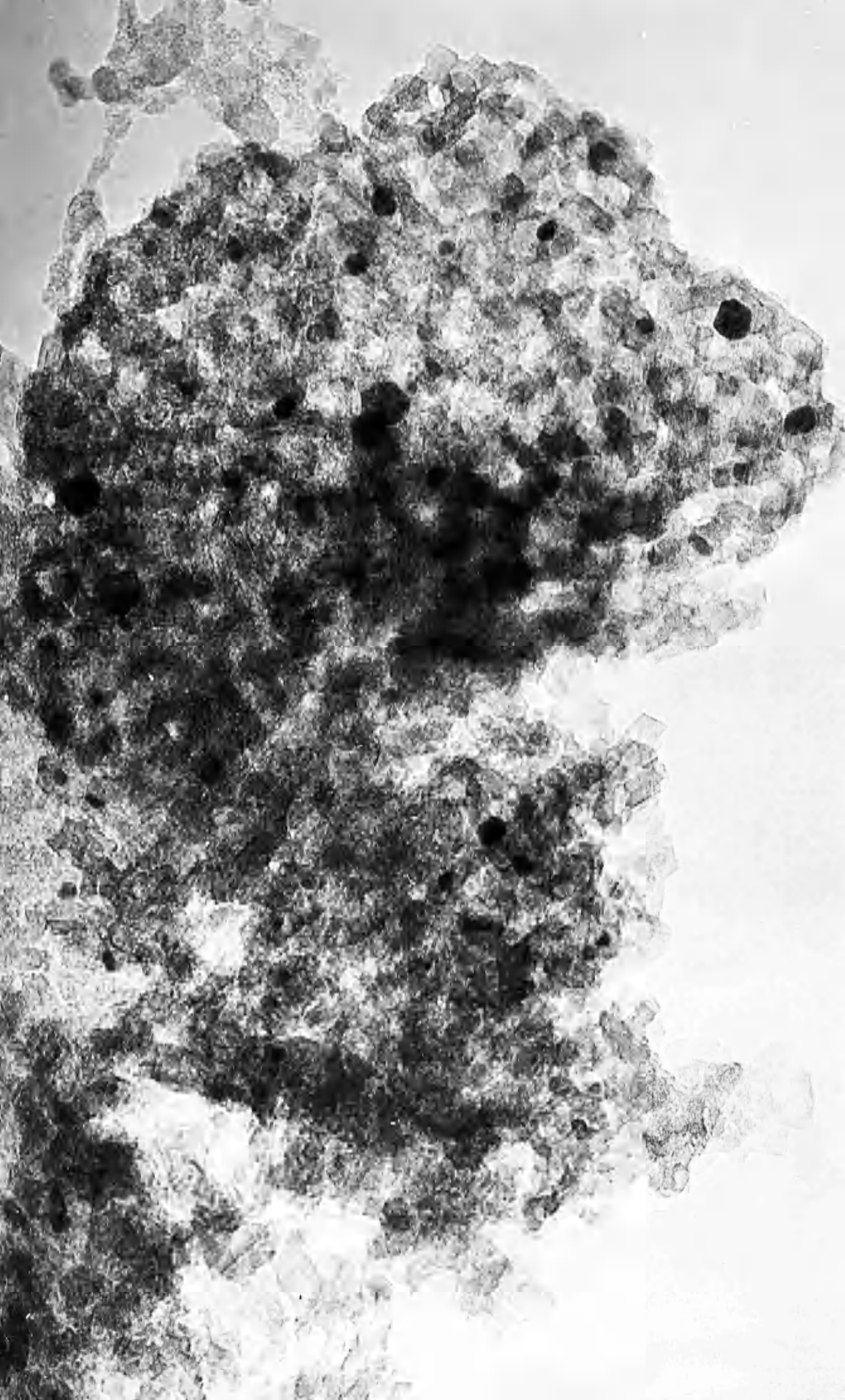

Plate 14

Highly dispersed platinum following oxychlorination treatment of fresh catalyst 1.

X 1.47 M

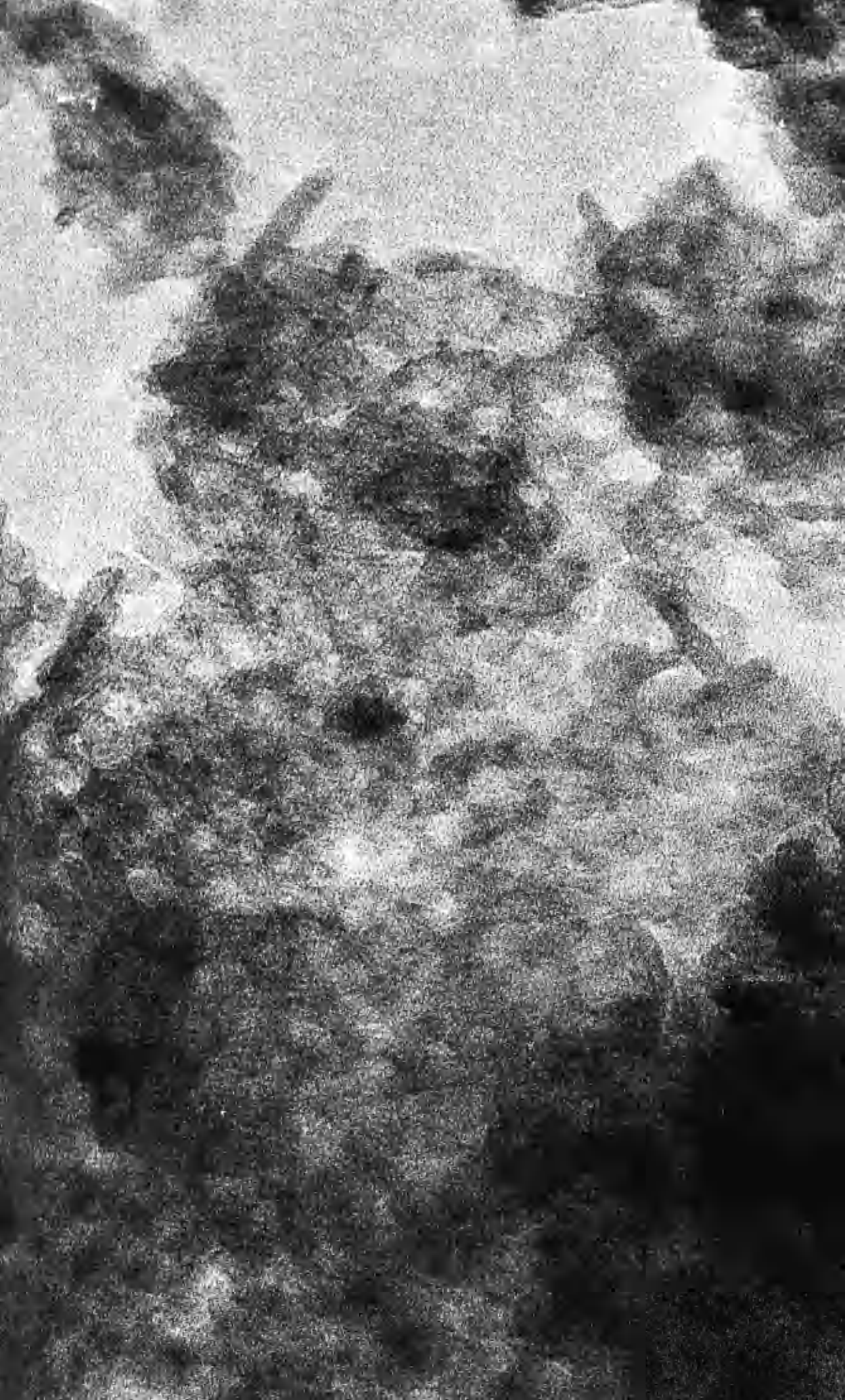

figure 5.11: Particle size distribution following oxychlorination treatment on a fresh catalyst (C1) at 480°C for 3 hours.

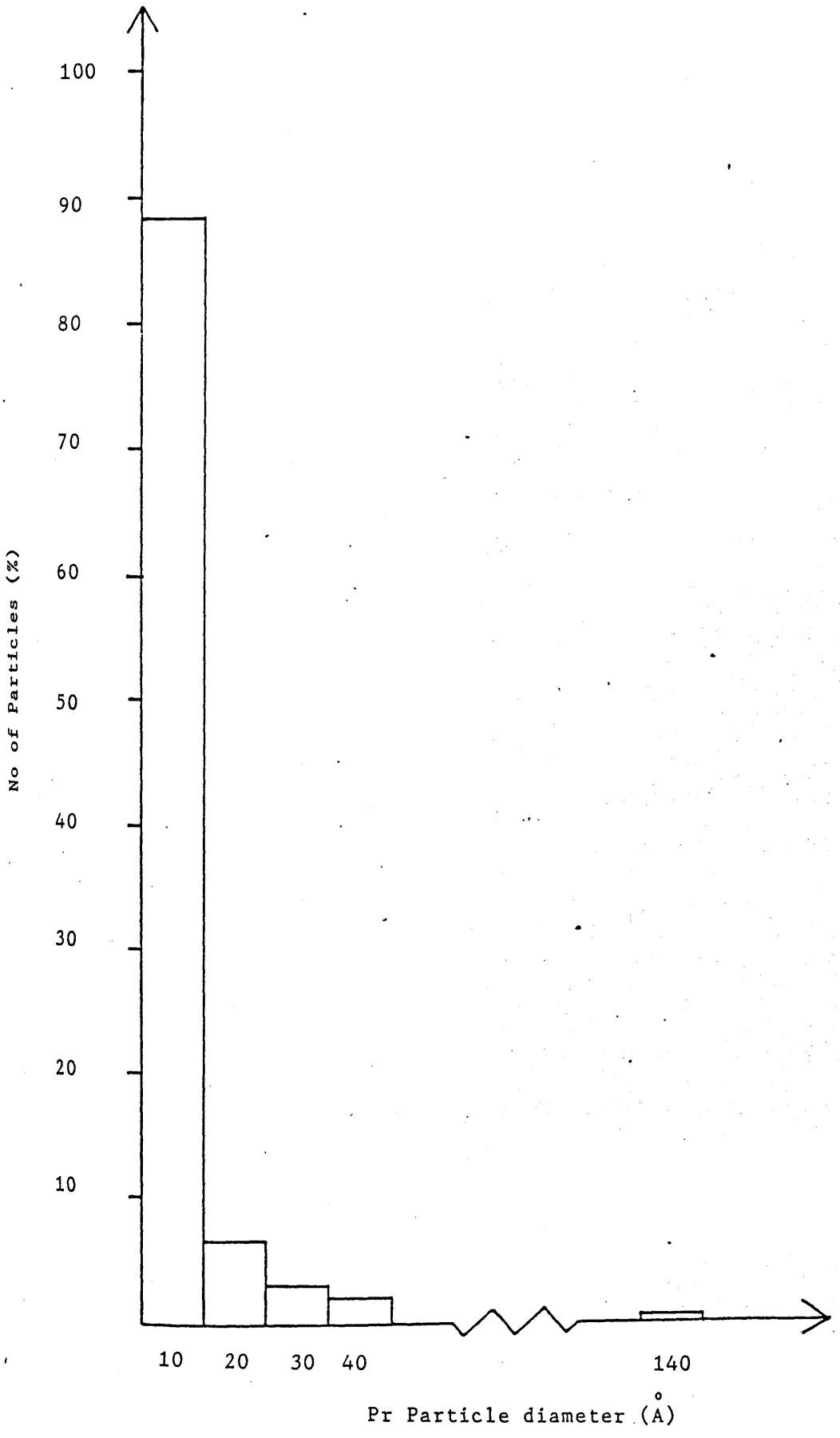

5.2 Catalyst 2 (C2)

Catalyst 2 was prepared in the same way as C1. Platinum was difficult to detect, by TEM, in the fresh catalyst indicating a mean Pt particle diameter below 10Å. After ageing at 600° C (Chap. 3) the particle size increased (Plate 15) with a mean particle diameter of about 79Å. The particle size distribution of the aged catalyst is indicated by figure 5.12.

Regeneration of the aged catalyst was attempted by three oxychlorination treatments, as explained in section 3.2.

Only TEM was used to study this series of catalysts. No attempt was made to gain a full particle size distribution, as the aim of the experiment was to determine if large Pt crystallites remain after pulse oxychlorination treatments.

After oxychlorination 2.1 large platinum particles were detected by TEM, as shown in Plate 16. Platinum particle sizes ranged up to 200Å in diameter.

The redispersion of sintered Pt was attempted by oxychlorination 2.2, by a series of 6 thirty minute oxychlorination/reduction cycles, as described in the experimental. Large platinum particles were observed after oxychlorination treatment (Plate 17). Several platinum crystallites greater than 50Å were observed ranging up to 190Å in diameter.

Plate 15

Sintered platinum particles following ageing of C2.

X 1.65M

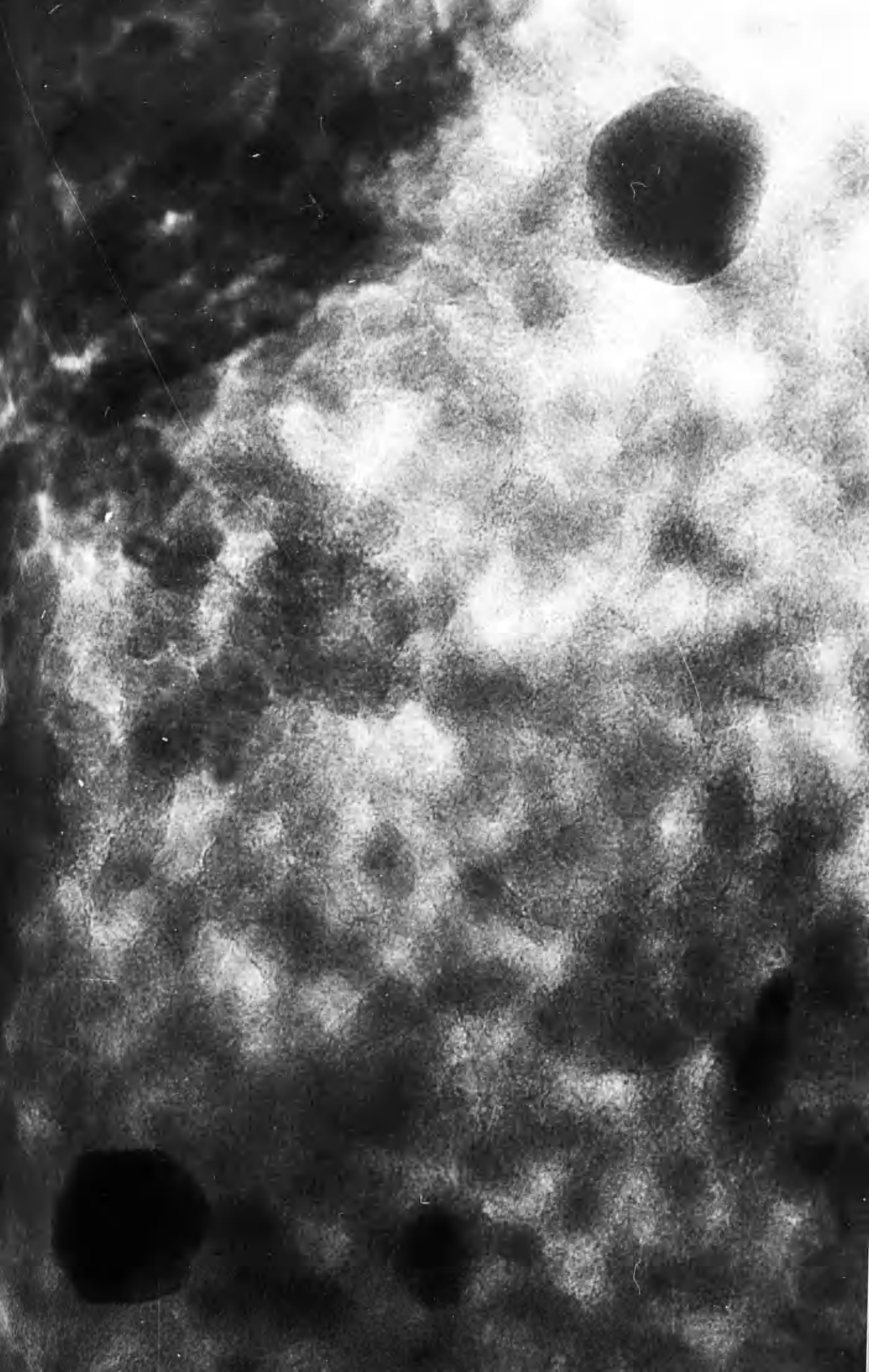

Figure 5.12: Particle size distribution following ageing of C2

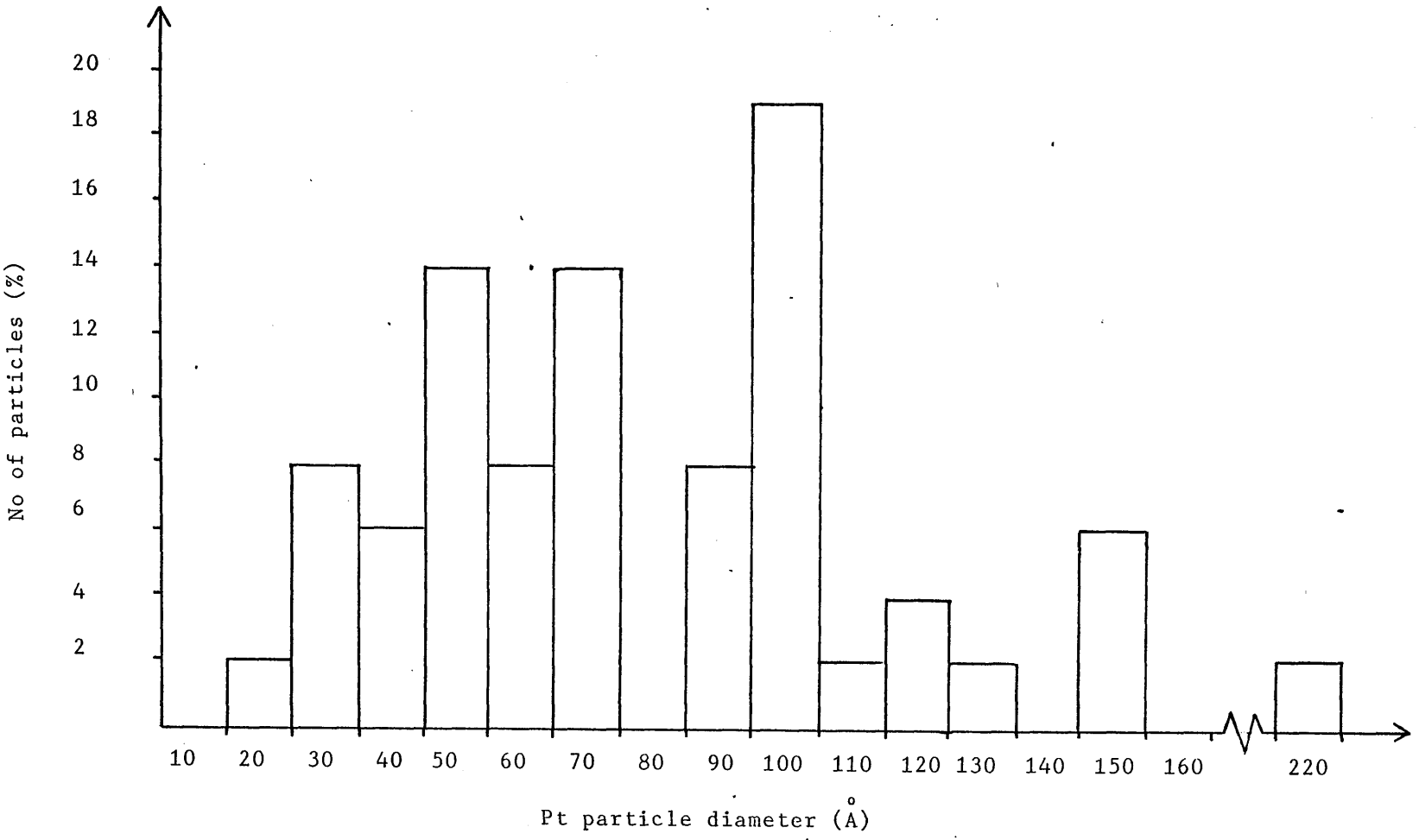

Plate 16

Sintered platinum particles remaining following oxychlorination treatment of C2.

X 2.34M

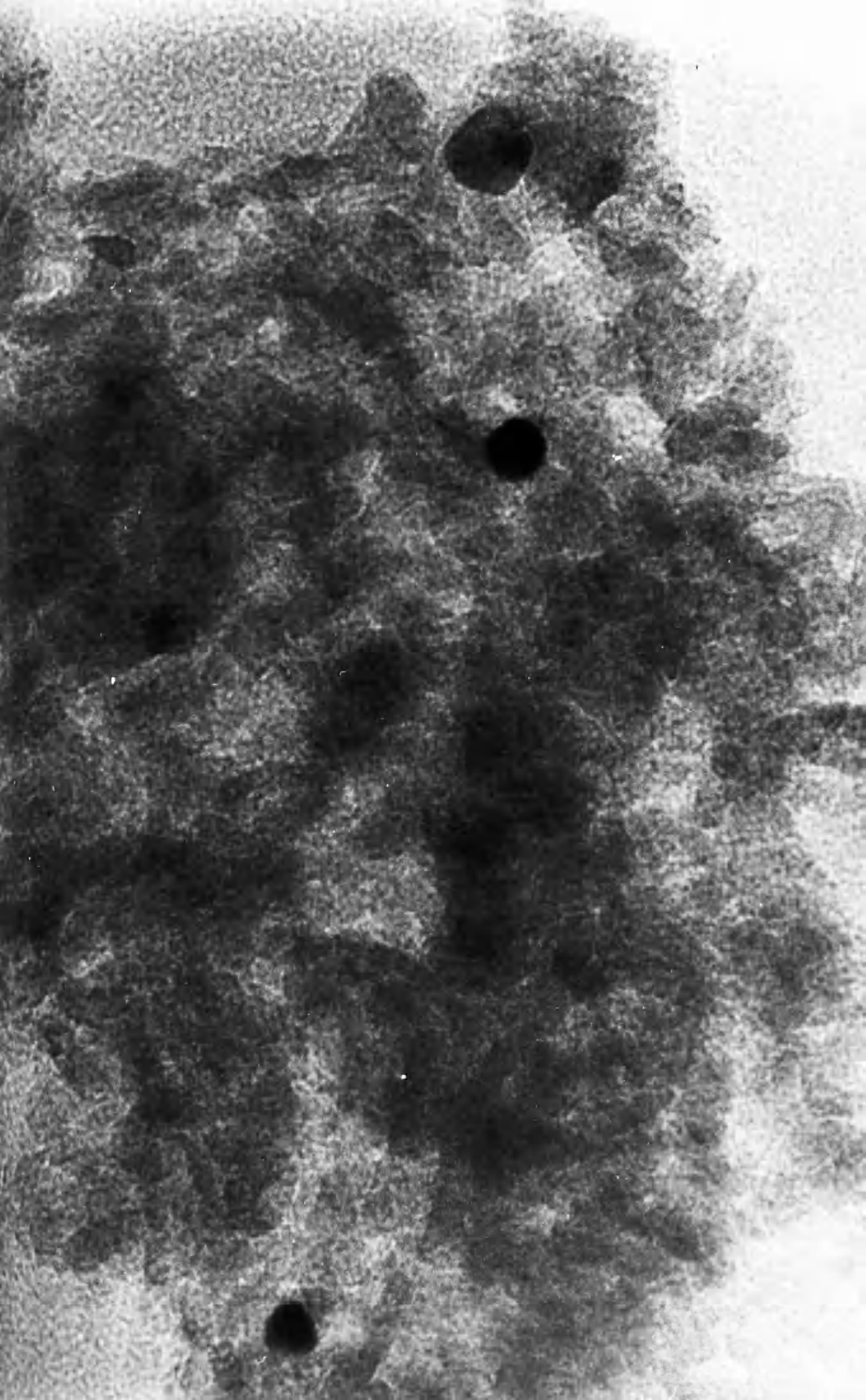

Plate 17

Large platinum particles remaining after 6 pulse oxychlorination cycles.

X 2.34M

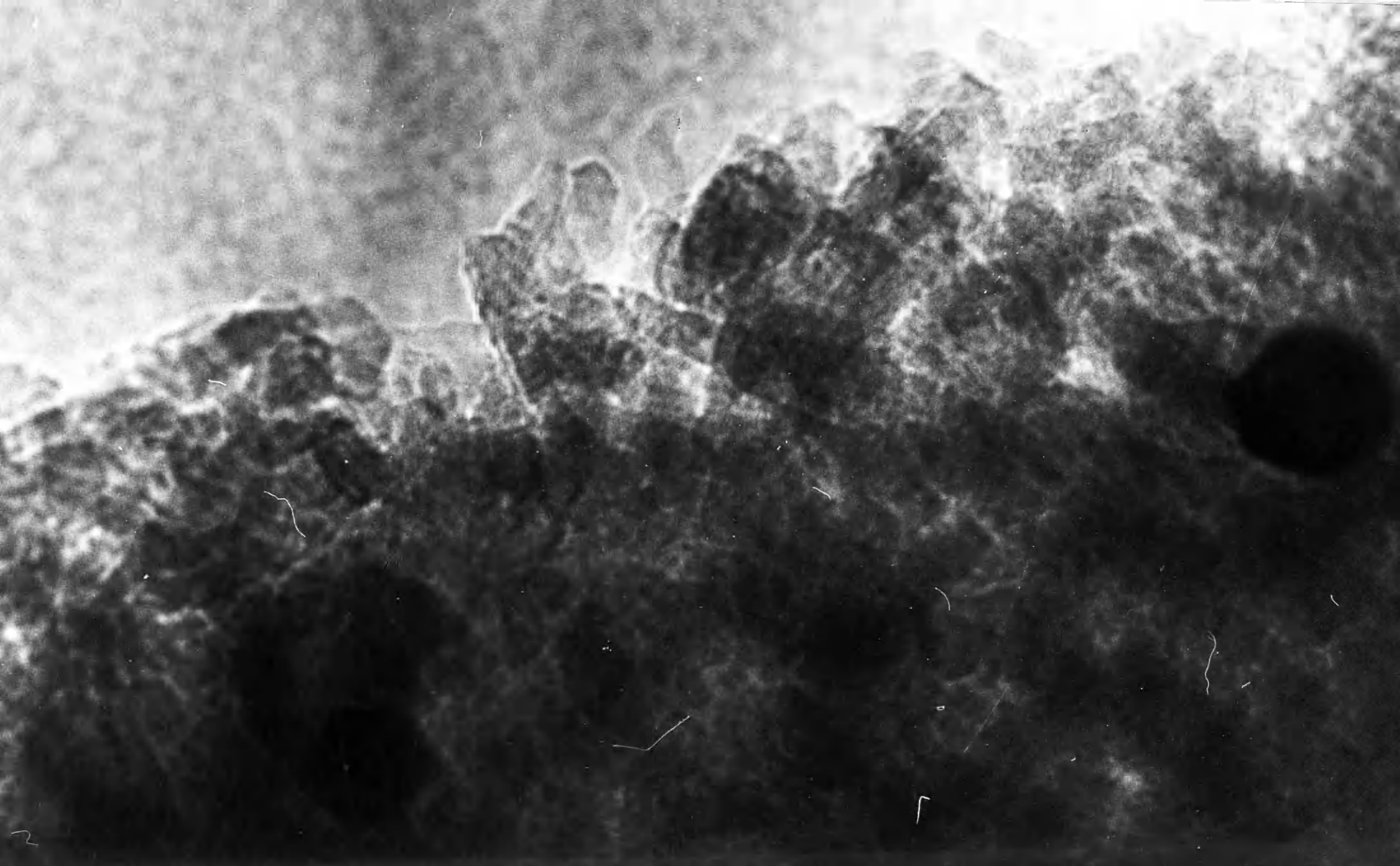

After 10 oxychlorination/reduction cycles (oxychlorination 2.3) large platinum crystallites were still observed (Plate 18).

No change in particle morphology was observed between platinum treated by oxychlorination 2.1 and the particles treated by the pulse oxychlorination/reduction cycles. In each case most of the platinum exists in the form of spherical particles.

Plate 18

Large platinum crystallites following 10 oxychlorination cycles.

X1.32M

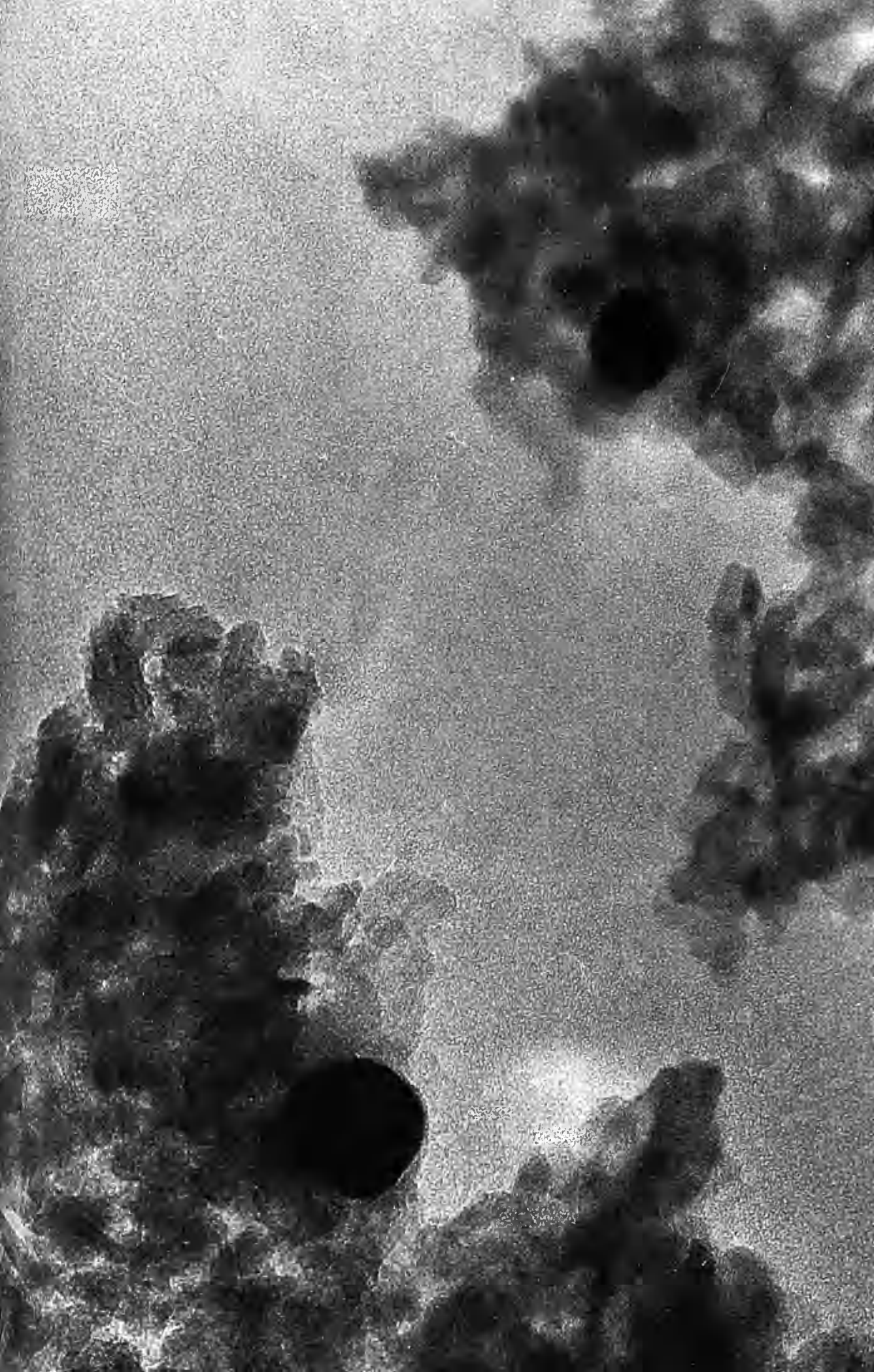

5.3 Catalyst 3

5.3.1 Catalyst Characterisation

The calcined Condea alumina was characterised, as explained in section 5.1, and impregnated with a predetermined amount of hexachloroplatinic acid. Neutron activation analysis confirmed that the catalyst contained 0.79 percent by weight platinum, and 0.86 percent by weight chlorine.

TEM examination showed that catalyst 3 had a mean Pt particle diameter of 16Å with a standard deviation $\sigma = \pm$ 8Å (Plate 19). The platinum was difficult to resolve in the fresh catalyst, indicating that most of the platinum exists at a size below the resolution limit of the microscope. The particle size distribution for the platinum resolved is shown in figure 5.13. CO chemisorption indicates that the fresh catalyst has a mean Pt particle diameter of 13.1Å. The chemisorption and TEM results from C3 are tabulated on Tables 5.5 and 5.6 respectively. X-ray diffraction analysis of the fresh catalyst shows that all of the platinum is below the resolution of the technique (<30Å).

Plate 19

Fresh catalyst 3, showing highly dispersed Pt crystallites.

X 1.47M

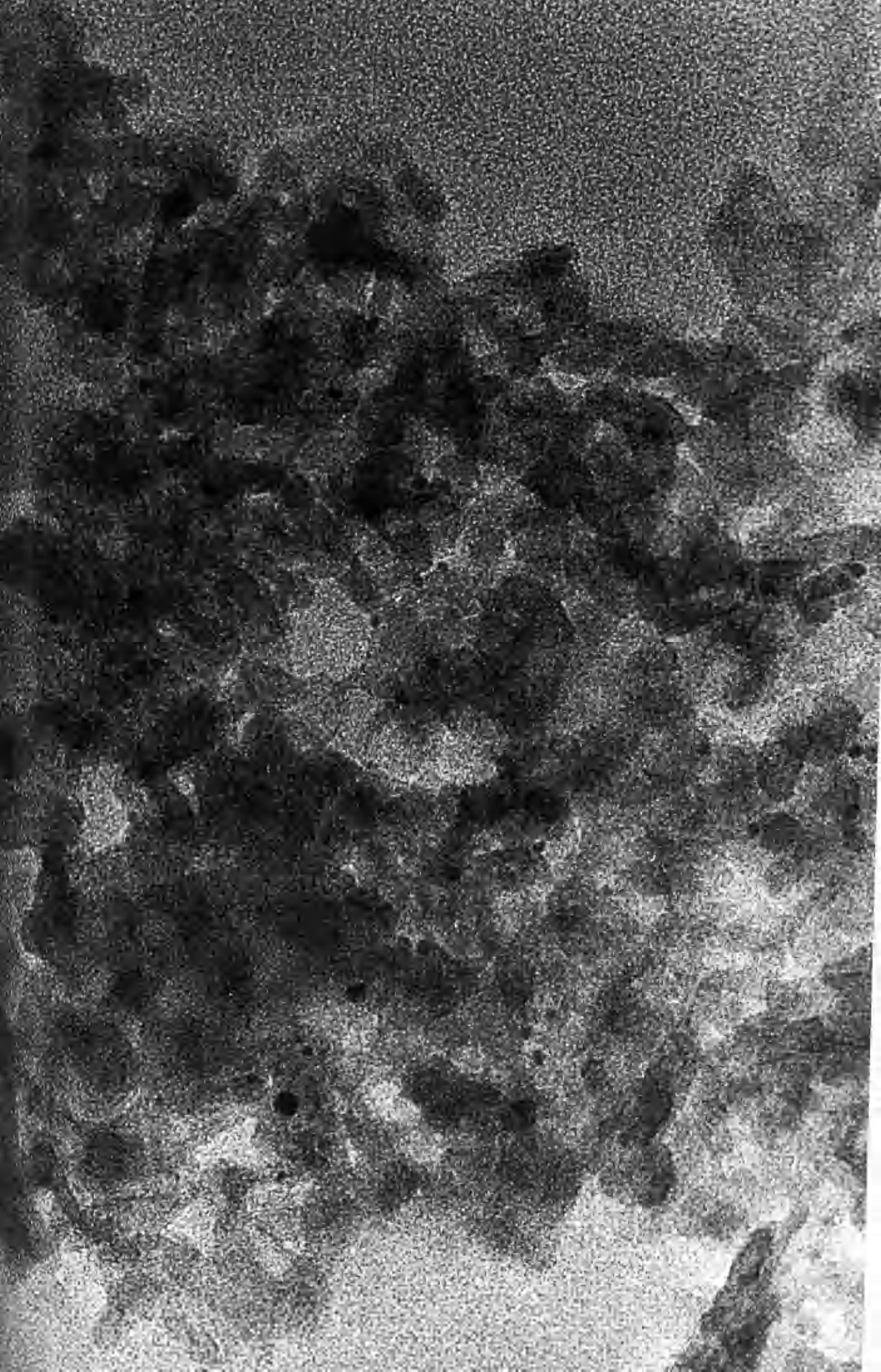

figure 5.13: Particle size distribution of fresh catalyst 3

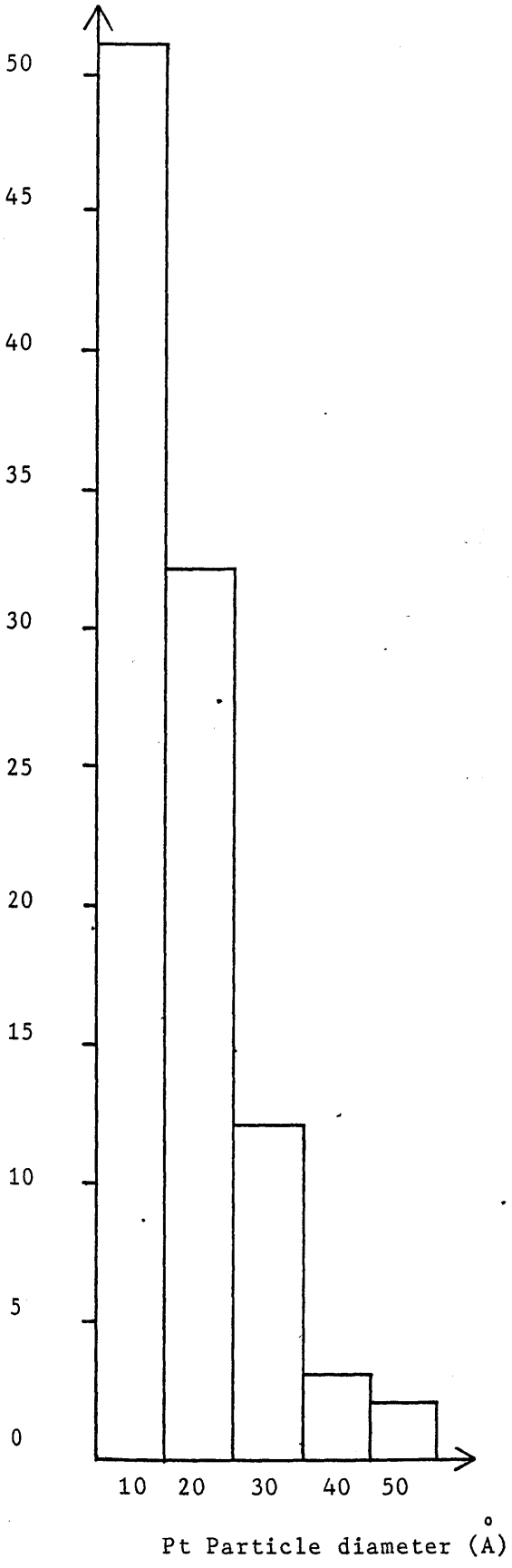

Table 5.5: CO chemisorption data for catalyst 3 following ageing and oxychlorination (oxy) treatments.

	CO Chemisorption	
	Surface Area (m^2/g)	Pt d_{calc} (Å)
fresh	1.7	13.1
2h sinter	0.6	37.1
4h sinter	0.3	74.3
2h sinter, oxy 3h	1.5	14.9
4h sinter, oxy 3h	0.64	34.8
4h sinter, oxy 9h	1.3	17.1
4h sinter, oxy 18h	0.04	552.4

Table 5.6: Electron Microscopy data for catalyst 3, following ageing and oxychlorination treatments.

	TEM		
	d_{mean} (Å)	σ (± Å)	n
fresh	16.2	8	59
2h sinter	13.9	6.3	305
4h sinter	49.0	44	412
2h sinter, 3h oxy	36.0	35.5	167
4h sinter, 3h oxy	119	114	207
4h sinter, 9h oxy	46.3	44	206
4h sinter, 18h oxy	87.0	65	183

Table 5.7: X-ray diffraction line broadening analysis (XRD) results for Catalyst 3, following ageing and oxychlorination (oxy) treatments.

	XRD	
	$\bar{d}$mean (Å)	% weight Pt visible
fresh	-	0
4h sinter	60	0.80
4h sinter, 3h oxy	93	0.67
4h sinter, 9h oxy	149	0.28
4h sinter, 18h oxy	124	0.17

5.3.2 Ageing of Catalyst 3

(i) 2 Hour Sinter

After ageing for 2 hours (sinter 3, section 3.2) the particle size appeared to increase as shown by TEM examination. Platinum was more easily resolved by comparison to the fresh catalyst. Plates 20 and 21 show platinum particles on the alumina following sintering for 2 hours. A mean particle size of 13.9Å was measured by TEM, with a standard deviation $\sigma = \pm$ 6Å. Figure 5.14 shows a particle size distribution for C3 following a 2h sinter. CO chemisorption data indicate an increase in particle size by comparison to the fresh catalyst. A mean particle diameter of 37.1Å was calculated from adsorption measurements (Table 5.5).

Plate 20

Typical area of C3 following ageing for 2 hours.

X 2.49·M

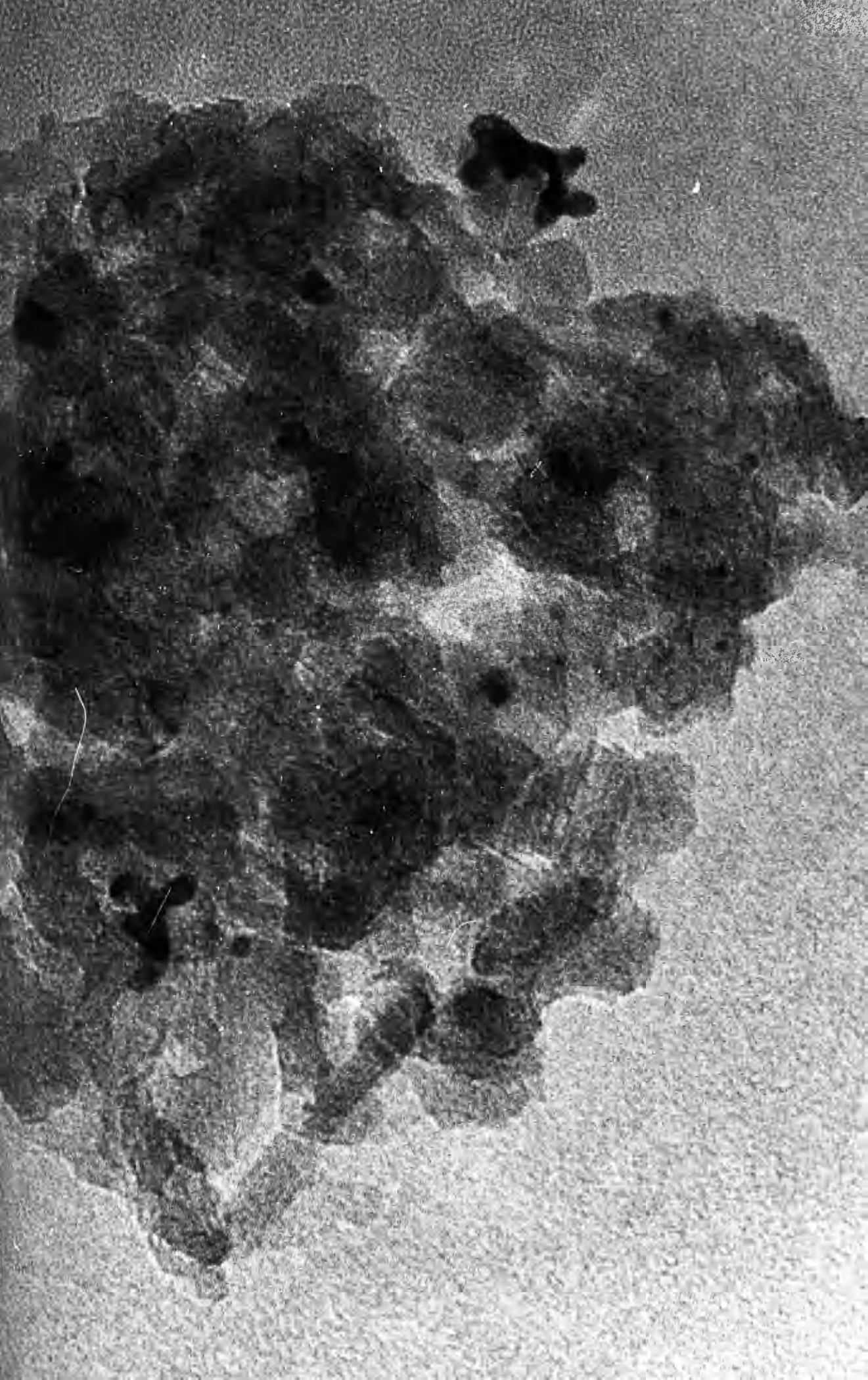

Plate 21

Typical area of C3 following ageing for 2 hours.

X 1.47 M

figure 5.14: Particle size distribution of catalyst 3 following sintering in 3% $O_2|N_2$ for 2 hours.

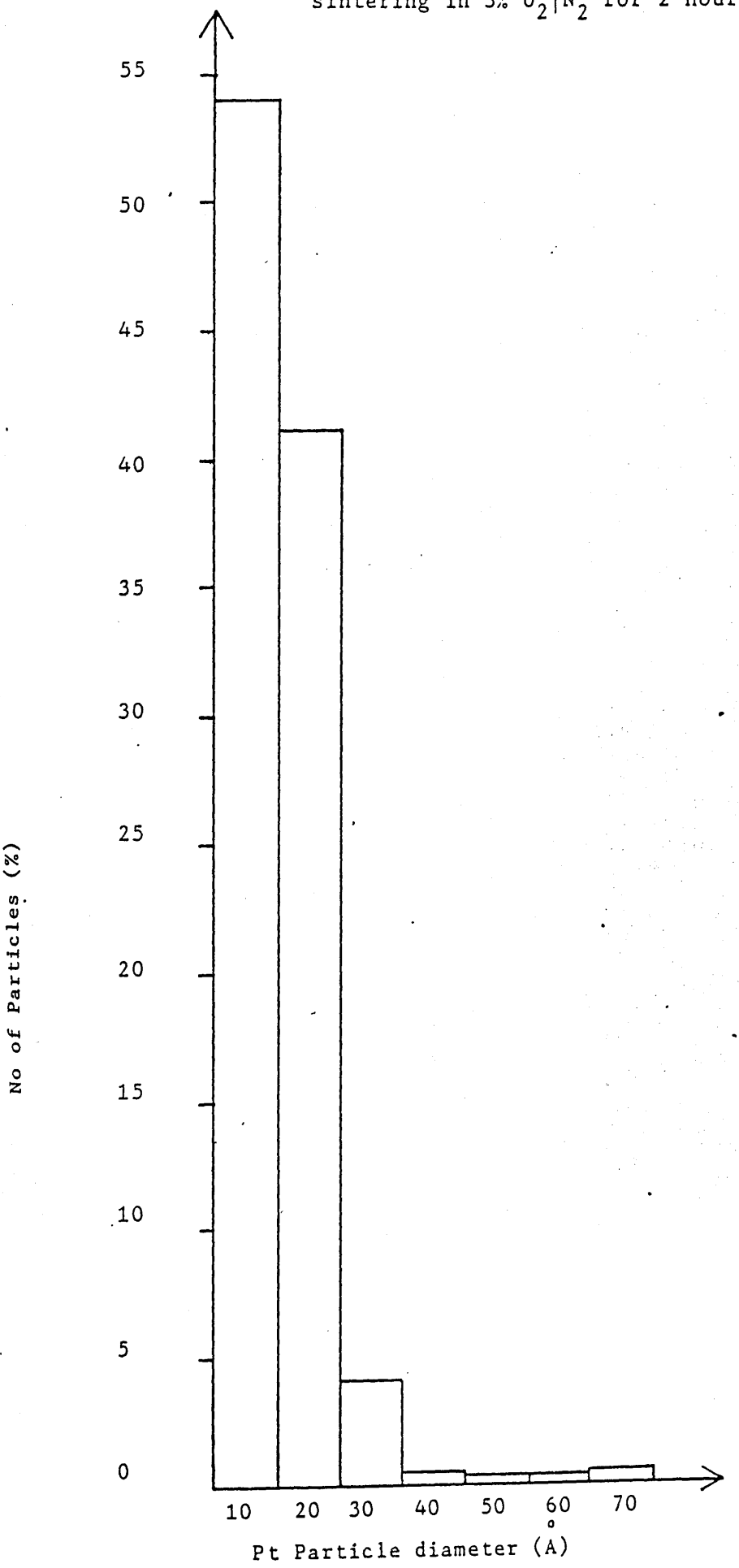

(ii) 4 Hour Sinter

The fresh catalyst, C3, was sintered in 3% O_2/N_2 at 600°C for 4 hours, as explained in the experimental section (sinter 4). An increase in particle size was observed by TEM. (Table 5.6). Plates 22 and 23 show large platinum crystallites following this treatment. The particle size distribution, measured from TEM, is shown by figure 5.15.

CO chemisorption results show an increase in platinum particle size following the 4 hour ageing treatment, as indicated in Table 5.5.

X-ray diffraction line broadening (XRD) indicates a mean particle diameter of 60Å, following ageing for 4h (Table 5.7). All of the platinum was detected, as indicated by quantitative XRD. The XRD trace of the platinum (311) reflection is shown in figure 5.16(a).

Neutron activation analysis found the Cl - level to be 0,78 w/o chlorine.

Plate 22

Typical area of C3 following ageing for 4 hours.

X 2.49 M.

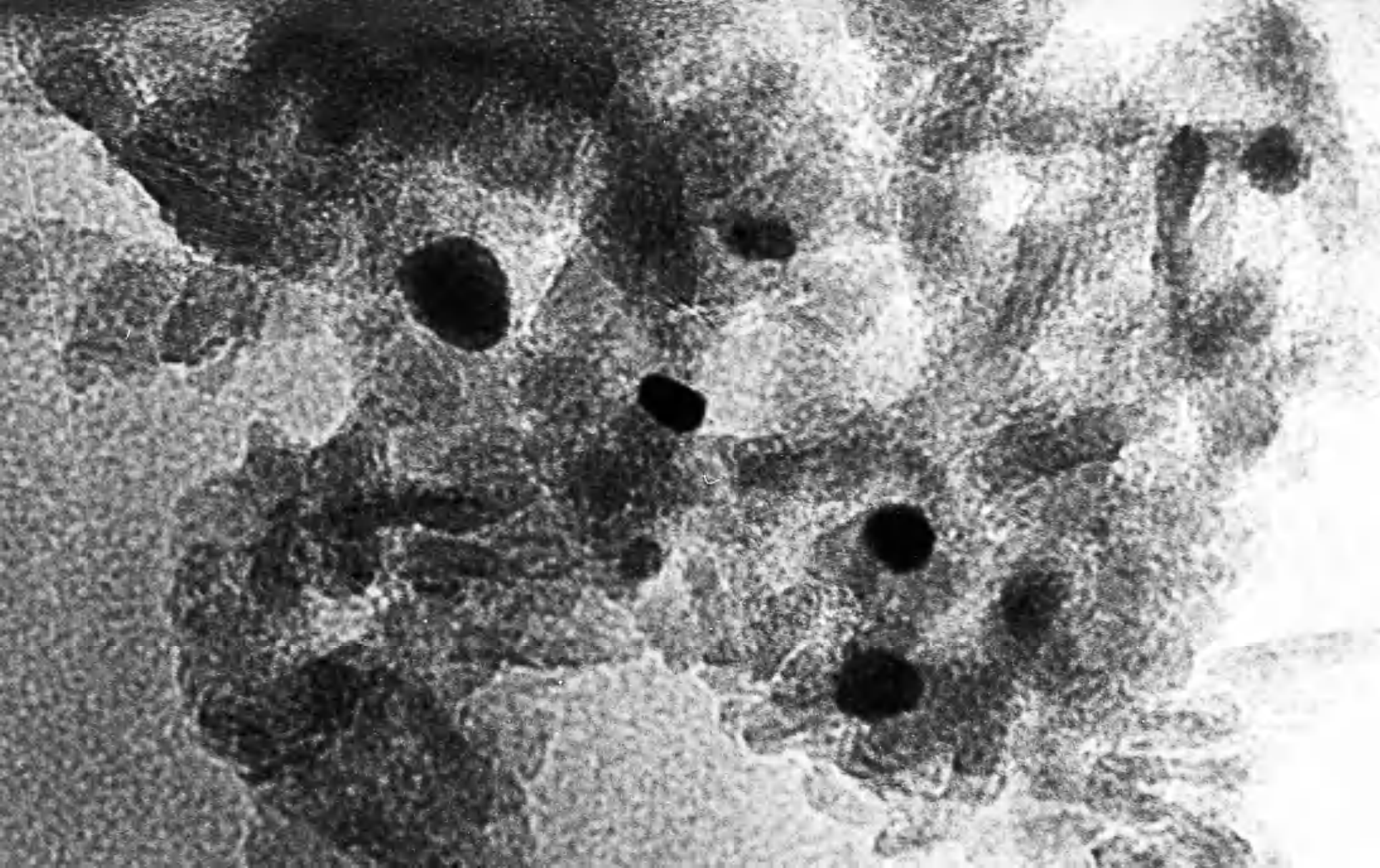

Plate 23

Sintered platinum particles following ageing of C3 for 4 hours.

X 1.41M

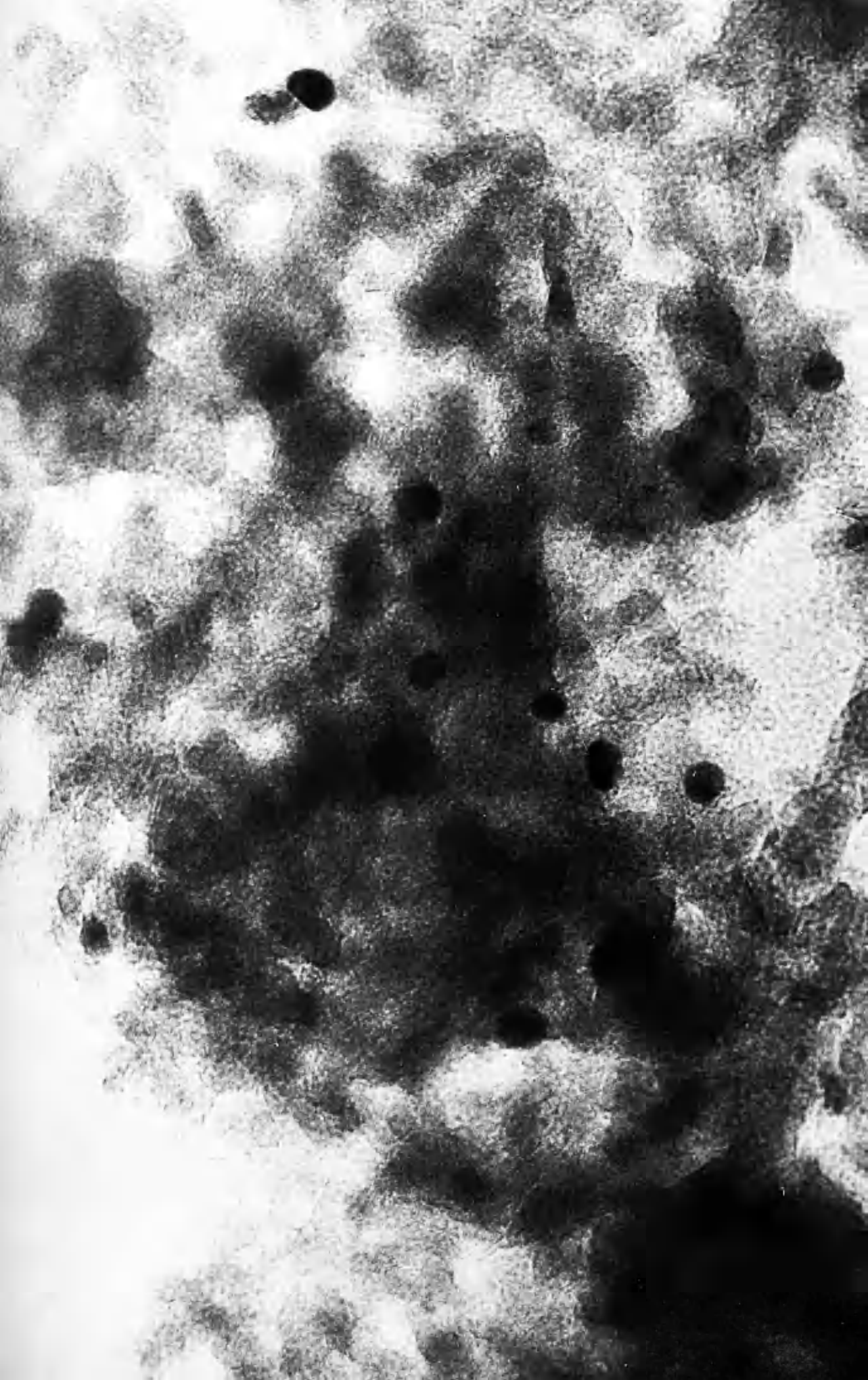

figure 5.15: Particle size distribution of catalyst 3 following sintering in 3% $O_2|N_2$ for 4 hours.

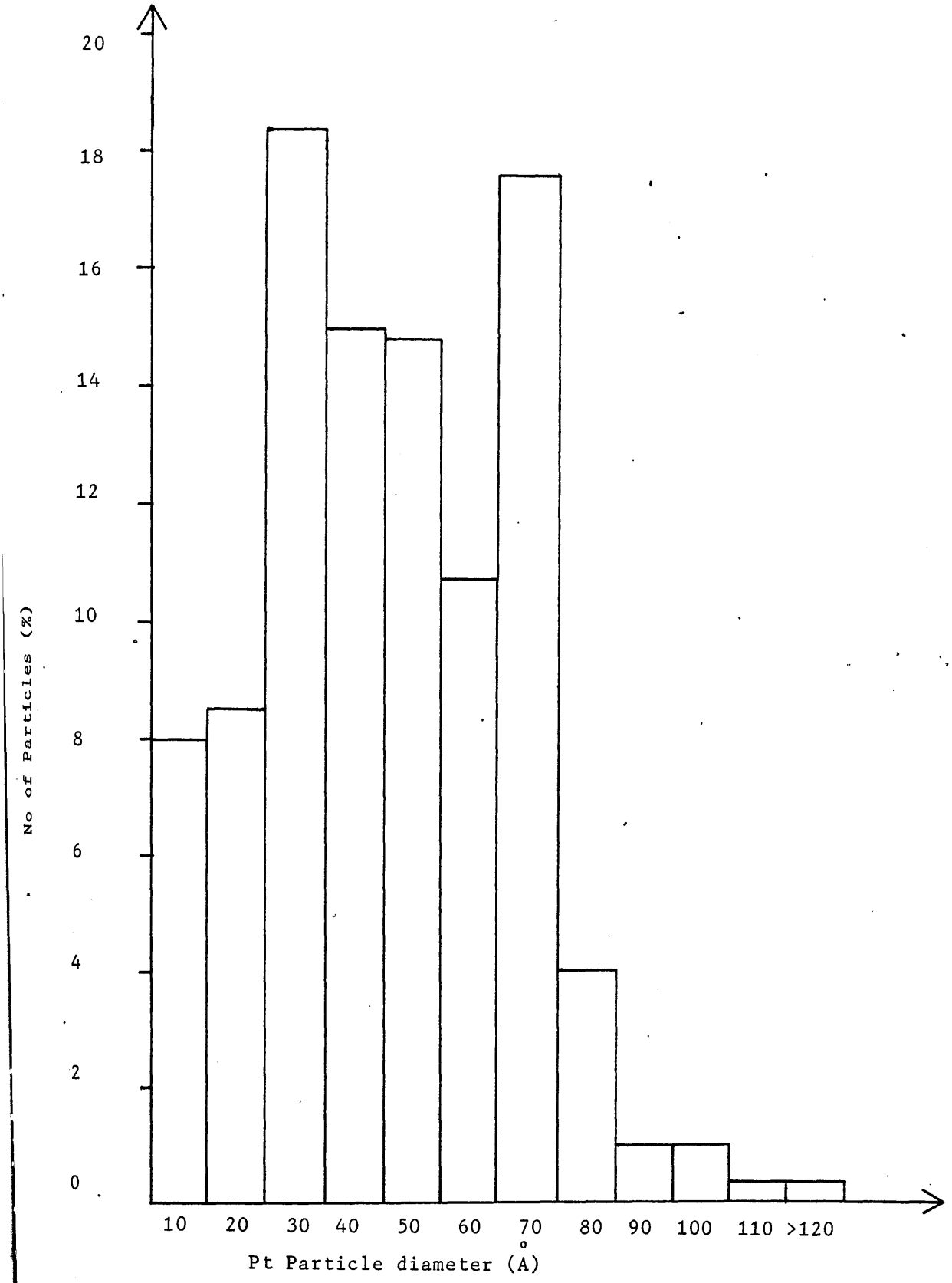

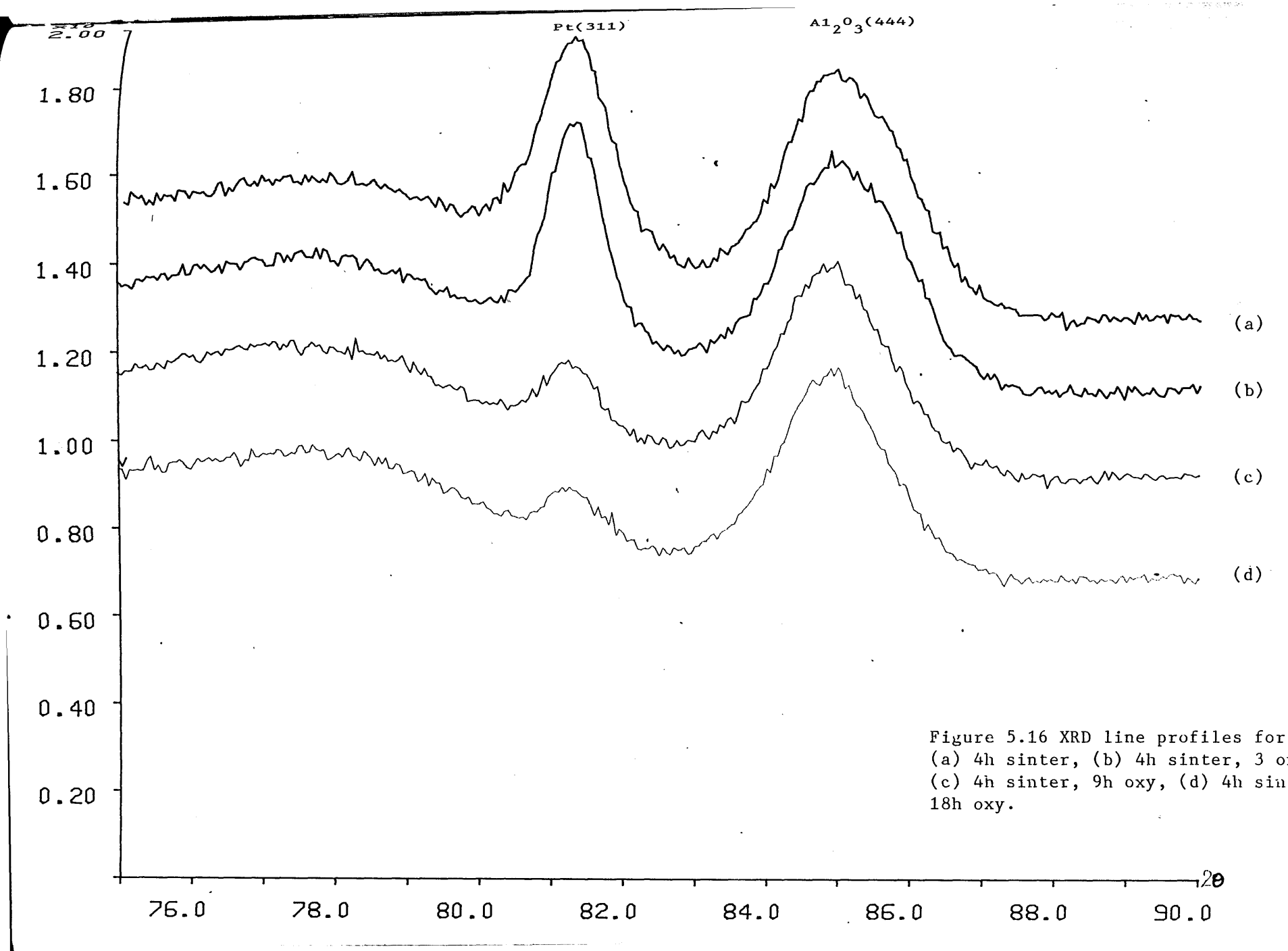

Figure 5.16 XRD line profiles for C3 (a) 4h sinter, (b) 4h sinter, 3 oxy, (c) 4h sinter, 9h oxy, (d) 4h sinter, 18h oxy.

figure 5.17: Particle size distribution of C3 following (i) Ageing for 2 hours (ii) oxychlorination for 3 hours.

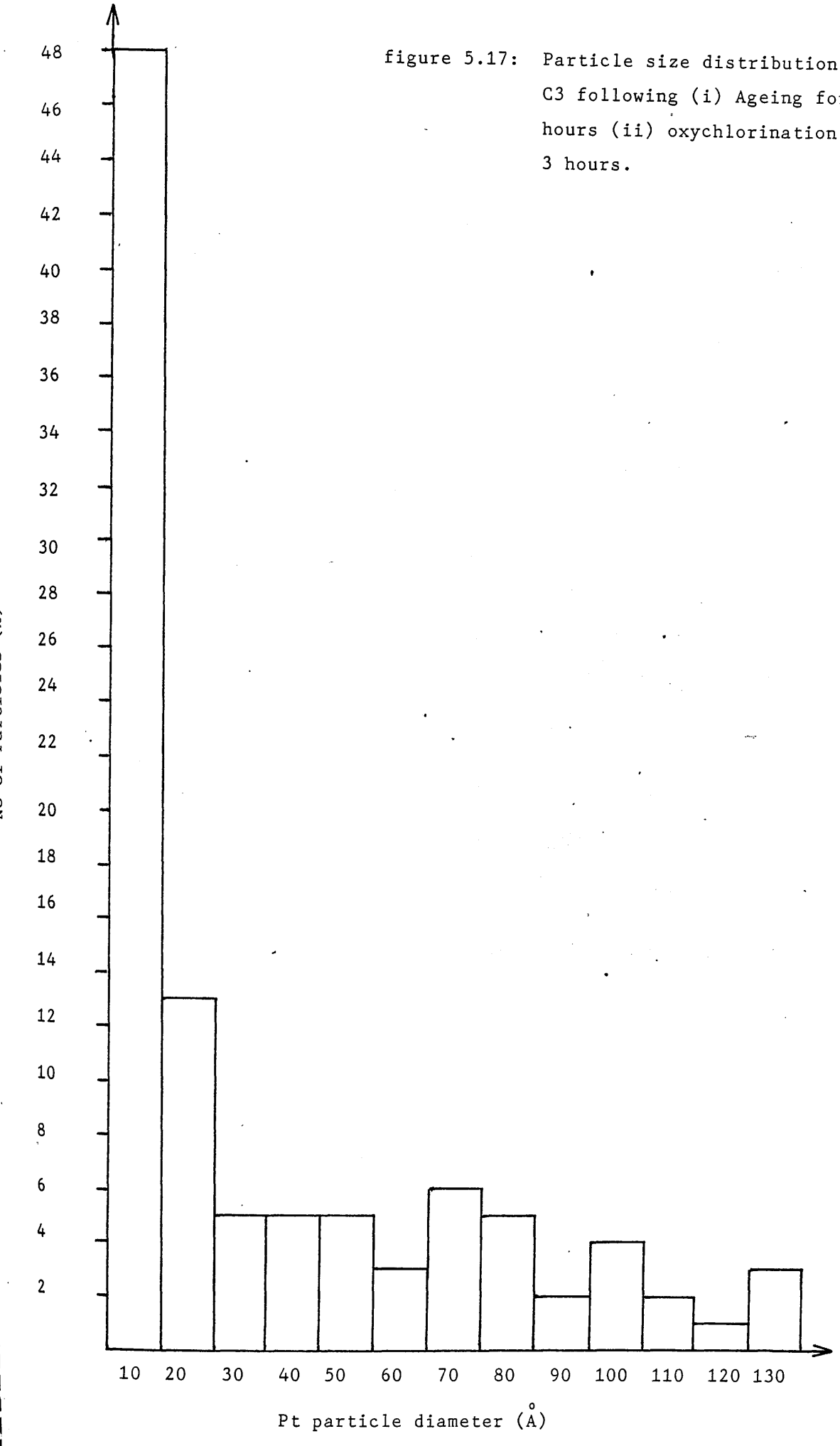

Plate 24

Highly dispersed Pt following oxychloriantion treatment of 2 hour sinter C3.

X1.68 M

(ii) Oxychlorination of a 4h sintered catalyst.

The 4h sintered catlayst was oxychlorinated for 3 hours, 9 hours and 18 hours by oxychlorination treatments 3.2, 3.3 and 3.4 respectively (chapter 3).

Neutron activation analysis was used to determine the amount of chlorine in the catalyst following each treatment (Table 5.8).

CO chemisorption results (Table 5.5) indicate an increase in surface area after oxychlorination treatment for 3h and a further increase in surface area following the 9h treatment. However after the 18h oxychlorination treatment the surface area, as determined by CO chemisorption, decreased to 0.04 m^2/g.

X-ray diffraction line profiles for catalyst 3 following each attempted regeneration are shown in figure 5.15. From this figure it can be seen that the width of the Pt (311) peak decrease with the time of oxychlorination. This indicates an increase in the size of the platinum crystallites. Values for the mean platinum particle size, calculated from XRD profiles, are shown on Table 5.7. The area under the Pt (311) Peak decreases with oxychlorination time (figure 5.18), and hence the amount of platinum detected by X-ray analysis ('visible' Pt) decreases. (Table 5.7).

TEM results are tabluated in Table 5.6. After oxychlorination for 3 hours the platinum appeared to be sintered. Plate 25 shows sintered platinum crystallites following a 3h 'regeneration' treatment. Very few small Pt particles (<30Å) have been resolved as indicated in the particle size distribution (figure 5.19).

Table 5.8: Neutron activation analysis to test Cl - content of Catalyst 3, following oxychlorination treatments.

	Percent by weight Cl
fresh	0.86
sinter 4h	0.78
sinter 4h, oxy 3h	0.93
sinter 4h, oxy 9h	1.14
sinter 4h, oxy 18h	1.16

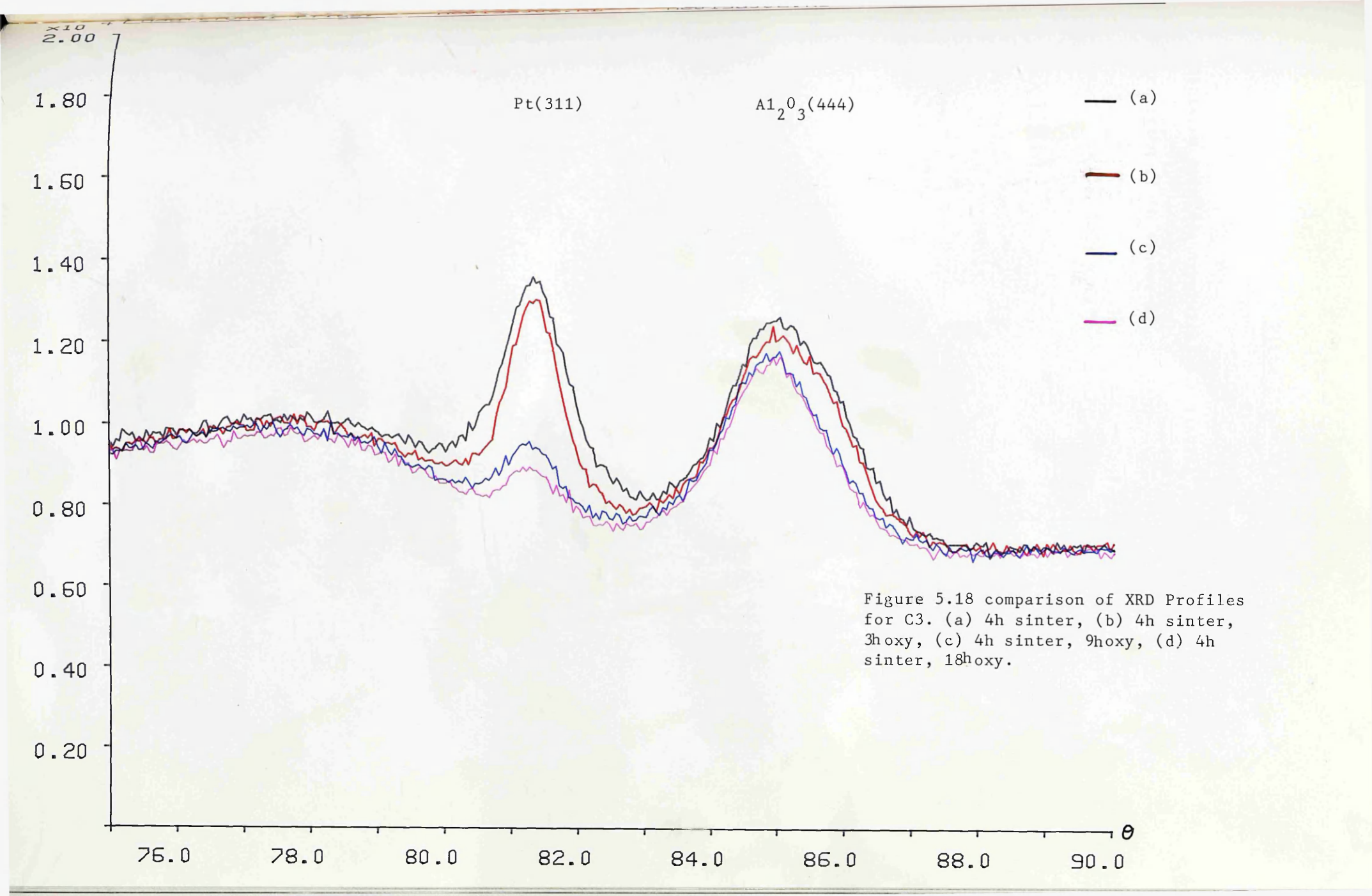

Figure 5.18 comparison of XRD Profiles for C3. (a) 4h sinter, (b) 4h sinter, 3hoxy, (c) 4h sinter, 9hoxy, (d) 4h sinter, 18hoxy.

Plate 25

Sintered paltinum crystallites following 3h oxychloriantion treatment of 4h sinter C3.

X1.38 M

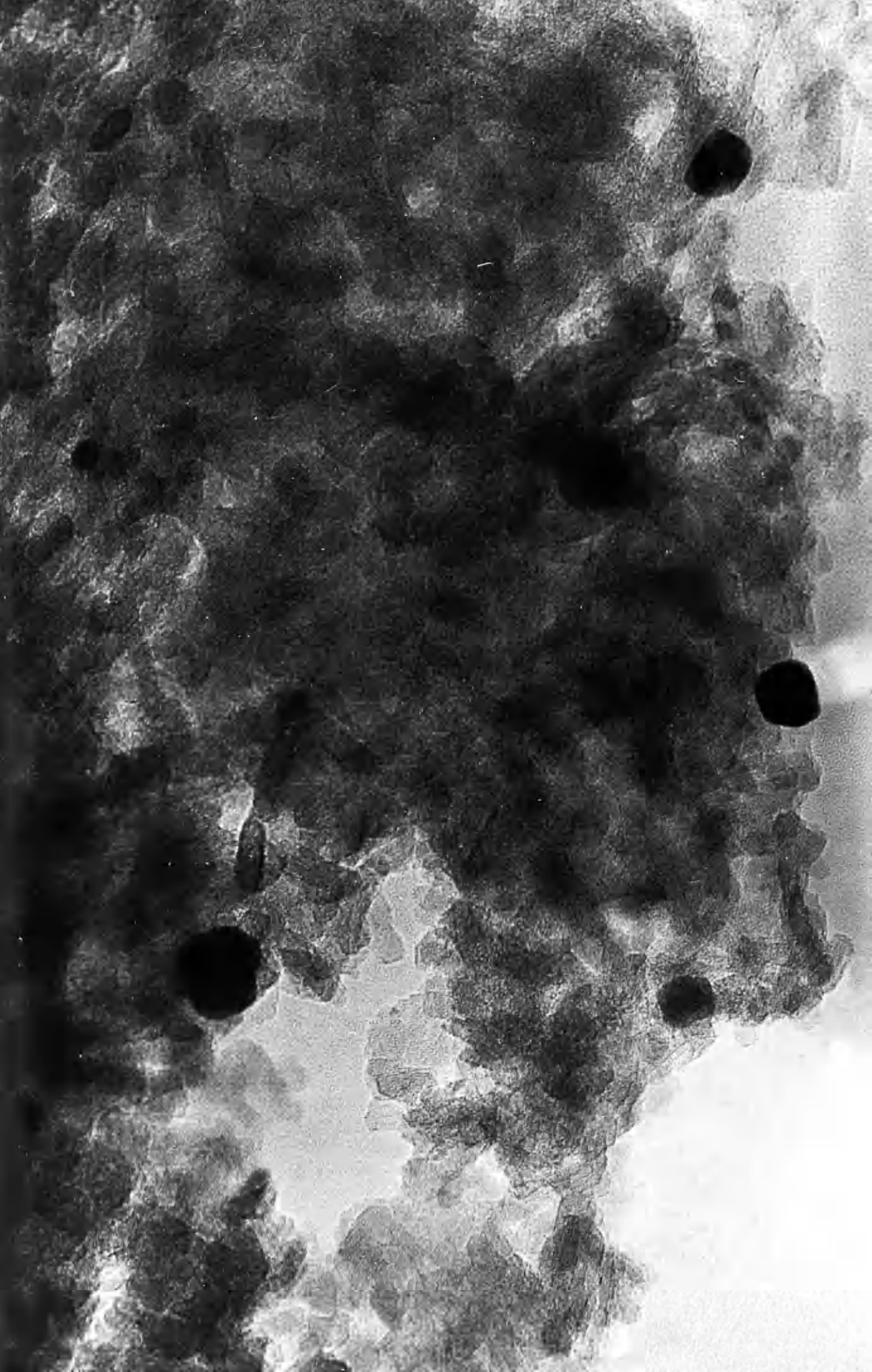

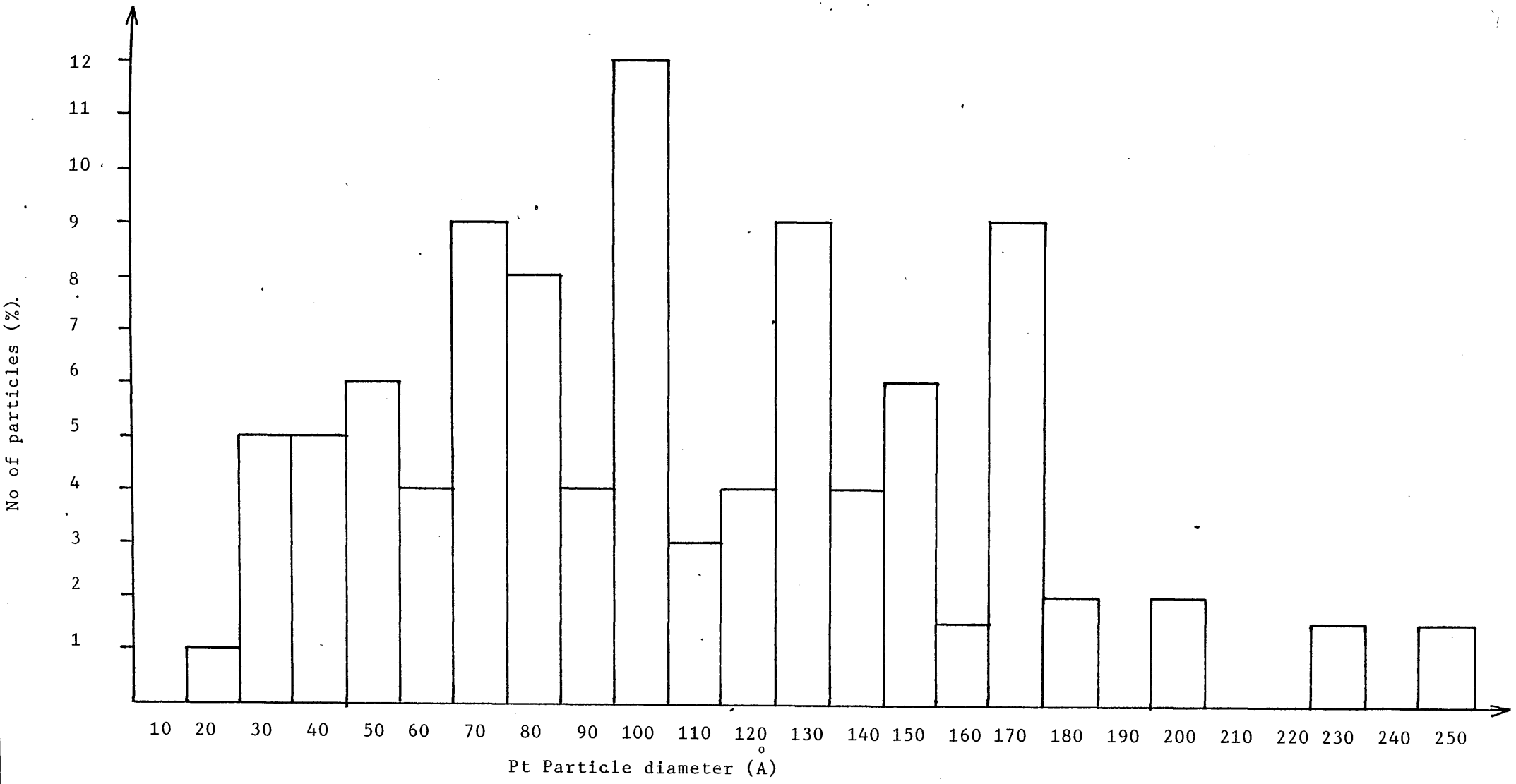

Figure 5.19: Particle size distribution of C3 following (i) Ageing for 2 hours (ii) Oxychlorination for 3 hours.

Plate 26

Typical area of C3 following oxychlorination for 9 hours.

X1.29M

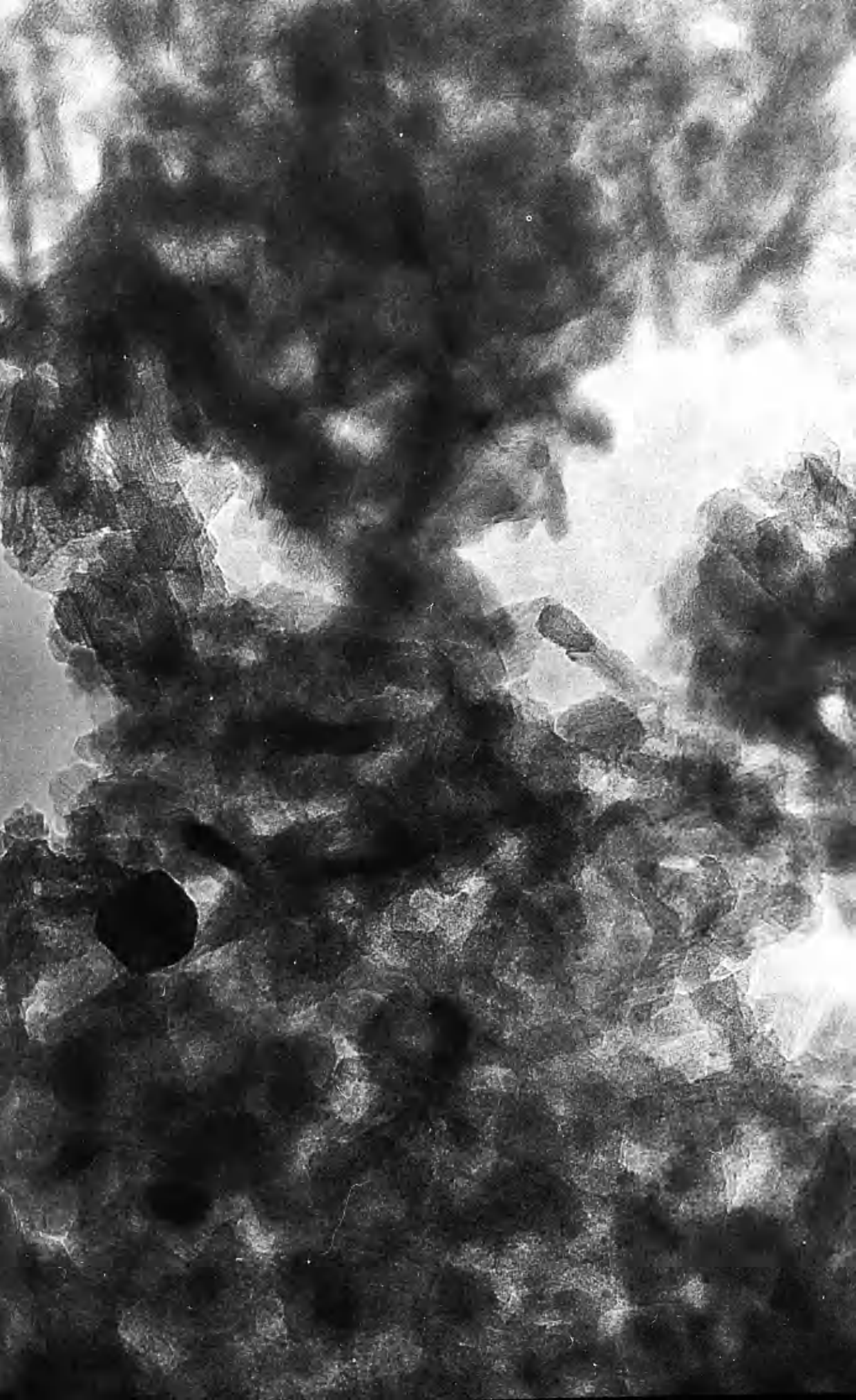

Plate 27

Large platinum particles remaining following oxychloriantion for 9 hours of C3.

X1.32 M

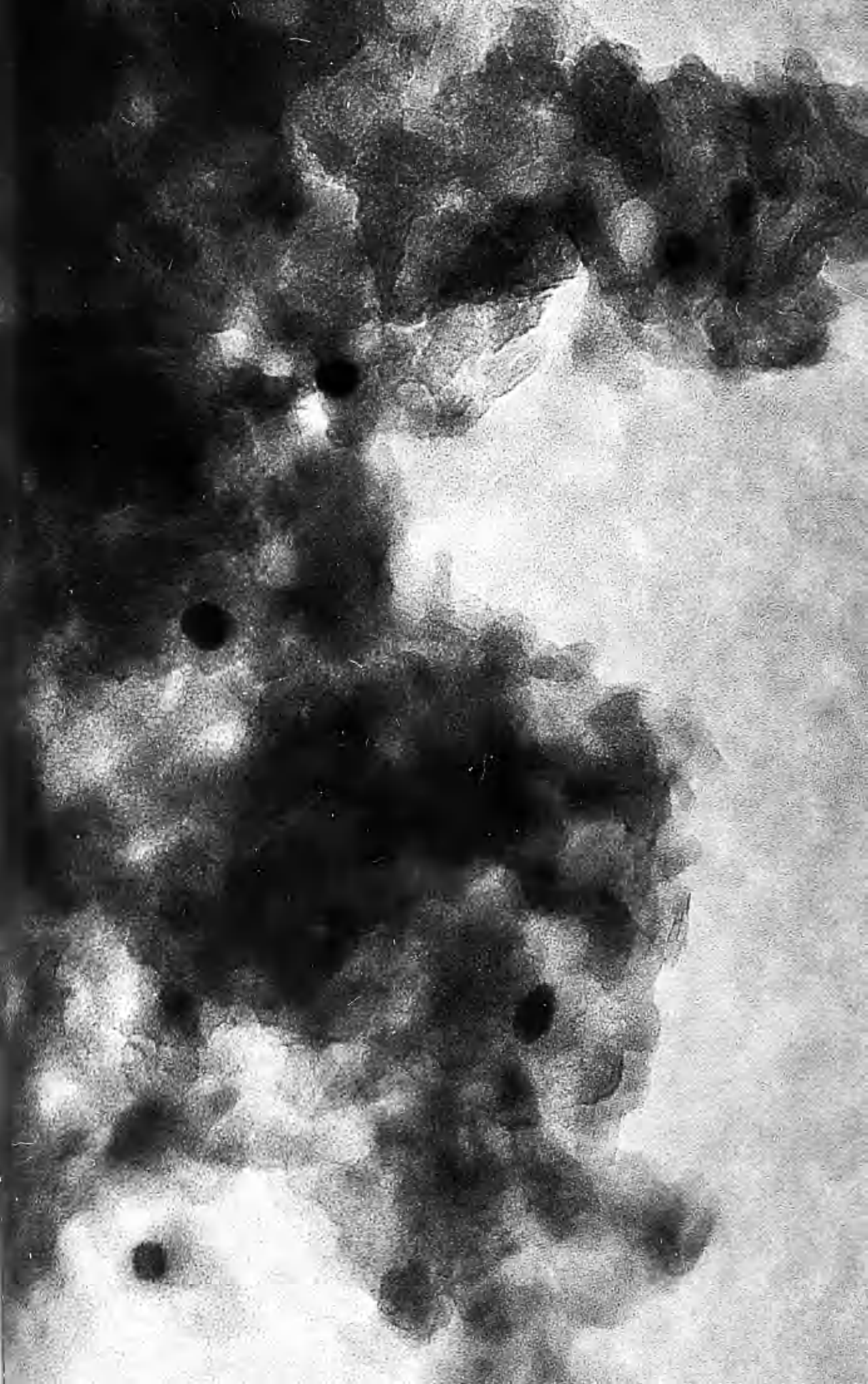

figure 5.20: Particle size distribution of C3 following (i) Ageing for 4 hours (ii) oxychlorination for 9 hours.

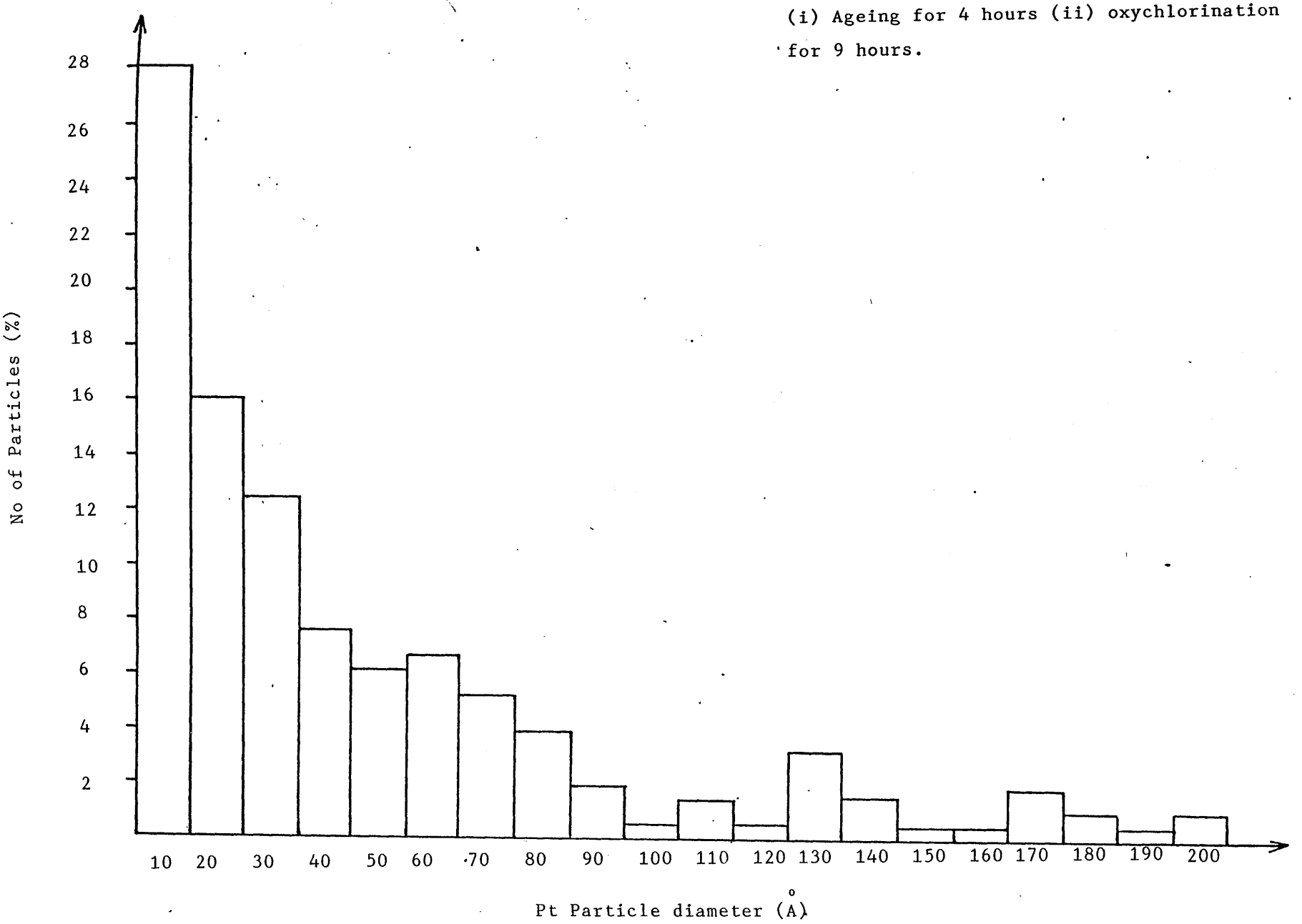

TEM examination of the catalyst following the 9h oxy treatment suggests some redispersion of the sintered Pt particles as very little platinum was detected on the alumina, indicating that most of the platinum exists below the resolution limit of the microscope (<10Å). Plate 26 shows small Pt particles following oxychlorination for 9h. Some large particles remain after this treatment as shown by Plate 27 and the particle size distribution (figure 5.20).

Large sintered platinum particles are formed during the 18h oxychlorination treatment, as shown by TEM (Plates 28 - 29). This suggests that this treatment results in further sintering of the catalyst. However, although the detected platinum was highly sintered, platinum was less easily detected compared with the sintered catalyst. The Pt particle size distribution for the 18h oxychlorinated catalyst is shown in figure 5.21.

Plate 28

Large sintered platinum particles following oxychlorination for 18 hours of C3.

X 550,000

Plate 29

Large platinum particles on C3 following oxychlorination for 18 hours.

X1.59M

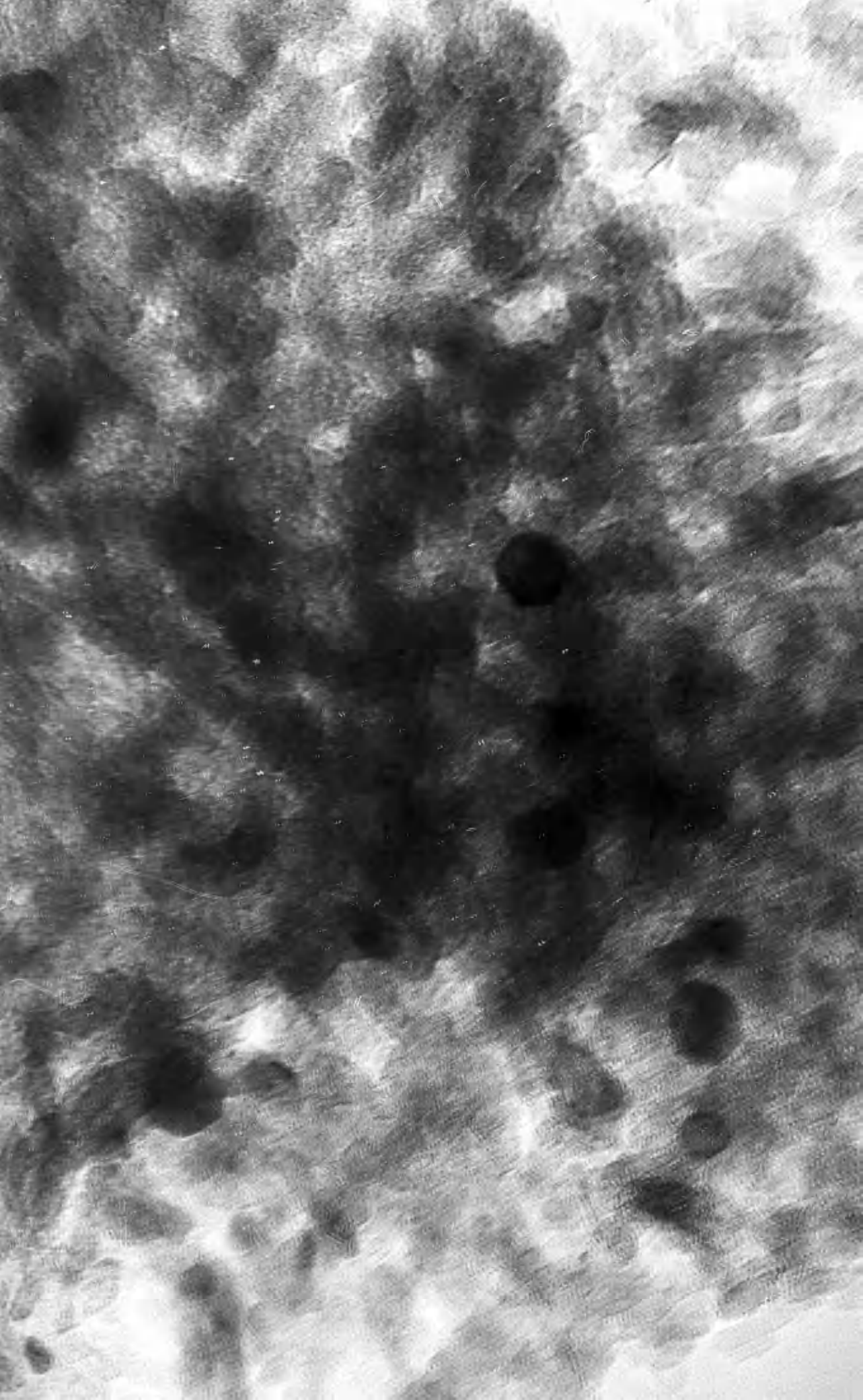

figure 5.21: Particle size distribution of C3 following (i) Ageing for 4 hours (ii) oxychlorination for 18 hours.

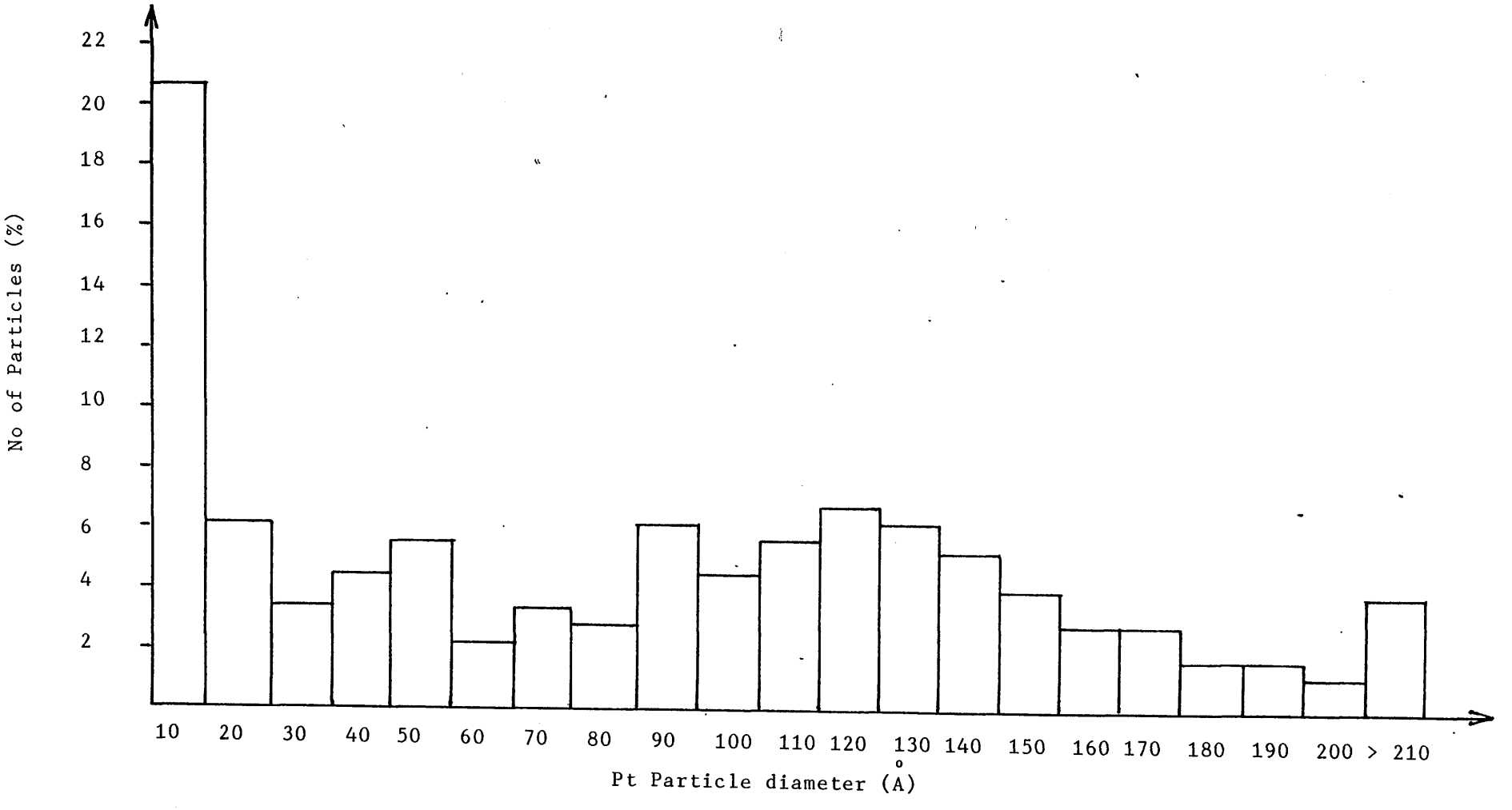

5.4 Oxychlorination of γ- Al_2O_3

The γ-Al_2O_3 was treated by an oxychlorination treatment (oxychlorination 1.6) with a high CCl_4 concentration. The alumina appeared unchanged by TEM examination and the electron diffraction was characteristic of γ-Al_2O_3, although a few areas of the alumina surface appeared affected by the treatment. Plate 30 shows an electron micrograph of an area of alumina following the oxychlorination. The selected area electron diffraction pattern is inset . 7.6Å lattice spacings can be clearly seen from the micrograph, which are not due to γ-Al_2O_3. The spacings calculated from the diffraction pattern are indicated on table 5.9 . The diffraction pattern (single spots) is characteristic of a material with large single crystals, unlike the polycrystalline ring - pattern of γ- alumina. This is in agreement with the long range lattices observed by TEM, suggesting single crystals of up to 500Å. The diffraction spacings have not been identified, by the A.S.T.M. index, as any aluminium oxide, hydroxide or oxychloride.

As TEM results suggest that a small amount of the γ- alumina may be affected by the oxychlorination treatment employed, X-ray diffraction profiles were obtained for the alumina before and after oxychlorination as shown in figure 5.22. No difference was observed between the two alumina samples, suggesting that no change occurs in the γ- alumina structure following the oxychlorination treatment employed.

The surface area of the alumina was determined before and after treatment. The untreated alumina had a surface area of 179 m^2/g, following oxychlorination the alumina surface area was measured as 198 m^2/g. Oxychlorination treatment with high CCl_4 concentration does not decrease the surface area of the alumina.

Plate 30

Area of alumina following oxychlorination with 1400ppm CCl_4. Electron diffraction pattern is insetted.

X 1.32M

TABLE 5.9

Diffraction spacings from diffraction Pattern Plate.30.

γ-Al_2O_3 following oxychlorination treatment.

8.4
4.0
2.69
2.24
1.79
1.22
1.34
1.08
1.68

figure 5.22: XRD profiles of γ-Al_2O_3 and γ-Al_2O_3 following oxy-chlorination.

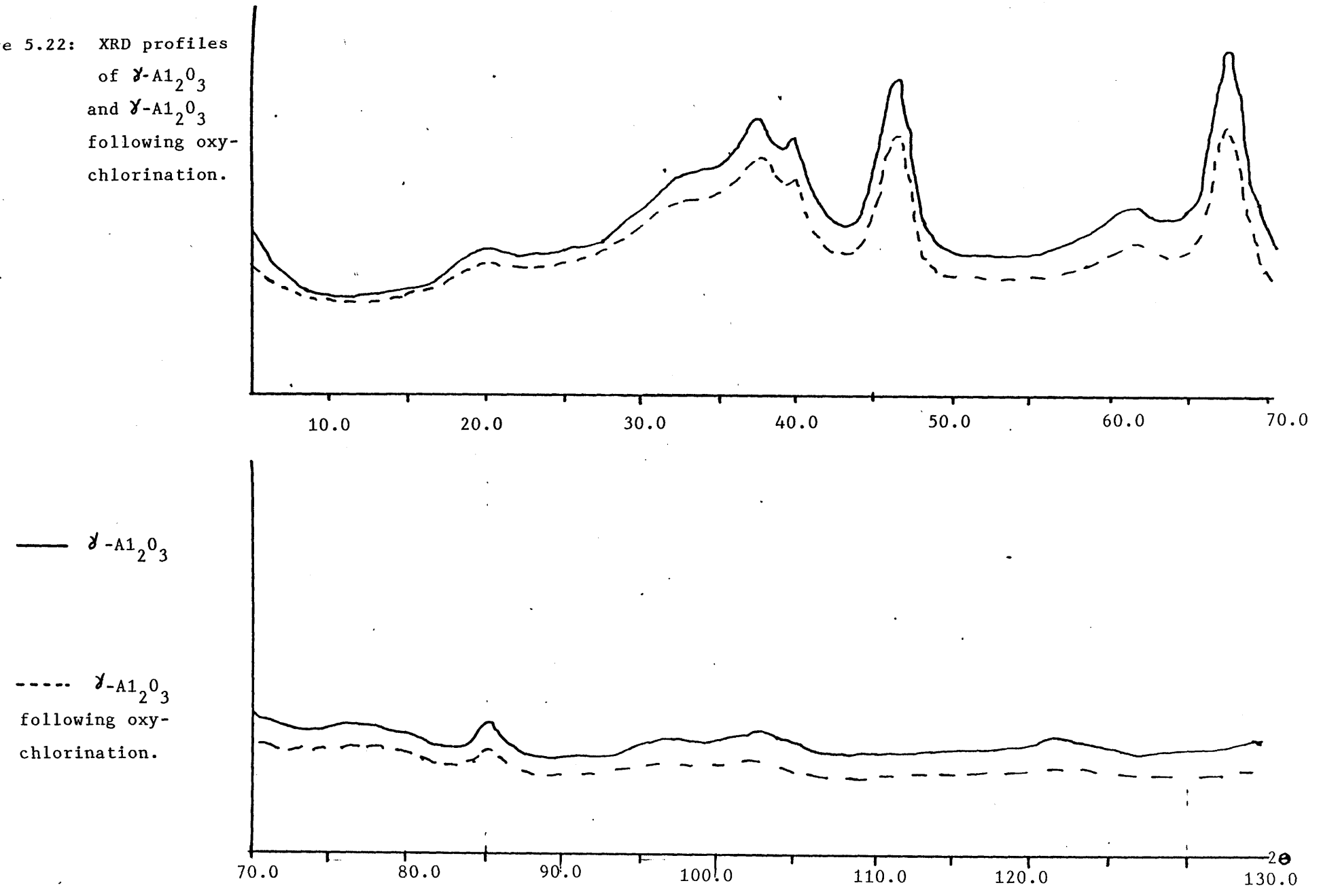

—— γ-Al_2O_3

----- γ-Al_2O_3 following oxy-chlorination.

5.5 Oxychlorination Treatment of a Pt Wire

A length of platinum wire was oxychlorinated by oxychlorination 1.1., as described in the experimental chapter. A scanning electron micrograph of the untreated platinum wire is shown in Plate 31. The surface of the platinum is very smooth, the extrusion lines, from the manufacture of the wire, can be clearly seen.

After oxychlorination treatment several pitted areas appear (Plate 32), suggesting the movement or errosion of the surface platinum on oxychlorination treatment.

Energy dispersive X-ray analysis found that Cl was present on both the untreated and the oxychlorinated wire.

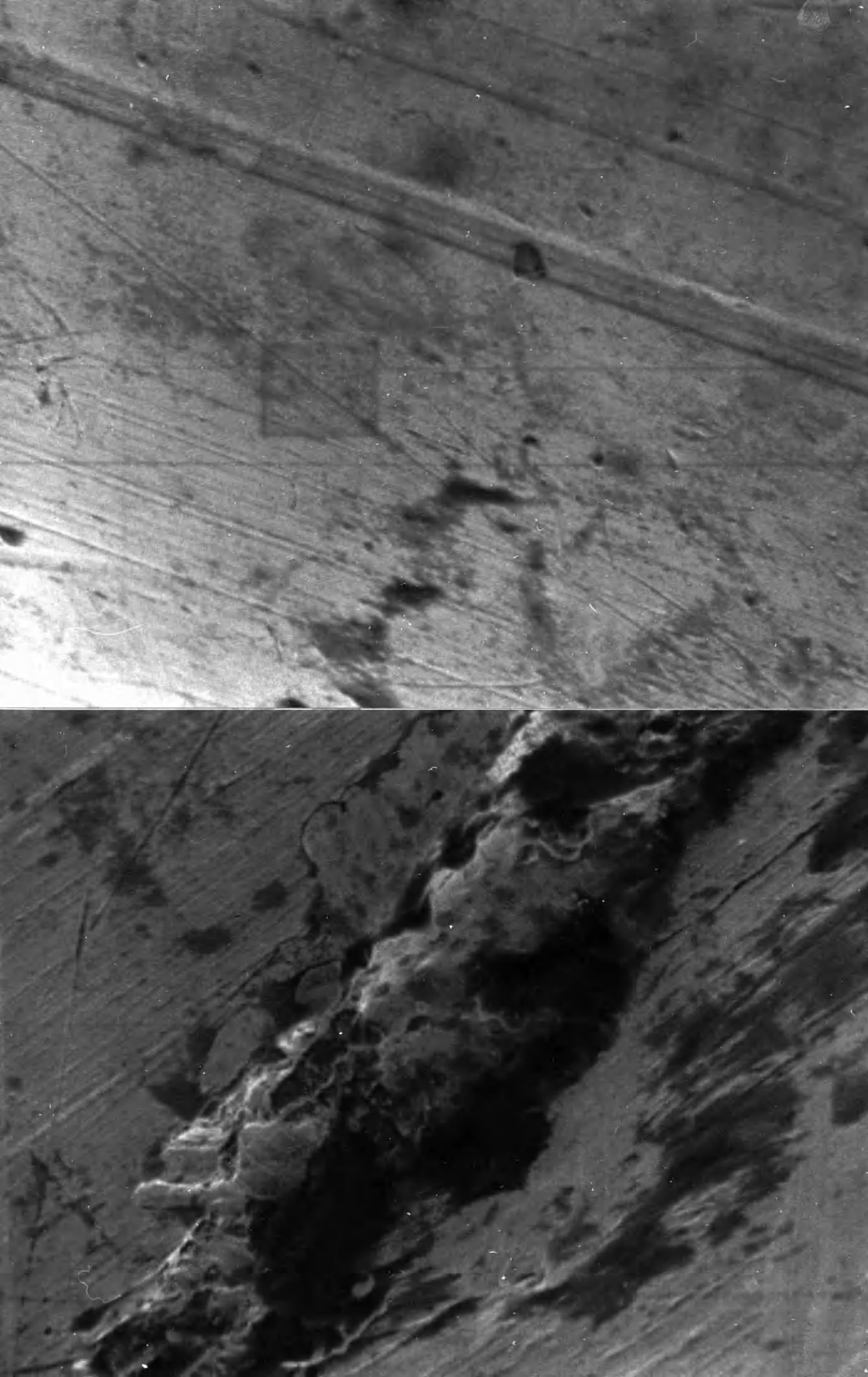

5.6 Stability of Pt (IV) oxide in the Electron Beam

A sample of Pt (IV) oxide was examined by the electron diffraction mode. A diffraction pattern was observed, consisting of diffuse rings typical of an amorphous material. This pattern rapidly changed to sharp rings characteristic of a polycrystalline material. The diffraction pattern is shown by Plate 33.

The measured periodicities were found to compare well with the tabulated values for platinum (Table 5.10), indicating that the Pt (IV) oxide is unstable in the electron beam being reduced to platinum metal.

TABLE 5.10. Measured electron diffraction periodicities and A.S.T.M. indexed X-ray diffraction data for Pt.

Electron diffraction	Pt A.S.T.M. Index		
d (Å)	d (Å)	I/I_o	hkl
2.27	2.265	100	111
1.94	1.962	53	200
1.39	1.387	31	220
1.19	1.183	33	311
1.13	1.132	12	222
0.98	0.981	6	400
0.89	0.900	22	331
0.87	0.877	20	420
0.82	0.801	29	422

Plate 33

Electron diffraction pattern of Pt (IV) oxide, following a few minutes under the electron beam.

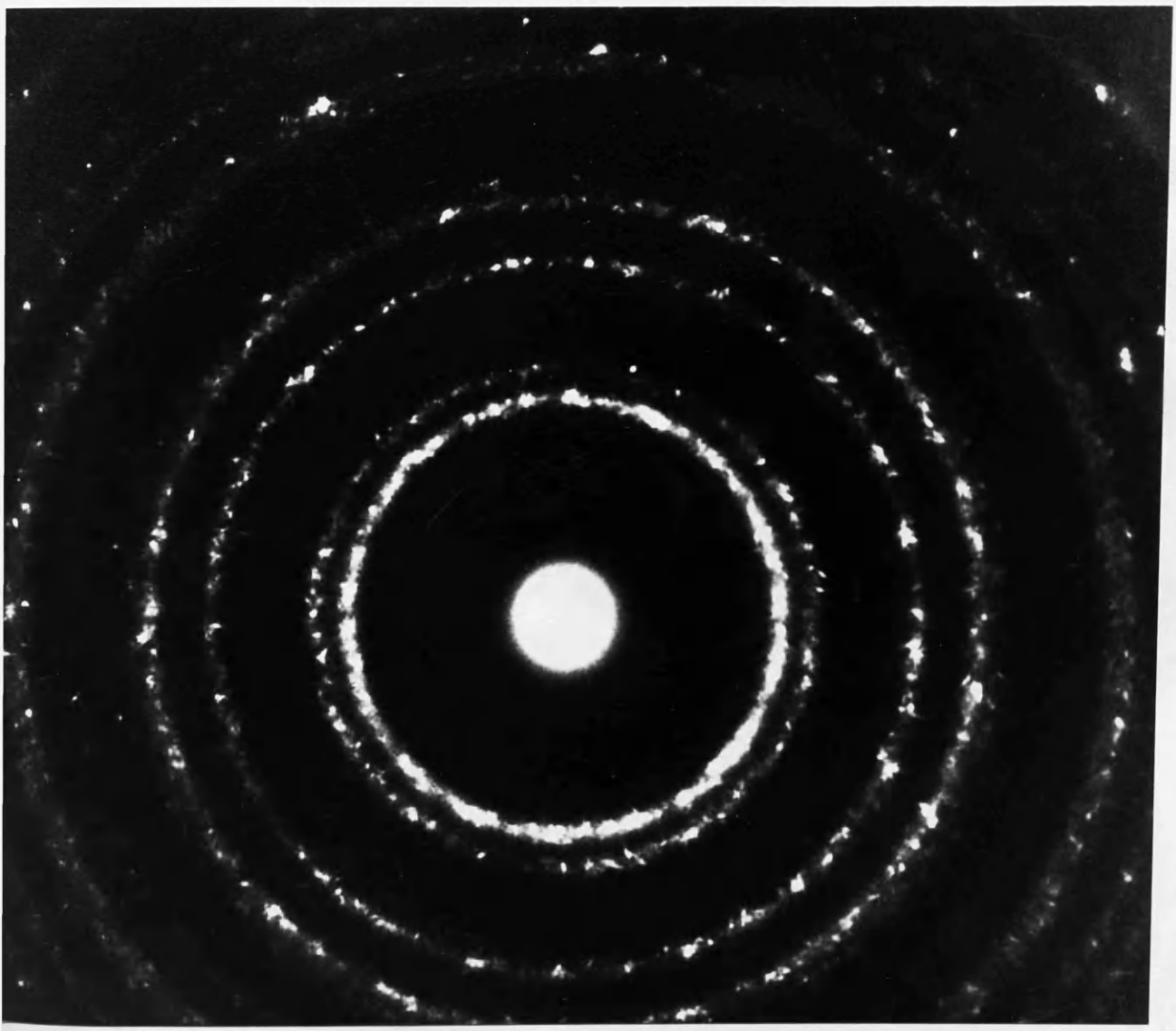

5.7: Micro-Reformer Runs

Table 5.11 shows the catalyst performance at 500°C, 300 psig in naphtha and n-heptane for all four catalyst samples tested. These results show little variation in activity between the catalyst samples, using naphtha as the feed. All catalysts studied behave as reforming catalysts.

Using n-heptane as the feed a better indication of aromatic production is obtained. The direct conversion of n-heptane to aromatics is shown by the toluene production. The toluene yield for the fresh catalyst is 19.5 w/o, on sintering this value is reduced to 12.4 w/o. The oxychlorination treatments increase the toluene yield to 19.0 w/o and 15.9 w/o, for the 9h and 18h oxychlorinations respectively.

Similarly comparing the total aromatic yield from each catalyst it can be seen that the fresh catalyst behaves as a good catalyst producing 22.3 w/o aromatics, on sintering the aromatic yield drops to 15.4 w/o. The aromatic yield is recovered to 21.8 w/o following the oxychlorination treatment for 9 hours.

The differences in activity between the treated catalyst samples can be shown by comparing the amount of unconverted n-heptane following the reforming cycle (Table 5.11). The fresh catalyst has 6.7 w/o unconverted n-heptane. This value increases to 7.6 w/o following the ageing treatment. Oxychlorination for 9 hours reduces this value to 4.8 w/o.

Table 5.11: Catalyst Performance at 500°C, 300 psig in naphtha and n-heptane. (H_2 : HC = 6:1 WHSV = 2.5h^{-1}) of C3 fresh; C3 sinter 4h; C3 sinter 4h, oxychlorination 9h (9h oxy); C3 sinter 4h, oxychlorination 18h (18h oxy).

All yields are wt %.

Feed	Naphtha					n-heptane			
Component	Naphtha Feed	C3 fresh	C3 sinter	C3 9h oxy	C3 18h oxy	C3 fresh	C3 sinter	C3 9h oxy	C3 18h oxy
C1		1.3	0.9	2.5	2.1	1.6	1.3	2.6	2.2
C2		2.0	1.6	2.8	2.4	4.2	4.3	5.1	4.7
C3		4.1	3.4	5.2	4.4	8.4	8.4	10.0	9.4
C4		5.6	4.8	7.1	6.0	11.5	11.8	13.8	13.0
C5+		85.4	87.7	80.8	83.6	72.8	73.0	67.0	69.1
5 Naphthenes	0.1	-	0.1	-	-	-	-	-	-
5 iso Paraffins	-	4.1	3.8	5.0	4.3	7.2	8.4	8.4	7.7
5 n-Paraffins	0.1	1.7	1.5	2.1	1.8	3.3	3.7	3.9	2.9
6 Naphthenes	4.3	0.4	0.6	0.5	0.5	0.2	0.2	0.3	0.8
6 iso Paraffins	4.5	9.2	8.6	9.7	9.5	4.5	4.4	5.4	5.0
6 n-Paraffins	6.4	3.3	3.3	3.1	3.3	0.8	1.3	1.6	1.5
7 Naphthenes	9.6	0.7	0.6	0.6	0.9	1.4	0.8	0.7	0.9
7 iso Paraffins	8.7	9.7	10.8	8.0	10.1	25.6	29.2	19.9	25.1
7 n-Paraffins	9.9	2.6	2.9	1.8	2.4	6.7	7.6	4.8	6.2
8 Naphthenes	9.9	0.4	0.2	-	0.5	-	-	-	-
8 iso Paraffins	11.0	4.9	7.1	2.6	4.5	0.8	1.1	0.4	0.5
8 n-Paraffins	9.6	4.1	1.5	0.5	0.9	-	-	-	-
9 Naphthenes	4.4	-	-	-	-	-	-	-	-
9 iso Paraffins	7.1	-	1.7	0.3	-	0.2	0.5	-	-
9 n-Paraffins	2.8	-	-	-	-	-	-	-	-
Benzene	0.7	3.5	3.8	4.7	4.2	0.8	0.5	1.5	1.1
Toluene	3.8	15.0	14.3	17.3	15.8	19.5	12.4	19.0	15.9
m+p-xylene	4.7	15.8	15.1	15.5	15.1	0.6	0.6	0.6	0.7
o-xylene	1.2	5.1	4.8	5.3	5.2	0.2	0.2	0.2	0.2
C9+Aromatics	0.4	7.1	7.1	3.8	4.0	1.2	1.7	0.5	0.9
Aromatics	-	46.5	45.1	46.7	44.3	22.3	15.4	21.8	18.7
Conversion n-heptane aromatics						25	17	23.7	20

The stability of the catalyst during the reaction is indicated by Table 5.12. The aromatic yield is recorded over the period of the reaction with n-heptane. These results show the fresh and 9 hour oxychlorination catalyst to be stable over the period of time studied. The sintered and 18 hour oxychlorination samples being less stable.

Table 5.12:-

Aromatic Yield from n-heptane V time on line at 500°C, 300 psig, H_2: HC = 6:1 WHSV = $25h^{-1}$.

Time (hours) / Yield Weight % on feed.

Catalyst.

Fresh C3	Hours	168	176	184	192	200	208										
	Yield	22.4	22.5	22.5	22.0	22.3	22.3										
C3	Hours	120	124	128	132	136	144	148	152	156	160	164	172	180	196	204	208
Sinter 4h,	Yield	20.9	18.8	18.6	20.1	17.3	16.9	17.3	16.7	16.4	16.4	16.4	15.6	15.2	15.3	15.4	15.3
C3	Hours	192	200	208	216	228	236	244	252	260	268	276					
Sinter 4h,	Yield	21.6	21.3	21.0	20.7	20.8	20.5	21.1	20.8	21.0	20.2	20.3					
Oxy 9h																	
C3	Hours	148	156	164	172	180	188	196	200	204	212	216	220				
Sinter 4h,	Yield	20.9	20.3	19.5	19.5	18.5	18.3	17.8	18.2	17.6	17.0	16.9	16.6				
Oxy 18h.																	

6. DISCUSSION: Identification of small platinum particles.

6. DISCUSSION: Identification of Small Platinum Particles.

Results from previous work (Spanner, 1984) suggest that sub - 10Å platinum particles may be formed following an attempted redispersion of sintered platinum particles by an oxychlorination treatment. As these small particles are apparently responsible for catalysis it is important that the size, shape and distribution of these particles are known. In a study of the redispersion of sintered platinum particles it is important that these small particles are resolved to give a more accurate particle size distribution. For these reasons one of the aims of this study was to resolve any sub - 10Å platinum particles formed as a result of the regeneration treatment.

In Spanner's work (1984), three techniques were used to characterise the catalyst; transmission electron microscopy (TEM); X-ray diffraction (XRD) and hydrogen chemisorption. The results are shown diagrammatically on figure 6.1. All three techniques found the fresh catalyst to be highly dispersed and the aged catalyst to consist of large sintered platinum crystallites. Conflicting results were obtained following an attempted redispersion by an oxychlorination treatment. Results from TEM and XRD indicated that the large particles formed during sintering were not apparently redispersed on oxychlorination treatment, although catalytic activity was regained and hydrogen chemisorption showed enhanced surface area. Results from quantitative XRD suggest that most of the platinum exists in the form of sub - 10Å platinum particles, 'invisible' to XRD and at the resolution limit of electron microscopy due to contrast effects. The results from the above study, together with results from this present study are reported (Butterly et al., 1986).

figure 6.1: Diagrammatic representation of previous results (Spanner, 1984) indicating the existance of sub-10Å Pt Particles.

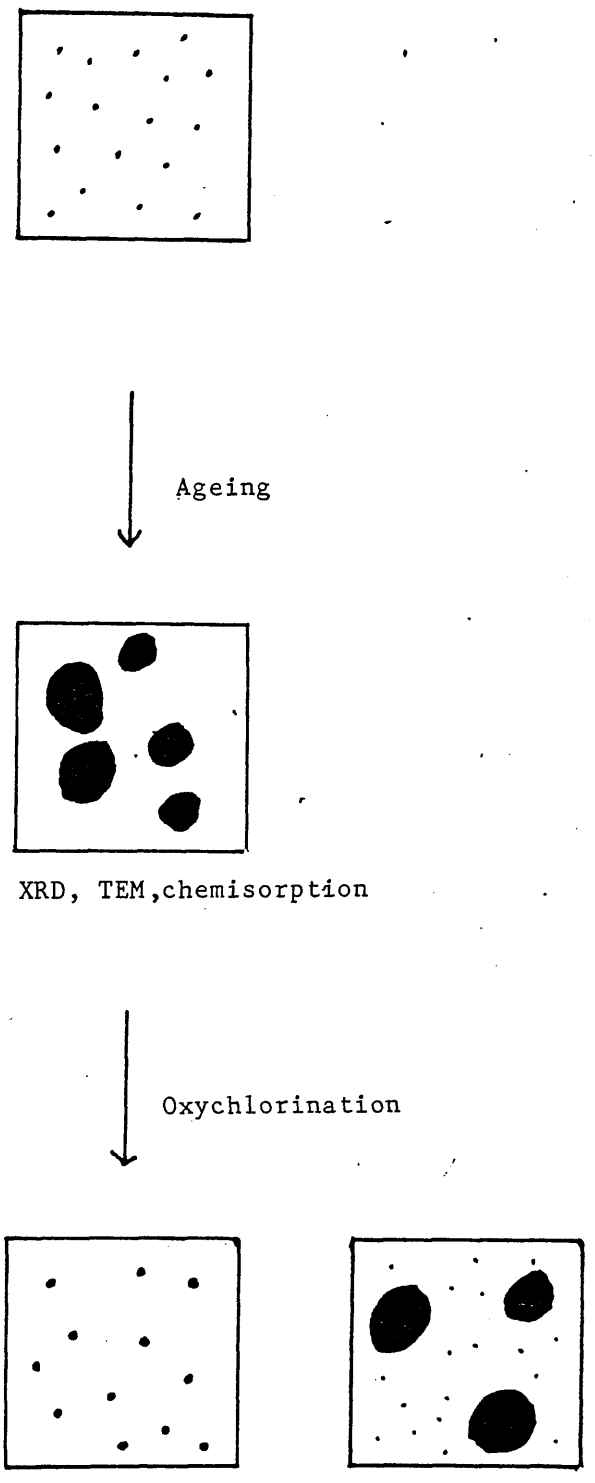

Results from this study support the results from Spanner (1984). TEM, XRD and CO chemisorption were used to characterise catalyst 3 following each stage in the ageing - regeneration cycle. Results are indicated in Tables 5.5 - 5.7. Catalytic activity was determined by passing n-heptane through a micro-reformer. Results show (Table 5.12) that the catalytic activity was initially high and decreased following the ageing treatment. Following oxychlorination treatment on the aged catalyst, the catalytic activity increased to a value similar to that of the fresh catalyst. Results at each stage in the ageing - regeneration cycle and the use of quantitative XRD to explain differences in results are discussed below.

Both CO chemisorption and TEM suggest that the platinum is highly dispersed in the fresh catalyst. No platinum is detected by XRD suggesting that all of the platinum exists at a size below the resolution of XRD (<30Å) as expected with a highly dispersed catalyst.

The aged catalyst appeared sintered by XRD, TEM and CO chemisorption. All of the platinum was detected by XRD as shown by quantitative XRD.

Following the attempted redispersion by oxychlorination in each case the catalyst shows an increase in particle size (compared with the aged catalyst) by electron microscopy and XRD mean particle size, although CO chemisorption shows an enhanced surface area. Considering quantitative XRD results: for oxychlorination for 3 hours the amount of platinum detected ('visible') to XRD was 0.67 w/o implying that 0.13 w/o Pt was undetected by XRD ('invisible'). XRD results were then compared to chemisorption results as follows:-

Surface areas were calculated from XRD results by assuming particle diameters for invisible platinum. The sum of the surface area from the 'invisible' Pt and the surface area due to the 'visible' Pt was then compared to the measured surface area from CO chemisorption.

$$\text{i.e.} \quad SA = SA_{(\text{visible Pt})} + SA_{(\text{invisible Pt})}$$

$$= \frac{6 \times 10^4}{d_{mean} \times \rho_{Pt}} \times \alpha\% + \frac{6 \times 4}{d_{est} \times \rho_{Pt}} \times Y\%$$

where

SA	=	Surface area (m^2/g)
d_{calc}	=	mean Pt diameter measured from XRD profile
d_{est}	=	Estimated Pt diameter for 'invisible' Pt
ρ_{Pt}	=	density of Pt
$\alpha\%$	=	w/o visible Pt
Y%	=	w/o invisible Pt

The deviation from the surface area (as measured by CO adsorption) was plotted against estimated 'invisible' platinum diameter, as shown in figure 6.2. From this graph it can be seen that the minimum deviation from the measured surface area would be achieved by assuming that the invisible platinum exists in the form of small crystallites with a mean diameter of 8.5Å.

Similarly following oxychlorination treatment for 9h, 0.28% by weight of platinum is invisible to XRD with a mean diameter of 149Å. Therefore 0.52 w/o Pt is 'invisible' to XRD. Following the above argument the minimum deviation from the measured surface area would be achieved by assuming a mean Pt diameter of 11.5Å for the 'invisible' Pt.

figure 6.2: Deviation from measured surface area of CO chemisorbed against 'invisible' Pt particle diameter.

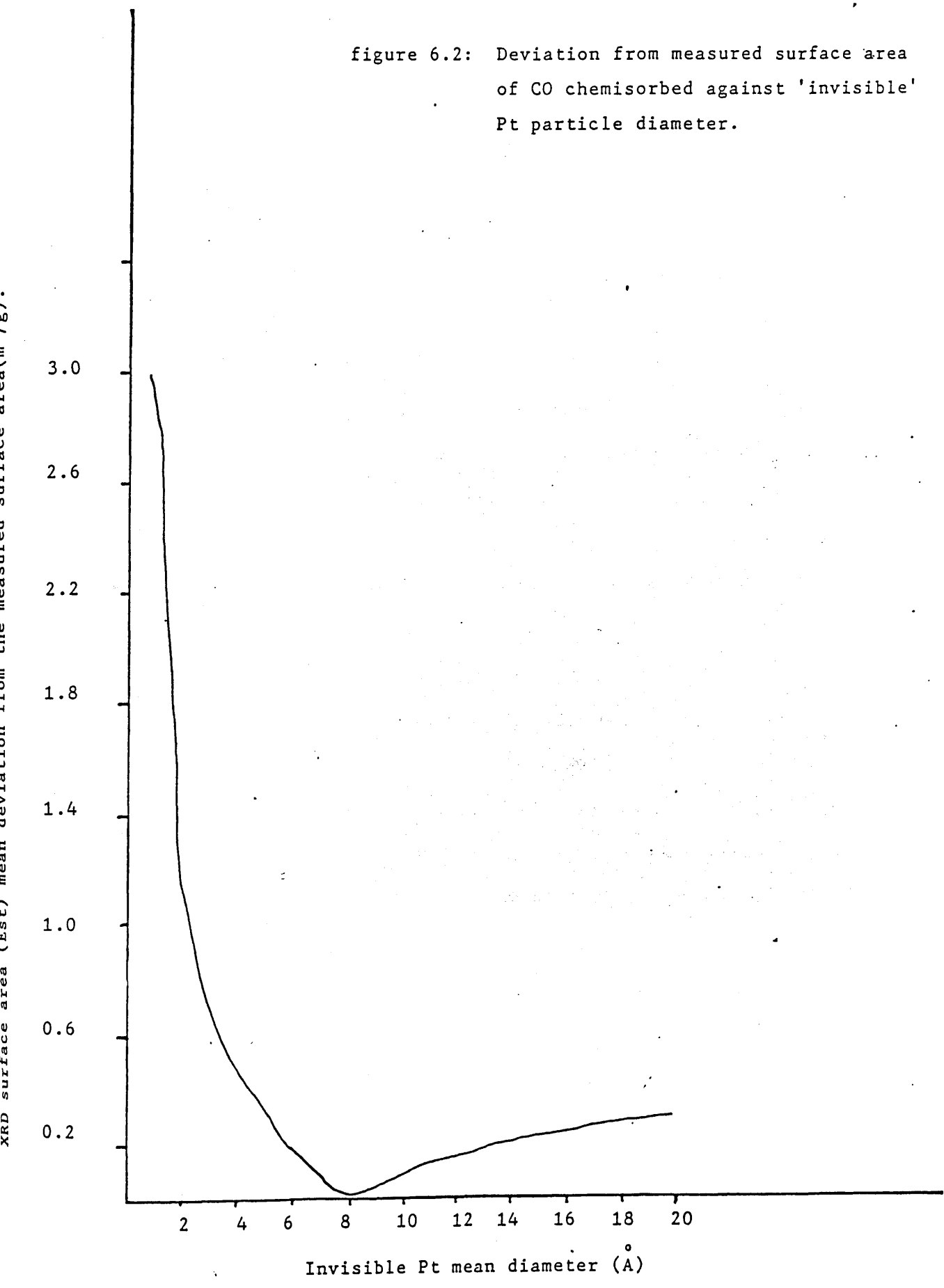

The results from this study could therefore be schematically represented by figure 6.1. In the case of the 9h oxychlorination, 65% of the platinum exists in the form of highly dispersed platinum.

As these sub - 10Å platinum particles are apparently responsible for catalysis (as the catalytic activity is regained following oxychlorination treatment) the size, shape and structure of these particles are important. One of the aims of this study was to resolve sub - 10Å platinum particles formed as a result of the regeneration treatment. Three methods were used to determine the nature of the highly dispersed metal, namely high resolution electron microscopy (HREM), bright field hollow cone illumination electron microscopy and an attempted 'staining' of the supported metal by a tellurium compound (Te-staining). The experimental procedure for each is outlined in chapter 3 and the results shown in chapter 4.

Several methods have been used to study the structure of supported catalysts, as explained in section 1.5. In particular high resolution electron microscopy (e.g. Treacy and Howie, 1980; Millward, 1980; Smith et al., 1983.) and dark field methods (Treacy, Howie and Wilson, 1978; Zenith et al., 1980; Freeman et al. 1977). The problems of using electron microscopy to study a system such as Pt/γ-Al_2O_3 were considered by Flynn, Wanke and Turner (1974). The major problems are due to contrast effects from the high contrast of γ - Al_2O_3 (Plate 6) which prevents small metal particles being detected. In this study three techniques have been used to overcome this problem.

(a) Hollow Cone Illumination - In which the contrast from alumina is reduced by the use of an annular aperture, which permits only contrast from the platinum to form the image.

(b) High resolution electron microscopy.

(c) Te-staining - This novel technique was used in which the catalyst was treated with a tellurium compound.

The results from each technique will be discussed.

Hollow cone illumination was used to enhance the contrast of the platinum crystallites against the alumina support. This technique is useful where the support scatters strongly due to a crystalline and irregular structure. The results are shown in section 4.1. The contrast from the alumina support is reduced using hollow cone conditions (Plates 1 and 2). This makes the platinum particles easier to detect, although high resolution information on platinum crystallites is lost using an annular aperture. For example particle D (Plate 1a) shows lattices extending in different directions suggesting a multiple twinned structure; using an annular aperture (Plate 1b) this information is lost.

Platinum (111) lattices are clearly shown on particles A and B, figure 2, using axial illumination. However with hollow cone illumination this structural information is lost.

Small platinum particles have been resolved using hollow cone illumination. Particle E (Plate 2) is not resolvable with axial illumination due to the high contrast from the support. However, removing this contrast with hollow cone illumination the particle is easily resolved.

Particle boundaries are more clearly defined in the hollow cone mode, although particle size and shape did not appear to change. This conflicts with results from a study on Pd/Al_2O_3 catalysts where an increase in mean particle size is reported using dark field hollow cone illumination, as compared to axial illumination.

Hollow cone illumination appears to be a useful technique for the resolution of small platinum particles masked by the high contrast of the alumina support. The main disadvantage of this technique is the loss in lattice structure. However, if both axial and hollow cone images are obtained for each area, both particle structure and small crystallites may be resolved.

Platinum metal chalcogenides are easier to prepare than the corresponding oxides. Platinum metals react readily with S, Se and Te without special conditions of pressure and temperature (Wold, 1986). In addition, platinum metal chalcogenides behave like alloys and show metallic luster and conductivity.

It was hoped that by the exposure of an active catalyst to Te, the Te would combine with platinum and act as an indicator (the high atomic number making an electron dense triatomic molecule with each platinum atom). Such a molecule would be discretely resolvable under high resolution electron microscopy. In this way the contrast from highly dispersed platinum particles would be greatly increased and so resolvable by TEM. This process has been termed Te-staining. The results are shown in section 4.2.

These results show that the attempted stainings with Et_2Te could not be used to enhance the contrast from highly dispersed platinum particles. High contrast particles were observed on the alumina support, which X-ray elemental analysis identified as containing Te with no Pt. Therefore, by staining with Te, Te particles could be mistaken for Pt particles in a particle size analysis. To be a useful 'staining' material the Et_2 Te would have to selectively react with the platinum and have no effect on the alumina support or the carbon film.

However, Te was detected on the carbon film and on the alumina support. No enhanced Te levels were detected, by X-ray elemental analysis, where platinum was detected. This implies that the Te is not combining with the platinum. In the second staining attempt where Et_2 Te was vapourised over a catalyst sample Te is detected on the carbon film and yet Pt is detected with no Te. Therefore by decreasing the amount of Et_2Te passing over the catalyst, Te residues are still detected on the support film, but the concentration is not high enough to react with all the platinum.

The Te compound was also found to be unstable under the electron beam (Plate 4). Diffraction patterns indicate that the material is initially amorphous (inset a), shown by the diffuse rings of the diffraction pattern, a few sharp spots are observed (inset b) following irradiation for 1 minute. After a few minutes the material appears crystalline (inset c) indicated by the sharp spot diffraction pattern. To be of use as a 'staining' material for TEM the Te compound would have to be stable under the electron beam.

The Te compound is therefore unselective in combining with platinum and is unstable in the electron beam. These results suggest the Te cannot be used, in this way, as a 'staining' material to resolve small platinum crystallites.

High resolution electron microscopy was used in an attempt to resolve the sub - 10Å particles indicated by XRD. The coherence and image contrast of the microscope were increased by using an LaB_6 pointed filament which produces a more coherent beam. In high resolution electron microscopy small particles are identified by a phase

contrast mechanism (see chapter 2). With larger particles the phase contrast effects are insignificant due to multiple scattering and so large particles are identified by diffraction contrast. As the platinum particle size decreases the defocus range over which small particles are detectable decreases (Flynn, Wanke and Turner, 1974). This makes the identification of small supported particles difficult. Zenith et al. (1980) found that the resolution of small platinum particles is strongly dependant on the relative orientation of the particles when a semi-crystalline support such as γ-Al_2O_3 is used. Therefore careful imaging conditions must be chosen before small platinum particles can be resolved.

With careful preparation and imaging conditions sub - 10Å Pt particles have been resolved following oxychlorination treatment (Plates 5A and 5B). The particles have a spherical morphology. However, not all of the sub - 10Å platinum particles have been detected as only the particles in the correct orientation at the defocus values used were resolved. High resolution electron microscopy has therefore proven the existence of platinum in a highly dispersed state giving a better particle size distribution, however the technique is not quantitative.

Figure 6.3 shows the particle size distribution of catalyst 3 following oxychlorination of a sintered catalyst for 9 hours. From this figure it is shown that, of the platinum resolved by TEM 56% of the platinum particles are below the resolution limit of XRD (i.e. <30Å in diameter). This is in agreement with results from quantitative XRD which suggests that a large percentage of the platinum crystallites exist at a size below the resolution limit of XRD. Similarly with the oxychlorination of sintered catalyst 1, following the standard

Figure 6.3: Particle size distribution of C3 following oxychlorination.

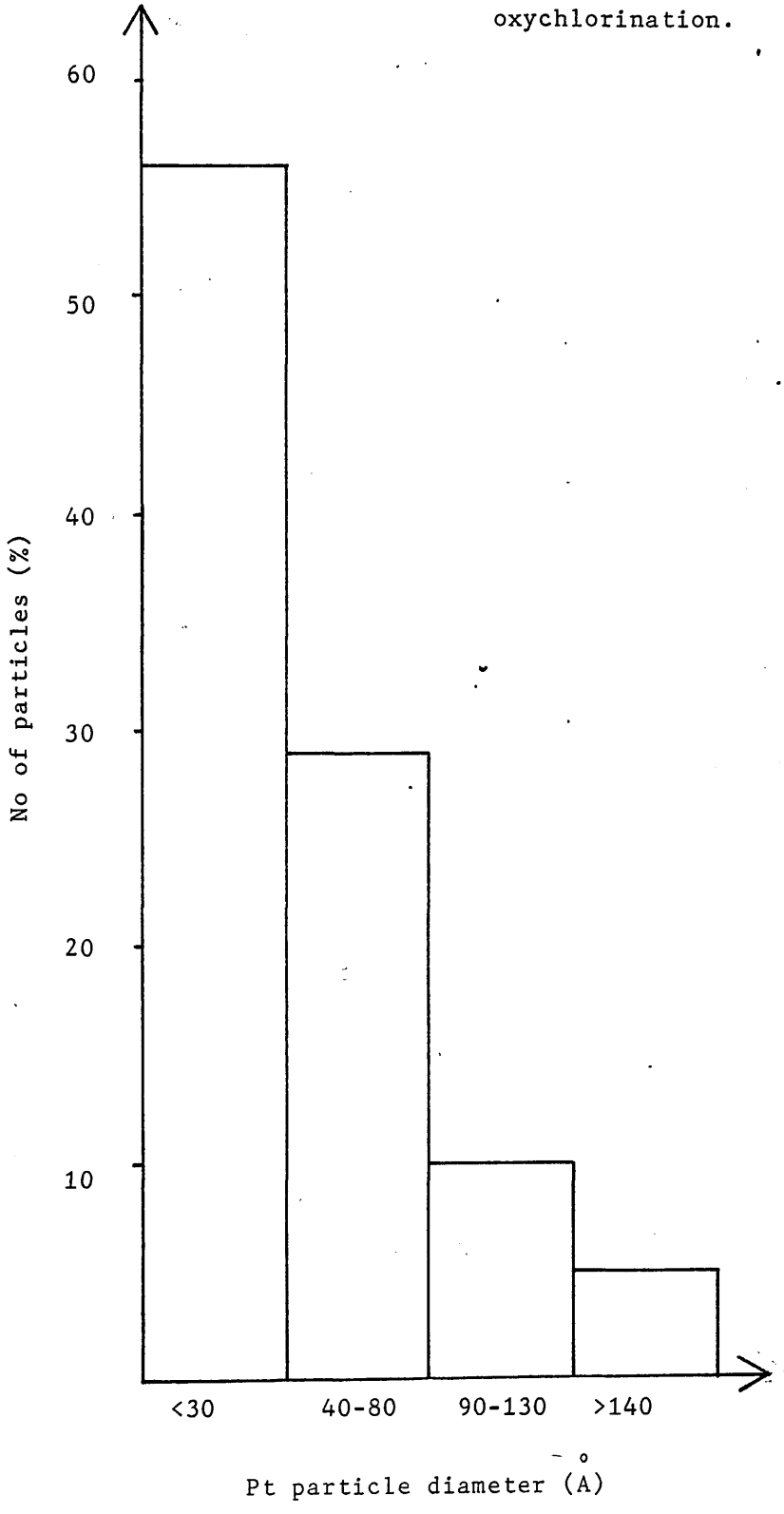

oxychlorination treatment (oxychlorination 1.1) 72% of the platinum particles, resolved by TEM, are below 30Å in diameter, and 56% of the paltinum particles resolved by TEM were below 10Å in diameter (figure 5.5).

Results from X-ray diffraction and gas adsorption suggest that following oxychlorination platinum exists in the form of highly dispersed platinum particles co-existing with large sintered particles (figure 6.1). Structural studies using hollow cone illumination and high resolution electron microscopy support this theory as high resolution electron microscopy has been used to identify the catalytically active species indicated by quantitative XRD.

7. DISCUSSION: Comparison of Characterisation Techniques.

7. DISCUSSION: Comparison of Characterisation Techniques.

Three techniques were used to characterise the catalyst following each treatment namely, transmission electron microscopy, selective gas chemisorption and X-ray diffraction line broadening analysis. Catalytic activity was determined from micro reformer runs on selected catalysts. The two major aims of this study were:

1. to determine, by high resolution electron microscopy, if sub-10Å platinum particles exist following oxychlorination treatment.

2. to gain a better understanding of the optimum regeneration treatment and to propose a model for the redispersion of platinum following oxychloriantion treatment.

The resolution of sub - 10Å particles is discussed in chapter 6. The second aim involves a structural study to determine changes in platinum particle size distribution following various treatments. As the actual particle size distribution can be obtained from electron microscopy, as compared to mean values obtained from other techniques such as gas adsorption and X-ray techniques, electron microscopy was therefore used to monitor changes in particle distribution. However, due to resolution limitations in an electron microscopic study of supported catalysts (e.g. Flynn, Wanke and Turner (1974)) gas adsorption results were compared to results from electron microscopy. With catalyst 3 X-ray diffraction results were also used for comparison.

Catalyst 1 fresh appears highly dispersed by electron microscopy (TEM) and good agreement is obtained with H_2 chemisorption results (chapter 5). Following an ageing treatment in 3% $O_2|N_2$ at 600°C for 4 hours the particle size is found to increase by TEM and a decrease in metal surface, surface area is indicated by H_2 chemisorption. Redispersion of the sintered platinum agglomerates was attempted by oxychloriantion 1.1 and the surface area, as indicated by hydrogen chemisorption measurements, is found to increase to a value similar to that of the fresh catalyst. Results from H_2 chemisorption are shown in table 5.2. TEM results show that some redispersion of sintered platinum particles occurs as shown in figure 5.5. TEM results are tabulated in table 5.4. In general electron microscopy results indicate larger mean particle sizes than chemisorption results. For example, following oxychlorination 1.2 a mean particle size is calculated from chemisorption results of 9Å, TEM results indicate a mean Pt particle size of 38Å. However, this is explained by the highly dispersed platinum particles being below the contrast limit of TEM as explained in chapter 6.

Initial chemisorption results use H_2 chemisorption. However, chemisorption measurements were carried out at ICI Wilton. Due to problems experienced at ICI with hydrogen measurements it was decided to change over all chemisorption measurements on Pt $|\gamma$-Al_2O_3 catalysts to CO chemisorption. For this reason later results use CO chemisorption. One of the main reasons for the change to CO chemisorption was due to problems of hydrogen spillover. Some catalyst samples appeared to show a dispersion greater than 1, indicating that either the H: Pt stoichiometry is greater than one or hydrogen spillover from the metal to the support is causing abnormal chemisorption values.

A series of reports on the characterisation of platinum|silica catlaysts (Bond et al., 1985) discusses the differences in adsorbates. Frennet and Wells (1985) consider the chemisorption of hydrogen on a platinum|silica catalyst. They report that the experimental value for the H: Pt stoichiometry can exceed 1:1. Four states of adsorbed hydrogen were found with two states being associated with hydrogen adsorbed on to the support. In the same series of reports (Wells, 1985) the chemisorption of carbon monoxide was considered. The nature of the adsorbed CO was determined by infrared spectroscopy. Results show that most of the CO is present in a linear form, two branched forms were identified at low concentrations. An adsorption stoichiometry for CO: Pt of 1:1 was suggested (Wells, 1985). Basically results from this series of papers suggests that H_2 chemisorption may have problems with spillover and the adsorption stoichiometry is disputed. CO chemisorption is in good agreement with electron microscopy results and an adsorption stoichiometry of 1:1 is proven. Differences in results in this study were obtained between H_2 chemisorption and CO chemisorption fresh C1, C1 sinter and C1 following oxychlorination 1.1 were studied by both CO and H_2 chemisorption. The mean particle sizes calculated from CO chemisorption are lower than those obtained from H_2 chemisorption. Both calculations assume a Pt: adsorbate ratio of 1:1. This suggests that some H_2 spillover may occur when using H_2 chemisorption to characterise the $Pt|Al_2O_3$ system. Other authors (e.g. Renouprez et al., 1974) found results from H_2 and CO adsorption to be in good agreement. However, it was not an objective of this study to determine the differences in chemisorption techniques, but to use chemisorption results to correlate with results obtained by electron microscopy.

In general trends shown by TEM results are backed by trends in chemisorption. For example, figure 7.1 shows results from both techniques

Figure 7.1: CO chemisorption results and TEM results V ageing - regeneration treatment on catalyst 1.

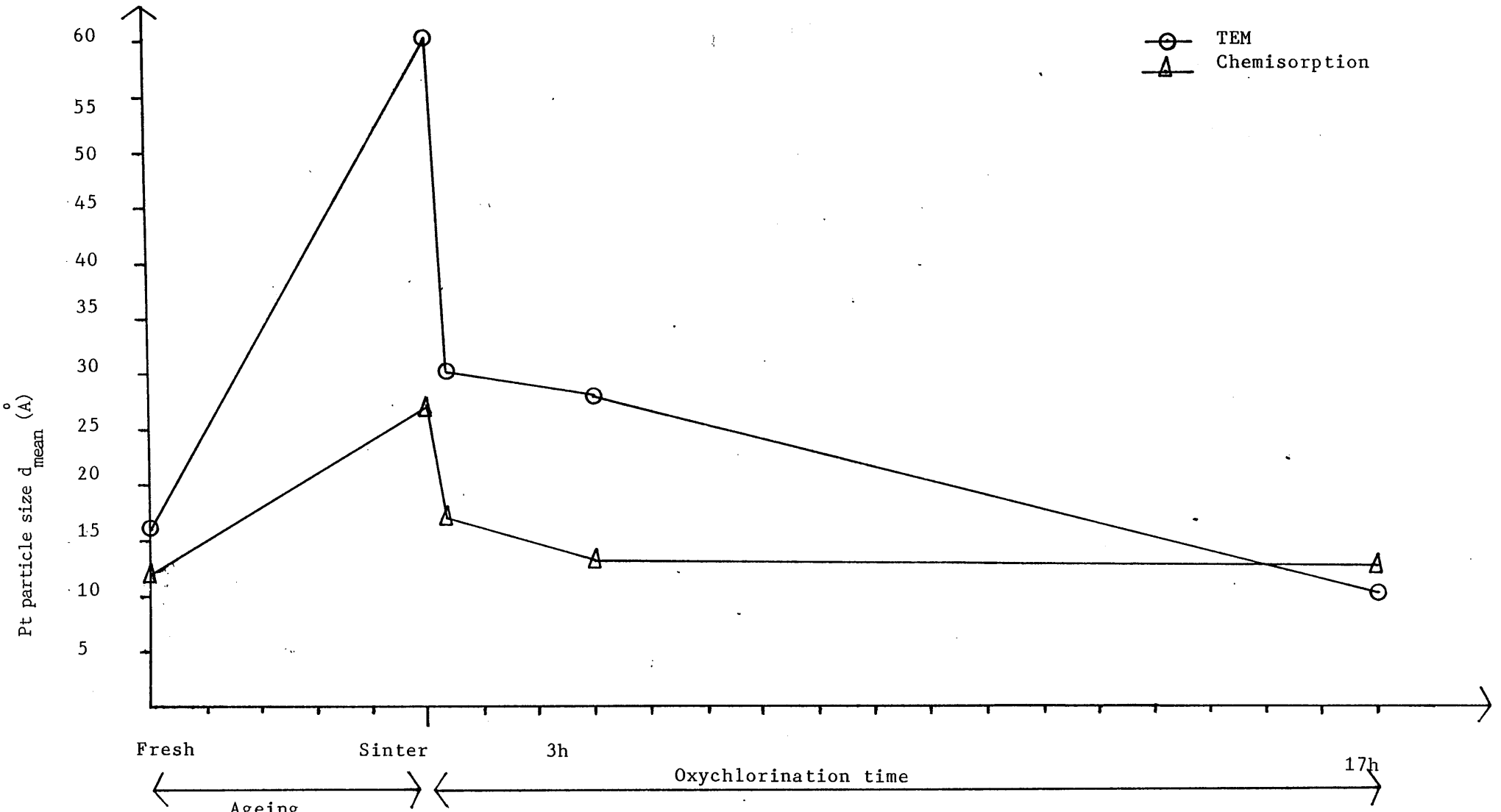

to characterise the Pt particle size of C1 following ageing and subsequent regenration treatments for 15 mins (oxychlorination 1.7); 3 hours (oxychlorination 1.1) and 17 hours (oxychlorination 1.8). The particle sizes increases by both methods following the ageing treatment and decreases with the time of oxychlorination. Again results from TEM indicate larger values for the mean platinum particle size. This is probably due to the large number of highly dispersed platinum crystallites, undetected by electron microscopy due to contrast limitations. However, as explained in chapter 6 a large number of 'small' platinum particles have been resolved in this study. Earlier work (White et al., 1983; Smith et al., 1983; Spanner et al., 1983) found no change in particle size by TEM following the regeneration treatment, although chemisorption measurements show an increase in metal dispersion. Therefore, a better agreement between characterisation techniques is obtained from these results. The TEM results have the advantage of showing how the particle size distribution changes with the time of oxychlorination, hence giving an indication of the mechanism of platinum redispersion. This will be further discussed in chapter 8.

Figure 7.2 shows changes in the mean platinum particle size with time of oxychlorination of catalyst 3 following sintering for 4 hours. In this case, CO chemisorption indicates an increase in platinum particle size following ageing. The particle size then decreases following oxychlorination for 3 hours and a further decrease in particle size following oxychlorination for 9 hours. However, TEM results suggest that no redispersion of platinum particles occurs following oxychlorination treatment. But rather an increase in platinum particle size occurs following oxychlorination for 3 hours. Similarly XRD results indicate

Figure 7.2: CO chemisorption TEM and XRD results V oxychlorination time for catalyst 3

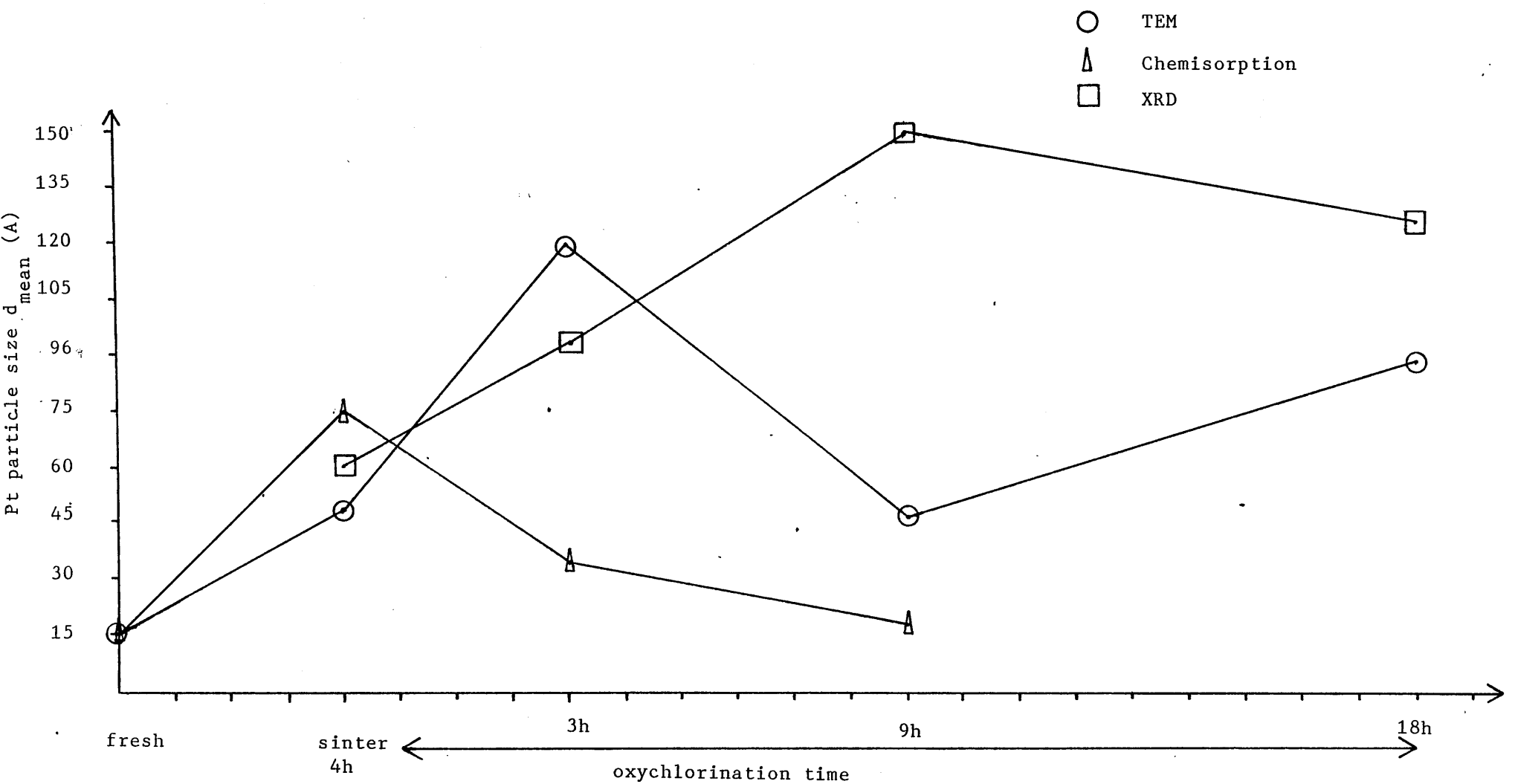

that no redispersion occurs following oxychlorination. Figure 7.3 plots the amount of platinum detected by XRD (i.e. the amount of platinum >30Å in diameter) against the time of oxychlorination. This shows that the longer the catalyst is oxychlorinated the more platinum <30Å. Mean platinum diameters for this 'invisible' platinum were calculated (see chapter 6) and found to be ~10Å in diameter. These particles are at the limit of resolution of TEM. By using a combination of techniques a great deal more information can be obtained about the catalyst. CO chemisorption results give an average surface area and hence mean particle size. TEM gives a good indication of the particle size distribution. XRD results together with TEM and gas adsorption results shows that a bimodel particle size distribution occurs following an attempted redispersion by oxychlorination treatment. Large platinum agglomerates co exist with highly dispersed platinum particles. Further, it is shown that the amount of platinum in the form of highly dispersed sub - 10Å particles increases with the time of oxychlorination.

Following oxychlorination for 18 hours CO chemisorption indicates a metal surface area of $0.04 m^2/g$. This value is very low conflicting with results from X-ray diffraction. Very large platinum particles were observed by microscopy but highly dispersed material was also observed following this treatment. Initially it was thought that surface chlorine levels may be very high following oxychlorination for 18 hours. This may affect the catalyst surface leading to error in the adsorption measurement. Neutron activation analysis was used to measure the Cl-content following each oxychlorination treatment (Table 5.8). No significant increase in chlorine is observed which could explain such a difference in surface area.

Figure 7.3: Amount of platinum detected by XRD (w|o) V time of oxychlorination

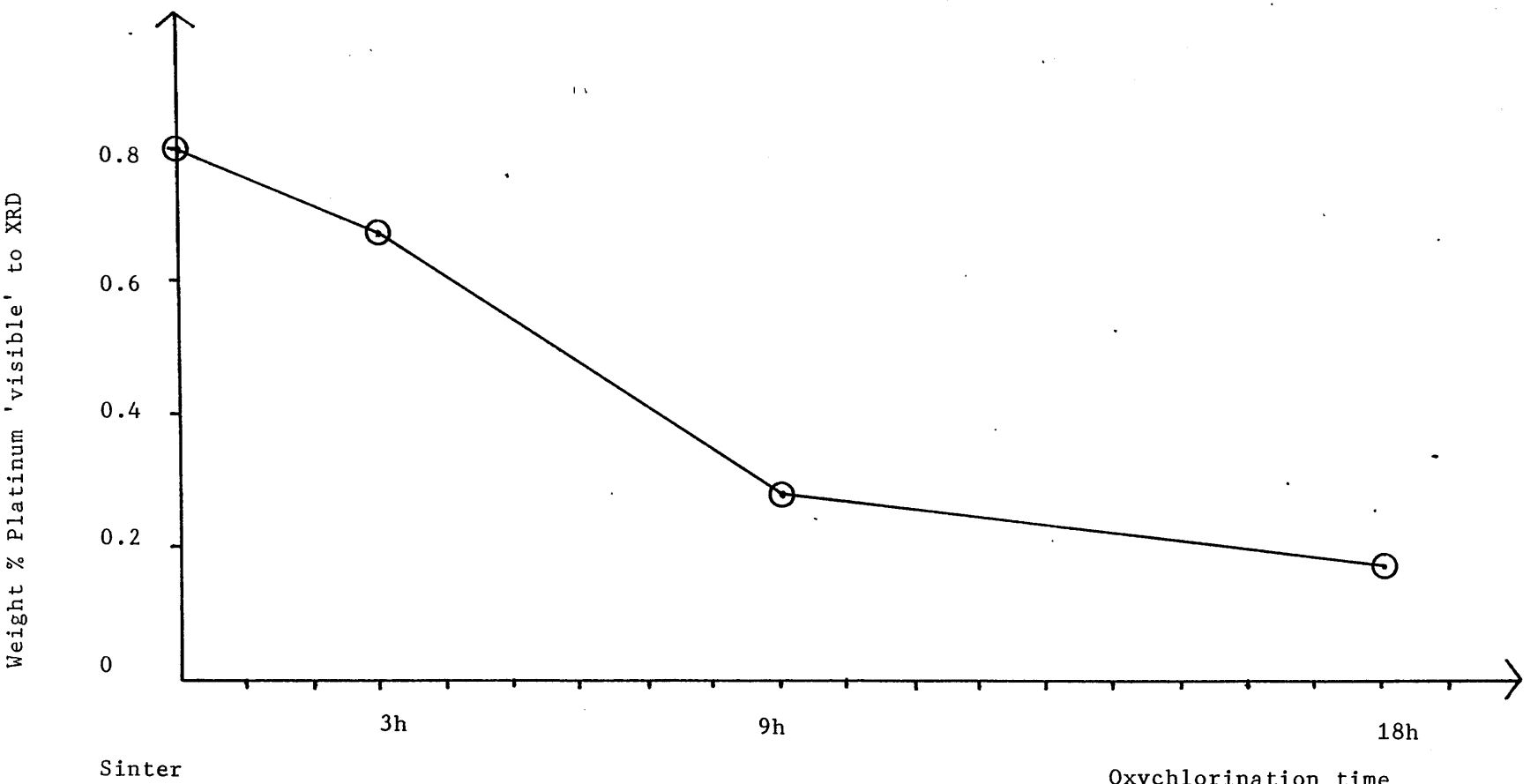

8: DISCUSSION: Catalyst Regeneration

8.1 The Effect of CCl_4 to Redispersion

8.2 The Effect of Ageing-Regeneration Time

8.3 Catalytic Activity

8.4 A Model for the Redispersion of Platinum on an Alumina Support

8. DISCUSSION: Catalyst Regeneration

Regeneration of platinum | alumina catalysts has been reported following an oxychlorination treatment (e.g. Spanner et al., 1983A; 1983B; Lieske et al., 1983; Stráguzzi et al., 1980). Microreformer results from this study indicate that the fresh catalyst (catalyst3) behaves as a good reforming catalyst. Following sintering by treatment in 3% $O_2|N_2$ at 600°C for 4 hours the catalytic activity decreased (sections 5.7). The catalytic activity was found to increase following each oxychlorination treatment on the sintered catalyst. The mean particle size, from gas adsorption and TEM, increased following the sintering treatment for 4 hours. Following oxychlorination treatment for 9 hours the surface area from CO chemisorption increased, indicating a decrease in Pt particle size.

It is suggested that the regeneration of catalytic activity is due to the redispersion of sintered platinum agglomerates by the oxychlorination. In this study a full structural study of the catalyst has been undertaken to find if regeneration of catalytic activity is due to the actual redispersion of sintered metal. High resolution studies were carried out as discussed in chapter 6 which indicate that a large fraction of the platinum exists in the form of small (<30Å in diameter) particles.

Two models have been proposed to explain the redispersion of platinum. Ruckenstein and Malhotra (1976) suggested that redispersion is due to the splitting of large platinum particles due to the build up in internal stresses caused by lattice mismatch occuring when platinum is oxidised to platinum oxide in an oxidising atmosphere. While redispersion has been proposed to occur (Ruckenstein and

Chu, 1979) via the spreading of a layer of a platinum oxide species on the alumina due to the decrease in surface tension as platinum is oxidised to platinum oxide. Both suggested mechanisms invoke the formation of a platinum-alumina-oxide complex being responsible for redispersion. McHenry et al. (1961) first suggested that oxidation promoted the formation of a Pt-alumina complex which he termed 'soluble' platinum. Johnson and Keith (1963) supported the formation of a Pt- Al_2O_3 complex in an oxidising environment, as large platinum crystallites were dispersed as a complex phase which then led to the increased Pt surface area on reduction.

One of the aims of this study was to study the catalyst after different stages and conditions of the ageing and oxychlorination treatments to give an indication of the mechanism of redispersion, and also to determine the nature of the platinum oxy - or oxychloride compound responsible for platinum redispersion following oxychlorination treatment. Several factors were considered such as the effect of oxychlorination time; the effect of CCl_4 in the oxychlorination treatment to the redispersion; the effect of sintering time to the time required to redisperse the metal; and the effect of platinum metal loading. The results of each will be discussed.

Initial work was carried out using a catalyst with 0.3% by weight (w|o) platinum on γ-Al_2O_3. This was chosen to be close to the metal loading in real reforming catalysts. However, the use of such a low metal loading had serious disadvantages in an electron microscopy study. The low metal loading made resolution of the Pt metal very difficult as there was very little platinum present. The concentration of metal was also too low for X-ray diffraction analysis and so only chemisorption results could be used to compare to results from microscopy. For these

reasons the later work was carried out using catalyst 3 with a platinum loading of 0.8w|o.

An example of the 0.3 w|o platinum loading is catalyst 1 (1). In this material the fresh catalyst consists of small platinum particles (<30Å) in diameter. After sintering in 3% O_2 in N_2 for 4 hours at 600°C the particle size was found to increase as determined by electron microscopy and the surface area from H_2 chemisorption decreased. The catalyst was then examined by TEM following an oxychlorination treatment (oxychlorination 1.1) before reduction. This was in the hope of detecting a platinum oxide or platinum oxychloride complex which may have been formed during the redispersion process. No such complex was detected by electron microscopy or electron diffraction. Following reduction in H_2 the platinum particle size was measured. The particle size distribution (figure 5.5) shows that the platinum has been redispersed although some of the platinum exists in the form of large (>80Å) platinum particles.

As no intermediate Pt oxide or oxychloride complex was detected, a specimen of Pt (IV) oxide was examined under the electron beam. The results (section 5.6) show that this compound is unstable under an electron beam, being reduced to platinum metal.

A piece of platinum wire was oxychlorinated and then studied by SEM. Energy dispersive X-ray analysis was used to detect any surface chlorides on the surface of the platinum. Cl was detected on the surface of the oxychlorinated wire. However, a low level of Cl was also detected on the wire before oxychlorination. It therefore seems unlikely that the redispersing material can be found by electron microscopy following the oxychlorination treatment employed. Other

workers have identified intermediate compounds during the redispersion of supported Platinum. Foger and Jaeger (1985) suggested that redispersion of sintered platinum particles occurs in 10% Cl_2 in N_2 at temperatures in the range 470 - 670K. Platinum chlorides were detected by electron diffraction, TEM, XRD and Ultraviolet diffuse reflectance spectoscopy. The authors report that redispersion occurs only if [Pt (IV) Cl_x] is formed.

Lieske et al., (1983) identified intermediates in the redispersion of platinum in oxygen by temperature programmed reduction. Two surface oxides α - and β - $[PtO_2]_s$ and two chlorine containing surface complexes, $[Pt^{IV}(OH)_x Cl_y]_s$ and $[Pt^{IV} O_x Cl_y]_s$ were detected. Redispersion of platinum in oxygen was reported possible only in the presence of chloride and the formation of $[Pt^{IV} O_x Cl_y]_s$ is suggested as the redispersing material. This was further supported by the fact that this compound can be formed between 500 - 600°C which is the temperatures where redispersion in an O_2 environment is reported.

8.1: The Effect of CCl_4 on Redispersion

Redispersion has been reported by many authors in an oxygen environment (e.g. Stulga et al. (1980); Ruckenstein and Chu (1979); Straguzzi et al. (1976); Fiedorow and Wanke (1976); Flynn and Wanke (1974); Sushuma and Ruckenstein (1987)),and also in chloride environment (Foger and Jaeger (1985). Lee and Kim (1984) reported that small amounts of chlorine in an oxygen atmosphere increased the amount of redispersion. To find the effect of CCl_4 on redispersion a series of experiments were carried out varying the CCl_4 conditions in the gas stream.

In this study redispersion was attempted by an O_2 treatment (oxychlorination 1.2) and by oxychlorination treatment (1.1) at 480°C. Both experiments were identical as described in the experimental section except that with oxychlorination 1.1 a 0.6% by weight Cl increase was attempted by injecting CCl_4 into the gas stream with a concentration of 400ppm CCl_4. In each case the gas flow rate was 0.8 l/h.

Results (section 5.1.3.) show that redispersion occured with both treatments. Chemisorption results indicated that the surface area returns to a level similar to the fresh catalyst suggesting complete redispersion of the sintered catalyst. TEM results showed that some redispersion occured although some large particles remained following each treatment. Figures 5.5 and 5.6 show the particle size distribution of catalyst 1 following oxychlorination 1.1 and oxygen treatment (oxy 1.2) respectively. The particle size distribution was moved to smaller particle sizes with CCl_4 (oxy 1.1). Mean particle diameters from TEM showed that from a mean particle size of 60Å for the sintered catalyst, oxygen treatment at 480°C decreased the mean particle size to

38Å. Oxychlorination treatment (oxy 1.1) decreased the particle size to 28Å. The CCl_4 in the gas stream therefore enhances the redispersion of sintered platinum particles.

These results are in agreement with results from Straguzzi, Aduriz and Gigola (1980) who reported that following a series of sintering - redispersion treatment on $Pt|Al_2O_3$ catalysts a decrease in the final dispersion was obtained unless the chlorine level of the catalyst was restored to its original level. The authors reported that redispersion occurs at 500°C but the addition of chlorine during oxygen treatment enhances the redispersion. Similarly Bournonville and Martino (1980) found that injection of CCl_4 into the O_2 gas stream at 650°C increased the surface area compared with the oxygen only case. Bishara et al., (1983) found the dispersion of the metallic phase in bimetallic reforming catalyst to be higher at higher chlorine levels in the catalyst. Addition of chlorine during the reactivation process resulted in a complete recovery of the catalytic activity.

Lietz et al., (1983) found that Cl was essential for redispersion to take place. They proposed that platinum surface atoms are oxidised to Pt (IV) and then attacked by Cl from the alumina , this migrates and can be subsequently reduced. Other authors (e.g. Dautzenberg and Wolters (1978)) suggested that Cl is needed before redispersion can occur.

The amount of CCl_4 passed over the catalyst was varied to 1 w|o and 2 w|o in oxychlorinations 1.3 and 1.4 respectively. Again chemisorption results indicated complete redispersion. TEM results showed that the platinum is highly dispersed following these treatments. A mean particle diameter of 43Å was found by TEM following oxychlorination 1.4, however very little platinum was detected following this treatment which suggests

that most of the platinum exists at a size undetected by electroon microscopy.

TEM results suggested that all of the platinum is highly dispersed to a value similar to the fresh catalyst following oxychlorination treatment 1.5 with a [CCl_4] of 800ppm. Figure 8.1 shows the decrease in mean particle size, as measured by TEM, with an increase in CCl_4 concentration. This indicates that an increase in CCl_4 concentration increases the redispersion of sintered paltinum agglomerates.

A 1400ppm CCl_4 concentration was used in oxychlorination 1.6. Large sintered platinum particles were detected as shown in plate 12. No redispersion is apparent from TEM results. It was thought that this may be due to the large CCl_4 concentration affecting the surface area of the γ-Al_2O_3 support. However, surface area measurements indicated no difference between γ-Al_2O_3 and γ-Al_2O_3 treated by oxychlorination 1.6.

XRD profiles (figure 5.22) showed no difference between the two samples. TEM results showed that a small amount of the alumina may be affected by the high CCl_4 treatment (plate 30), although not a significant amount to explain the observed differences. Bishara et al., (1983) found the surface area of reforming catalysts to increase with an increase in the gas flow of the regenerating gas. The flow rate of oxy 1.6 was only 0.2 l|hour and so may be too low for redispersion to occur.

The platinum dispersion is therefore increased with the addition of CCl_4 up to 800ppm. At higher CCl_4 concentrations less redispersion occured. This may be due to the lower gas flow rate used or there may be an optimum [CCl_4] required for maximum regeneration.

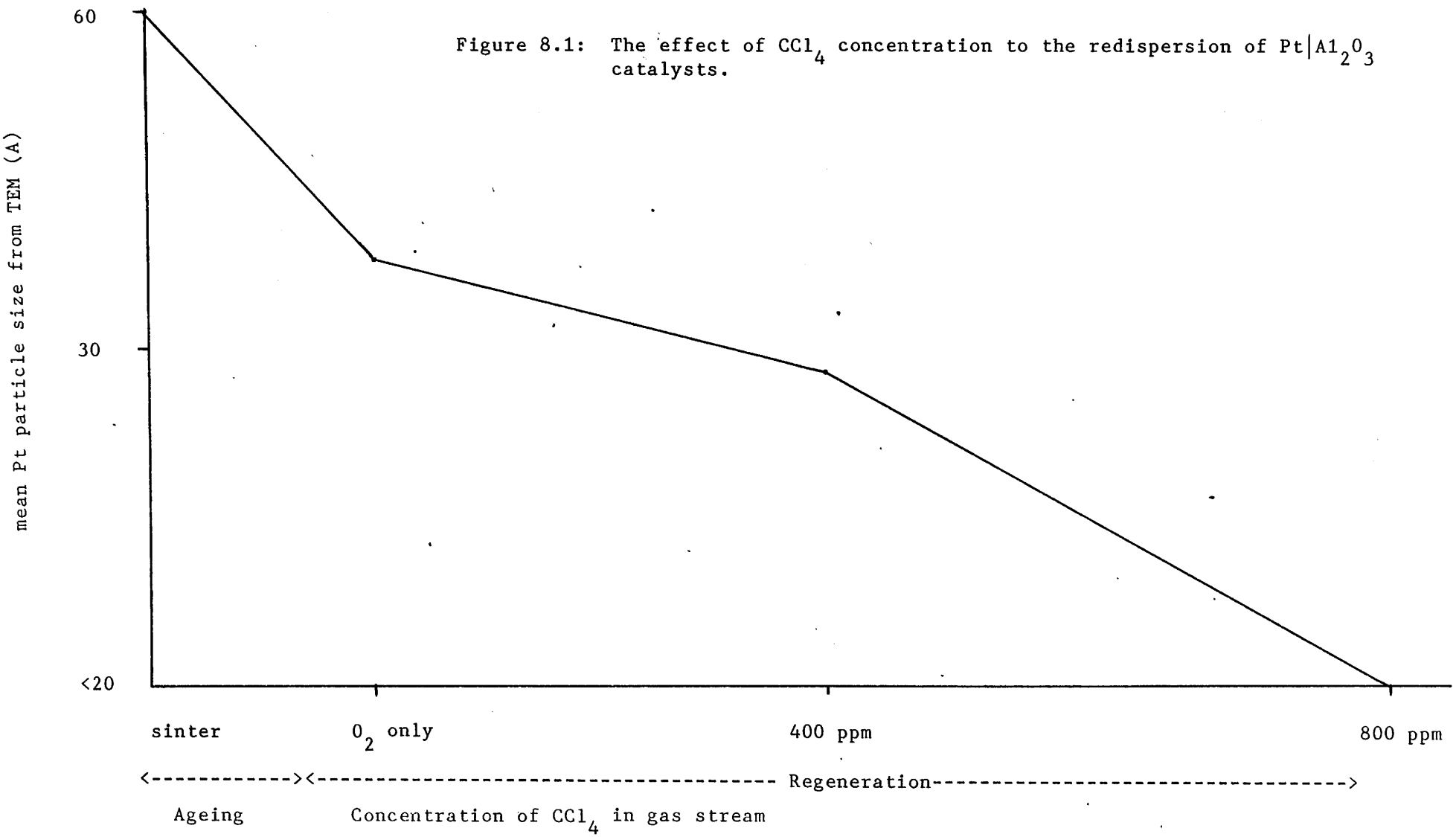

Figure 8.1: The effect of CCl_4 concentration to the redispersion of $Pt|Al_2O_3$ catalysts.

8.2 Effect of Ageing-Regeneration Times

The catalyst was treated at two temperatures in 3% $O_2|N_2$. At 600°C the platinum was found to sinter. At 480°C a decrease in particle size was observed. This has been reported by many authors. Fiedorow and Wanke (1976) on a study of an alumina supported platinum catalyst found that below 550°C O_2 treatment resulted in an increase in surface area. Above 550°C the dispersion decreased with increasing temperature. Redispersion was reported in oxygen as occuring via the spreading of platinum oxide. Decomposition of PtO_2 above 550°C prevents redispersion from occuring and so sintering of the platinum occurs. Similarly Ruckenstein and Malhotra (1976) from a TEM study of a model catalyst reported that treatment in air at 600°C for 24 hours results in an increase in particle size. At 500°C for 24 hours in air a decrease in particle size. Again redipersion is reported via the formation of platinum oxide. Sintering occured at 600°C as the oxide is not stable at this temperature. At higher temperatures sintering can occur more easily due to the higher energy of the platinum crystallites.

Previous work at Glasgow (Spanner et al., 1983A 1983B; White (1982) found no redispersion by TEM following oxychlorination treatment. The ageing treatments employed were severe. The catalysts were aged for 24 hours at 600°C prior to oxychlorination treatment. In this study the catalyst was given a mild sintering treatment for 4 hours at 600°C in 3% $O_2|N_2$. A second ageing treatment of 2 hours at 600°C in 3% $O_2|N_2$ was used with C3 to find the effect of ageing time on the time required for redispersion.

After ageing for 2 hours the platinum was easily detected compared with the fresh catalyst, as shown on plates 20-21. Following ageing for 4 hours the particle size of C3 was found to increase as shown on plates 22-23.

The platinum metal loading does not appear to greatly influence the ageing of the catalyst as C1 (0.3w|o Pt) following the ageing treatment has a mean platinum particle size of 60Å. The mean particle size of C3 (0.8 w|o Pt) following ageing was measured as 49Å.

The time of 'regeneration' was varied as explained in sections 5.1.3 and 5.3.3. C1 was oxychlorinate for 15 minutes (oxy 1.7), 3 hours (oxy 1.1) and 17 hours (oxy 1.8). Figure 7.1 shows the decrease in platinum particle size , by TEM, with an increase in oxychlorination time. Differences in chemisorption and electron microscopy results are discussed in chapter 7. TEM results show that after 15 minutes the mean particle size decreased and over 70% of the platinum exist at a size of <30Å in diameter (figure 5.10). After 3 hours there was a further decrease in platinum particle size with over 50% of the particles resolved by TEM with a diameter of <15Å in diameter (figure 5.5).

The dramatic decrease in mean particle size following oxychlorination for 15 minutes indicated that there may be two stages in the redispersion process. The initial increase in dispersion may be due to the spreading of Pt oxide following oxidation of medium sized (50-80Å) platinum crystallites. Stopping the redispersion after 15 minutes the amount of smaller particles (<30Å) is therefore increased. The larger particles take longer to spread and so the decrease in mean particle size is less dramatic over 3 hours than 15 minutes. Following redispersion for 17

hours the platinum is completely redispersed. Dadyburjor (1980) suggested a two stage mechanism for redispersion whereby splitting of large platinum particles occurs at short redispersion times. At longer regeneration times and smaller particles a thermodynamic model was proposed based on the spreading of platinum oxide due to decrease in surface tension as platinum is oxidised to platinum oxide.

However, in this case splitting does not appear to explain the redispersion process as large particles are said to split more readily (Dadyburjor, 1980) than smaller particles. Large agglomerates remained following an attempted redispersion for 3 hours.

Quantitative XRD results are correlated with results from CO chemisorption and TEM following oxychlorination treatments on C3 (chapter 7). These results suggest that the amount of highly dispersed platinum increased with time of oxychlorination. TEM and XRD showed that the size of large platinum agglomerates following oxychlorination treatment increased with treatment time. These results indicate that a sintering process is taking place in competition with the redispersion mechanism. Whereby some regeneration is occuring but unstable Pt particles are sintering by an Ostwald ripening process and so large particles are growing at the expense of small platinum particles. Particle growth by a ripening process would occur more readily with C3 as the interparticle distance would be less with the higher metal loading. With C1 the distance between particles is greater compared with C3 as shown by electron microscopy (plates 9 and 23). The migration time would be higher and so less sintering would occur.

The metal loading of the catalyst affected the regeneration process. Complete redispersion of C1 (o.3 wt % Pt) occured after oxychlorination for 17 hours whereas large platinum agglomerates remained following oxychlorination for 3 hours, 9 hours and 18 hours of C3 (o.8 wt % Pt). Yao, Sieg and Plummer (1979) found two phases of Pt - oxide on an $Pt|Al_2O_3$ catalyst in oxygen, a dispersed phase where Pt oxide and a 3 - D phase where Pt is present in form of crystallites. At low platinum concentrations the metal could be dispersed by heat treatment in air at 500°C. At high metal concentrations large particles remain following this treatment. Following reduction, catalysts with a low platinum loading were completely dispersed. With higher metal loadings only small particles were redispersed during heat treatment in oxygen. Large crystallites remain intact. These results compare well with the results of this study. Complete dispersion occured with low metal loading (C1) and large agglomerates co-existed with highly dispersed material with higher metal loading (C3).

The time required for redispersion increased with the sintering time, i.e. the size of the metal crystallites prior to oxychlorination treatment. Oxychlorination of C3 following sintering for 2 hours appeared, by TEM and CO chemisorption, to be highly dispersed after 3 hours.

No sintering was observed following oxychlorination of fresh catalyst 1, indicating that oxychlorination of a 0.3 wt % Pt catalyst does not result in any sintering of the platinum.

8.3: Catalytic Activity

The catalytic activity of catalyst 3 was determined by passing naphtha and n-heptane over the catalyst in a lab-scale micro reformer (section 5.7). Initial experiment used a naphtha feed to determine the catalytic activity. The components in the feed are indicated on Table 5.11. The fresh catalyst behaved as a reforming catalyst increasing the fraction of branched and aromatic compounds in the naphtha. Following sintering for 4 hours in 3% $O_2|N_2$ at 600°C the catalytic activity did not significantly change. However McHenry et al., (1960) proposed that dehydrogenation of naphthenes only requires 0.1 wt % platinum, but that cyclization of paraffin requires more. Since low severity tests in naphtha result in dehydrogenation of naphthenes to aromatics, it is possible for a sintered catalyst to appear to perform well if 0.1 wt % platinum is well dispersed. The sintering treatment carried out in this experiment was not severe suggesting that a significant amount of platinum was highly dispersed for dehydrogenation reactions to occur. For this reason a second test was carried out using n-heptane. This tests exclusively for cyclization performance. Differences were observed between the four catalysts. The fresh catalyst performed well in the direct conversion of n-heptane to toluene with a conversion of 19.5 wt %. Sintering the catalyst decreased this to 12.4 wt % following oxychlorination for 9 hours.

Similarly the amount of unconverted n-heptane increased with the aged catalyst and is reduced to a level similar to the fresh catalyst following oxychlorination treatment. These results show that sintering decreases the catalytic activity. The catalytic activity can be recovered by an oxychlorination treatment. Further, results show that oxychlorination treatment for long times may affect the stability of the catalyst.

Following oxychlorination for 18 hours the activity of the catalyst was stable up to 172 hours. Whereas following oxychlorination for 9 hours the catalyst was stable over the period of time studied.

Particle measurements from XRD and TEM indicate that following an 18 hour oxychlorination treatment the platinum exists as large sintered agglomerates co-existing with highly dispersed material. The fall in catalytic activity may be due to sintering of the paltinum during reforming due to a ripening process where large stable platinum particles grow at the expense of large agglomerates. This would explain the initial high activity which falls off with time. Following oxychlorination for 9 hours the particle size distribution was less bimodel ie. the amount of small highly dispersed material was lower and the large particles were on average smaller than the 18h oxychlorinated catalyst. This catalyst should therefore be more stable.

8.4: A Model for the Redispersion of Pt on a γ-Al_2O_3 Support

Redispersion of supported platinum has been attributed by means of two models. The crystallite splitting model explains redispersion as being due to the fracture of platinum crystallites. This is due to the build up in internal stresses caused by lattice mismatch as platinum is oxidised to platinum oxide (Ruckenstein and Malhotra, 1976; Dadyburjor, 1980; Gollob and Dadyburjor, 1981). Redispersion is also reported as occuring via the formation of a layer of platinum oxide across the support due to the decrease in surface tension as platinum is oxidised to platinum oxide (e.g. Ruckenstein and Chu, 1979; Ruckenstein and Pulvermacher (1973); Baker (1980); Sushuma and Ruckenstein (1987)). The basis of the spreading mechanism is the decrease in surface tension as platinum is oxidised to platinum oxide. For a crystallite in thermodynamic equilibrium the three surface tensions are related through Young's equation

$$\sigma_{gs} - \sigma_{ms} = \sigma_{mg} \cos\theta$$

where σ is the surface tension; the subscripts ms, mg and gs refer to the metal-substrate, metal-gas and gas-substrate interfaces; θ is the contact angle. When a metal is oxidised to its corresponding metal oxide $\sigma_{gs} - \sigma_{ms} > \sigma_{mg}$ hence the contact angle $\theta \rightarrow 0$ causing a surface layer of metal oxide to wet the alumina support. In a reducing atmosphere the metal oxide is reduced to metal which does not wet the support hence redispersing the sintered metal. A theoretical approach to redispersion via spreading is explained by Ruckenstein (1979). Attempted redispersion of the sintered catalyst (C1) by oxychlorination treatment resulted in a decrease in particle size as shown in plate 5A. A comparison of the sintered and oxychlorinated catalysts are indicated in the histograms in figure 8.2. It is evident that the number of large particles (>130Å) remained approximately constant, whereas the number of small particles (<30Å) had doubled following redispersion. This

Figure 8.2: A comparison of the Pt particle size distribution of the sintered and oxychlorinated catalyst.

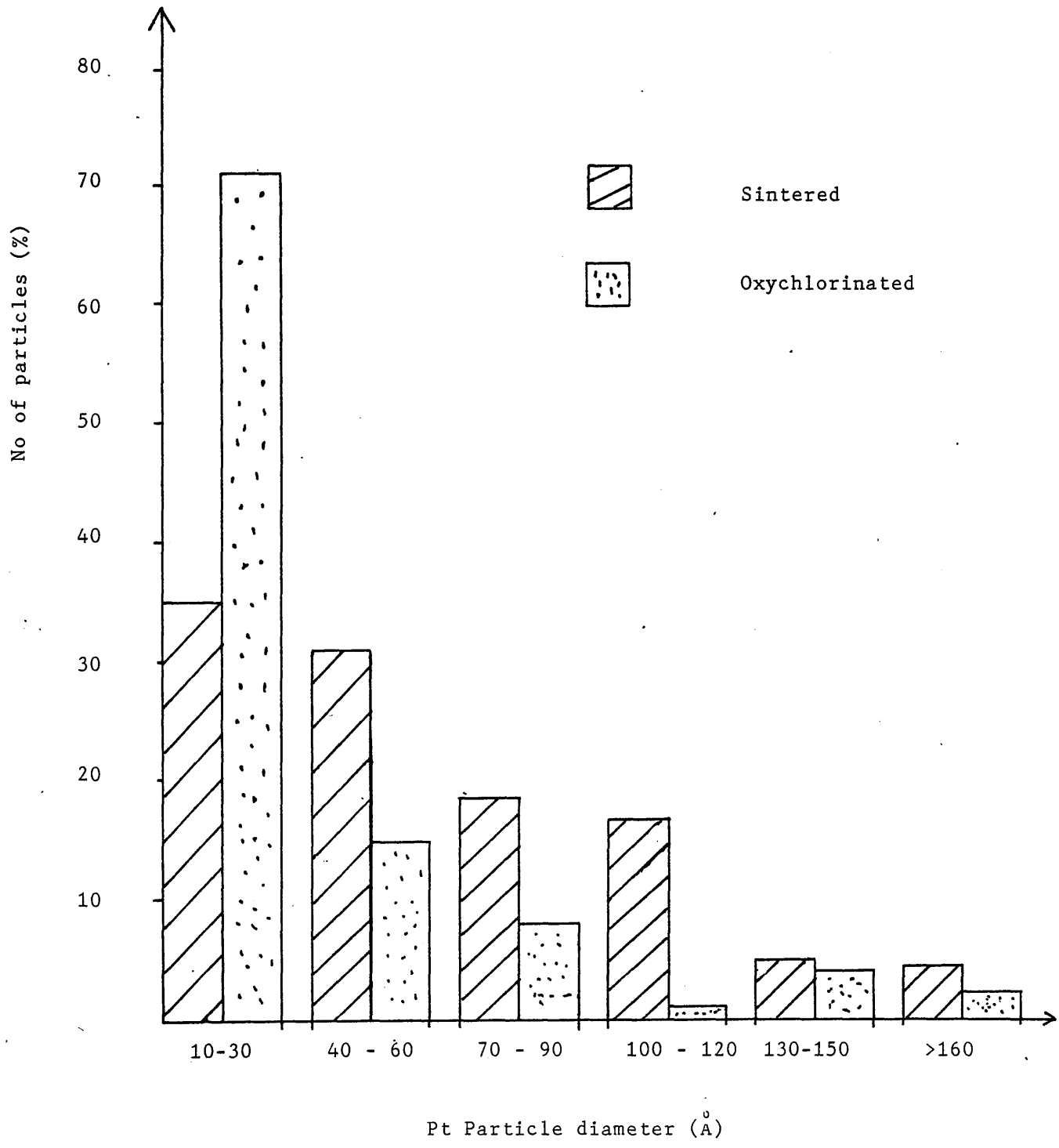

suggests that the crystallite splitting model is not a good representation of platinum redispersion, in the present system, as large particles are said to fracture more readily than smaller particles (Dadyburjor, 1980). Dadyburjor (1980) suggested that two stages occur in the redispersion of sintered agglomerates. Splitting occured at short regeneration times with large particles and spreading is the dominant mechanism with smaller particles and longer regeneration times. With a splitting mechanism the number of large particles should decrease rapidly and then dispersion should increase with treatment time due to a spreading mechnaism. However, in this study large crystallites remained following oxychlorination for 15 minutes and 3 hours on C1. Large agglomerates were detected following oxychlorination treatment of C3 for up to 18 hours. Large particles have been reported following regeneration treatments in other studies (e.g. Yao et al., 1979; Stulga et al., 1980; White 1982; Spanner 1984). According to the crystallite splitting model the increase in dispersion should be independent of the surface area of the support (Fiedorow and Wanke (1976)) as no interaction with the support is inferred. Baker (1980) reported that redispersion occurs by the wetting (spreading) of the support by a platinum oxide, redipersion is affected by the nature of the support. Similarly Lee and Kim reported differences in dispersion with different supports. No redispersion occurs with a SiO_2 support.

The results from this study may be explained by invoking the formation of a mobile platinum oxide or oxychloride species. An oxide layer may form on the surface of large particles and spread across the alumina support. After reduction some redispersion would occur. The platinum particle diameter would not significantly change as large crystallites may be protected by a surface layer of oxide, preventing further oxidation as shown in figure 8.3. Long redispersion times are required

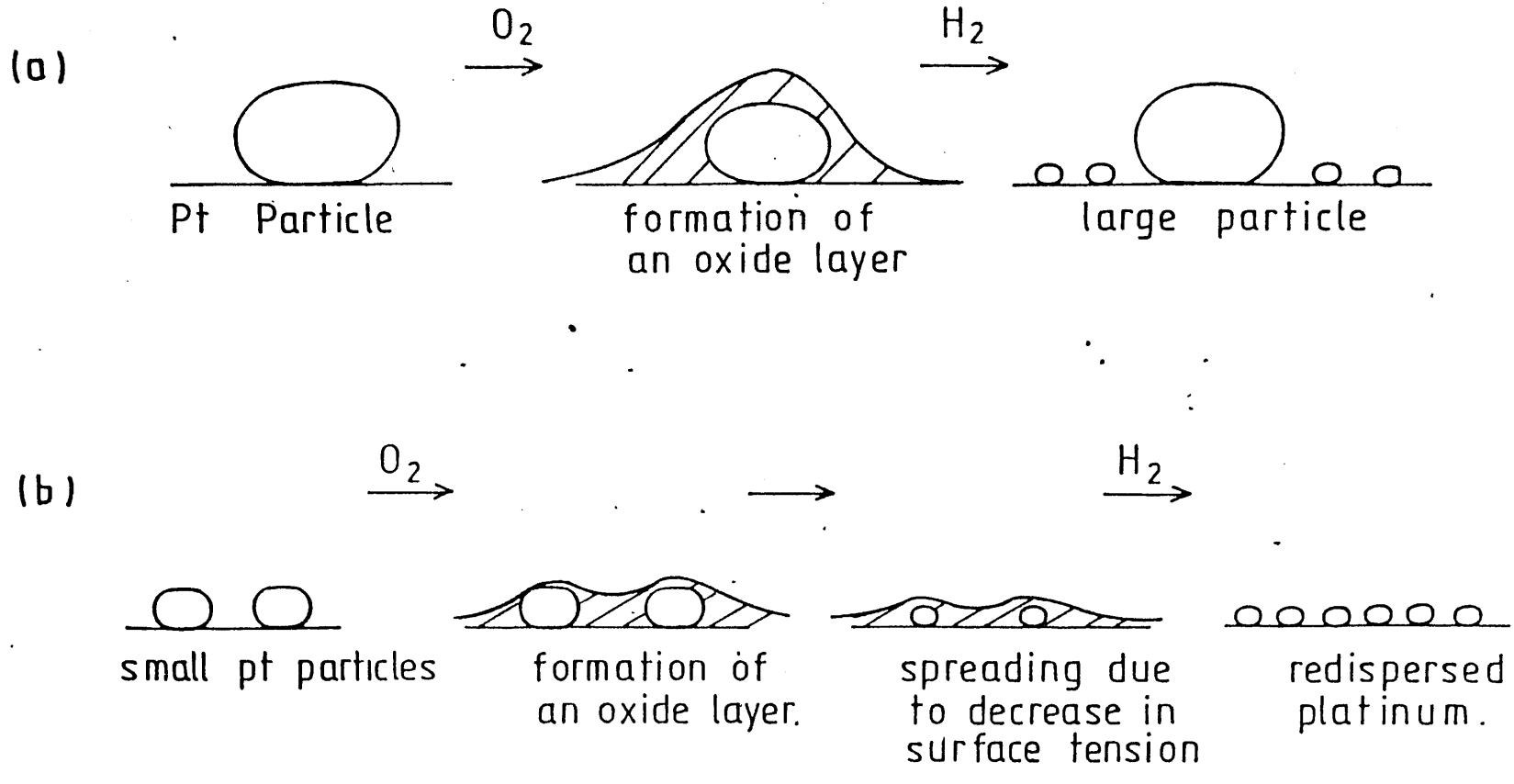

Figure 8.3 Model for the redispersion of platinum in a $pt/\gamma-Al_2O_3$ catalyst, following on oxychlorination treatment.
(a) large platinum particles. (b) small platinum particles.

before these large particles can completely 'spread' across the alumina. For this reason oxychlorination treatment of Cl results in complete redispersion.

No intermediate complex was identified from this study, although the increase in dispersion in the presence of CCl_4 indicates that a platinum oxychloride complex was responsible for redispersion. Scanning electron micrographs of platinum before and after oxychlorination (plates 31 and 32) show that the surface of the paltinum was erroded following oxychlorination treatment. This may be due to the movement, 'spreading', of a platinum oxide or oxychloride during the treatment. This backs the spreading model for redispersion.

As long times are required to redisperse sintered platinum agglomerates, a series of experiments were carried out where the catalyst was oxychlorinated for a short time and then reduced. This process was repeated several times (section 5.2). It was hoped that the large platinum would redisperse some platinum. These 'pulse' oxychlorination - reduction cycles were carried out in an attempt to reduce the protective layer of platinum oxide on the surface of large particles of platinum. Some occurring redispersion at the edges of the large particles. It was hoped that further oxychlorination treatment would produce more highly dispersed material. The oxide layer protecting the platinum from further oxidation would be removed by pulsing with short oxychlorination treatments. The time required for regeneration could hopefully be decreased. Results (section 5.2) show that the pulse treatments were not successful. The platinum was found to severely sinter following 10 oxychlorination - reduction cycles. This indicates that the surface oxide does not form a rate limiting impermeable layer.

Results from C3 agree well with the results from C1. In each case redispersion increased with the time of oxychlorination treatment. However with C3 the size of the large particles increased with oxychlorination time. As the size of large particles increased with regeneration time there must be a competing mechanism whereby regeneration is occuring but unstable highly dispersed Pt particles are sintering by an Ostwald ripening mechanism and so large particles are growing at the expense of small platinum particles. The basis of Ostwald ripening is the growth of larger particles at the expense of smaller ones. Small particles have a larger surface energy than larger particles and therefore the driving force of sintering would be an overall decrease in surface energy (Wynblatt and Gjostein (1975)).

The model proposed for the redispersion of supported platinum crystallites is via the formation of platinum oxide (or oxychloride) on the surface of the platinum agglomerates and spreads out due to a decrease in surface tension as platinum is oxidised. Large particles are protected from further oxidation by a layer of platinum oxide and so longer regeneration times are required to redisperse these particles. The dispersion increases with oxychlorination time. With higher metal loading catalysts a sintering mechanism competes with the regeneration process and large particles grow by an Ostwald ripening process. However, the regeneration process is the dominant mechanism.

9. CONCLUSIONS

9. CONCLUSIONS

The main aims of this study were to:

(a) Identify any sub-10Å platinum particles that may exist following oxychlorination treatment.

(b) To determine if platinum redispersion occurs following an oxychlorination treatment.

(c) To attempt to propose a model for the redispersion of platinum agglomerates.

The following conclusions are made from this study:

(i) X-ray diffraction line broadening analysis indicates that following oxychlorination treatment for 18 hours 80% of the platinum exists in a highly dispersed state, below the resolution limit of X-ray diffraction.

(ii) Comparing quantitative XRD results to chemisorption results a mean particle diameter of 10Å is calculated for the 'invisible' platinum.

(iii) Both hollow cone illumination and high resolution electron microscopy show that the small particles indicated by X-ray diffraction exist.

(iv) Using a combination of techniques it has been shown that redispersion of platinum agglomerates occurs following oxychlorination treatment. Further, it has been shown that the amount of redispersion increases with times of oxychlorination.

(v) A model has been proposed where redispersion occurs via the spreading of a layer of a platinum oxide across the alumina support. On reduction the oxide is reduced to platinum. The amount of redispersion increases with the concentration of CCl_4 in the gas stream so a platinum oxychloro-complex may be responsible for redispersion.

(vi) The amount of redispersion appears to be dependant on the platinum metal loading of the catalyst as C1 (0.3% by weight Pt) is completely redispersed after 17 hours and C3 (0.8% by weight Pt) has large platinum agglomerates following oxychlorination for 18 hours. This suggests that Ostwald ripening occurs during oxychlorination. This competes with redispersion. At lower metal loadings interparticle separation is greater and hence more redispersion occurs at a given regeneration time.

(vii) Catalytic results from a lab-scale microreformer show that the catalytic activity decreases following the ageing treatment employed. The catalytic activity is restored to its original value following oxychlorination treatment for 9 hours and 18 hours. However the stability of the catalyst is poorer following oxychlorination for 18 hours. This may be due to instabilities in particle size due to large particles growing at the expense of smaller particles. The particle size distribution is less bimodel following oxychlorination for 9 hours and so less ripening occurs. This suggests an optimum redispersion time of 9 hours.

REFERENCES

ADLER S.F. and KEAVNEY J.J. (1960) J. Phys. Chem., 64, 208.

AHMED H., (1971) Proc. 25th Anniv. Meeting EMAG, 30, Institute of Physics, London.

ALLPRESS J.G., HERVAT F.A., MOODIE A.F. and SANDERS J.V. (1972) Acta. Cryst., A28, 528.

ANDERSON R.B., McCARTNEY J.T., HALL W.K. and HOFER L.J.E. (1947) Ind. Eng. Chem., 39, 1618.

ANDREWS K.W., DYSON D.J. and KEOWN S.R. (1968) In "Interpretation of Electron Diffraction Patterns", Adam Hilger, London.

ARAI H., SEIYAMA T., HARAKAWA M. and TOMINAGA H. (1980) from 'Catalyst Deactivation' (B. Delmon, G.F. Froment, Eds), Elsevier Scientific Publishing Company, Amsterdam, P. 167.

A.S.T.M. Index (1965), Publication P.O. 15 - 15i.

AVERY N.R. and SAUNDERS J.V. (1970) J. Catal., 18, 129.

BAIRD T. (1982) RSC Specialist Periodical Report - Catalysis, Vol, 5, P. 172.

BAKER R.T.K. (1980) J. Catal., 63, 523.

BAKER R.T.K., PRESTRIDGE E.G. and GARTEN R.L. (1979A) J. Catal., 56, 390.

BAKER R.T.K., PRESTRIDGE E.G. and GARTEN R.L. (1979B) J. Catal., 59, 293.

BASSET J.M., DALMAI-IMELIK G., PRIMET M. and MUTIN R. (1975) J. Catal., 37, 22.

BISHARA A., MURAD K.M., STANISLAUS A. ISMAIL M. and HUSSAIN S.S. (1983) Appl. Catal., 7, 351.

BOND G.C. and WELLS P.B. (1985) Appl. Catal., 18, 221.

BOURNOVILLE J.P. and MARTINO G. (1980) in "Catalyst Deactivation" (B. Delmon and G.F. Froment, Eds) Elsevier Scientific Publishing Co., Amsterdam, P. 159.

BRITISH PATENT (1958) 760, 476.

BRITISH PATENT (1969), 1, 134, 144.

BUTT J.B. (1984) Catalysis - Science and Technology, 6, 1.

BUTTERLY L.J., BAIRD T., FRYER J.R., DAY M. and NORVAL S. (1986) Proc. XIth Int. Cong. on Electron Microscopy, Kyoto, P. 1775.

CIAPETTA F.G., DOBRES R.M. and BAKER R.W. (1958) In "Catalysis" (Emmett P.H., Ed) Reinhold, New York, Vol VI, pp 495-692.

CIAPETTA F.G. and WALLACE D.N. (1971) Catal. Rev., 5, 67.

CHU Y.F. and RUCKENSTEIN E. (1977) Surf. Sci., 67, 517.

CHU Y.F. and RUCKENSTEIN E. (1978) J. Catal., 55, 281.

COSSLETT V.E. (1951) In "Practical Electron Microscopy", Oxford University Press, London.

COSSLETT V.E. (1970) Inst. Elect. Eng., 117, 1489.

COSSLETT V.E. (1980) Proc. R. Soc. London, A370, 1.

COSSLETT V.E. (1981A) Contemp. Phys., 22, 3.

COSSLETT V.E. (1981B) Contemp. Phys., 22, 147.

COWLEY J.M. (1975) In "Diffraction Physics", North Holland, Amsterdam. P. 221.

COWLEY J.M. and MOODIE A.F. (1957) Acta. Cryst., 10, 609.

CREWE A., EGGENBERGER D.N., WALL J. and WALTER L.J. (1968) Rev. Sci. Inst., 39, 576.

CUSAMANO J.A., DEMBINSKI G.W. and SINFELT J.H. (1966) J. Catal., 5, 471.

DADYBURJOR D.B. (1979) J. Catal., 57, 504.

DADYBURJOR D.B. (1980) In "Catalyst Deactivation" (B. Delmon and G.F. Froment, Eds) Elsevier Scientific Publishing Co., Amsterdam, P. 341.

DAUTZENBERG F.M. and WOLTERS H.B.M. (1978) J. Catal., 51, 26.

DAVIS B.H. and VENUTO P.B. (1969) J. Catal., 15, 363.

de BROGLIE L. (1924) Phil. Mag., 47, 446.

DEOROUANEE.G., CHLUDZINSKI J.J. and BAKER R.T.K. (1984) J. Catal., 85, 187.

EMMETT P.H. and BRUNAUER S. (1937) J. Am. Chem. Soc., 59, 310.

ENGLISH C.A. and VENABLES J.A. (1971) Proc. 25th Anniv. Meeting, EMAG, 40, Institute of Physics, London.

ENGLISH C.A. and VENABLES J.A. (1972) Proc. 5th European Conf. on E.M., Manchester, Inst. Phys. Conf. Ser: 14, 172.

FIEDOROW R.M.J. and WANKE S.E. (1976) J. Catal., 43, 34.

FIEDOROW R.M.J. and WANKE S.E. (1978) J. Catal., 51, 193.

FLYNN P.C., WANKE S.E. and TURNER P.S. (1974) J. Catal., 33, 233.

FLYNN P.C. and WANKE S.E. (1974A) J. Catal., 34, 390.

FLYNN P.C. and WANKE S.E. (1974B) J. Catal., 34, 400.

FOGER K. and JAEGER H. (1985) J. Catal., 92, 64.

FOGER K., HAY D. and JAEGER H. (1985A) J. Catal., 96, 154.

FOGER K., HAY D. and JAEGER H. (1985B) J. Catal., 96, 170.

FRANCK J.P. and MARTINO G.P. (1985) In "Deactivation of Reforming Catalysts" from Chemical Industries Vol. 20, 205, (J. Oudar and H. Wise, Eds) Mercel Dekker Inc., New York.

FREEMAN L.A., HOWIE A. and TREACY M.M.J. (1977) J. Microscopy, 111, 165.

FRENNET A. and WELLS P.B. (1985) Appl. Catal., 18, 243.

FRYER J.R. (1979) "The Chemical Applications of Transmission Electron Microscopy", Academic Press Inc. (London) Ltd.

FRYER J.R. (1983) Mol. Cryst. Liq. Cryst., 96, 275.

GANESAN P., KUO H.K., SAAVEDRA A. and ANGELIS R.J. (1978) J. Catal., 52, 310.

GATES B.C., KATZER J.R. and SCHUIT G.C.A. (1979) "Chemistry of Catalytic Processes", McGraw Hill, New York. P. 259.

GOLLOB R. and DADYBURJOR D.B. (1981) J. Catal., 68, 473.

GOODMAN P. and MOODIE A.F. (1974) Acta. Cryst., A30, 280.

GUENIN M., BREYSSE M. and FRETY R. (1984) J. Mol. Catal., 25, 119.

HAINE M.E. and MULVEY T. (1954) Proc. 3rd Int. Conf. E.M., London, P. 698.

HALL C.E. (1953) "An Introduction to Electron Microscopy" McGraw-Hill Book Company Inc., New York.

HALL C.E. and HINES R.L. (1970) Philos. Mag., 21, 1175.

HARRIS P.J.F. (1986) J. Catal., 97, 527.

HARRIS P.J.F., BOYES E.D. and CAIRNS J.A. (1983) J. Catal., 82, 127.

HAYES (1973) Ger. Offen., 2,320,807.

HEINEMANN H., MILLS G.A., HATTMAN J.B. and KIRSCH F.W. (1953) Ind. Eng. Chem., 45, 130.

HEINEMANN K. and POPPA H. (1970) Appl. Phys. Lett., 16, 515.

HEINEMANN K. and POPPA H. (1972) Appl. Phys. Lett., 20, 122.

HILLIER J. and VANCE A.W. (1945) In "Electron Optics and the Electron Microscope", Wiley, New York.

HOLLAND F., FRYER J.R. and BAIRD T. (1983) Inst. Phys. Conf. Ser., No. 68, 19.

HOWIE A. (1980) In "Characterisation of Catalysts", (Thomas J.M. and Lambert R.M., Eds) Wiley, Chichester. P. 89.

IIJIMA S. (1977) Optik., 48, 193.

JOHNSON M.F.L. and KEITH C.D. (1963) J. Phys. Chem., 67, 200.

KAY D. (1965) "Techniques for Electron Microscopy" (1965) Blackwell Scientific Publications Ltd., Oxford.

KNOLL M. and RUSKA E. (1932) Ann. d. Physik., 12, 607.

KRAKOW W. and HOWLAND L.A. (1976) Ultramicroscopy, 2, 53.

LANKHORST P.P., de JONGSTE H.C. and PONEC V. (1980) In "Catalyst Deactivation", (Delmon and Froment, Eds) Elsevier Scientific Publishing Co., P. 43.

LEE T.J. and KIM Y.G. (1984) J. Catal., 90, 279

LEMAITRE J. (1984) In "Characterisation of Heterogeneous Catalysts". (F. Delannay, Ed.), Marcel Dekker Inc., New York., P. 29.

LIESKE H., LIETZ G., SPINDLER H. and VOLTER J. (1983) J. Catal., 81, 8.

LIETZ G., LIESKE H., SPINDLER H., HANKE W. and VOLTER J. (1983) J. Catal., 81, 17.

LYNCH D.F. and O'KEEFE M.A. (1972) Acta. Cryst., A28, 536.

McHENRY K.W., BERTOLACINI R.J., BRENNAN H.M., WILSON J.L. and SEELIG H.S. (1960) In "Proceedings 2nd. Int. Cong. on Catalysis, Paris, Vol. 2., P. 2295 (paper 117).

MacIVER D.S., TOBIN H.H. and BARTH R.T. (1963) J. Catal., 2, 485.

McVICKER G.B., GARTEN R.L. and BAKER R.T.K. (1977) 5th. Canadian Symposium on Catalysis.

MATYI R.J., SCHWARTZ L.H. and BUTT J.B. (1987) Catal, Rev.-Sci.Eng., 29, 41.

MILLS G.A., HEINEMANN H., MILLIKEN T.H. and OBLAD A.G. (1953) Ind. Eng. Chem., 45, 134.

MILLS G.A., WELLER S. and CORNELIUS E.B. (1960) In "Proceedings 2nd. Int. Cong. Catalysis"., Paris, Vol. 2., P. 2221 (paper 113).

MILLWARD G.R. and JEFFERSON D.A. (1978) In "Chemistry and Physics of Carbon" (Ed., P.L. Walker Jr.) 14, 1, Marcel Dekker Inc., New York.

MILLWARD G.R. (1980) J. Catal., 64, 381.

MURATA Y., BAIRD T. and FRYER J.R. (1976) Nature, 263, No. 5576, 401.

NIXON W.C., AHMED H., CATTO C.J.D., CLEAVER J.R.A., SMITH K.C.A., TIMBS A.E., TURNER P.W. and ROSS P.M. (1977) EMAG., 13.

OIKAWA (1970) Ultramicroscopy, 4, 181.

PINES D. (1956) Rev. Mod. Phys., 28, 184.

PINES D. (1963) In "Elementary Excitations in Solids", New York.

PINES H. and HAGG W.O. (1960) J. Am. Chem. Soc., 82, 2471.

POPPA H. and HEINEMANN K. (1980) Optik., 56, 183.

RENOUPREZ H., HOANG-VAN C. and COMPAGNON P.A. (1974) J. Catal., 34, 411.

ROTHSCHILD W.G., YAO H.C. and PLUMMER H.K. (1986) Langmuir, 2, 588.

RUCKENSTEIN E. (1980) In "Growth and Properties of Metal Clusters", (J. Boubdon, Ed.), Elsevier Scientific Publishing Co., Amsterdam, P. 57.

RUCKENSTEIN E. and CHU Y.F. (1979) J. Catal., 59, 109.

RUCKENSTEIN E. and LEE S.H. (1987) J. Catal., 104, 259.

RUCKENSTEIN E. and MALHOTRA M.L. (1976) J. Catal., 41, 303.

RUCKENSTEIN E. and PULVERMACHER B. (1973) J. Catal., 29, 224.

SANDERS J.V. (1986) Ultramicroscopy, 20, 33.

SASHITAL S.R., COHEN J.B., BURWELL R.L. and BUTT J.B. (1977) J. Catal., 50, 479.

SAXTON W.O. (1978) Optik, 49, 505.

SCHERZER O. (1949) J. Appl. Phys., 20, 20.

SHERRER P. (1918) Goett. Nachr., 2, 98.

SINFELT J.H., HURWITZ H. and ROHROR J.C. (1962) J. Catal., 1, 481.

SINFELT J.H. (1981) Catalysis - Science and Technology, Vol. I (J.R. Anderson and M. Boudart, Eds) Springer - Verlag, P. 257.

SLINKIN A.A. (1980) Russ. Chem. Rev., 49, 771.

SMITH D.J., CAMPS R.A., FREEMAN L.A., HILL R., NIXON W.C. and SMITH K.C.A. (1983) J. Microscopy, 130, 127.

SMITH D.J., WHITE D., BAIRD T. and FRYER J.R. (1983) J. Catal., 81, 107.

SPANNER M. (1984) Unpublished Work, Glasgow University.

SPANNER M., BAIRD T., FRYER J.R. and FREEMAN L.A. (1983A) Inst. Phys. Conf. Ser., No. 68, 267.

SPANNER M., BAIRD T. and FRYER J.R. (1983B) Inst. Phys. Conf. Ser., No. 68, 271.

SPENADEL L. and BOUDART M. (1960) J. Phys. Chem., 64, 20.

SPENCE J.C.H. (1981) "Experimental High Resolution Electron Microscopy", Clarendon Press, Oxford.

STRAGUZZI G.I., ADURIZ H.R. and GIGOLA C.E. (1980) J. Catal., 66, 171.

STULGA J.E. and WYNBLATT P. (1980) J. Catal., 62, 59.

SUSHUMA I. and RUCKENSTEIN E. (1987) J. Catal., 108, 77.

TANAKA M. and OGASAWARA S. (1970A) J. Catal., 16, 157.

TANAKA M. and OGASAWARA S. (1970B) J. Catal., 16, 164.

THON F. and SIEGEL B.M. (1970) B. Bunsen. Ges. Phys. Chem., 74, 1116.

TREACY M.M.J., HOWIE A. and WILSON C.J. (1978) Phil. Mag., A38, 569.

TREACY M.M.J. and HOWIE A. (1980) J. Catal., 63, 265.

TURKEVICH J. (1945) J. Chem. Phys., 13, 235.

U.S. Patent (1960) 2, 922, 767.

U.S. Patent (1969) 3, 415, 737.

U.S. Patent (1976) 3, 953, 368.

U.S. Patent (1976) 3, 981, 283.

Van NORDSTRAND R.A., LINCOLN A.J. and CARNEVALE A. (1964) Anal. Chem., 36, 819.

WANKE S.E. and FLYNN P.C. (1975) Catal. Rev.-Sci. Eng., 12, 93.

WARREN B.E. and AVERBACH B.L. (1950) J. Appl. Phys., 21, 595.

WELLS P.B. (1985) Appl. Catal., 18, 259.

WHITE D. (1982) Ph.D. Thesis, Glasgow University.

WHITE D., BAIRD T., FRYER J.R., FREEMAN L.A., SMITH D.J. and DAY M. (1983) J. Catal., 81, 119.

WILLIAMS R.C., FISHER H.W. (1970) J. Mol. Biol., 52, 121.

WOLD A. (1971) Advances in Chemistry, No. 98, P. 171.

WOLF R.J. and JOY D.C. (1971) Proc. 27th EMAG, 34, Institute of Physics.

WYNBLATT P. and AHN T-M (1975) Mat. Sci. Res., 10, 83.

WYNBLATT P. and GJOSTEIN N.A. (1975) In "Progress in Solid State Chemistry Vol. 9" (J.O. McCaldin and S. Somorjai, Eds.) Pergamon Press, P. 21.

YAO H.C., SIEG M., PLUMMER H.K. (1979) J. Catal., 59, 365.

YATES (1973) Ger. Offen., 2, 212, 204.

ZENITH J., CONTRERAS J.L., DOMINGUEZ J.M., YACAMAN M.J. (1980) J. Microsc. Spectrosc. Electron, 5, 291.

ZWORKIN V.K., MORTON G.A., RAMBERG E.G., HILLIER J. and VANCE A.W. (1945) In "Electron Optics and the Electron Microscope", Wiley, New York.

Inst. Phys. Conf. Ser. No. 90: Chapter 2
Paper presented at EMAG 87, Manchester, 8–9 September 1987

A model for the regeneration of Pt/γ-Al_2O_3 reforming catalysts

L J Butterly, T Baird, J R Fryer, M Day*

Chemistry Department, University of Glasgow, Glasgow G12 8QQ.
* I.C.I. Chemicals and Polymers Group, Wilton, TS6 8JE.

ABSTRACT: A model is proposed to explain the redispersion of sintered platinum crystallites, following an oxychlorination treatment on an aged Pt/γ-Al_2O_3 reforming catalyst. Transmission electron microscopy and hydrogen chemisorption have been used to study the catalyst at each stage in the ageing - regeneration cycle employed. Highly dispersed platinum crystallites have been resolved following oxychlorination, indicating successful redispersion of sintered crystallites.

1. INTRODUCTION

Platinum metal supported on alumina is used industrially as a reforming catalyst, converting linear hydrocarbons to unsaturated, cyclised and isomerised species. With prolonged use the platinum tends to agglomerate and carbon is deposited on the surface of the alumina, decreasing the catalytic activity. The catalyst can be reactivated by burning off the carbonaceous residues in oxygen and redispersing the platinum by an oxychlorination treatment.

Two models have been proposed to explain the redispersion of platinum:
(i) The Crystallite Splitting Model - where redispersion is due to the splitting of large Pt particles (Ruckenstein and Malhotra, 1976).
(ii) Redispersion by Spreading - where redispersion occurs via the spreading of a layer of platinum oxide species on the alumina, due to the decrease in surface tension as platinum is oxidised to platinum oxide (Ruckenstein and Chu, 1979).

This paper reports the results of high resolution electron microscopy (HREM) studies of the catalyst after each stage in the ageing - regeneration process, in an attempt to explain platinum redispersion.

2. EXPERIMENTAL

The catalyst was prepared by impregnating Condea alumina granules (400-100 μm, surface area 200m^2/g) with a predetermined amount of hexachloroplatinic acid, H_2PtCl_6.

© 1987 IOP Publishing Ltd

The samples were calcined in a muffle furnace at 500°C for 5 hours, chlorided by slowly injecting dilute HCl into the gas flow, and then reduced in hydrogen at 460°C for 24 hours. Neutron activation analysis confirmed that the catalyst contained 0.31% by weight of platinum. Ageing of the fresh catalyst was achieved by sintering in 3 v/o O_2 in N_2 at 600°C for 4 hours.

Redispersion of the sintered catalyst was attempted by an oxychlorination treatment at 480°C in 3v/o O_2 in N_2, the chlorine being obtained from CCl_4 in N_2 which was slowly added to the gas stream over 3 hours at 400ppm.

High resolution electron microscopy was used to measure the platinum particle size distribution at each stage in the ageing - regeneration cycle. Samples were ground to a fine powder, suspended in de-ionised water, dried on to carbon-coated specimen grids and examined in a JEOL 1200-EX transmission electron microscope. Platinum particle sizes were calculated from H_2 chemisorption data by assuming a simple spherical particle geometry and a H:Pt ratio of 1:1.

3. RESULTS AND DISCUSSION

Particle size data obtained from HREM and H_2 chemisorption, for fresh sintered and regenerated catalysts are shown in Table 1. High resolution electron microscopy of the fresh catalyst suggests that the platinum is highly dispersed, reflecting a successful preparation, as indicated in figure 1.

After ageing HREM and chemisorption both revealed an increase in platinum particle size. Figure 2 shows typical sintered platinum crystallites.

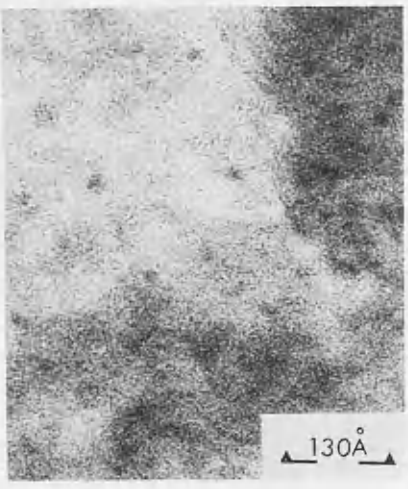

figure 1: fresh catalyst showing highly dispersed Pt crystallites.

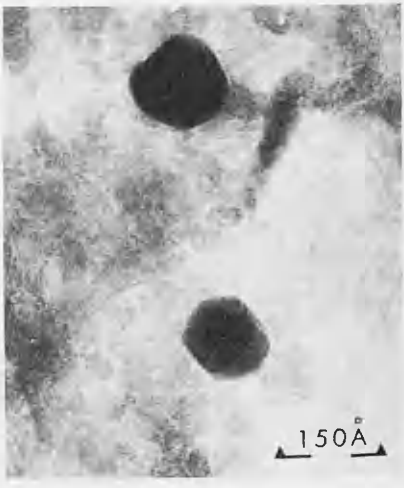

figure 2: aged catalyst displaying typical sintered Pt particles.

Table 1: Statistical data for fresh (F), sintered (S) and oxychlorinated (OXY) catalysts.

	F	S	OXY
H_2 Chemisorption Vm (ml/g)	0.204	0.047	0.234
H_2 Chemisorption d(calc.) (nm)	1.2	5.4	1.1
TEM mean diameter d(mean) (nm)	1.6	5.6	2.8

Attempted redispersion of the sintered catalyst by oxychlorination treatment indeed resulted in a decrease in particle size as shown by HREM (figure 3) and a corresponding increase in hydrogen uptake.

Particle size distributions of the sintered and oxychlorinated catalysts are indicated in the histograms in figure 4. It is evident that the number of large particles ($\rangle$ 130Å) remains approximately constant, whereas the number of small particles ($\langle$ 30 Å) has doubled following redispersion. This suggests that the crystallite splitting model is not a good representation of platinum redispersion, in the present system, as large particles are said to fracture more readily than smaller particles (Dadyburjor, 1980). The results may be explained by invoking the formation of a mobile platinum oxide or oxychloride species. Subsequent reduction of atomically dispersed oxide on the support would then lead to redispersion.

An oxide layer may form on the surface of the large particles and spread across the alumina support , after reduction some redispersion would occur. The platinum particle diameter would

igure 3: sub-10Å Pt
articles on alumina
llowing oxychlorination.

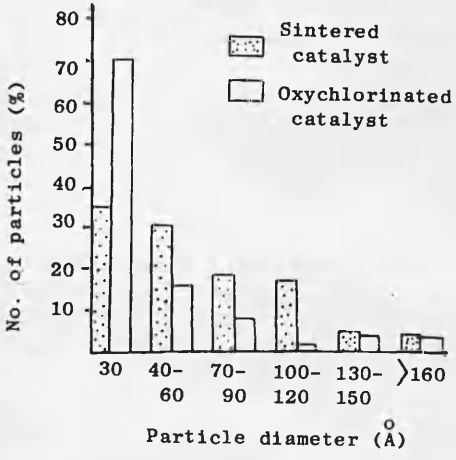

Figure 4: A comparison of the sintered catalyst and the catalyst following an oxychlorination.

not significantly change as large crystallites may be protected by a surface layer of oxide, preventing further oxidation as shown in figure 5.

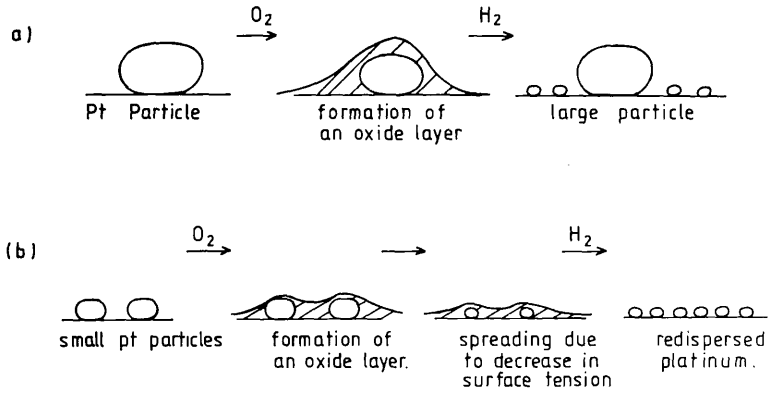

figure 5 Model for the redispersion of platinum in a pt/γ-Al_2O_3 catalyst, following on oxychlorination treatment. (a) large platinum particles. (b) small platinum particles.

4. REFERENCES

Dadyburjor D B 1980, Catalyst Deactivation, Delmon B and Froment G F Eds. (Elsevier Sci. Publishing Co. Netherlands) pp341

Ruckenstein E, Chu Y F 1979 J. Catal. 59 109.

Ruckenstein E, Malhotra M L 1976 J. Catal. 41 303.

Proc. XIth Int. Cong. on Electron Microscopy, Kyoto, 1986

CATALYTIC SITES IN Pt/γ-Al_2O_3 REFORMING CATALYSTS.

L.J. BUTTERLY[1], T.BAIRD[1], J.R. FRYER[1], M.DAY[2] and S. NORVAL[2]

(1) Department of Chemistry, University of Glasgow, Glasgow G12 8QQ. Scotland. U.K.
(2) I.C.I. Petrochemicals and Plastics Division, Wilton, Cleveland, England. U.K.

Previous studies (1,2) have shown that platinum (0.3-1.0 w/o) dispersed on γ-alumina converts linear hydrocarbons (naphtha feed) to cyclic products such as benzene and toluene, increasing the octane rating of the naphtha. In the course of this reaction the platinum tends to agglomerate and carbon forms on the surface of the alumina decreasing the catalytic activity. The catalytic activity can be regained by burning off the carbon with oxygen and redispersing the platinum by an oxychlorination treatment. Our previous work (1,2,3) has considered the structure of the reactivated platinum particles. Results from TEM and XRD (Table 1) indicate that the large platinum particles formed during sintering were not apparantly redispersed on oxychlorination treatment, although catalytic activity was regained and hydrogen chemisorption showed enhanced surface area.

X-ray diffraction analysis was carried out by measuring line broadening of the Pt (311) reflection. Quantitative XRD was used to measure the amount of Pt being detected by comparison to standards of known w/o Pt. It was found that only 0.4 w/o Pt was detected on a 0.83 w/o Pt catalyst, suggesting that over 50% of the platinum was in the form of sub-30Å particles. These are apparantly responsible for catalysis and therefore the shape, size and structure of the particles are important. Monolayer volumes were estimated from XRD results by assuming particle diameters, for Pt not detected by XRD, and comparing to the measured monolayer volumes from hydrogen chemisorption. Figure 1 shows the XRD estmated monolayer volumes' mean deviation from the measured monolayer volume of hydrogen chemisorbed, against the 'invisible' Pt particle diameter for many catalysts of differing treatments. The minimum mean deviation from the measured monolayer volume is found by assuming a Pt particle diameter of 9Å.

High resolution electron microscopy has been used to resolve the catalytically active species indicated by quantitative XRD. Figure 2 shows sub-10Å Pt particles on the alumina support, following oxychlorination treatment.

REFERENCES:

(1) Spanner. M., Baird. T., Fryer. J.R., Freeman. L.; Inst. Phys. Conf. Ser. No. 68: 3, 267 (1983)
(2) Spanner. M., Baird. T., Fryer, J.R.; Inst. Phys. Conf. Ser. No. 68: 8, 271 (1983)
(3) White. D., Baird. T., Fryer. J.R., Freeman. L.A., Smith. D.J. and Day M.; J. Catal. 81,119, (1983)

Table 1: Statistical data for fresh (F), sintered (S) and oxychlorinated (OXY) catalysts.

	F	S	OXY
H_2Chemisorption Vm(ml/g)	0.405	0.112	0.345
H_2Chemisorption d(calc)(nm)	1.69	6.11	1.98
TEM diameter d (nm)	3.2	15	16.6
XRD fourier average (nm)	3.0	10.4	10.8
Ratio of aromatic products to unreformed n-heptane.	25:1	1.1:1	28.5:1

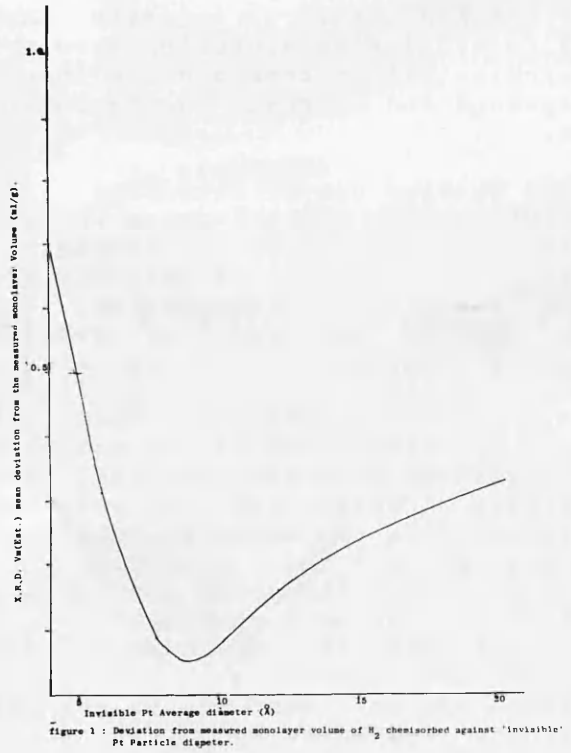

figure 1 : Deviation from measured monolayer volume of H_2 chemisorbed against 'invisible' Pt Particle diameter.

Figure 2: sub-10Å Pt particles on γ-alumina, following oxychlorination

GLASGOW UNIVERSITY LIBRARY